AD-A194 450 INDIAN OCEAN VALIDATION(U) COAST GUARD ALEXANDRIA VA OMEGA NAVIGATION SYSTEM CENTER E R SWANSON ET AL. 01 SEP 87 USCG-ONSCEN-02-87 1/2

UNCLASSIFIED F/G 17/7 NL

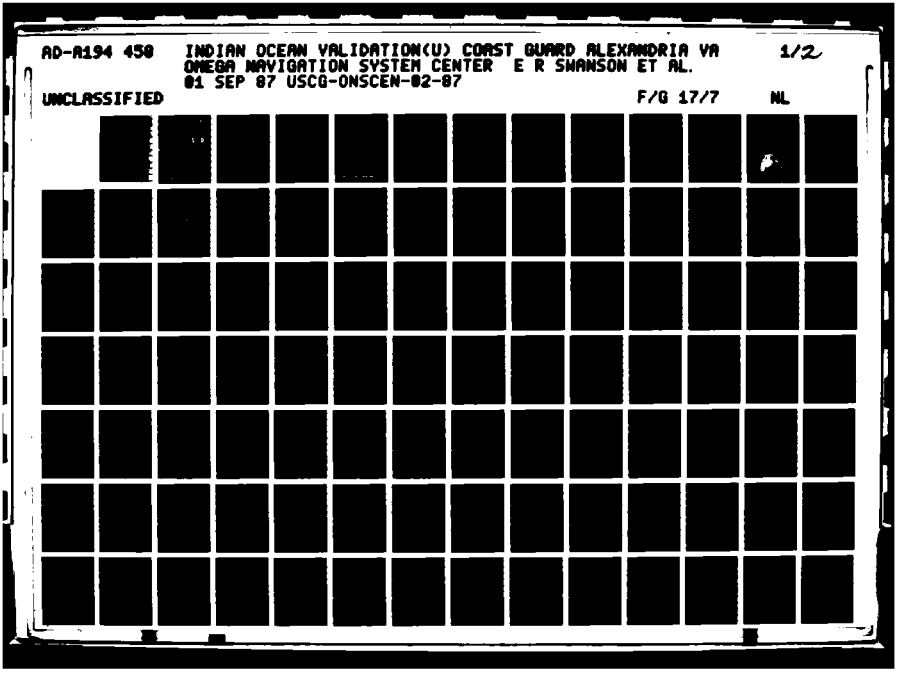

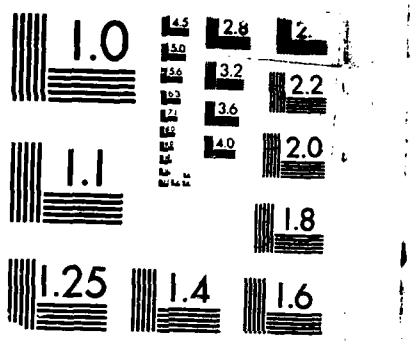

MICROCOPY RESOLUTION TEST CHART

BUREAU OF STANDARDS-1963-A

INDIAN OCEAN VALIDATION

by

E. R. Swanson
and
C. P. Kugel

1 SEPT. 1987

Abstract

Results from the Indian Ocean validation conducted during 1983 are presented. Existing coverage theories were largely confirmed in the region except that an interference boundary for the use of Japan at night in Western Australia should be relocated. The supported coverage theories indicate potential accuracy of 2 nmi (c.e.p.) or better throughout the region on a 24-hour basis except in the important trade route from the Red Sea, around the tip of India, through the Straits of Malacca, and into the South China Sea. On the trade routes accuracies as poor as five miles may occasionally occur.

CONTENTS

LIST OF FIGURES

SECURITY CLASSIFICATION OF THIS PAGE

ADA194458

REPORT DOCUMENTATION PAGE

1a. REPORT SECURITY CLASSIFICATION: UNCLAS	1b. RESTRICTIVE MARKINGS
2a. SECURITY CLASSIFICATION AUTHORITY	3. DISTRIBUTION/AVAILABILITY OF REPORT: UNLIMITED
2b. DECLASSIFICATION/DOWNGRADING SCHEDULE	
4. PERFORMING ORGANIZATION REPORT NUMBER(S): CG-ONSCEN-02-87	5. MONITORING ORGANIZATION REPORT NUMBER(S)
6a. NAME OF PERFORMING ORGANIZATION: USCG-OMEGA NAV. SYS. CENTER; 6b. OFFICE SYMBOL (If applicable): G-ONSC	7a. NAME OF MONITORING ORGANIZATION
6c. ADDRESS (City, State, and ZIP Code): OMEGA NAVIGATION SYSTEM CENTER, 7323 TELEGRAPH ROAD, ALEXANDRIA, VA. 22310-3998	7b. ADDRESS (City, State, and ZIP Code)
8a. NAME OF FUNDING/SPONSORING ORGANIZATION: SAME AS 6a.; 8b. OFFICE SYMBOL (If applicable)	9. PROCUREMENT INSTRUMENT IDENTIFICATION NUMBER
8c. ADDRESS (City, State, and ZIP Code)	10. SOURCE OF FUNDING NUMBERS: PROGRAM ELEMENT NO. / PROJECT NO. / TASK NO. / WORK UNIT ACCESSION NO.

11. TITLE (Include Security Classification): INDIAN OCEAN VALIDATION

12. PERSONAL AUTHOR(S): ERIC SWANSON + CARL KUGEL

13a. TYPE OF REPORT	13b. TIME COVERED FROM ____ TO ____	14. DATE OF REPORT (Year, Month, Day): 1987 SEPT. 1	15. PAGE COUNT

16. SUPPLEMENTARY NOTATION

17. COSATI CODES: FIELD	GROUP	SUB-GROUP

18. SUBJECT TERMS (Continue on reverse if necessary and identify by block number): REGIONAL VALIDATION (INDIAN OCEAN) FOR THE OMEGA NAVIGATION SYSTEM

19. ABSTRACT (Continue on reverse if necessary and identify by block number)

INCLUDED WITH DOCUMENT (1ST PAGE)

20. DISTRIBUTION/AVAILABILITY OF ABSTRACT: ☒ UNCLASSIFIED/UNLIMITED ☐ SAME AS RPT. ☐ DTIC USERS	21. ABSTRACT SECURITY CLASSIFICATION: UNCLAS
22a. NAME OF RESPONSIBLE INDIVIDUAL: RANDOLPH J. DOUBT	22b. TELEPHONE (Include Area Code): 703-866-3890; 22c. OFFICE SYMBOL: G-ONSC

DD FORM 1473, 84 MAR — 83 APR edition may be used until exhausted. All other editions are obsolete.

SECURITY CLASSIFICATION OF THIS PAGE

EXECUTIVE SUMMARY

Omega validations are intensive studies of regions with multiple goals:

1. To characterize signal coverage in the region.
2. To determine potential accuracy of the Omega system.
3. To assess performance of existing equipment.

The latter goal is very much tertiary. Equipments from various manufacturers differ and are all suboptimal in different ways. Better receivers are being developed as Omega is better understood and software modified.

Omega coverage considerations extend well beyond the simple existence of adequate signal levels with respect to atmospheric noise i.e., Signal-to-Noise Ratio (SNR). Indeed, SNR is rarely a problem and, if so, will be obvious to the users of a manual receiver and easily annunciated by an automatic receiver. Thus, SNR limitation should not lead to hazardous conditions. A more subtle and more important limitation is that occasionally present in the Omega signal structure itself. The signal structure must allow the measured phase to be related to position on the ground. One would prefer a single propagation mechanism to convey signals directly from stations to receivers at any location and time. This is not the case. Occasionally, dominant signals will be received over the "long" path propagating not directly but over half way around the world. Also, anomalies may occur over short paths if several propagation modes are supported. This "modal" interference tends to occur at night on westbound paths near the magnetic equator. These types of "self-interference" are especially troublesome as they cannot necessarily be determined from the received signals themselves. A priori coverage guidance is necessary for proper signal utilization. Verifying coverage guidance is a major goal of Omega validation.

The measurement program took place from the summer of 1982 to the fall of 1983. Ground monitors modified to allow amplitude measurement were operated at Perth, Singapore, Bahrain, Diego Garcia and Pretoria. The analysis was also based on long term measurements conducted at other land sites in and around the Indian Ocean. Special shipboard-Magnavox 1105 installations were

made to obtain Omega phase error data at sea on three merchant ships. Most importantly, a dedicated U.S. Coast Guard C-130H aircraft flew a well-planned set of flight legs searching for modal interference at night. The aircraft was equipped with special instrumentation which produced considerably more data than heretofore available from validations. The aircraft also carried a conventional Litton LTN-211 receiver as well as inertial and Global Positioning System (GPS) equipments. The analysis also exploited long term measurements conducted at land sites in and around the Indian Ocean.

This validation has been analyzed with special attention to coverage models. The now conventional coverage overlays have only recently become available at 13.6 kHz as well as 10.2 kHz., and can be quite different. Also, a highly integrated parametric global model for Omega coverage at 10.2 kHz has been developed. The parametric model predicts not only station coverages for any particular time of day, but also Omega system accuracy as would be achieved by an ideal receiver.

The validation results are quite supportive of the models. Of particular interest is the verification of 13.6 kHz coverage especially as compared with coverage at 10.2 kHz. This is the first validation analysis for which global 13.6 kHz coverage overlays have been available. Prediction of unique modal limitations northeast of Liberia on 13.6 kHz at night amounts to a considerable triumph for full-wave prediction theory and the overlay construction methods. A boundary change in the 10.2 kHz modal interference region for Japan is as much supportive of the overall method as it is corrective of a particular error. This particular instance is one in which the 10.2 kHz parametric coverage proved more accurate than the overlays on which it was largely based. Not only was the general parametric coverage prediction good, the assumed error budgets for phase prediction also were validated. This adds considerable credibility to parametric predictions of system accuracy throughout the Indian Ocean, in particular and by extrapolation, for global forecasts as well. Omega is much better understood as an entity than it was a few years ago.

The models indicate an accuracy capability of 2 nmi (c.e.p.) or better throughout the region on a 24-hour basis with the unfortunate exception of the trade routes from the Red Sea, around the tip of India, through the Straits of Malacca, and up the South China Sea. When signal paths from both Australia and Japan are dark, there is a small region in which signals from neither station can be used and where the usable stations provide only poor geometry. Fix accuracies as poor as 5 nmi (c.e.p.) may then occur. This small area warrants intensive local study. Differential Omega might help mitigate errors.

Although of tertiary concern in the validation, the performance of the LTN-211 flown on the validation flights was noteworthy as an example of existing equipment. On the positive side, the set navigated continuously throughout the entire validation effort maintaining a median accuracy of about two miles. Considering the miles flown, duration of the test, intervening Omega station outages, various weather conditions, and the fact the flights were deliberately planned to investigate signal limitations, this level of system performance and robustness is exemplary. Comparison with other aids indicated no truly gross errors ever occurred. However, landing errors larger than four miles (but less than ten miles) were measured. At least some of these were apparently the result of inadequate coverage guidance being incorporated into the LTN-211 at the time of the validation. The exceptions emphasize the need for coverage guidance.

INDIAN OCEAN VALIDATION
ABRIDGED REPORT

This abridgement and the full report are divided into six sections:

1. Overview
2. Coverage Theory
3. Equipment Deployment
4. Spot Comparison: Theory and Observation 1800 GMT
5. Individual Station Coverage Analysis
6. System Coverage and Error Characterization

Appendices to the full report provide additional detail on coverage prediction and field strength prediction.

OVERVIEW:

The Omega validation program has evolved over the years into a coordinated sequence of geographic "validations" where intensive resources in both instrumentation and analysis are applied to determine Omega coverage. Functionally, the process is a traditional one in the establishment and operation of navigation aids. Presumably there was a "validation" program of some type to assure the effectiveness of the first radio beacon. More recently Loran-C has undergone "calibrations". The Loran-C efforts and Omega validations share the characteristics that not only is the signal availability and utility in an area determined, a data base is also gathered from which the essential phase characteristics of the signals can be better calibrated and, hence, used in the future. Loran-C or Omega regional validations or calibrations are essentially single efforts to be conducted once. This is in contrast to the periodic measurement and re-certification conducted on airport approach aids by the Federal Aviation Administration (FAA). FAA aids are at much higher frequency and their performance can be affected not only by slow equipment aging but, also, by unrelated new construction near airports which can change the radio field through introducing reflections. For both Omega and Loran-C, a few well placed monitors are sufficient to determine any slow changes which may occur. Additionally, localized programs may occasionally be

warranted. One example is the effort conducted by the U.S. Coast Guard and SERCEL prior to installing differential Omega beacons. Another example of particular relevance to this validation would be intensive investigation of Omega coverage near Singapore and the Straits of Malacca. This is an area of very heavy traffic, both marine and air. It is also an area where Omega coverage is not only poor but difficult to assess. Local long term assessment with attention to seasonal changes is warranted. Use of Differential Omega should be considered.

Whereas past validation efforts have made use of such predictions as may have been available, this validation analysis is strongly coupled to the now existing theory. This is in consonance with the multiple goals of a validation effort:

1. Characterize signal coverage in the region. That is, define the radio physics and signal environment in which an Omega receiver must operate.
2. Determine potential Omega accuracy using an idealized receiver.
3. To a much lesser extent, obtain an estimate of the accuracy of present Omega equipment.

The de-emphasis on present equipment functioning is important and essential to a system validation. Accuracy can improve as software is improved based on a better understanding of signal characteristics; thus, the de-emphasis on actual performance of equipments during the evaluation itself.

It is noteworthy that this is the first evaluation for which signals from all eight Omega stations, including Australia, have been available.

COVERAGE:

The term "coverage" requires amplification. The fundamental measurement in Omega is that of the phase of a radio signal and the essential expectation is that changes of phase can be related to changes of position on the ground. An additional requirement is to measure the phase in a timely fashion in the presence of noise. In practice the signal level, that is, Signal-to-Noise Ratio (SNR), is almost always adequate to permit timely phase measurement. As can be seen by perusing the detailed station coverage

diagrams, most Omega signals can be received at almost all locations almost all of the time. The few exceptions are primarily due to the "shadow" effect of regions of extremely high attenuation such as Greenland and Antarctica. The critical problem is that the structure of the signals may not permit navigation. That is, a signal may be of high amplitude but the structure itself renders the signal unsafe for use. A particularly dangerous aspect of this structural limitation is that there is no way by which a receiver can necessarily identify such signals based on their characteristics as received. A priori guidance on usage is a major reason for undertaking validation in general and developing coverage guidance in particular.

Phenomena leading to an unsuitable signal structure have been referred to as "self-interference". That is, energy propagates from transmitter to receiver by a desired modeled mechanism and various other interfering mechanisms as well. Self-interference is recognized to occur near transmitters roughly equivalent to the skywave-groundwave interference experienced with other systems. Additionally, Omega coverage models recognize an interference near the antipode of a transmitter where energy can arrive from all directions. Other self-interference phenomena include long path interference wherein the signal propagated over half way around the world dominates that received over the shorter path, and "modal" interference.

Omega propagation may be best viewed as occurring within a spherical waveguide formed between the earth and the ionosphere. During daytime illumination conditions, the waveguide may be rather simplistically represented. The signal field may exhibit some complexity "near" transmitters, but after a short distance, a single mode will dominate and, therefore, phase will vary regularly with distance. The "first" is that which will be present during the day and that for which the Predicted Propagation Corrections (PPCs) were developed.

At night propagation may be very much more complex and the full interaction of the Omega signals and the ionospheric magneto-plasma needs to be considered. Various propagation modes may be supported and "modal interference" may extend over large regions. Primarily in response to

strategic communications requirements, the Naval Ocean Systems Center (NOSC) has spent tens of millions of dollars developing computer models which properly represent the interaction. The Analytical Sciences Corporation (TASC) has spent millions more applying the models to Omega. These full-wave computations form the basis of all modern coverage studies. The computer model provides guidance on how the Omega signal structure may vary in space or time which may then be verified or modified by a validation effort.

There are three coverage approaches of importance to the present validation: 1) overlay, 2) parametric, and 3) local. The interrelationships between the models are developed in more detail in the full report. Key aspects follow.

The overlay method of presenting coverage information was the first of the methods employed. Initially, coverage for a single station at a single idealized day or night propagation condition was computed. These were originally done only at 10.2 kHz but have since been extended to 13.6 kHz. Figure 1 is an example showing modal interference regions for La Reunion

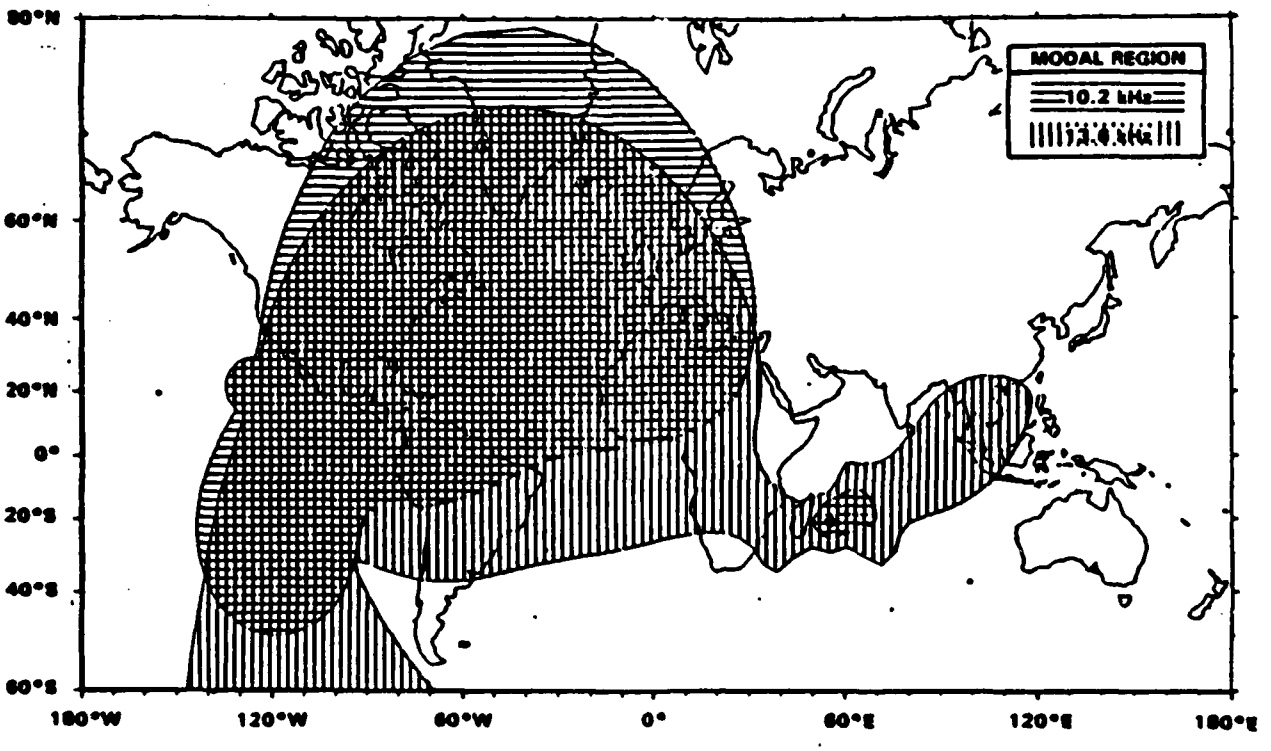

Figure 1. Overlay Coverage Showing Modal Interference Limitations for Omega La Reunion at Night

at both 10.2 and 13.6 kHz. Signal-to-Noise contours also were computed and regions free of modal interference and where the SNR exceeded a threshold were identified as providing good coverage. Coverages from the eight stations at the particular idealized illumination condition were then overlayed to obtain "spaghetti" diagrams to explicit system coverage. Figure 2 shows an example reflecting later extensions to a particular time of day. The overlay approach does have some advantages. The spatial extent of coverage limitations as shown, for example, in Figure 1, provides an excellent starting point from which to plan validation efforts. (It further illustrates the need for elaborate computations as one would not otherwise expect the extreme difference in coverage between 10.2 and 13.6 kHz northeast of La Reunion). Individual station coverage diagrams, e.g., Figure 1, or the composite diagrams, e.g., Figure 2, can also be used by a navigator to determine useful signals. Further, the coverage boundaries readily can be identified during a validation and boundaries moved if necessary. However, overlays are severely limited in several ways--particularly in predicting the accuracy to be provided.

The parametric and local approaches both employ apparently equivalent optimal weighting by which potential accuracy can be deduced if all signals are used to best advantage. That is, poor signals providing good geometry are properly "traded-off" against good signals of poor geometry. Additionally, the parametric approach incorporates a modeling of Omega propagation parameters which is compatible with the processing now done within modern receivers to compute PPCs. Although currently developed only for 10.2 kHz, results from the parametric approach have been used at least equally with overlays in this validation. The parametric approach provides two outputs: (1) Individual stations coverages are produced in a form where various types of signal limitations are indicated and the nature of the limitation shown, e.g., Figure 3. and (2) System coverage maps show accuracy to be obtained throughout the world at various specific times or alternatively computed throughout the 24-hour day (cf. Figure 4). The parametric formulation is quite powerful in providing coverage guidance, but lacks the ease of making local adjustments inherent with overlays.

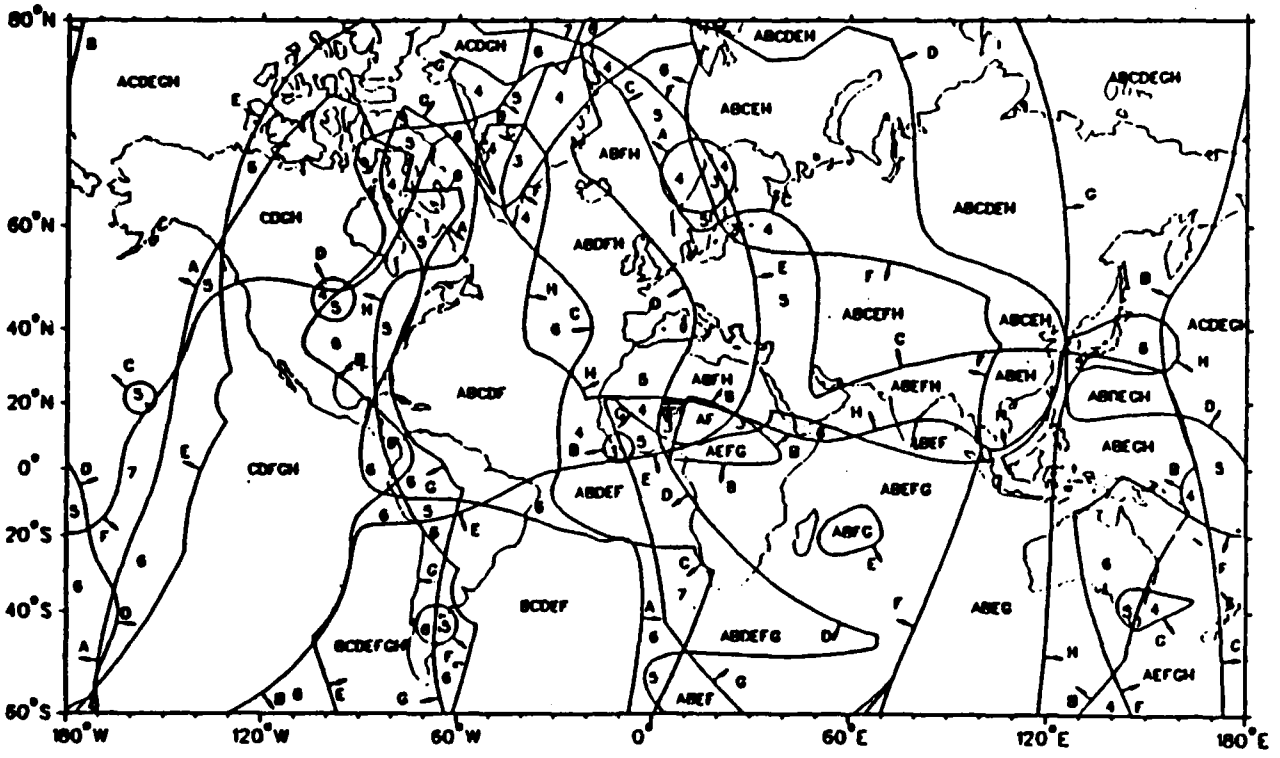

Figure 2. Compoposite Coverage, 1800 GMT in August (-30 db SNR).

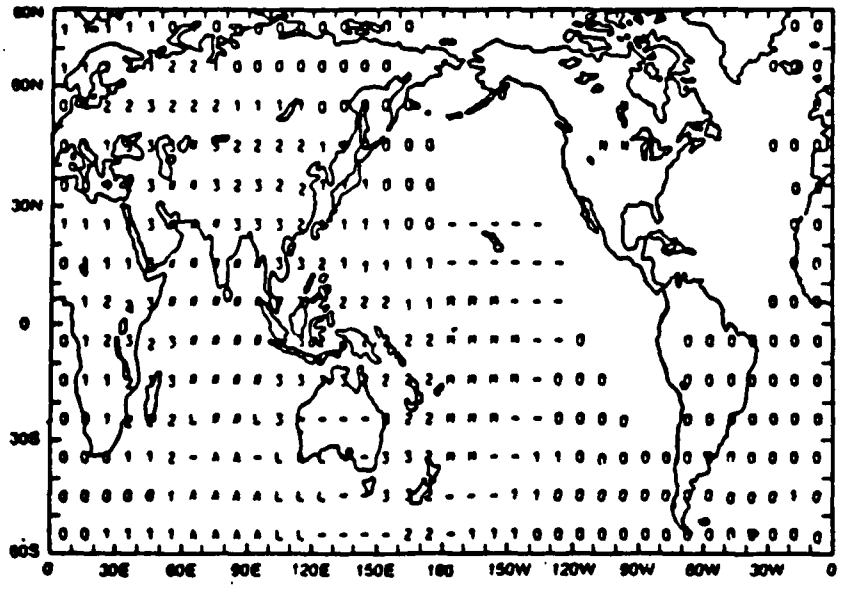

Figure 3. Parametric Coverage for an Individual Station Showing Coverage for Omega North Dakota at 0600 GMT (Vernal Equinox). KEY: Self-Interference: M = Modal, L = Longpath, N = Near, A = Antipodal, - = Perturbed but usable; SNR: (Blank) = SNR > 0 db in 100 Hz Bandwidth, 0 = 0≤ SNR < -10db, 1 = -10≤ SNR< -20, etc, # = SNR≤ -40 db.

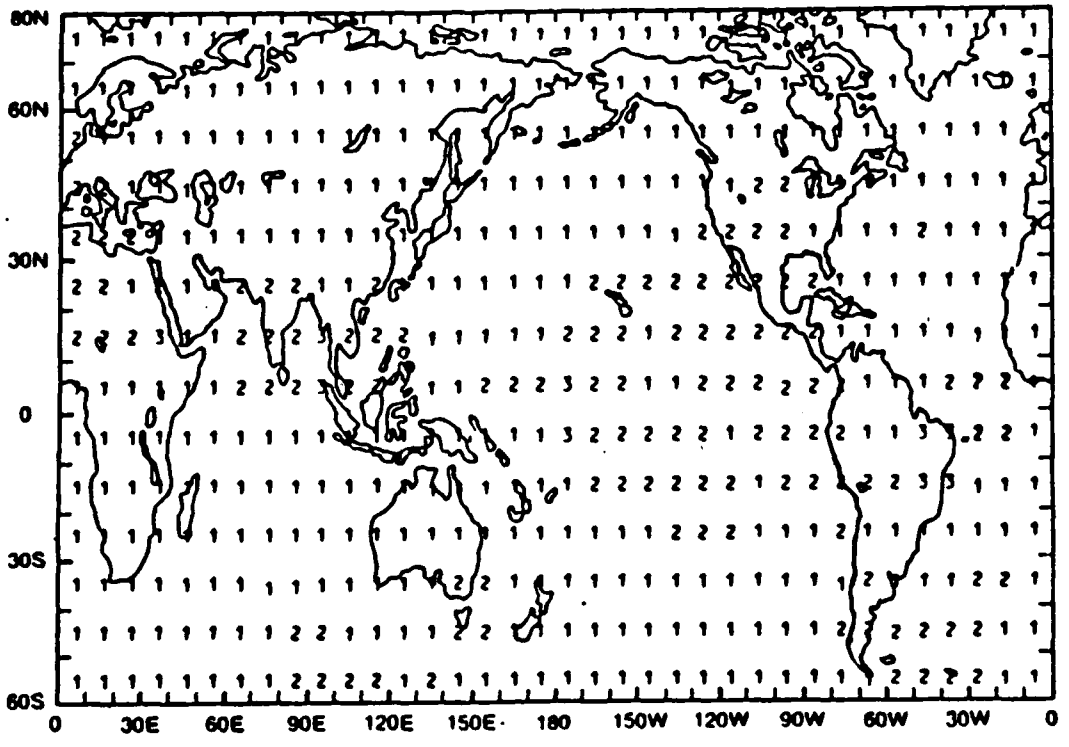

Figure 4. 24-hour System Coverage (figures show median accuracy in n.mi. c.e.p.). (Derived from parametric model using 10.2 kHz alone).

The local method was developed specifically to obtain a measure of optimum system accuracy in a validation region. It has been previously used only in the north Pacific validation. While this method and the parametric both incorporate an appropriate combinational optimization, the methods of characterizing the errors and coverage are quite different. Although the local method has been fully applied to the validation and is discussed in the full report, the results are believed less credible than those from the parametric approach.

EQUIPMENT DEPLOYMENT:

As with previous validations, the Indian Ocean validation was a coordinated effort to gather diverse types of synergistic data from which the key aspects of Omega coverage could be determined. The major measurement portions were:

1. In-flight measurements on dedicated flights.
2. Long term measurement of temporal variation at fixed sites.
3. Shipboard data from ships transiting the area.

Both amplitude and phase measurements were made in-flight and at the fixed sites. Figure 5 shows the Indian Ocean areas, flight paths for the dedicated flights, the fixed sites, and ship transit areas.

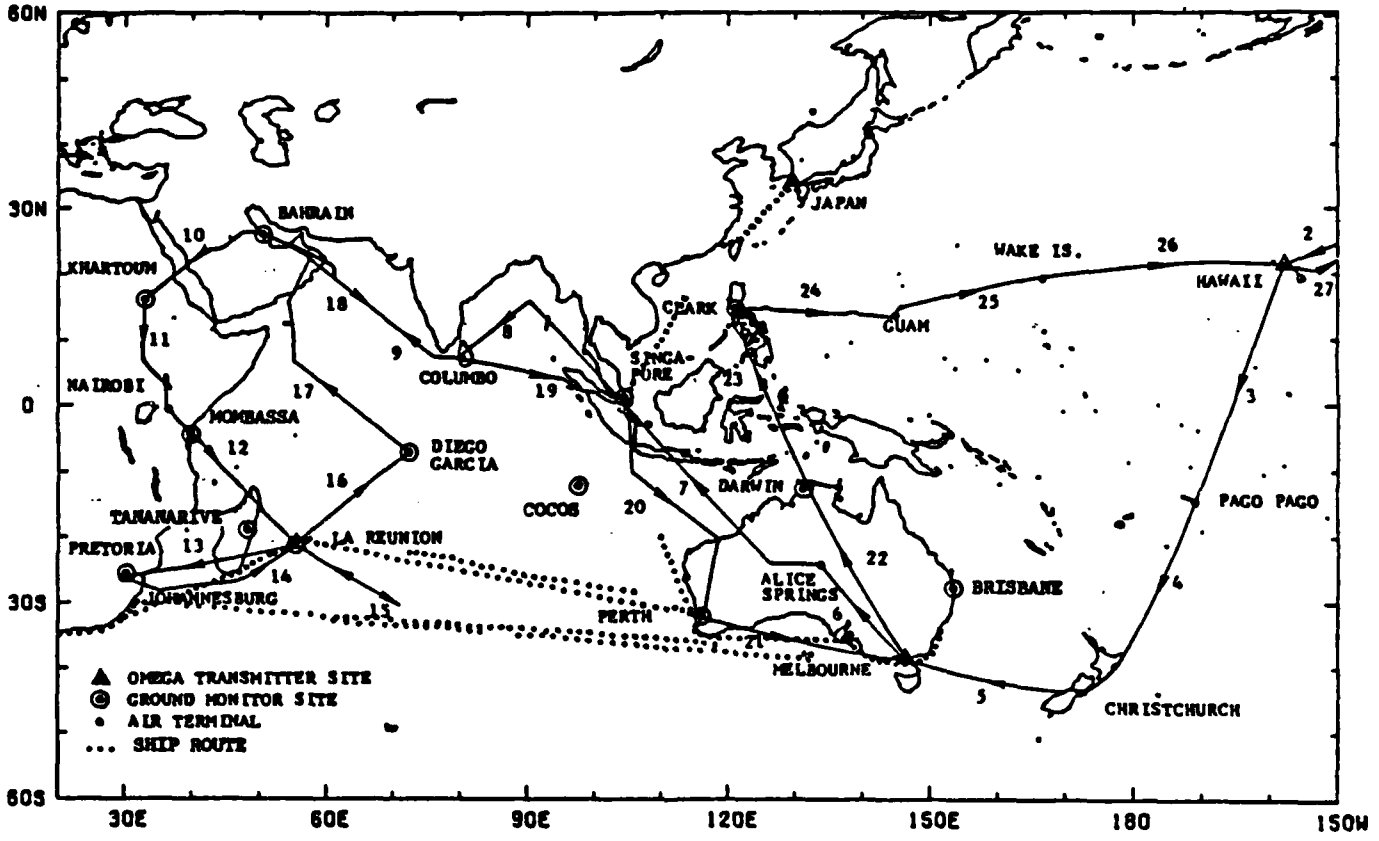

Figure 5. Indian Ocean Flights, Voyages and Monitoring.

Airborne instrumentation for this validation was unique. The principle data gathering device was a modified Litton LTN-211 Omega navigation receiver. The LTN-211 typically measures at least three of the four commutated Omega frequencies. At each frequency this receiver ordinarily measures signals from seven of the eight Omega stations and uses one segment

to inject a reference signal into the antenna to calibrate the receiving system. Typically, injection was is on top of a relatively weak Omega signal and is done at a relatively high level so as to swamp the incident Omega signal. Ordinarily, measurements of the injection are used internally for calibration and not output. In this validation a weak signal nearly equal to the noise was injected and the phase tracking data for the injection was output as well as being used internally. Of particular interest was the measured phase variance on the injected channel which can be related to the Signal-to-Noise Ratio. Since the absolute voltage level of the injection was known, this allowed measurement of the prevailing noise level. For this purpose an omnidirectional whip antenna was used instead of the usual loop. As is ordinarily done within the LTN-211, phase variances on the other signals also were computed. As the signal-to-noise ratio relates to the phase variance and since the nominal noise level could be determined from measurements on the injection channel, the signal amplitude of each of seven Omega stations could be measured. A few problems were, however, anticipated and experienced. The most significant problem was a loss of quality due to the effect of the noise on other measurements. The aircraft was also equipped with an Inertial Navigation System (INS) and a Global Positioning System (GPS) receiver. In particular, it was the intention that the GPS be used to determine biases in the INS.

A second unmodified LTN-211 was also installed with a conventional loop (H-field) antenna. This equipment was used to assess airborne navigational performance.

SPOT COMPARISON OF PREDICTED AND OBSERVED COVERAGE - 1800 GMT:

A convenient means of checking the adequacy of the 10.2 kHz parametric coverage prediction is available by combining results noted in two papers published in the Proceedings of the 1984 Seattle meeting of the International Omega Association. In one, Kugel presented receiver utilization of signals at various points throughout the region at 1800 GMT. Signals on which modal interference was noted also were identified. Swanson presented a method of estimating coverage at particular times of day including 1800 GMT. Thus, we wish to compare coverage as noted in Kugel's Figure 5 with that computed by

Swanson for 1800Z. Conveniently, the flights were conducted at nearly the same illumination conditions for which calculations were made. Seasonal differences could cause the noise to be slightly different.

Observed coverage combined with coverage assessment(s) are discussed summarized tabularly in the full report. Many features were noted. Perhaps most importantly, of the observations noted by Kugel as undergoing interference, all were predicted to be disturbed. The primary objective of coverage studies is to indicate where signals may be used safely. Coverage indications were developed conservatively so as to attempt to assure signal deletion if necessary even at the expense of occasionally deleting signals which were usable. There were, however, a significant number of instances where modal interference was expected but where Kugel did not note it.

Signals were expected to be unperturbed at better than -20 db Signal-to-Noise Ratio (SNR) in 100 Hz bandwidth in 45% of the samplings. In these circumstances, tracking was nearly solid. In only three percent of the instances did the receiver tracking less than 100% of the time, but even for these exceptions the average tracking was 90%. This suggests that there was nothing grossly noisy about the aircraft itself or the installation, and further, suggests that the particular method for predicting estimated SNRs is reasonably accurate.

Actual signal usage was highly supportive of the theoretical model. One would also hope that signals in the range from -20 to -30 db could be reliably tracked. The table shows this range to be about the tracking limit with the observed usage ranging from 100% to none. The SNR tracking limit for the particular installation appears nearer -30 db than -20db. Generally, signals which were predicted to be usable were in fact used by the receiver. Unfortunately, some improper signal usage also was noted. That is, some "use" was made of signals which were predicted and observed to be undergoing self-interference.

Whereas comparison of theoretically projected signal availability and actual signal use was reasonable and meaningful, comparison of predicted

accuracy from an optimal receiver using only 10.2 kHz with that from an actual receiver using three of the four Omega frequencies is much less meaningful. Not the least of the various problems is that the true location of the aircraft at 1800 GMT was not known. The location of the aircraft was known before take-off and after landing. Theoretical predictions indicate abnormally poor fix accuracy (4 mile c.e.p. or more) at 1800 GMT in a generally equatorial belt from Khartoum through Colombo to Singapore but accuracy of 1-2 miles otherwise. For flights airborne at or near 1800 GMT half of the abnormally poor landing errors were in the equatorial belt. Otherwise, errors on landing were typically slightly over two miles. Typical errors before takeoff were slightly better than one mile. Considering dissimilarities in theoretical model and actual implementation and the crudeness of the spot comparison, the agreement is better than might be expected.

INDIVIDUAL STATION COVERAGE ANALYSIS:

As previously noted, potential utility of a signal in a particular area at a particular time depends primarily on the signal structure and secondarily on the prevailing Signal-to-Noise Ratio. The structure can be described in terms of the severity of competing types of self-interference: modal interference, long path interference, or proximity to the transmitter or antipode. Signal self-interference, particularly modal interference, will be addressed first.

Modal components combining to form a resultant signal cannot be directly observed experimentally. Nor, under typical receiving conditions at a stationary receiver, would it be apparent whether a signal was received over the long or short propagation path. Thus, indirect methods and scientific inference must be used in coverage assessment. It is also a reason coverage assessment is so important; practical receivers are very limited in the means they may employ to detect self-interference.

One of the best methods of assessing signal character is to measure a signal while flying radially or nearly radially toward or away from a station. Although it is the character of the phase behavior which is of primary interest, it is more convenient to measure amplitude. If only one

mode is present, both phase and amplitude will vary regularly. If there are competing modes, neither will vary regularly. Since accurate knowledge of position is needed to interpret phase measurements which vary through a complete cycle each wavelength, amplitude is examined as knowledge of position need be only approximate to support interpretation. As amplitude also varies temporarily one prefers to examine data measured while entire propagation paths remain dark. Abnormal variation of amplitude with distance from a transmitter suggests the presence of modal interference. A complication is identification of a region where a single mode may be dominate but not the mode usually prevalent and assumed for Omega. These areas may be inferred since they are contained within other regions where a modal interference boundary has been identified. They may also be inferred if fixed site temporal variations have been recorded. Since the usually-assumed dominant mode is expected during the day, an irregular temporal variation may indicate a change of modal dominance.

Interpretation of airborne amplitude recordings may be limited for a number of reasons including flight tangential to a station bearing instead of radially, poor signal reception, or other factors. One advantage of conducting the assessment with attention to theoretical coverage approaches is that this tends to validate the global coverage assessment methods themselves. Thus, confidence is gained beyond the simple agreement that may occur at a particular location and time. In this the detection of any unambiguous exceptions is particularly important. As Einstein observed, no number of experiments can prove a theory true, but it only takes one to prove it false. In interpreting records, mainly incompatibilities were noted. As theoretical coverage boundaries are defined to correspond with very nearly the maximum possible interference fades, interference was noted to occur on validation records at a somewhat less severe criterion.

Observed signal coverages are compared with exceptions on a station by station basis in the full report. Significant findings and deviations from expectations can be summarized according to phenomena as follows.

Signal-to-Noise Ratio limitations were generally about as expected. Whether the few deviations were due to abnormally favorable or unfavorable flight conditions or atmospheric noise at the particular time of flight cannot be determined. When flown, the Norway signal was observed to be better than expected in South Africa but worse in southern Australia. The Hawaiian 10.2 kHz signal exhibited a brief period of utility near South Africa as expected by the parametric coverage model, but which would not have been expected based on coverage overlays. North Dakota was received better in East Africa than expected, but Australia was weaker in the Arabian Sea than predicted.

Important modal interference limitations predicted for the region were mainly confirmed by the validation. This was demonstrated impressively by measurements of 13.6 kHz from La Reunion northeast of La Reunion. One of the most obvious features of the flights was the extensive modal interference on 13.6 kHz northeast of the station. This was observed on all flights where it would have been expected. As predicted, the region extends at least to Singapore (cf. Figure 1). This is a very much more extensive limitation than predicted or observed for equivalent 10.2 kHz signals. All in all, prediction of the 13.6 kHz limitations is a considerable triumph for full-wave theory and adds considerable credibility to all full-wave predictions.

One significant difference between published and observed coverage was observed. This occurred on the 10.2 kHz signal from Japan to Western Australia near Perth. Circumstances limiting the use of this signal are unusual and described in detail in full report. Three modes compete which leads to a situation in which coverage is limited near Perth, but not at either greater or lesser distances along the same radial. Further, in contrast to more usually prevailing conditions, coverage at 10.2 kHz is limited in this local region while coverage at 13.6 kHz is not.

A study of the near-field region surrounding the Australian station suggests that a land based study such as the survey conducted about North Dakota would be useful.

One unexplained variation was noted. The field strength of Norway exhibited an anomalous variation in the Bay of Bengal. It occurred on both

Flights 8 and 19 and can be associated with bearing from Norway rather than time of day. It is imperceptible at 10.2 kHz, noticeable at 11 1/3 kHz and marked at 13.6 kHz. This type of effect has not been observed before. It appears confined to a small geographic region.

All in all, individual station coverages were close to that which was, or should have been, expected.

SYSTEM COVERAGE:

In the previous section, the structural suitability of signals for navigation was assessed together with their adequacy with respect to atmospheric noise sources. This is a necessary but not sufficient part of determining system coverage. Additionally, it is necessary to determine the inaccuracies which may be induced in the phase measurements which will eventually be processed to obtain a fix. In this way the performance of an optimum receiver can be assessed.

The 10.2 kHz parametric model was shown in the previous section to predict modal boundaries reasonably well. By inference, the model can, thus, also predict the statistical effect on accuracy of a multimode signal environment where competing modes may cause errors but not lane slippage. Similarly, one expects the effects of noise to be statistically modeled reasonably well. Other errors include the inherent phase repeatability from day to day due to minor ionospheric differences, σ_r, and the predictive error, σ_p, due to inability to predict the long term average phase properly. The existing error budget has been:

TABLE I

ERROR BUDGET FOR 10.2 kHz PARAMETRIC MODEL

Path Illumination	σ_r	σ_p
Day	3 cec	4 cec
Night	5	4
Transition	4	15

We must now compare this error budget with actual observations in and around the Indian Ocean.

Fixed land based monitoring has long been conducted worldwide including the region. A subset of semi-monthly phase difference measurement blocks from sites in and around the Indian Ocean over a several year period was selected. This very large data base then was processed by the method used in the North Pacific validation. Of particular interest are cumulative statistics for the median random propagational variation, median "absolute phase error", and median "rms variation about the absolute phase error". Since two propagation paths contribute to a phase difference measurement, the random propagational variation so obtained is equivalent to $\sqrt{2}\,\sigma_r$ while $\sqrt{2}\sigma_p$ is equivalent to the rss combination of the other two terms. Estimates were made for 24-hours, "Day" and "Night". During the "Day", σ_r computes to be 2.6 cec while 4.1 cec is obtained at night or on a 24-hour basis. Obviously, the agreement appears to be excellent. However, there is an important difference. As used within the parametric model, "Day" or "Night" applies as the entire propagational path is illuminated or dark. In combining the *Indian Ocean ground* based statistics, "Day" was taken to be from 0500 - 0700 GMT while "Night" was 1700 - 1900 GMT. While these periods reasonably represent the region, they do not represent the component propagation paths forming a phase difference. By parametric standards, most of statistical entries in the cumulative tables represent transitional propagation conditions. Thus, the long established error budgets could be slightly conservative. The interpretive distinctions between "Day" and "Night" become much more important in comparing estimates of σ_p as the gross prediction bias during transitions can be expected to override the nominal "Day" and "Night" estimates. Computation yields σ_p = 9.2 cec (Day), 9.6 cec (Night) and 10.7 cec (24-hr). By comparison, a path or collection of paths undergoing transition one third of the time would be expected to yield an rms bias of 9.3 cec while one undergoing transition half the time would yield 11.0 cec. Since

the actual illumination mix has not been determined, the agreement can only be called nominal. However, the results are certainly compatible with the assumed budget.*

Day and night predictive biases also may be assessed through perusal of average phase difference errors measured for the semi-monthly data blocks under the appropriate illumination conditions. This was done manually for the various locations in and around the Indian Ocean to determine: 1) whether the nominal 4 cec error budget for predictive errors was realistic and 2) whether any particular stations/sites, or lines of position exhibited anomalous errors. Predictive biases over single paths appear about 4 cec or slightly less during the day and 4 cec or slightly more at night. No anomalous predictive biases were found.

Another estimate of phase measurement errors can be obtained from actual observations at sea on several merchant ships. These ships were especially instrumented with Magnavox MX 1105 receivers to provide meaningful comparisons of measurements from Omega with those from Navsat. Ordinarily, such comparisons yield only differences which cannot properly be attributed to one system or another. Whereas Navsat provides outstanding accuracy to a docked ship, accuracy degrades at sea. Should high ship dynamics result in large unknown set and drift, Navsat fixes may well be worse than those obtained with Omega. For the installations discussed here, merchantmen were operating on ordinary trade routes with very low dynamics. Further, speed and heading were automatically input to the Navsat equipment while special cubic spline smoothing was employed in making the fix comparisons. Under the arranged conditions, it is believed that usually most of the discrepancy can be attributed to Omega. To avoid complexity introduced by combining various lines of position to obtain a fix, the best comparison for the present

* Similar estimates were also made for 13.6 kHz, although the utility of these is somewhat moot as the parametric model is not yet extended to this frequency. Estimates of ρ averaged 10% higher corresponds to a 17% greater navigational precision because of the shorter wavelength. Estimates of r were markedly lower ranging from 2.1 to 3.8 cec. These suggest that in multi-frequency fixing, the 13.6 kHz accuracy will dominate.

purposes will be that of phase difference discrepancies between the various lines of position which can be measured and the Navsat indicated ship position. The median line of position error obtained from the median errors on each of several voyages from each of the several ships was 15.5 cec at 10.2 kHz. This suggests a typical instantaneous measurement error of $15.5\sqrt{2}$ = 11.0 cec over each of the component propagation paths which may by compared with the rss combination of σ_r and σ_p as measured over 24-hours at land sites, viz: $\sqrt{4.1^2 + 10.7^2}$ = 11.5 cec. Apparently, the observed phase discrepancies at 10.2 kHz at sea are in good agreement with those observed on land and, as previously shown, in agreement with the assumed error budget.*

It is not reasonable to attempt a similar comparison of airborne phase measurements. Although a Global Positioning System (GPS) receiver was carried, there were few periods of common operation. Further, asynchronism in the data recording could prove significant at aircraft speeds.

The foregoing and the previous sections indicate that individual station coverages at 10.2 kHz are well represented by the parametric model and further that the assumed error budget is reasonable. Therefore, accuracy forecasts based on the parametric model are credible in the Indian Ocean region. Figures 6, 7, 8 and 9, reproduced from the 1984 Seattle meeting of the International Omega Association, show accuracy expected from an optimal receiver using 10.2 kHz transmissions alone. They may be considered validated for the Indian Ocean. The figures show excellent accuracy at 0000 and 0600 GMT throughout the Indian Ocean while figures for 1200 and 1800 GMT show somewhat poorer accuracy in many areas with markedly worse accuracy at times in a belt from the Arabian Sea through Sri Lanka, the Bay of Bengal, Singapore, the Straits of Malacca, and into the South China Sea. Occurrence of periods of poor accuracy in this belt has long been recognized. It is nearly equitorial and signals propagated at night from the east cannot be used in this region because of modal interference. Those signals which are usable all arrive from the west and, therefore, present poor geometry. It is ironic

* The median discrepancy at 13.6 kHz was 11% higher indicating 17% higher accuracy capability using 13.6 kHz.

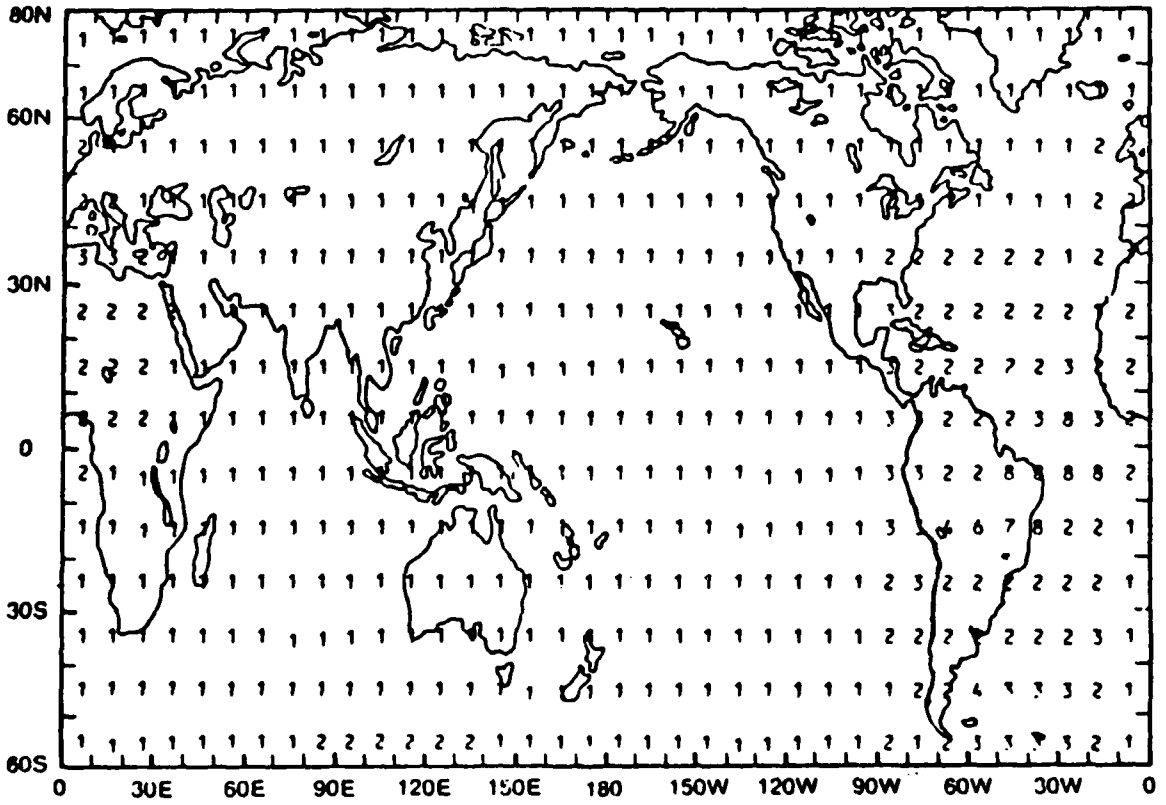

Figure 6. System Coverage at 0000 GMT (n.mi., c.e.p. using 10.2 kHz alone).

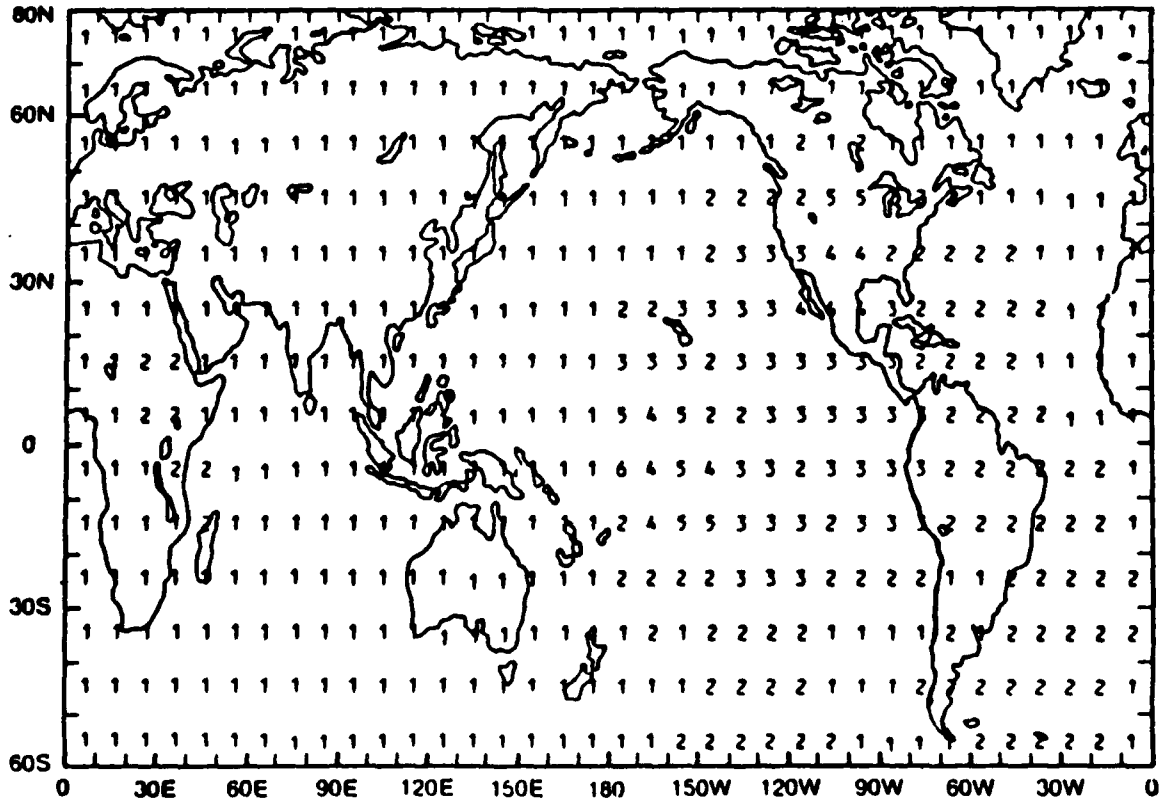

Figure 7. System Coverage at 0600 GMT (n.mi., c.e.p. using 10.2 kHz alone).

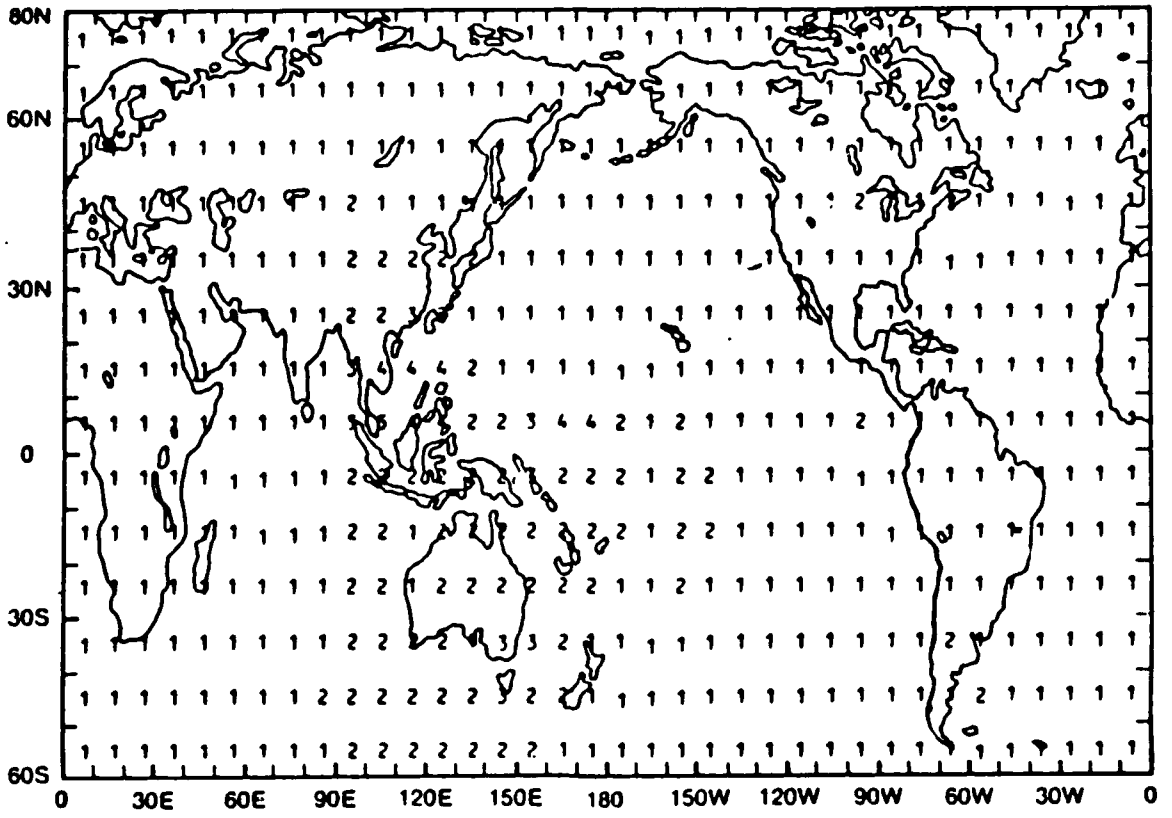

Figure 8. System Coverage at 1200 GMT (n.mi., c.e.p. using 10.2 kHz alone).

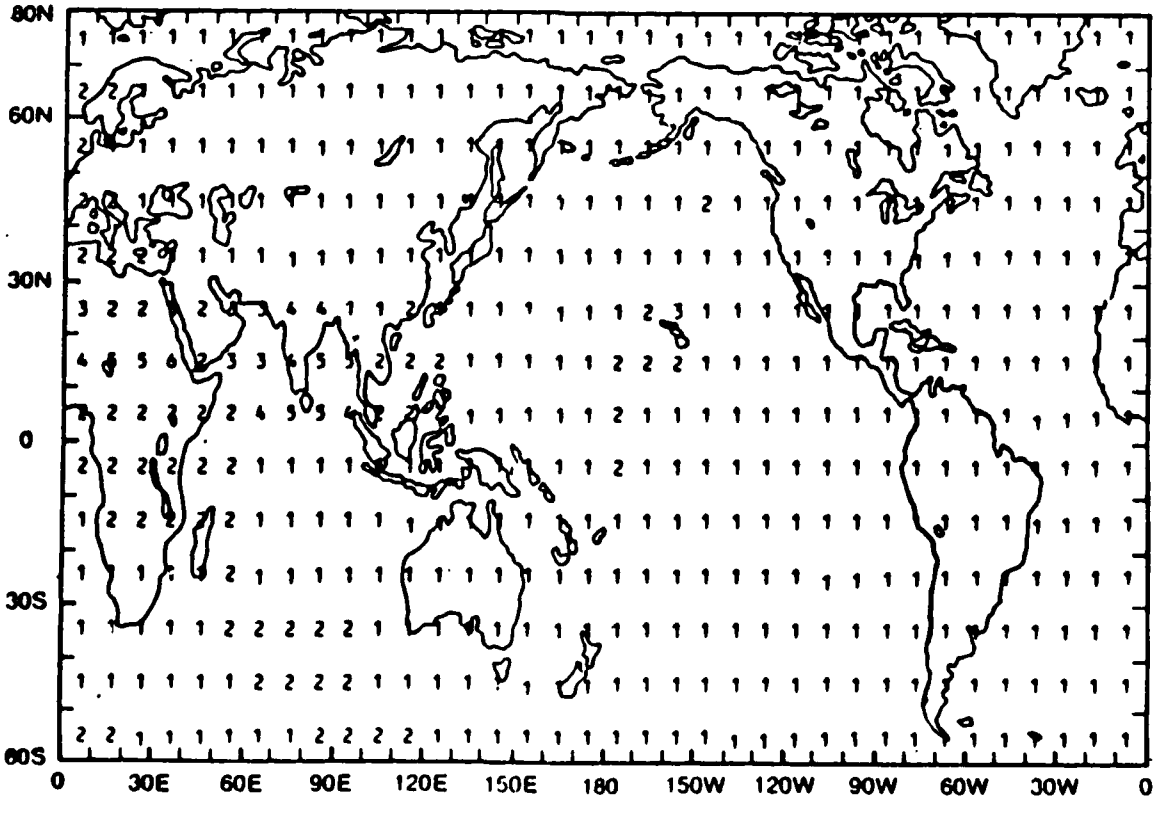

Figure 9. System Coverage at 1800 GMT (n.mi., c.e.p. using 10.2 kHz alone).

that the worst accuracy is located on the heaviest trade routes. The areas near Singapore and the Straits of Malacca warrant further study. Currently, use of Japan and Australia is precluded here because of modal interface. However, the boundaries are rather close and a detailed regional study might indicate it safe to use Japan or Australia in this important region. Additional data should be gathered during the forth-coming western Pacific validation.

Accuracy of an optimum multi-frequency Omega receiver is conjectural since the parametric model has not yet been extended beyond 10.2 kHz. Optimal use of 13.6 kHz would not be expected to help much in the belt of poorest accuracy since modal limitations on 13.6 kHz are even more severe than at 10.2 kHz. Certainly, however, the general accuracy would improve. In particular, in the unusual case where noise introduces significant inaccuracy, a four-frequency Omega receiver would have about twice the accuracy of a single frequency receiver.

Perhaps one of the more important results from this validation is the credence added to the parametric model itself. The model has many uses. It can be used as a tool for system analysis. Accuracy can be predicted not only for optimum conditions but for suboptimum conditions as well. An important set of suboptimal conditions is that arising from station outages. Validation of the parametric model also means particular receiver implementations can be emulated. The model may also be used to assess the potential accuracy from possible differential Omega installations. It is also applicable to assessing anticipated performance on proposed routes. Probably the important application will be incorporation of the model in receivers so as to improve accuracy and radically reduce the probability of rare large errors.

A traditional output from area validations has been a composite coverage diagram. Figure 10 shows such a diagram indicating the 10.2 kHz signals which are usable throughout the region. The boundaries primarily reflect nighttime modal limitations, but have been drawn with attention to other limitations as well. The navigator should select lines of position from the signals indicated with attention to geometry and station maintenance schedules. It is advisable to consult other coverage guidance to determine the types of limita-

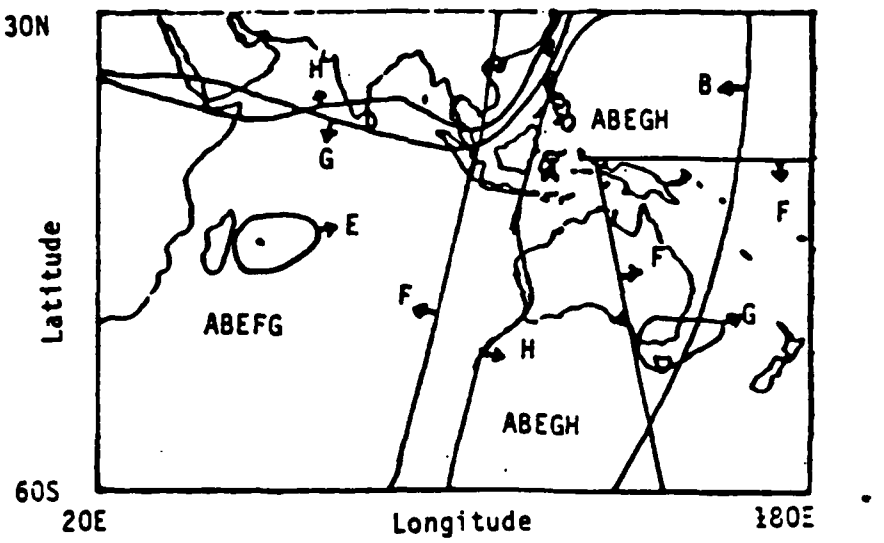

Figure 10. Preferred Stations for 24-hour Service

tions which may be expected at various times. For example, parametric individual station coverages for idealized day and night conditions will show the propagationally limiting conditions. Of the coverages indicated, Norway (A) may be weak at times in the southeast, but is usable if it can be received. Additionally, North Dakota (D) will provide usable, if occasionally weak, signals off South Africa. Also, North Dakota and Hawaii (C) will be occasionally useful in the northeast. Both Australia (G) and Japan (H) cover nearly the entire region during periods when the respective propagation paths are illuminated. "Daytime" long path limitations occur on Australia in the Red Sea and on Japan off East Africa as well as near-field limitations immediately around the stations. Some use of Argentina (F) in southwest Australia may be possible when Antarctica is dark.

The actual performance of widely-sold Omega receivers is of some, if tertiary, interest. The Magnavox MX 1105 receivers used at sea are combined Omega/Navsat units. Because of the way these receivers were being used navigationally, they provided valid phase errors but not true Omega fix errors. Thus, there are no shipboard fix comparisons.

One of the two airborne Litton LTN-211 receivers was allowed to operate in the usual way using a loop antenna. Unfortunately, the location of the aircraft was rarely known precisely when airborne even though the aircraft was

equipped with an Inertial Navigation System (INS) as well as a Global Positioning System (GPS) receiver. The GPS satellite "window" rarely occurred during flights and the receiver failed half way through the validation while the INS proved less accurate than the Omega sets. While detailed airborne accuracy assessment is not supported, gross performance experience can be noted. In nearly two hundred hours of flight time, neither receiver failed. This is consistent with the high mean time between failure (MTBF) expected for a mature commercial avionic product. Occasional in-flight inter-comparisons between the two Omega sets, often using different signals, or between either Omega and the INS suggests that fixes were never in error by much more than the errors on landing. This is particularly noteworthy when it is remembered that the flights were especially selected to investigate areas of modal interference.

When the aircraft was on the ground, it could be confidently located at least to an uncertainty corresponding to the size of the airfield. Table II shows the median accuracy obtained using the LTN-211 with loop antenna using three frequencies on takeoffs and landings. The table has been separated into two columns depending on whether the parametric coverage model for 10.2 kHz alone indicates an accuracy of about one mile or two miles or more for the particular location and time of each takeoff and landing.

TABLE II

LTN-211 MEDIAN ACCURACY

	Expected Accuracy	
	~1 nmi	≳2 nmi
Takeoff	1.1 nmi	0.7 nmi
Landing	2.1	4.9
Median	1.6	2.8

The overall median accuracy from the actual LTN-211 receiver using three frequencies is of the order predicted by the parametric model for an ideal receiver using 10.2 kHz alone. Looking in more detail, important differences

are noted. First, the takeoff errors are markedly less than those on landing. This may relate to the recent initialization and the long tracking time constants used by the LTN-211 on the ground. In this case the landing errors would be more valid. Secondly, too many large errors of over four miles were observed on landing. The occasional occurrence of larger errors is a matter of grave concern because of the possible impact on safety. An Omega receiver should be in error by more than four miles only very rarely. Large errors on landing occurred at Alice Springs (4.9 nmi), Nairobi (9.9 nmi), Singapore (5.0 nmi), Sri Lanka (6.4 nmi), Khartoum (7.6 nmi), and Melbourne (6.4 nmi). Of these, only the errors at Singapore and Sri Lanka can be reasonably attributed to the possible effects of poor signal availability and geometry. It is speculated that the other four may have been the result of poor signal utilization within the LTN-211. The only coverage guidance incorporated in the LTN-211s used was that for 10.2 kHz as guidance for 13.6 kHz was published less than two months before the start of the validation. Two of the landing errors, Alice Springs and Melbourne, could have resulted from using inappropriate near-field criteria from Omega Australia at 13.6 kHz compared with that for 10.2 kHz. Comparison of nighttime modal interference differences between 10.2 kHz and 13.6 kHz suggests that it would almost have been surprising if there were not large landing errors at Khartoum and Nairobi. For the flight to Khartoum, major coverage differences between 10.2 kHz and 13.6 kHz were theoretically indicated for stations B, C, E, and H, while for the flight to Nairobi differences occur on B, E, and G. Although coverage differences could have led to improper signal utilization and, hence, large landing errors at several other sites, it is speculated that redundant processing techniques within the LTN-211 prevented large errors elsewhere. All in all, the few large landing errors seem to provide graphic examples of the need for validation and coverage guidance.

Operationally, during flights especially selected to study modal interference, tracking and navigation were continuous throughout the entire region. The error on landing was always less than 10 miles. Use of proper coverage guidance could probably have reduced or eliminated the few larger errors. Typical accuracy was probably about two miles. Although the LTN-211 software can and is being improved, the actual navigation experienced represents a considerable accomplishment.

CONCLUSIONS

By far the most important result of the validation was the demonstrated correspondence between theory and measurement. Even the modification of the Japanese coverage boundary in west Australia was reflective of clerical limitations in originally drawing the boundary rather than limitations of full-wave propagation theory. Full-wave overlays for both 10.2 and 13.6 kHz were well supported as was the parametric coverage for 10.2 kHz. Coverage studies and the validation process have combined to render the system as an entity much better understood now than it was a few years ago.

Theoretical calculations indicate an accuracy capability of 2 nmi (c.e.p.) or better throughout the region on a 24-hour basis with the unfortunate exception of the trade routes from the Red Sea, around the tip of India, through the Straits of Malacca, and up to the South China Sea. When signal paths from Australia and Japan are both dark, about 1500 GMT, there is a small region directly astride the trade routes where neither Australia nor Japan can be used and the usable stations provide poor geometry. Fix accuracies as poor as about 5 nmi (c.e.p.) may then occur. However, intensive additional study of this small region is warranted. Installation of Differential Omega may be desirable. Uncertainties in the boundary locations are such that either Australia, Japan or both may actually prove usable.

Performance of the LTN-211 flown on the validation flights was noteworthy: both for what it did right and what it did wrong. On the positive side, the set navigated continuously throughout the entire validation effort maintaining a median accuracy of about two miles. Considering the duration of the test, miscellaneous intervening Omega station outages, various weather conditions, and the fact the flights were deliberately planned to investigate problems, this level of system performance and robustness is exemplary. Comparison with other aids indicated that no truly gross errors ever occurred. However, a few larger (but less than ten mile landing errors did occur. At least some of these apparently resulted from inadequate coverage guidance being incorporated into the LTN-211 at the time of the validation. The exceptions emphasize the need for coverage guidance.

Begin Full Report

INTRODUCTION

For some years the Omega Navigation System Operations Detail (ONSOD) has assessed the utility of signals through a series of regional validations (Doubt, 1984). Previous efforts have included the South Pacific (Karkalik, et al., 1978), North Atlantic (Campbell, et al., 1980), North Pacific (Levine and Woods, 1981) and South Atlantic (Watt, et al., 1983). The report presents the results from the validation of the Indian Ocean conducted in 1983.

Over the years, the Omega validation program has evolved into a corrdinated sequence of geographic "validations" where intensive resources in both instrumentation and analysis are applied to determine Omega coverage. Functionally, the process is a traditional one in the establishment and operation of navigation aids. Presumably there was a "validation" program of some type to assure the effectiveness of the first radio beacon. More recently Loran-C has undergone "calibrations". The Loran-C efforts and Omega validations share the characteristics that not only is the signal availability and utility in an area determined, a data base is also gathered from which the essential phase characteristics of the signals can be better calibrated and, hence, used in the future. Loran-C or Omega regional validations or calibrations are essentially single efforts to be conducted once. This is in contrast to the periodic measurement and re-certification conducted on airport approach aids by the Federal Aviation Administration (FAA). FAA aids are at much higher frequency and their performance can be effected not only by slow equipment aging but, also, by unrelated new construction near airports which can change the radio field through introducing reflections. For both Omega and Loran-C, a few well placed monitors are sufficient to determine any slow changes which may occur. Additionally, localized programs may occasionally be warranted. One example is the effort conducted by the U.S. Coast Guard and SERCEL prior to installing differential Omega beacons. Another example of particular relevance to this validation would be intensive investigation of Omega coverage near Singapore and the Straits of Malacca. This is an area of very heavy deep draft marine and air traffic. It is also an area where Omega coverage is not only poor but difficult to assess. Local long term assessment with attention to seasonal changes is warranted. Use of Differential Omega should be considered.

Whereas past validation efforts have made use of such predictions as may have been available, this validation analysis is strongly coupled to the now

existing theory. This is in consonance with the multiple goals of a validation effort:

1. Characterize signal coverage in the region. That is, define the radio physics and signal environment in which an Omega receiver must operate.
2. Determine potential Omega accuracy using an idealized receiver.
3. To a much lesser extent, obtain an estimate of the accuracy of present Omega equipment.

The de-emphasis on present equipment functioning is important and essential to a system validation. Accuracy can improve as software is improved based on better understanding of signal characteristics; thus, the de-emphasis on actual performance of equipments during the evaluation itself.

It is noteworthy that this is the first evaluation for which signals from all eight Omega stations, including Australia, have been available.

OVERVIEW

This report is divided into six sections:

1. Overview
2. Coverage Theory
3. Equipment Deployment
4. Spot Comparison: Theory and Observation 1800 GMT
5. Individual Station Coverage Analysis
6. System Coverage and Error Characterization

supplemented by three appendices:

A. Amplitude Prediction
B. Individual Station Coverages at 10.2 kHz at Specified Times
C. Alternative Coverage Analysis

The text has been written primarily for completeness and is necessarily lengthy. A full reading of the report will eliminate any need to read the abridged report which is a proper abridgement and does not introduce additional material. However, illustrations appearing in the abridgement also have not been reproduced in the main body. Page and figure numbers in this document follow the convention that a single number refers to the abridged report section while a compound number, such as 1-1 refers to a particular page or figure in the specified section of the main body, e.g., Section One, Figure 1.

Section 2, Coverage Theory, contains two major portions. The first is a general discussion of what is meant by "coverage" and introduces the three major coverage methodologies: overlay, parametric and local. This first section is equivalent to material contained in the adbridgement. A second section discusses fix mathematics in detail. Specifically, it reformulates work originally published by Lee in a manner more appropriate to Omega coverage prediction. Although the reformulation has been in use in parametric coverage prediction for some years, it has not previously been published. A complete local coverage assessment was also conducted but is not considered as credible as the parametric or overlay assessments. It has been incorporated into an Appendix (C) primarily for completeness.

Section 3 decribes the equipment and its deployment. It describes the airborne equipment in more detail than the equivalent section of the abridged report. Additionally, brief descriptions of fixed site and shipboard instrumentation is included.

Section 4, Spot Comparison: Theory and Observation at 1800 GMT, is equivalent to that in the abridgement except that full quantative comparison tables are developed instead of simply stating the results.

Section 5, Individual and Station Coverage Analysis, differs substantially from the equivalent section in the abridgement. Both sections provide the same general introductory comments but the abridgement proceeds to an immediate summary of coverages by type of limitation. The full sections belabors coverage from each station in detail. Additionally, more background and rationale is provided on the methodology of deducing Omega coverage from airborne radial measurements of signal amplitude.

Section 6, System Coverage and Error Characteristics, and the report conclusions are identical between full report and abridgement.

Appendix A, Amplitude Prediction, contains a comparison of 10.2 kHz measure amplitude with predictions obtained from the amplitude prediction model used in the program to make parametric coverage maps. The compiled amplitudes come from a variety of sources but, combined, form a credible data base of precise measurements.

Appendix B, Individual Station Coverages at 10.2 kHzx at Specified Times, presents a full set of parametric predictions for individual station coverages at 0000Z, 1200Z, and 1800Z at the vernal equinox. These were prepared in conjuction with other illustrations presented here and in Swanson (1984) but have not been published as a complete set. They proved useful in evaluating the specific stations coverages discussed in Section 5.

Appendix C, Alternative Coverage Analysis, provides the complete results of a coverage assessment using the "local" method as was originally developed and applied to assess coverage in the North Pacific. It is not considered as credible as the parametric coverage assessment in this region but is included as an appendix since the method has been used in a previous validation.

Extensive references are provided. Three Data Supplements augment this report. They are not usually specifically referenced in this report itself but are listed on page R-6.

2. COVERAGE THEORY

COVERAGE FUNDAMENTALS:

The term "coverage" requires amplification. The fundamental measurement in Omega is that of the phase of a radio signal and the essential expectation is that changes of phase can be related to changes of position on the ground. An additional requirement is to measure the phase in a timely fashion in the presence of noise. In practice the signal level, that is, Signal-to-Noise Ratio (SNR), is almost always adequate to permit timely phase measurement. As can be seen by perusing the detailed station coverage diagrams, most Omega signals can be received at almost all locations almost all of the time. The few exceptions are primarily due to the "shadow" effect of regions of extremely high attenuation such as Greenland and Antarctica. The critical problem is that the structure of the signals may not permit navigation. That is, a signal may be of high amplitude but the structure itself renders the signal unsafe for use. A particularly dangerous aspect of this structural limitation is that there is no way by which a receiver can necessarily identify such signals based on their characteristics as received. A priori guidance on usage is a major reason for undertaking validation in general and developing coverage guidance in particular.

Phenomena leading to an unsuitable signal structure have been referred to as "self-interference". That is, energy propagates from transmitter to receiver by a desired modeled mechanism and various other interfering mechanisms as well. Self-interference is recognized to occur near transmitters roughly equivalent to the skywave-groundwave interference experienced with other systems. Additionally, Omega coverage models recognize an interference near the antipode of a transmitter where energy can arrive from all directions. Other self-interference phenomena include long path interference wherein the signal propagated over half way around the world dominates that received over the shorter path, and "modal" interference.

Omega propagation may be best viewed as occurring within a spherical waveguide formed between the earth and the ionosphere. During daytime illumination conditions, the waveguide may be rather simplistically represented. The signal field may exhibit some complexity "near" transmitters, but after a short distance, a single mode will dominate and, therefore, phase will vary regularly with distance. The "first" is that which

will be present during the day and that for which the Predicted Propagation Corrections (PPCs) were developed.

At night propagation may be very much more complex and the full interaction of the Omega signals and the ionospheric magneto-plasma needs to be considered. Various propagation modes may be supported and "modal interference" may extend over large regions. Primarily in response to strategic communications requirements, the Naval Ocean Systems Center (NOSC) has spent tens of millions of dollars developing computer models which properly represent the interaction. The Analytical Sciences Corporation (TASC) has spent millions more applying the models to Omega. These full-wave computations form the basis of all modern coverage studies. The computer model provides guidance on how the Omega signal structure may vary in space or time which may then be verified or modified by a validation effort.

There are three coverage approaches of importance to the present validation: 1) overlay, 2) parametric, and 3) local. Key aspects follow.

The overlay method of presenting coverage information was the first of the methods employed. Initially, coverage for a single station at a single idealized day or night propagation condition was computed. These were originally done only at 10.2 kHz but have since been extended to 13.6 kHz. Figure 1 is an example showing modal interference regions for La Reunion at both 10.2 and 13.6 kHz. Signal-to-Noise contours also were computed and regions free of modal interference and where the SNR exceeded a threshold were identified as providing good coverage. Coverages from the eight stations at the particular idealized illumination condition were then overlayed to obtain "spaghetti" diagrams to explicit system coverage. Figure 2 shows an example reflecting later extensions to a particular time of day. The overlay approach does have some advantages. The spatial extent of coverage limitations as shown, for example, in Figure 1, provides an excellent starting point from which to plan validation efforts. (It further illustrates the need for elaborate computations as one would not otherwise expect the extreme difference in coverage between 10.2 and 13.6 kHz northeast of La Reunion). Individual station coverage diagrams, e.g., Figure 1, or the composite diagrams, e.g., Figure 2, can also be used by a navigator to determine useful

signals. Further, the coverage boundaries readily can be identified during a validation and boundaries moved if necessary. However, overlays are severely limited in several ways--particularly in predicting the accuracy to be provided.

The parametric and local approaches both employ apparently equivalent optimal weighting by which potential accuracy can be deduced if all signals are used to best advantage. That is, poor signals providing good geometry are properly "traded-off" against good signals of poor geometry. Additionally, the parametric approach incorporates a modeling of Omega propagation parameters which is compatible with the processing now done within modern receivers to compute PPCs. Although currently developed only for 10.2 kHz, results from the parametric approach have been used at least equally with overlays in this validation. The parametric approach provides two outputs: (1) Individual stations coverages are produced in a form where various types of signal limitations are indicated and the nature of the limitation shown, e.g., Figure 3. and (2) System coverage maps show accuracy to be obtained throughout the world at various specific times or alternatively computed throughout the 24-hour day (cf. Figure 4). The parametric formulation is quite powerful in providing coverage guidance, but lacks the ease of making local adjustments inherent with overlays.

The local method was developed specifically to obtain a measure of optimum system accuracy in a validation region. It has been previously used only in the north Pacific validation. While this method and the parametric both incorporate an appropriate combinational optimization, the methods of characterizing the errors and coverage are quite different. Although the local method has been fully applied to the validation and is discussed in Appendix C, the results are believed less credible than those from the parametric approach.

STATION vs. SYSTEM COVERAGE:

There is an inherent duality in addressing coverage. One may be referring to signal coverage from a particular transmitter or one may be referring to navigational coverage provided by the navigation system as an entity.

The system user is concerned with the quality of the navigation which will be available to him. This is measured in terms of typical accuracy, probability of large error, equipment reliabilities, etc. Of these, maps showing anticipated accuracy are most desired.* Often a series of maps may be produced to account for seasonal, diurnal, or other variations.

Navigation system experts will be concerned with the specific operation of the various component parts of navigation systems. These include both receivers and transmitters. A specific concern is the ability of the transmitter to radiate a signal which may be received and usefully interpreted by a receiver. That is, individual station coverage is of interest to the navigation system expert in optimizing performance of the navigation system as a whole. Individual station coverages may be viewed as tools for the system expert in much the same way as reliability studies balancing performance of antenna systems, tuning facilities, transmitters, and commercial power availability. Whereas the user does not need to care what caused an outage, the details are of intense interest to the system engineer who is trying to affect improvements.

It is becoming increasingly important to keep a proper functional distinction between the needs of the navigator and the needs of the navigation system expert. Not too long ago the navigator himself was often an integral part of the fix reduction process. To a substantial extent, the navigator was also the "system" expert. In some areas this duality continues to exist. For example, celestial navigation requires the navigator shoot the stars, perform the reduction, and plot the fix himself. In the process, he develops a "feel"

* Arguably, a more important measure is the probability of having an error greater than some prescribed value, such as the width of a traffic corridor. Safety is more associated with the probability of unusual large errors; fuel savings is, however, related more to typical accuracy.

for such individual measurement errors as may have occurred due to ship's motion or poor visibility and the effect of these errors on the "system" in terms of the divergences of fix triangles plotted on a chart. The navigator thus possesses a sense of the fix accuracy (indeed he even knows the direction of the error ellipse) when it comes time to determine a safe course for conning the ship. As equipment becomes increasingly automated, it is important that this fundamental sense of fix accuracy and reliability continue to be provided to the navigator. It will no longer be provided by the fix reduction process itself; it must be specifically provided by the navigation system expert.

In the case of Omega, the situation is further exacerbated by the redundancy of useful inputs available to a good receiver. It has been shown statistically that there is about a 50/50 chance of useful signals being available from 7 of the 8 Omega stations (Swanson, 1984b). Considering each station radiates time shared transmissions at four frequencies, this implies a tremendous amount of navigationally useful information. The navigator cannot reasonably be expected to consider the possible permutations, combinations, and weightings of signals as may occur within a modern receiver. He must be given functionally useful guidance on anticipated performance in terms he can understand and apply: e.g., accuracy measured in nautical miles.

The foregoing does not mean there is no need for indivudual station coverage studies. There is still a need for these by system experts as they more closely depict the physical limitations and provide a good vehicle for refining system knowledge and developing better coverage displays for users. However, except for a few users of older receivers. navigators should not be burdened with coverage overlays. Such an approach forces users to become system experts. There are two problems with forcing users to become system experts. The first is that the users are already busy and car best use time elsewhere. The second is the level of training necessary for them to be able to use the systems safely. It is far better that the user be provided with accuracy information in immediately useful terms.

HISTORICAL PERSPECTIVE

It may be no editorial exaggeration to assert that the coverage of radio navigation systems is studied from before they are implemented until the day they are turned off...and possible afterward. Certainly studies of the accuracy to be expected from Omega or its predecessor systems has been conducted from the initial proposal for Radux by J. A. Pierce (1947). Pierce also included results of a systematic study of individual station coverages for proposed station sitings in the first report of the Omega Implementation Committee (Pierce, et. al. 1964). Unfortunately, neither Pierce's approach or any other documented systematic approach was followed in actual station sitings. The first map showing anticipated accuracy capbility of the then exising Omega net was by Swanson in 1963.

A problem with all early work on coverage was an inherent misunderstanding of the importance of modal interference. Early system tests were conducted using transmitters located variously in Hawaii; San Diego, California; Whidbey Island, Washington; Forestport, New York; Balboa, Panama Canal Zone; Criggion, U.K.; Aldra, Norway; and Trinidad. While geographically diversified in many ways, these sites all lie in a range of geomagnetic latitudes from about 22 to 68°, that is, in a belt which would correspond to the temperate latitudes if it were geographic. More importantly, modal interference is particularly important near the equator. Except for what turned out to be critically important ionospheric propagational considerations, nothing exceptional was expected near the equator. That is, ionospheric height was expected to differ little* from that in the temporate latitudes while ground conductivities were similar to those experienced at the temporate latitudes. This was a different circumstance from that expected in the Arctic (and Antarctic) where the ionosphere was known or expected to be substantially different from that elsewhere due to particles entering at the auroral zone and potential chemical effects due to prolonged illumination or darkness. Further, ground conductivities in the Arctic were known to have marked effects on vlf signals. Contributing to an experimental emphasis in the Arctic and temporate latitudes was system geometry. Early arrangements provided good fixing over

* Possibly some differences could exist from the influence of the equatorial electrojet.

much of North America and the North Atlantic Ocean and also over the Arctic; they did not support position fixing near the equator. Thus, circumstances and known problem areas were both such as to result in minimal equatorial experience prior to the system being declared in Interim Operational Status.

The foregoing is not to say that the potential for propagational problems at night near the equator was not recognized technically, nor that nothing was done to attempt to investigate equatorial progagation within the constraints of the existing system. Geomagnetic limitations in the data base were recognized early. Further, it was recognized that spherical geometry leads to much of the world being located near the equator while little is near the poles. The Navy Electronics Laboratory (NEL, now NOSC) gathered data in North West Africa using ships of opportunity. In 1966-67 extensive data were gathered in South America under Federal Aviation Administration (FAA) sponsorship following earlier less extensive work by the Naval Research Laboratory. These measurements were primarily line-of-position propagational measurements rather than fixing measurements due to the system geometry. Further, they were restricted to less than a dozen sites. As Einstein once observed, no number of experiments can prove a theory right, but it only takes one exception to prove it wrong. Unfortunately, the exception was simply not observed.* Thus, technical concern over the adequacy of the geomagnetic diversity reflected in the data base compounded by an increasingly theoretical case on the complexity of propagation under equatorial conditions was not supported by one solid observation of Omega signals.

It was not until 1967 that Pappert, Gossard, and Rothmuller published the first theoretical paper to report results of a program on vlf propagation which fully allowed for earth curvature, ionospheric inhomogeneity and anisotropy (Pappert, et al. 1967). This "full wave" program has proven to be

* In hindsight this is not too surprising. Equatorial limitations are only severe at night and on azimuths to the west. The few circumstances which might have shown problems presumably exhibited constructive interference so that the observed phase differences were not far from that expected from a simple first mode dominant model. Detailed transitional complexities at sunrise or sunset which might have shown interference could not be ambiguously interpreted because of low radiated power, e.g., 185 watts from Forestport.

a critical development in the evolution of Omega coverage studies. In its initial form, however, it was hard to run. Skill was required to be certain that all significant propagation modes had, indeed, been found. Also, needed geophysical input such as electron density profiles were not as well known as they are now. These factors acted to produce prudent skepticism when results differed significantly from expectations using long standing simplistic models. While confidence developed over a period of years, Omega implementaion decisions continued to be made based on older overly simplistic ideas. Even as the theoretical model acquired credibility from many successful predictions at other frequencies, there remained no unambiguous Omega data showing exceptions to expectations based on more simplistic ideas. From a management view, there was little reason to change course.

Over a period of years, intrinsic propagational coverage limitations were recognized as of importance and studies of individual station coverage limitations were conducted. Initially these systematically applied NOSC developed extensions of the original full wave program to produce "radials" showing anticipated field variation at 10.2 kHz moving outward from stations along various azimuths (Gupta, 1975). This worked progressed by stages then producing coverage maps for 10.2 kHz under idealized day and night conditions (Gupta et al. 1980a; Gupta et al. 1980b) and later extended the work to 13.6 kHz still under idealized conditions (Gupta and Morris, 1983). Later this work was extended to specific (GMT) times of the day (DMA, 1981; Gupta and Morris, 1984; Gupta et al, 1985). As previously noted, these approaches have advantages for the expert in that they closely conform to the physics of propagational limitations. They suffer in not providing a clear idea of the accuracy to be obtained.

More recent work combines realistic parameterizations of propagational limitations with optimal fixing arithmeic to produce realistic maps of system coverage, in nmi anticipated fix accuracy. This work is described in more detail in the following section.

FIX MATHEMATICS

It is necessary to explore the mathematical foundations of optimum fixing using redundant information as is offered by Omega. As noted earlier, this is necessary not only to develop an optimum receiver but also to intelligently assess Omega capability inasmuch as there is no limit to the number of ways in which information can be combined suboptimally. Fortunately, two excellent theoretical works have been published within the last decade or so.

Lee (1975a, 1975b) published papers addressing the problem of obtaining an optimum fix from a hyperbolic multilateration system such as Omega, while later Levine and Woods (1982) published a derivation especially considering the need for optimum Omega fixing. Both works are just short of mandatory reading for the serious student of radio navigation systems. Since the works differ substantially in style, a comparison of the two works may be in order. A good way to introduce the comparison is to compare the backgrounds of the two principal authors. Both hold degrees from MIT. However, Lee obtained his doctorate there in electrical engineering while Levine obtained his doctorate at CALTECH in theoretical physics. To a substantial degree, the derivations reflect these difference in training. Lee's work is structured within the general notation of optimal estimation. Critical insights derive from the properties of matrix identities. Levine's work has a straightforward approach executed with clarity. Statistical optimizations and ensemble averaging are done explicitly with attention to requirements, if any, of the underlying statistical distributions. Despite the perhaps greater clarity of the Levine work, a summary of the Lee work will be presented here. There are two reasons for this apparently perverse choice. First, Lee's work is the immediate antecedent of an assessment of optimal Omega accuracy by Thompson (1977) which is in turn the antecedent of recent work by Swanson (1983, 1984a) used as a basis of accuracy assessment in this report. Secondly, Lee develops a unique insight wherein system accuracy can be likened to moments of inertia in a center of mass coordinate system wherein each radio signal source has an associated "mass" related to the associated information quality. As will be seen, this insight is extremely powerful once grasped. Further, as moments of interia are well understood, programming becomes very straightforward by analogy. Except as noted, the following is an abridgement of Lee's 1975 paper but characterized explicitly for Omega.

We consider N signals propagated from each of N stations over paths of

length d1, d2, ... as shown in Figure 2.1.

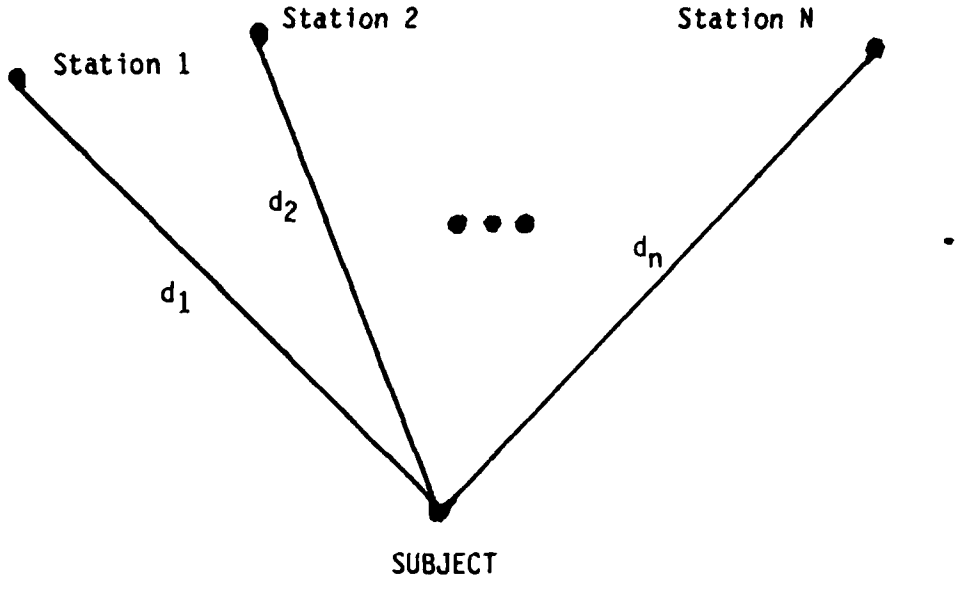

Figure 2-1. Problem Geometry

The phase (or phases) over each path can in principal be processed to obtain equivalent times of arrival (TOA) over each path.

$$t_1 = T_1 + d_1/c$$

$$t_2 = T_2 + d_2/c$$

$$\vdots$$

$$t_N = T_N + d_N/c \qquad (1)$$

where

t_j = the TOA of the signal from the jth station

T_j = the (unknown) time at which the signal was transmitted

d_j = the distance from the actual position of the jth station to the (unknown) position of the subject

c = the signal velocity

In principal Omega is synchronized so that $T_1 = T_2 = \ldots = T_j = T_0$. That is, all transmissions may be treated as though they occurred at some common time T_0 which, however, is not precisely known at the receiver. Thus, in principal, the receiver position can be determined by expressing the d_j in terms of the (known) station coordinates and the (unknown) receiver coordinates and solving (1) for the receiver coordinates and T_0.

In practice, the exact values of the quantities t_j, and d_j in (1) are not available. Instead, approximations t_j^* and d_j^* of t_j and d_j are available as follows:

t_j^* = the measured TOA of a signal or signals from the jth station

d_j^* = the distance from the assumed position of the jth station to the (unknown) position of the subject.

The quantities t_j^*, T_0, and d_j^* are not related by (1). Instead, t_j^*, T_0, and d_j^* satisfy the following equations:

$$t_1^* = T_0 + d_1^*/c + \epsilon_1$$

$$t_2^* = T_0 + d_2^*/c + \epsilon_2$$

$$\vdots$$

$$t_N^* = T_0 + d_N^*/c + \epsilon_N \qquad (2)$$

where ϵ_i is an error term that accounts for TOA errors due to such factors as:

Omega ground station synchronization

environmental noise

signal self interference
day to day phase variability
long term prediction bias
anomalous propagation
instrumentation error
local electromagnetic interference and platform noise, etc.

Since the errors ϵ_j are normally not known, the subject position cannot be determined exactly. Instead, the position can only be approximated (estimated) from (2) with the accuracy of the approximation depending upon the magnitudes of the errors ϵ_j.

Error Assumptions

Throughout it is assumed that the errors ϵ_j can be modeled as uncorrelated zero-mean random variables. That is if $\bar{\epsilon}$ denotes the vector of errors ϵ_j.

$$\bar{\epsilon} = \begin{bmatrix} \epsilon_1 \\ \epsilon_2 \\ \cdot \\ \cdot \\ \cdot \\ \epsilon_N \end{bmatrix} \qquad (3)$$

then it is assumed that

$$E[e] = 0 \qquad (4)$$

where E denotes expectation. Moreover, it is assumed that the covariance matrix P_ϵ of the ϵ_j takes the form

$$P_\epsilon \triangleq E(\epsilon \epsilon')$$

$$= \begin{bmatrix} \sigma_1^2 & & \mathbf{0} \\ & \sigma_2^2 & \\ & & \ddots \\ \mathbf{0} & & \sigma_N^2 \end{bmatrix}$$

where the prime denotes transposition. In considering the general multilateration problem, Lee noted: "The assumptions (4) and (5) appear reasonable for many applications, provided the TOA's are precorrected for mean anomalies of the signal propagation medium [6], [7], [9]". In the specific case of Omega, the nature of the error sources indicates that many important errors will be uncorrelated. Others, such as long term prediction bias, will be unknown but fixed and therefore "correlated" at any given location. Inclusion of predictive biases within the error budget is essentially equivalent to considering an ensemble of fixes all of which are based on the same type of predictive methods with each having errors characteristic of the preditive model but not the specific location. Implications of this will be discussed in a subsequent section on model limitations.

Equations for TOA Differences

Although unnecessary from the viewpoint of determining receiver position, it is customary to eliminate the unknown T_0 from (2) prior to determining (estimating) position. The elimination can be accomplished in many ways. For present purposes, it is assumed that T_0 is eliminated by subtracting each equation from its predecessor*. The resulting system of N-1 equations takes the form

$$t_1^* - t_2^* = (d_1^* - d_2^*)/c + (\epsilon_1 - \epsilon_2)$$

$$t_2^* - t_3^* = (d_2^* - d_3^*)/c + (\epsilon_2 - \epsilon_3)$$

$$\vdots$$

$$t^*_{N-1} - t^*_N = (d^*_{N-1} - d_N^*)/c + (\epsilon_{N-1} - \epsilon_N) \qquad (6)$$

* The results obtained in subsequent sections are valid regardless of how T_0 is eliminated. cf. (Lee, 1975a).

Note that the error terms in (6) can be expressed as follows in matrix notation:

$$\begin{bmatrix} \epsilon_1 - \epsilon_2 \\ \\ \epsilon_{N-1} - \epsilon_N \end{bmatrix} = H\epsilon$$

where ϵ is given by (3) and

H = a $(N-1) \times N$ matrix of the form

$$\left.\begin{bmatrix} 1 & -1 & 0 & \cdots & 0 & 0 \\ 0 & 1 & -1 & \cdots & 0 & 0 \\ & & & \ddots & & \\ 0 & 0 & 0 & \cdots & 1 & -1 \end{bmatrix}\right\} N-1 \text{ rows} \qquad (7)$$

$\longleftarrow$ N columns $\longrightarrow$

Consequently, the covariance matrix P_Δ for the error terms in (6) can be expressed in terms of that for the ϵj as follows:

$$P_\Delta = E\left\{ \begin{bmatrix} \epsilon_1 - \epsilon_2 \\ \vdots \\ \epsilon_{N-1} - \epsilon_N \end{bmatrix} \begin{bmatrix} (\epsilon_1 - \epsilon_2) & \cdots & (\epsilon_{N-1} - \epsilon_N) \end{bmatrix} \right\}$$

$$= E\left\{(H\epsilon)(H\epsilon)'\right\}$$

$$= HP_\epsilon H'.$$

Positional Errors with Optimal Processing

Let R be (2 x 1) vector that specifies the actual subject position in a tangent plane on the surface of the earth. A number of different methods exist for "solving" the TOA equations (6) for R.* Each method can be viewed as defining a (2 x 1) vector function (estimator)

$$R = f(t_1^*, t_2^*, \ldots, t_N^*)$$

that approximate R, given the values t_1^*, t_2^*, ... t_N^*.

The linearized least-squares procedures is one such method. The procedure involves linearizing the TOA equations about a point sufficiently close to the subject so that the linearization error are negligible compared to the rms TOA errors σ_1, σ_2, ..., σ_N. The subject position R relative to the reference point is then approximated by the vector R that minimizes the quadratic error measure

$$Q = \left[(\epsilon_1 - \epsilon_2)\cdots(\epsilon_{N-1} - \epsilon_N)\right]\left[P_\Delta\right]\begin{bmatrix} \epsilon_1 - \epsilon_2 \\ \epsilon_2 - \epsilon_3 \\ \vdots \\ \epsilon_{N-1} - \epsilon_N \end{bmatrix}$$

$$= (H\ )'P^{-1}(H\ ). \qquad (8)$$

The linearized counterparts of (6) take the form

* See Bancroft (1985) for a recent discussion on solution or a more generalized form.

$$t_1^* - t_2^* = 1/c(\delta_1^* - \delta_2^*) + 1/c(i_1 - i_2)\bullet R + (\epsilon_1 - \epsilon_2)$$

$$t_2^* - t_3^* = 1/c(\delta_2^* - \delta_3^*) + 1/c(i_2 - i_3)\bullet R + (\epsilon_2 - \epsilon_3)$$

$$\vdots$$

$$t_{N-1}^* - t_N^* = 1/c(\delta_{N-1}^* - \delta_N^*) + 1/c(i_{N-1} - i_N)\bullet R + (\epsilon_{N-1} - \epsilon_N) \qquad (9)$$

where

δ_j^* = the distance from the assumed position of the jth beacon to the reference point

i_j = (1 x 2) unit vector pointing from the subject to the jth beacon (see Fig. 2.2)

R = (2 x 1) vector specifying the subject position relative to the reference point (see Fig. 2.2).

It is assumed that the vectors i_j and R are expressed in terms of a convenient Cartesian coordinate system (X', Y', Z') centered at the subject.

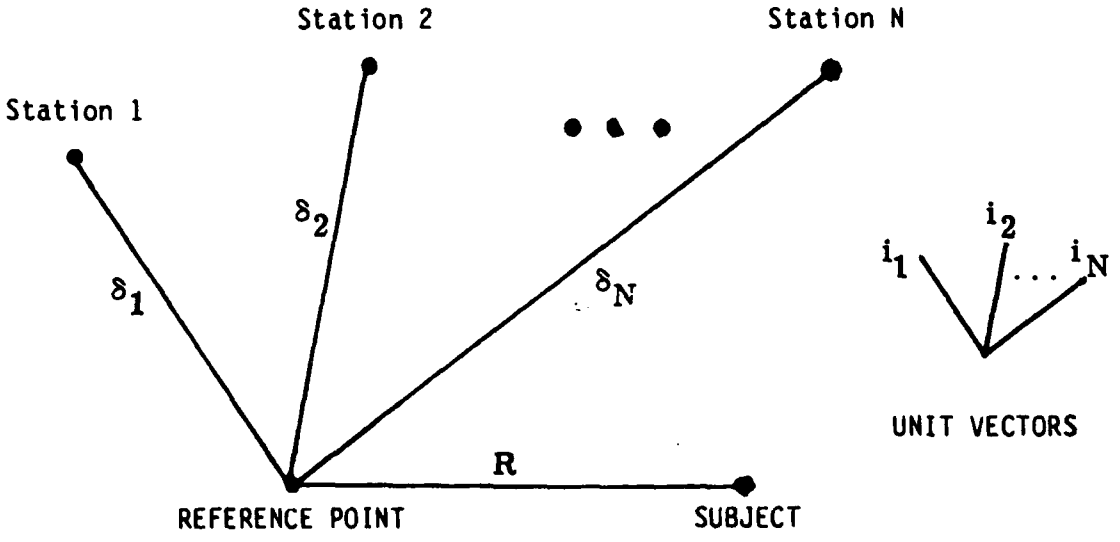

Figure 2-2 Analytic Definitions

For the purpose of minimizing (8), it is advantageous to rewrite (9) in matrix notation as follows:

$$HT^* = (1/c)H\delta^* + (1/c)HFR + H\epsilon \qquad (10)$$

where

$$T^* = \begin{bmatrix} t_1^* \\ \cdot \\ \cdot \\ \cdot \\ t_N^* \end{bmatrix}$$

$$\delta^* = \begin{bmatrix} \delta_1^* \\ \cdot \\ \cdot \\ \cdot \\ \delta_N^* \end{bmatrix}$$

$$F = \begin{bmatrix} i_1 \\ \cdot \\ \cdot \\ \cdot \\ i_N \end{bmatrix} \quad \left.\vphantom{\begin{bmatrix} a \\ b \\ c \\ d \\ e \end{bmatrix}}\right\} N \text{ rows}$$

and H and ϵ are given by (7) and (3), respectively.

Use of (10) in (8) yields

$$Q(R) = [HT^* - (1/c)H^* - (1/c)HFR]' P_\Delta^{-1} [HT^* - (1/c)H\delta^* - (1/c)HFR].$$

The minimizing condition that

$$dQ = -(2/c)dR'F'H'P_\Delta^{-1}[HT^* - (1/c)H\delta^* - (1/c)HFR]$$

equals zero for all vector differentials dR requires that

$$0 = F'H'P_\Delta^{-1}[HT^* - (1/c)H\delta^* - (1/c)HFR]. \qquad (11)$$

Solution of (11) produces the estimator

$$\hat{R} = [F'H'P_\Delta^{-1}HF]^{-1}F'H'P_\Delta^{-1}[cHT^* - H\delta^*] \qquad (12)$$

Use of (10) in (12) shows that the error, $\hat{R} - R$, in calculated position is related to ϵ as follows:

$$\hat{R} - R = c[F'H'P_\Delta^{-1}HF]^{-1}F'H'P_\Delta^{-1}H\epsilon .$$

Clearly, $\hat{R} - R = 0$ if $\epsilon = 0$. More generally, $E[\hat{R} - R] = 0$ provided $E[\epsilon] = 0$. Therefore, the estimator (12) is unbiased. The associated covariance matrix for the error $\hat{R} - R$ is as follows:

$$P_{\Delta R} = E[(\hat{R} - R)(\hat{R} - R)']$$

$$= c^2[F'H'P_\Delta^{-1}HF]^{-1}$$

$$= c^2[F'H'(HP_\epsilon H')^{-1}HF]^{-1} \qquad (13)$$

The least-squares result (12) represents only one possible estimate of the subject position R. Other workable estimators can be readily devised. According to Markov's theorem [11], however, the least-squares estimator is optimal in the sense that it produces the smallest mean-squared error of all estimators that satisfy the following (weak) conditions.

Condition:

1) The estimator is unbiased.

2) For the error magnitudes of interest, the estimator is linear in the ϵ_j. That is,

$$\hat{\mathbf{R}} = \mathbf{R} + \mathbf{A}\epsilon$$

where the matrix A is independent of the ϵ_j.

Accordingly, in what follows when we return to the main discussion, we restrict attention to the errors generated by the least-squares procedure.

Thus far, this abridgement has followed Lee's work almost exactly. It will now be prudent to diverge briefly.

Geometric Dilution of Precision (GDOP)

We now pause in the mathematical development to note the historical evaluation of the term "Geometric Dilution of Precision" (GDOP) and its application. "GDOP" is a technical term used in radio navigation to partition errors between those which might be obtained under reasonably ideal geometric circumstances and those which may occur with particular geometric arrangements. Some radio navigation systems have more or less constant ranging errors due, for example, to more or less constant instrumental errors on each measurement. Thus, the concept of GDOP may be useful to suggest opeational degradations of performance throughout a coverage area due to differences in the relative placements of usable signal sources. Like most jargon, GDOP has a proper meaning and application within expert circles. Also, like most jargon, it is easily misapplied. It is not a suitable substitute for an estimate of the accuracy of a particular system. A brief sketch of the development of the term GDOP was presented several years ago by Swanson (1978) who noted no mention of the term in the most then current navigational references; but an historical reference to GDOP as only the relative divergence of hyperbolic lines while the then, and present, modern use of the term would apply to both the relative divergences and crossing angles of lines of position. That is, the complete geometric effects. While attention of the earlier work was directed especially to the traditional case of signals from three stations on the surface of the earth combining to yield

a two dimensional fix, one would expect modern usage to still lump all geometric effects into a single term "GDOP". This is no longer so easy to do in modern over-determined systems while attempting to retain the original partitioning between signal quality and purely geometric effects. The definition almost must be such that additional stations lower GDOP even though their placement may be equivalent to improving quality on existing stations. (Otherwise, how close would additional stations have to be to be "co-located")? Consider the geometries depicted in Figure 2-3. Figure(a) shows an observer optimally located in the center of a three station network. Figure (b) shows the observer in the center of an optimally located four station network. Other factors being equal, the accuracy will be better in the center of the four station network than in the center of the three station network. Is this due to better "geometry"? Both arrangements are optimum for the assets used. Now consider(c) where a fourth station has been added to the

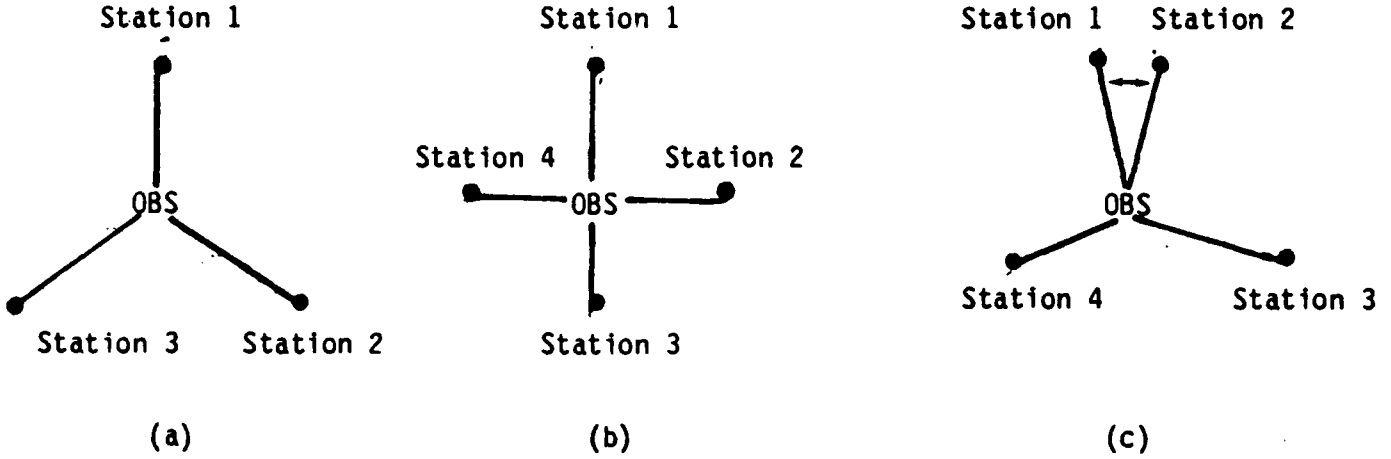

Figure 2-3. Hypothetical Hyperbolic System Geometries

three station network in such a way as to be co-located with an existing station. The accuracy from system (c) will be better than from (a) assuming the errors tracking the co-located stations are not perfectly correlated. Has this improved geometry? The problem illustrated in the foregoing is essentially one of attempting to apply strictly geometric ideas to address the more fundamental issue of anticipated accuracy. This is a mistake which would not be made by a navigation system user who would automatically think in terms of accuracy or, perhaps, relative accuracy compared with some nominal or

optimum accuracy. It is a mistake which would only be made by navigation system experts whose thinking has been clouded by a once applicable jargon. Were it not for redundancy, relative accuracy can indeed be expressed entirely in geometric terms.

We now diverge from Lee's original work by avoiding any explicit definition of "GDOP" preferring instead to use the term "Relative Accuracy". We are now at liberty to consider various possible accuracy references. One choice is to normalize in terms of the accuracy available in the center of a four station network as shown in Figure 3b. If all stations provide the same ranging accuracy and the errors are uncorrelated, then because of the hyperbolic geometry accuracy on the north-south line-of-position will be $\frac{1}{2}(\sqrt{2}\,\sigma)c$ which will be the same as that on the east-west line-of-position. Fix accuracy will then be

$$\sqrt{(\tfrac{1}{2}\sqrt{2}\,\sigma c)^2 + (\tfrac{1}{2}\sqrt{2}\,\sigma c)^2} = \sigma c$$

That is, for stations providing signals of equal quality, Relative Accuracy may be defined as the ratio of actual accuracy to the standard ranging error. This is identically equivlent to the ad-hoc normalization to the center of a symetric four station pattern. The definition is also equivalent, in this case, to that used by Lee for GDOP. Using this definition, relative accuracy will improve as more stations are added. Indeed, for stations uniformly distributed in azmiuth and providing uncorrelated signals of equal quality, it can be shown that the Relative Accuracy is approximately $2/\sqrt{N}$.*

A problem arises when all stations do not provide signals of equal

* This convenient variation with $\sqrt{N}$ suggests the possibility of an alternative definition wherein the square root of the number of stations is incorporated into the normalization. For example, defining Relative Accuracy as the ratio of the actual accuracy to the product of the velocity of light and the timing uncertainty if the location were known. This definition would emphasize geometric effects as it would produce near unity relative accuracy except when all stations were in more or less the same direction. The definition is not used here as it would hide the important advantages of redundancy to the user who, as noted, is indeed interested in relative accuracy. There might, however, be some use for it in expert circles as a definition for GDOP.

quality. What we wish to do is define Relative Accuracy as the ratio of actual accuracy to some effective ranging error, σ^*c:

$$\text{Relative Accuracy} = RA = \sqrt{\sigma_x^2 + \sigma_y^2} \Big/ \sigma^* c$$

What we must now do is define σ^* in the event all signals are not of equal quality. Probably the best choice is simply to prescribe a particular value of σ^* suitable for the circumstances being studied. An alternative is:

$$(\sigma^* c)^2 = \frac{N}{\sum \frac{1}{(\sigma_j c)^2}}$$

which has the computational property of being well behaved so long as the variances are non-zero as is to be expected. Whatever definition is chosen, the mathematics now follows identically with that developed by Lee. Computationally, the different interpretation of σ^* will result in poor signals receiving low weights in the combinational arithmetic while stations providing good signals will be weighted by associated masses near unity. Signals with infinite variance will require no special treatment.

For the purpose of assessing accuracy, it is convenient to rewrite the covariance matrix (13) as follows:

$$P_{\Delta R} = (\sigma^* c)^2 \Gamma$$

$$= (\sigma^* c)^2 \begin{bmatrix} \Gamma_{xx} & \Gamma_{xy} \\ \Gamma_{xy} & \Gamma_{yy} \end{bmatrix} \qquad (14)$$

Use of (13) in (14) shows that the Γ matrix is defined by the relationship

$$\Gamma = \left[\frac{1}{\sigma^* 2}\right] \left[F'H'(HP_\epsilon H')^{-1} HF \right]^{-1} = \left[F'H'(HP_\eta H')^{-1} HF \right]^{-1} \qquad (15)$$

where P_η denotes the normalized covariance matrix

$$P_n = \begin{bmatrix} (\sigma_1/\sigma^*)^2 & & & 0 \\ & (\sigma_2/\sigma^*)^2 & & \\ & & \ddots & \\ 0 & & & (\sigma_N/\sigma^*)^2 \end{bmatrix}$$

All conventional accuracy measures can be expressed easily in terms of Γ. For example, the ratios of the mean-squared errors in the X', Y' directions to the squared effective ranging error are given by

$$\sigma_x^2/(\sigma^* c) = \Gamma_{xx} \tag{16}$$

$$\sigma_y^2/(\sigma^* c) = \Gamma_{yy} \tag{17}$$

Similarly, the ratio of total mean-squared error $\left[\sigma_x^2 + \sigma_y^2\right]$ to the effective ranging error is given by

$$(\sigma_x^2 + \sigma_y^2)/(\sigma^* c)^2 = \Gamma_{xx} + \Gamma_{yy} \tag{18}$$

And Relative Accuracy is given by

$$RA = (\Gamma_{xx} + \Gamma_{yy})^{\frac{1}{2}} \tag{19}$$

Note that the functions of the Γ_{ij} that appear in the right-hand sides of (16) through (19) can be interpreted as error magnification factors that indicated how much the basic ranging error is magnified by the station geometry.

Two Useful Interpretations of Γ^{-1}

We now demonstrate that the inverse of the Γ matrix (15) possesses two extremely simple interpretations in terms of system geometry.

Let L denote Γ^{-1}. That is, let

$$L = F'H'(HP_nH')^{-1}HF \tag{20}$$

In an Appendix to Lee's original paper, it is shown that the matrix factor $H'(HP_nH')^{-1}H$ can be calculated from the expression

$$H'(HP_nH')^{-1}H = \left[I - MU(U'MU)^{-1}U'\right] \cdot M \left[I - U(U'MU)^{-1}U'M\right] \quad (21)$$

where

$$M = P_n^{-1} \quad (22)$$

and

$$U' = \underbrace{\left[1, 1, 1 \ \ldots \ 1\right]}_{N} \quad (23)$$

Use of (21) in (20) shows that

$$L = K'MK \quad (24)$$

where

$$K = \left[I - U(U'MU)^{-1}U'M\right] F \quad (25)$$

Equation (25) can be developed as follows:

$$K = \left\{ I - \left[1/\sum_{j=1}^{N} m_j\right] \begin{bmatrix} 1 \\ 1 \\ 1 \\ \cdot \\ \cdot \\ \cdot \\ 1 \end{bmatrix} \left[m_1, m_2, \ \ldots \ m_N\right] \right\} \begin{bmatrix} i_1 \\ i_2 \\ i_3 \\ \cdot \\ \cdot \\ \cdot \\ i_N \end{bmatrix}$$

$$= \begin{bmatrix} i_1 - \bar{i} \\ i_2 - \bar{i} \\ \cdot \\ \cdot \\ \cdot \\ i_N - \bar{i} \end{bmatrix} \quad (26)$$

where m_j denotes the typical diagonal element of M,

$$m_j = (\sigma^*/\sigma_j)^2 \quad (27)$$

and

$$\mathbf{i} = \left[1/\left(\sum_{j=1}^{N} m_j \right) \right] \sum_{j=1}^{N} m_j \mathbf{i}_j \qquad (28)$$

To interpret the matrix L, assume that the following construction is carried out.

Placement of masses on unit circle:

1) Draw a circle of unit radius with center at the subject position O.
2) Draw the vectors $\mathbf{i}_1, \mathbf{i}_2, \cdots, \mathbf{i}_N$ from the point O.
3) Place masses of value $m_j = (\sigma^*)^2/\sigma_j^2$ $(j = 1,2 \cdots, N)$, respectively, at the points where the unit vectors $\mathbf{i}_1, \mathbf{i}_2, \cdots, \mathbf{i}_N$ terminate at the circle (see Fig. 2-4).

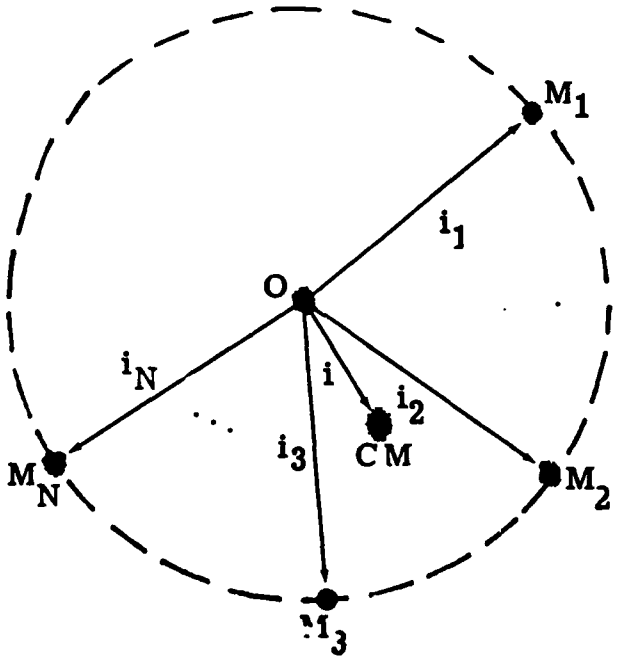

Figure 2-4. Geometric Interpretation

The vector $\mathbf{i}$ specified by (28) can be interpreted as pointing from the point O to the center of mass CM of the mass configuration, as shown in Fig. 2-4. Likewise, the vector difference $\mathbf{i}_j - \mathbf{i}$ contained in the jth row of the matrix K can be interpreted as a vector pointing from CM to the m_j. Thus, if (X, Y) denotes a Cartesian coordinate system centered at CM, and differing

from the system (X', Y') only by translation, then the elements of the jth row of K are simply the coordinates X_j and Y_j of the mass m_j in the system (X, Y). That is,

$$K = \begin{bmatrix} X_1 & Y_1 \\ \cdot & \cdot \\ \cdot & \cdot \\ \cdot & \cdot \\ X_N & Y_N \end{bmatrix} \tag{29}$$

The desired formulation of L follows directly from (25) and (29):

$$L = \begin{bmatrix} \sum_{j=1}^{N} m_j X_j^2 & \sum_{j=1}^{N} m_j X_j Y_j \\ \sum_{j=1}^{N} m_j X_j Y_j & \sum_{j=1}^{N} m_j Y_j^2 \end{bmatrix} \tag{30}$$

$$= M_H \times \begin{bmatrix} (1/M_H) \sum_{j=1}^{N} m_j X_j^2 & (1/M_H) \sum_{j=1}^{N} m_j X_j Y_j \\ (1/M_H) \sum_{j=1}^{N} m_j X_j Y_j & (1/M_H) \sum_{j=1}^{N} m_j Y_j^2 \end{bmatrix} \tag{31}$$

where m_j are given by (27), X_j and Y_j denote the coordinates of m_j measured from the center of mass, and is given by:

$$M_H = \sum_{j=1}^{N} (\sigma^*)^2 / (\sigma_j)^2 \tag{32}$$

Equation (30) asserts that the entries in L are simply the <u>moments and</u>

products of inertia of the mass configuration $m_1, m_2, \ldots, m_N$. By contrast, (31) asserts that the entries in the L matrix can be regarded as averages of the second-order products X^2, XY, and Y^2 over the set of masses.

This insight provided by Lee is extremely valuable both from the viewpoint of programming the equations and from the insight offered in assessing simple geometries. Indeed, it is often possible to estimate the accuracy expected from simple station arrangements in one's head! When programming, otherwise fairly obtruse equations are given the reality long implanted into the technical mind through teachings of center of mass and moments of inertia. Lee provided several examples in his original paper (Lee, 1975a) and also used the approach in a companion paper (Lee, 1975b). One example from his first paper follows.

Sample Calculation of Γ Matrix

An example is given here to illustrate the ease with which the Γ marix and typical error measures can be calculated.

A review of the previous derivation shows that the orientation of the coordinate system (X, Y, Z) can be chosen freely. Accordingly, the coordinate system here is selected to produce a diagonal Γ. The example also assumes that the mean-squared errors σ_j^2 $[j = 1 \ldots N]$ have the common value σ^2, so that

$$(\sigma*)^2 = \sigma^2$$

and

$$m_j = 1 \quad [j = 1, 2 \ldots N]$$

Consider three stations having equal 120 degree separations from the subject.

The unit vectors $i_1, \cdots i_3$ and the masses $m_1 \cdots m_3$ for the constellation are shown in Figure 2-5. Clearly, the center of mass CM of the configuration m_1, m_2, m_3 is at the origin.

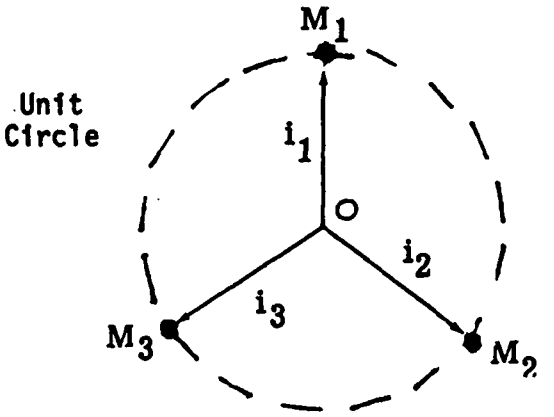

Figure 2-5. Geometry of Example

Therefore,

$$\Sigma X_j^2 = \Sigma Y_j^2 = 3/2$$

$$\Sigma X_j Y_j = 0$$

Consequently,

$$L = \begin{bmatrix} 3/2 & 0 \\ 0 & 3/2 \end{bmatrix}$$

and

$$\Gamma = \begin{bmatrix} 2/3 & 0 \\ 0 & 2/3 \end{bmatrix}$$

Thus, for example,

$$\sigma_x^2/(\sigma c)^2 = 2/3$$

and the relative accuracy is

$$RA = (2/3 + 2/3)^{1/2} = 2/\sqrt{3}$$

SYSTEM COVERAGE COMPUTATION

Optimal fix mathematics, however elegantly developed, does not by itself provide a working tool for the development of coverage diagrams for specific systems. First, the generalized mathematics as just presented must be applied specifically to the system of interest. Application of Lee's work to Omega requires incorporation of error models for the actual propagation conditions as well as detailed specification of such factors as station locations. Second, appropriate displays must be available so as to show maps of accuracy or provide other readouts of interest. Considerable effort, both in analysis and programming, thus must be expended in both of these areas to produce working coverage assessment tools.

Lee's work was first applied to Omega by Thompson (1977). Thompson considered the navigational error to be expected from such sources as: Omega ground station synchronization error, noise induced perturbation, multipath, random propagation variations and residual propagation errors. Results included contour maps of anticipated Omega accuracy and histograms of accuracy distribution. Unfortunately, Thompson based his propagation modeling on a 1969 work of Scott which in turn incorporated 1964 field prediction work of Swanson. Although the 1964 conclusions were, in fact, restricted to temperate latitudes, at the time of writing there was little reason to believe they would be grossly inapplicable to some equatorial propagation. Thus the outstanding formal error integration was compromised by a propagation routine which was completely inadequate for equatorial propagation at night.

Thompson generously made his work available to Swanson (1983; 1984a) who extended it primarily through the incorporation of more realistic propagation models and error budgets. The displays were also changed in several ways but especially so as to indicate the cause of propagational limitations on signals

from individual stations such as modal interference, long path interference, etc. (Figure 3). Accuracy for the system as an entity was changed from the contour display used by Thompson to a numeric display (Figure 4). Details of interest to this validation are discussed in subsequent sections.

The distinction between the coverage assessment program and the underlying theory can perhaps be emphasized by noting that the program has some application even where the underlying theory as developed by Lee is not applicable! Examples might be an evaluation of system errors as might occur from very large Sudden Phase Anomalies (SPA's) or Polar Cap Absorptions (PCA's). These are caused, respectively, by sudden X-ray or proton emissions from the sun causing ionospheric changes. The effect of these events on various paths is highly correlated thus invalidating one of the assumptions in the underlying derivation. However, the effects can be well predicted using only information ordinarily computed within the coverage assessment program. Thus a slight change in the program can lead to a major new assessment capability.

3. EQUIPMENT DEPLOYMENT

Measurements

As with previous validations, the Indian Ocean validation was a coordinated effort to gather diverse types of synergistic data from which the key aspects of Omega coverage could be determined. The major measurements portions were:

1. In-flight measurements on dedicated flights.
2. Long term measurement of temporal variation at fixed sites.
3. Shipboard data from ships transiting the area.

Both amplitude and phase measurements were made in-flight and at the fixed sites. Figure 5 (modified from Kugel, 1984) shows the Indian Ocean areas, flight paths for the dedicated flights, the fixed sites, and ship transit areas.

Airborne Measurements

Airborne instrumentation for this validation was unique. The experimental procedures for this effort have been previously described by Kugel (1984) and will only be summarized here. The principle data gathering device was a modified Litton LTN-211 Omega navigation receiver. The LTN-211 typically measures at least three of the four commutated Omega frequencies. At each frequency this receiver ordinarily measures signals from seven of the eight antenna to calibrate the receiving system. Typically injection is on top of a relatively weak Omega signal and is done at a relatively high level so as to swamp the incident Omega signal. In this validation a weak signal was injected and the phase tracking data for the injection output as well as being measured phase variance on the injected channel which can be related to the signal-to-noise ratio. Since the absolute voltage level of the injection was known, this allowed a measure of the prevailing noise level. For this purpose an omnidirectional whip antenna was used instead of the usual loop. As is ordinarily done within the LTN-211, phase variances on the other signals were also computed. Since the signal-to-noise ratio could be related to the phase variance and since the nominal noise level could be determined from measurements on the injection channel, this allowed a measure of the signal

amplitude of each of seven Omega stations. A few problems were, however, anticipated and experienced.

If signals are exceptionally strong, the phase variance is very small and amplitude cannot be measured with any accuracy. Effectively, a saturation condition is reached. In this case, however, the signals were sufficiently large that they could be measured incoherently on a Hewlett-Packard spectrum analyzer. Another problem was the need to find an appropriate injection level below saturation which would nevertheless swamp out the actual Omega signal on the injection segment. This proved usually possible to do. A more severe limitation was the recording scatter (noise) introduced by the measurement process. Especially under adverse conditions, the whip antenna would produce more noise than the magnetic loop usually used in commercial installations. Thus, the inherent measurement sensitivity was lower than would be normally available. The other problem was that noise does vary from one segment to the next. Noise scatter on the injection track is directly reflected as signal scatter on each measured signal. This was occasionally quite apparent by comparing scatter on amplitude recordings of different stations at the same frequency. Highly correlated pertubations could be attributed to noise on the injection channel.

Thus, the measurement approach proved a mixed blessing. On the one hand, it produced vastly more data than has heretofore been available from validations. On the other hand, the quality of the recordings was somewhat compromised. Since interpretation is so crucially dependent on nuances in variation between the amplitudes versus distance variations at different frequencies, the scatter induced by the measurement process is particularly regretted.

A second LTN-211 was also installed with a conventional loop (H-field) antenna. This equipment was used to process airborne navigational performance.

A block diagram of the aircraft installation is shown in Figure 3-1 while the components are described in more detail in the Aircraft Equipment Inventory, Table 3-I.

The flight routes were shown in Figure 5 except for an initial shakedown flight from St. Petersburg, Florida to San Diego, California via the North Dakota transmitter and flights between San Diego and Hawaii. Specific airport locations and nomenclature are given in Table 3-II while the actual flight schedule is shown in Table 3-III. Flights encompassed a 6-week period from 14 August until 26 September 1983, and all were made at night except for flights 14 and 27. Although all flights originally were designed to follow radial routes from specific transmitters, operational and political constraints often resulted in significant variations. For example:

(1) Flight 8 was intended to continue an Australian radial through to New Delhi, but permission for a night flight over India was not granted.
(2) Flight 10 was to be toward Liberia, but the only airway which could be flown in Saudi Arabia and, Egypt would not permit an overflight.
(3) Flight 11 had to avoid both Ethopian and Ugandan airspace.
(4) Having originated in South Africa, Flight 14 had to avoid Madagascar.
(5) Flight 19 had to be broken into two legs when a fueling problem prevented the aircraft from making the flight from Columbo to Australia.

The flight plan was arranged to provide overflights of certain land based monitors and transmitters to provide calibration of the airborne equipment (Table 3-IV).

Fixed Sites

Three types of fixed sites are of interest in this validation:

(1) Transmitter sites as listed in Table 3-V.

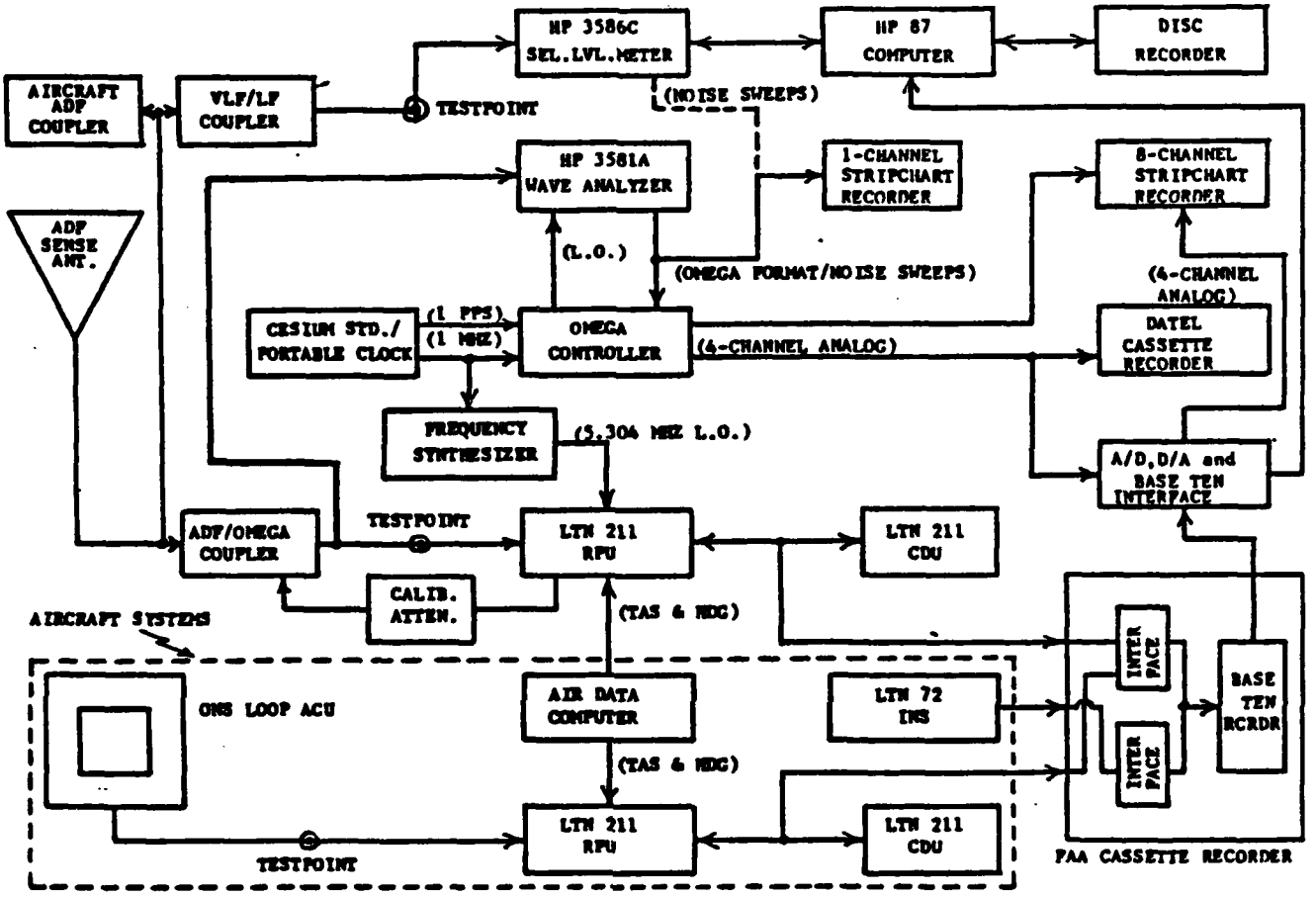

Figure 3-1. Block Diagram for C-130 Aircraft Equipment

TABLE 3-I

AIRCRAFT EQUIPMENT INVENTORY

EQUIPMENT TYPE	MANUFACTURER-MODEL NO.	DIMENSIONS INCHES H	W	D	WT LBS	INPUT POWER V	HZ	W
ONS CONTROL/DISPLAY UNIT	LITTON 211	5	6	4	4	115	400	24
ONS RECEIVER/PROCESSOR UNIT	LITTON 211	8	8	20	26	115	400	62
ONS LOCAL OSCIL SYNTHESIZER	SYNTEST SI-102	4	9	10	3	115	400	5
CESIUM STANDARD/FLYING CLOCK	HEWLETT-PACKARD E21-5061A	16	17	20	140	115	400	75
WAVE ANALYZER	HEWLETT-PACKARD 3581A	8	11	19	30	115	400	10
SELECTIVE LEVEL METER	HEWLETT-PACKARD 3586C	8	19	17	50	115	400	150
ANALOG/DIGITAL INTERFACE	NOSC	5	8	8	3	115	400	<1
CASSETTE TAPE RECORDER 1	FAA/BASE TEN SYSTEMS	8	8	13	15	115	400	20
12V POWER SUPPLY(2)	LAMBDA LM 260	3	4	7	5	115	400	<30
LIGHT		-	-	-	-	115	400	100
115V,60HZ INVERTER	KGS ELECTRONICS SPS-306B	4	8	14	18	28	DC	400
COMPUTER CONTROL/DISPLAY	HEWLETT-PACKARD 87	8	17	18	22	115	60	50
FLEXIBLE DISC DRIVE(DUAL)	HEWLETT-PACKARD 82901M	4	17	15	20	115	60	90
STRIPCHART RECORDER(8-CHNL)	WATANABE INST MC6715-8	10	17	10	40	115	60	100
STRIPCHART RECORDER(1-CHNL)	ESTERLINE-ANGUS	6	10	15	13	115	60	6
ADF/OMEGA ANTENNA COUPLER	LITTON 458880-03	3	3	6	1	12	DC	<1
ADF/VLF/LF ANTENNA COUPLER	NOSC	3	2	6	1	12	DC	<1
OMEGA/VLF/LF CONTROLLER	NOSC	4	17	10	5	12	DC	<25
CASSETTE TAPE RECORDER 2	NOSC/DATEL	7	5	10	5	12	DC	<2
CALIBRATION ATTENUATOR(2)	HEWLETT-PACKARD 355D/355C	3	4	6	2	-	-	-
SIGNAL DISTRIBUTION PANEL	NOSC	3	19	6	1	-	-	-

TABLE 3-II

AIRPORTS

IDENT. STD	IDENT. ICAO	SITE/TERMINAL NAME	LOCATION	COORDINATES LAT	LONG	LST-GMT
ASP	ASAS	ALICE SPRINGS RAAFB	ALICE SPRINGS,AUSTRALIA	23 48S	133 53E	+0855
AWK	PWAK	WAKE ISLAND AFLD	WAKE ISLAND	19 17N	166 38E	+1105
BAH	OBBI	BAHRAIN INTL	MUHARRAQ,BAHRAIN	26 16N	50 38E	+0325
CHC	NZCH	CHRISTCHURCH INTL	CHRISTCHURCH,NEW ZEALAND	43 29S	172 32E	+1130
CMB	VCBI	KATUNAYAKE INTL	COLUMBO,SRI LANKA	7 11N	79 54E	+0520
CRK	RPMK	CLARK AB	LUZON,PHILIPPINES	15 11N	120 33E	+0800
DRW	ADDN	DARWIN INTL	DARWIN,AUSTRALIA	12 25S	130 52E	+0845
GUM	PGUM	AGANA NAS	AGANA,GUAM	13 29N	144 48E	+0940
JNB	FAJS	JAN SMUTS ARPT	JOHANNESBURG,SOUTH AFRICA	26 08S	28 14E	+0155
KRT	HSSS	KHARTOUM ARPT	KHARTOUM,SUDAN	15 36N	32 34E	+0210
MEL	AMML	MELBOURNE INTL	MELBOURNE,AUSTRALIA	37 40S	144 50E	+0940
NAX	PHNA	BARBERS POINT NAS	EWA,OAHU,HAWAII	21 19N	158 05W	-1030
NBO	HKNA	JOMO KENYATTA INTL	NAIROBI,KENYA	1 19S	36 56E	+0230
NKW	FJDG	DIEGO GARCIA ATOLL	CHAGOS ARCHIPELAGO	7 18S	72 24E	+0450
PER	APPH	PERTH INTL	PERTH,AUSTRALIA	31 56S	115 58E	+0745
PIE	KPIE	CLEARWATER CGAS	CLEARWATER,FLORIDA	27 55N	82 41W	-0530
PPG	NSTU	PAGO PAGO INTL	AMERICAN SAMOA	14 20S	170 43W	-1125
RUN	FMEE	GILLOT ARPT	LA REUNION ISLAND	20 53S	55 31E	+0335
SAN	KSAN	SAN DIEGO INTL	SAN DIEGO,CALIFORNIA	32 44N	117 11W	-0750
SIN	WSAC	CHANGI INTL	SINGAPORE	1 21N	103 59E	+0655

TABLE 3-III

FLIGHT ITINERARY (C-130)

FLT	DEPARTURE					ARRIVAL					FLT
NO.	ID*	DATE	GMT	T	LT	ID*	DATE	GMT	T	LT	HRS
01	PIE	08/14	2227	-0400	1827	SAN	08/15	0842	-0700	0142	10.2
02	SAN	08/17	0554	-0700	2254	NAX	08/17	1458	-1000	0458	9.1
03	NAX	08/18	0622	-1000	2022	PPG	08/18	1505	-1100	0405	8.7
04	PPG	08/19	0602	-1100	1902	CHC	08/19	1352	+1200	0152	7.8
05	CHC	08/21	0846	+1200	2046	MEL	08/21	1354	+1000	2354	5.1
06	MEL	08/22	0839	+1000	1839	ASP	08/22	1328	+0930	2258	4.8
07	ASP	08/23	1058	+0930	2028	SIN	08/23	2021	+0800	0421	9.4
08	SIN	08/26	1317	+0800	2117	CMB	08/26	2052	+0530	0222	7.6
09	CMB	08/27	1252	+0530	1822	BAH	08/27	2045	+0300	2345	7.9
10	BAH	08/28	2240	+0300	0140	KRT	08/29	0346	+0200	0546	5.1
11	KRT	08/29	1717	+0200	1917	NBO	08/29	2133	+0300	0033	4.3
12	NBO	08/30	1632	+0300	1932	RUN	08/30	2234	+0400	0234	6.0
13	RUN	08/31	1440	+0400	1840	JNB	08/31	2105	+0300	0005	6.4
14	JNB	09/03	0702	+0300	1002	RUN	09/03	1309	+0400	1709	6.1
15	RUN	09/04	1455	+0400	1855	RUN	09/04	2242	+0400	0242	7.8
16	RUN	09/05	1452	+0400	1852	NKW	09/05	2023	+0600	0223	5.5
17	NKW	09/09	1412	+0600	2012	BAH	09/10	0038	+0300	0338	10.4
18	BAH	09/12	1343	+0300	1643	CMB	09/12	2157	+0530	0327	8.2
19	CMB	09/14	1246	+0530	1816	SIN	09/14	1834	+0800	0234	5.8
20	SIN	09/15	1022	+0800	1822	PER	09/15	1852	+0800	0252	8.5
21	PER	09/17	1130	+0800	1930	MEL	09/17	1718	+1000	0318	5.8
22	MEL	09/18	1042	+1000	2042	DRW	09/18	1748	+0930	0318	7.1
23	DRW	09/19	1027	+0930	1957	CRK	09/19	1725	+0800	0125	7.0
24	CRK	09/20	1235	+0800	2035	GUM	09/20	1842	+1000	0442	6.1
25	GUM	09/23	0904	+1000	1904	AWK	09/23	1425	+1200	0225	5.4
26	AWK	09/24	0754	+1200	1954	NAX	09/24	1523	-1000	0523	7.5
27	NAX	09/26	1511	-1000	0511	SAN	09/26	2338	-0700	1638	8.5

TABLE 3-IV

OVERFLIGHTS

NO.	FLT		XMTRS	RCVRS
01	PIE	SAN	DAK	
02	SAN	NAX	HAW	
03	NAX	PPG	HAW	
04	PPG	CHC		
05	CHC	MEL	AUS	
06	MEL	ASP	AUS	
07	ASP	SIN		SINGA
08	SIN	CMB		SINGA
09	CMB	BAH		BAHR2
10	BAH	KRT		BAHR2
11	KRT	NBO		
12	NBO	RUN	LAR	
13	RUN	JNB	LAR	PRETO
14	JNB	RUN	LAR	PRETO
15	RUN	RUN	RUN,RUN	
16	RUN	NKW	RUN	DIEGO
17	NKW	BAH		DIEGO,BAHR2
18	BAH	CMB		BAHR2
19	CMB	SIN		SINGA
20	SIN	PER		SINGA,PERTH
21	PER	MEL	AUS	PERTH
22	MEL	DRW	AUS	
23	DRW	CRK		
24	CRK	GUM		
25	GUM	AWK		
26	AWK	NAX	HAW	
27	NAX	SAN	HAW	

TABLE 3-V

OMEGA TRANSMITTERS

IDENT	SITE NAME	LOCATION	COORDINATES LATITUDE	COORDINATES LONGITUDE	LST-GMT
A. TRANSMITTERS					
NOR	OMEGA NORWAY	ALDRA,NORWAY	66 25 12.6N	13 08 12.5E	+0050
LIB	OMEGA LIBERIA	MONROVIA,LIBERIA	6 18 19.1N	10 39 52.4W	-0045
HAW	OMEGA HAWAII	HAIKU,OAHU,HAWAII	21 24 16.8N	157 49 51.5W	-1030
DAK	OMEGA NORTH DAKOTA	LA MOURE,NORTH DAKOTA	46 21 57.3N	98 20 08.8W	-0635
LAR	OMEGA LA REUNION	LA REUNION(FRANCE)	20 58 27.0S	55 17 23.1E	+0340
ARG	OMEGA ARGENTINA	TRELEW,ARGENTINA	43 03 12.9S	65 11 27.4W	-0420
AUS	OMEGA AUSTRALIA	WOODSIDE,AUSTRALIA	38 28 52.5S	146 56 06.5E	+0950
JAP	OMEGA JAPAN	TSUSHIMA,JAPAN	34 36 52.9N	129 27 12.6E	+0840

TABLE 3-VI

CALIBRATED FIXED RECEIVER SITES

BAHR2	BAHRAIN	MANAMA,BAHRAIN	26 12 33.0N	50 36 28.5E	+0320
DIEGO	DIEGO GARCIA	DIEGO GARCIA ATOLL	7 16 42.0S	72 21 52.8E	+0450
PERTH	PERTH	PERTH,AUSTRALIA	31 56 11.9S	115 58 36.6E	+0745
PRETO	PRETORIA	PRETORIA,SOUTH AFRICA	25 44 49.8S	28 16 35.4E	+0155
SINGA	SINGAPORE	SAMBAWANG,SINGAPORE	1 27 52.8N	103 49 47.4E	+0655

(2) Calibrated fixed receiving sites where both phase differences and amplitude were measured (Table 3-VI).

(3) Normal phase difference monitoring sites forming a part of the global Omega monitoring network.

The use of overflights to calibrate the airborne instrumentation has already been noted and is described in more detail by Kugel (1984). A total of 15 transmitter overflights were performed using Hawaii, North Dakota, La Reunion and Australia. Because some of these involved flying both toward and away from the antenna the required distance, 20 effective calibration flights were available. With 4 frequencies being monitored on each flight, a total of 80 estimates of signal behavior was obtained.

After the known relative gain variation with frequency of the antenna systems were accounted for, the ensemble of 100-km intercept-offsets were adjusted to provide an average system radiated power of 10 kw. The resulting values for individual stations and/or frequencies was then interpreted as the deviation of that signal from the assumed system average. Overall statistical summaries of these results indicated that all stations were within 0.5 dB of the correct level with an uncertainty of the same magnitude. Flights toward an antenna tended to show approximately 0.5 dB more signal than those departing the antenna. Some such differences might be expected given the location of the antennas with respect to the large mass of metal represented by the vertical stabilizer and the rapidly changing geometry during the overflight period.

Five special receiving sites were also instrumented and calibrated so as to measure long term temporal variation amplitude (Table 3-VI). The measurement approach was equivalent to that used aboard the aircraft: at each

frequency, a known weak signal level was used for injection on the calibration channel and the amplitude inferred by comparison of the phase variances on the signal tracking channels as compared with that on the calibration channel. However, each receiving site was calibrated by measurement. While calibration of an aircraft antenna while the aircraft is on the ground is somewhat dubious due to the unusual ground proximity and other factors, a fixed ground based receiving antenna can be calibrated at leisure with confidence that the environmental details prevailing during calibration will be the same as those experienced in use. Field strength measurements for calibration were obtained my measuring the voltage induced on a loop antenna of known geometry. At all sites the loop antenna could be reasonably located so as to be free of such field perturbations as might be caused by nearby objects. The measurement technique entailed preamplification, measurement using a tunable radio frequency voltameter (wave analyzer) and subsequent recording on a strip chart recorder. This technique has proven quite satisfactory for the stronger Omega signals unless local noise conditions are exceptionally high. Since there are several Omega signals available for calibration, each one which was of sufficient amplitude was used in turn. First, the antenna was directed to optimize the received signal, then measurements were made at all frequencies. The strip chart recorder was operated at sufficient speed that the individual station bursts could be recognized. Since the amplitude of all stations was recorded on the strip chart while the antenna was optimized for each in turn, this provided a considerable redundancy to assure reasonableness of measurements. For this validation, two antennas were used alternatively thus providing further redundancy. Equipment details are summarized in Table 3-VII.

TABLE 3-VII

CALIBRATION EQUIPMENT

EQUIPMENT TYPE	MANUFACTURER-MODEL NO.	DIMENSIONS INCHES H	W	D	WT LBS	INPUT POWER V	HZ	W
ONS LOOP ANTENNA	TRACOR H-FIELD BRICK	3	6	6	6	12	DC**	1
BRIEFCASE LOOP ANTENNA	NOSC	17	12	5	5	--	--	--
PRE-AMPLIFIER	NOSC	2	6	3	2	12	DC*	1
WAVE ANALYZER	HEWLETT-PACKARD 3581A	8	11	19	30	12	DC*	10
STRIPCHART RECORDER(1-CHNL)	ESTERLINE-ANGUS	6	10	15	13	12	DC*	6

* CONTAINS INTERNAL BATTERY
**REQUIRES EXTERNAL BATTERY

The third category of fixed sites are those which form a part of the on-going global Omega monitoring program. These sites measure long term temporal variation of phase or phase differences which are subsequently compiled in the Omega MASTERFILE used to refine Predicted Propagation Correction (PPC's). As these measurements are on-going, no special effort was needed as a part of the validation effort to support the measurements. They were, however, pertinent to the overall data analysis. Especially relevant were those from within the region including data from Darwin, Brisbane and Cocos (Australia), Clark AFB and Cubi Point NAS (Philippines), Khartoum (Sudan), Mombasa (Kenya), and Tananarive (Malagasy Republic). Also relevant are phase measurements at monitors associated with each Omega transmitting station. For this validation measurements at La Reunion were especially valuable. A partial summary of data is incorporated into Appendix C.

Shipboard Measurements

Seaborne measurements were also integrated into the validation. There are advantages and a number of serious drawbacks to shipboard monitoring. An advantage is obvious from Figure 5: the extensive ship transits passing through the southeast Indian Ocean--a region devoid of both monitors and flight paths. Thus, data were obtained from a region which was not otherwise sampled. A second advantage is the demonstration that the Omega signals could actually be received on whips working in the area. This is a practical result of direct concern to Omega equipped mariners.

Other aspects of shipboard data collection including limitations are discussed in the section on analysis.

Arrangements were made for installation of receivers capable of receiving both Omega and Navsat (Transit) signals on three merchantmen which normally operated in the area: MV. Mishva, MV. Siena and MV. Neder. From June through August 1983, the Magnavox MX 1105 receivers provided meaningful comparisons of measurements from Omega with those from Navsat. Ordinarily, such comparisons yield only differences which cannot properly be attributed to one system or another. Whereas Navsat provides outstanding accuracy to a docked ship, accuracy degrades at sea. Should high ship dynamics result in large unknown

set and drift, Navsat fixes may well be worse than those obtained with Omega. For the installations discussed here, the merchantmen were operating on ordinary trade routes with very low dynamics. Further, speed and heading were automatically input to the Navsat equipment while special cubic spline smoothing was employed in making the comparisons. Under the arranged conditions, it is believed that usually most of the discrepancy can be attributed to Omega.

4. SPOT COMPARISONS

SPOT COMPARISON OF PREDICTED AND OBSERVED COVERAGE - 1800 GMT:

A convenient means of checking the adequacy of the 10.2 kHz parametric coverage prediction is available by combining results noted in two papers published in the Proceedings of the 1984 Seattle meeting of the International Omega Association. In one, Kuger (1984) presented receiver utilization of signals at various points throughout the region at 1800 GMT. Signals on which modal interference was noted also were identified. Swanson (1984a) presented a method of estimating coverage at particular times of day including 1800 GMT. Thus, we wish to compare coverage as noted in Kugel's Figure 5, reproduced here as Table 4-I, with that in Appendix B which contains a full set of individual station coverage diagrams computed in preparation of Swanson's Seattle paper.

TABLE 4-I.

OMEGA SIGNAL PERCENTAGE USAGE NEAR 1800 UT(LTN 211 WITH H-FIELD ANTENNA)

FLT	LOCATION	NOR			LIB			HAW			DAK			LAR			ARC			AUS			JAP		
NO.	LAT LONG	102	113	136	102	113	136	102	113	136	102	113	136	102	113	136	102	113	136	102	113	136	102	113	136
07	7S 111E	99	100	100	77	100	100	4	7	8	CAL	CAL	CAL	100	100	100	0	0	0	100	100	100	0*	0*	0*
08	15N 90E	100	100	100	100	100	100	4	3	26	0	2	1	100	100	100	CAL	CAL	CAL	0*	0*	0*	30*	30*	27*
09	19N 61E	100	100	100	100	100	100	21	38	46	0	0	0	100	100	100	CAL	CAL	CAL	0*	0*	0*	59*	26*	100
11	13N 33E	100	100	100	100	100	100	CAL	CAL	CAL	39	51	39	71*	70*	98*	100	100	100	16	17	7	16	18	7
12	6S 41E	100	100	100	100	100	100	CAL	CAL	CAL	0	0	0	100	100	93*	100	100	100	100	100	100	0	0	0
13	24S 42E	88	100	100	100	100	100	CAL	CAL	CAL	0	1	1	100	100	100	100	100	100	100	100	100	0	0	0
15	28S 67E	100	100	100	100	100	100	0	0	0	CAL	CAL	CAL	100	100	89*	100	100	100	100	100	100	0*	0*	0
16	13S 65E	100	100	100	100	100	100	0	0	0	CAL	CAL	CAL	100	92*	100	100	100	100	100	100	100	0*	0	0*
17	3N 60E	100	100	100	100	100	100	CAL	CAL	CAL	0	0	0	100	100	100	100	100	100	80	100	100	0	0	0
18	15N 66E	100	100	100	100	100	100	OFF	OFF	OFF	0	0	0	100	100	100	CAL	CAL	CAL	0*	0*	0*	46*	42*	61*
19	1N 102E	100	100	100	100	100	100	OFF	OFF	OFF	0	0	0	100	100	100	CAL	CAL	CAL	100	100	100	0*	0*	0*
20	28S 117E	100	100	100	100	100	100	OFF	OFF	OFF	CAL	CAL	CAL	100	100	100	0	2	2	100	100	100	0*	0*	0
21	38S 146E	83	100	100	100	100	100	0	0	0	CAL	CAL	CAL	100	100	100	100	100	100	0*	0*	0*	100	100	100
22	13S 131E	100	100	100	CAL	CAL	CAL	0*	0*	0*	6	16	25	100	100	100	94	100	100	100	100	100	100	100	100
23	16N 121E	100	100	100	100	100	100	0*	0*	0*	48	100	100	100	100	100	CAL	CAL	CAL	0*	0*	0*	100	100	100
24	14N 142E	100	100	100	100	95	91	48*	67*	68*	10	29	33	100	100	100	CAL	CAL	CAL	100	100	100	100	100	100

NOTES: 1. All data for 1700-1900UT except FLT 19 ends at 1835, FLT 20 at 1851, FLT 21 at 1717, FLT 22 at 1744, FLT 23 at 1727 and FLT 24 at 1846.
2. (*) indicates significant amplitude variations probably caused by modal interference effects.

Before proceeding with the comparison itself, it will be useful to expand on the background of the referenced works. Also, although the intent of the comparison is straightforward, several complications need to be addressed.

The predicted coverage was computed for illumination conditions close to those experienced during the validation. The noise, however, was for spring rather than fall. A comparison of noise maps for the two periods suggests that noise in the fall would be roughly the same. (Specifically, computations were made for the vernal equinox while the validation was conducted near the autumnal equinox).

Kugel based 1800 GMT coverage on the period 1700 - 1900 GMT and tabulated coverage for 16 flights but several flights (numbers 19 through 24) ended prior to 1900. For these flights, theoretical coverage was also checked at 1200 GMT. If the indicated coverage was different from that at 1800 GMT, it too was tabulated for comparison. Since observations were displaced in distance as well as time from 1800Z, the coverage indicated on the maps was read for the region surrounding the 1800Z location. In some instances up to six different coverage assessments were obtained for a particular observation by Kugel.

Observed and computed coverages were first tabulated in one rather large and complicated table, Table 4-II. Each square shows observed and predicted coverage for a particular station on a particular flight near 1800Z. On the left is the signal usage as indicated by Kugel (from Table 4-I). At the right is the predicted coverage (or coverages) from Appendix B summarized according to code shown in Table 4-III which, in turn, is essentially that previously

TABLE 4-II

10.2 KHZ OBSERVED AND PREDICTED COVERAGE AT 1800 GMT

FLIGHT NUMBER	STATION NORWAY		LIBERIA		HAWAII		N. DAKOTA		LA REUNION		ARGENTINA		AUSTRALIA		JAPAN	
7	99	1	77	2	4	2 3	CAL	3 #	100	B	0	# 3	100	-	0*	M/-/0
8	100	0	100	0	4	L -	0	# 3	100	B	CAL	1	0*	M	30*	M -
9	100	0	100	0 B	21	L	0	#	100	B	CAL	1	0*	M	59*	M
11	100	0	100	B	CAL	2/3 L	39	2	71*	M	100	1	16	M -	16	M -
12	100	1	100	0	CAL	L A	0	3/2/#	100	- B	100	1	100	1 -	0	M
13	88	1	100	0	CAL	L A	0	2 3	100	- N	100	0	100	1 0	0	M
15	100	1	100	1 0	0	- 3	CAL	# -/A	100	B/N/-	100	0	100	0 B	0*	M
16	100	0 1	100	0 1	0	L -	CAL	#	100	B N	100	0	100	0 -	0*	M
17	100	0	100	0	CAL	L	0	#	100	B -	100	1 0	80	- M	0	M
18	100	0	100	0 B	OFF	L	0	#	100	B	CAL	1	0*	M	46*	M
19	100	0 1	100	0 1/2	OFF	2/L/3	0	#	100	B	CAL	#/2/3	100	M -	0*	M
20	100	1	100	0 2	OFF	1/2 2/1	CAL	L -	100	B	0	# -	100	B	0*	-/0/M
21	83	1/2 1	100	1/0 2	0	M/- 1/0	CAL	M -/3	100	0/B B	100	1/#/0 0/3/#	0*	N/B N/B	100	0/B 0/B
22	100	1/2 1	CAL	0/1 2	0*	M 2/1	6	M/- 3/2	100	0/B B	94	1/# #/2	100	-/B -/B	100	B/0/- 0/B/-
23	100	1 1	100	2/1 0	0*	M 2/1	48	2/- 2/3	100	0 B	CAL	#/L/- #/-	0*	M/- M/-	100	-/M/B -/M/B
24	100	1 1	100	2 0/1	48*	M 0/1	10	1/-/M 2	100	0 B	CAL	- 3	100	-/0/M	100	B

NOTE: Key shown in Table 4-III

TABLE 4-III

COVERAGE DISPLAY CODE

Character	Limitation/Meaning	Elaboration
N	Near	Within 1 Mn of station and potentially subject to skywave-groundwave interferences
A	Antipode	Within 2 Mn of antipode and subject to antipodal interference
#	No Signal	SNR worse than -40 dB in 100 Hz bandwidth
M	Modal	Second mode dominates or is within one dB of first mode
L	Long Path	Long path dominant or equal to short
-	Disturbed	Unwanted self interference within 10 dB; either long path or second mode
3	SNR in -30's	$-40 < SNR \leq -30$ dB in 100 Hz bandwidth; usable by well installed good receiver
2	SNR in -20's	$-30 < SNR \leq -20$ dB in 100 Hz bandwidth
1	SNR in -10's	$-20 < SNR \leq -10$ dB in 100 Hz bandwidth
0	SNR in -0's	$-10 < SNR \leq -0$ dB in 100 Hz bandwidth
B	Loud and Clear	Signal should be well received by poorly installed mediocre receiver under water

TABLE 4-IV

10.2 kHz COVERAGE COMPARISON SUMMARY
(Percent of observations)

Predicted Coverage	Observed Signal Utilization Unless Modal					Modal (*)
	100%	67-100%	34-66%	0-33%	0%	
SNR > 0	12					
0 ≤ SNR < -10	19					
-10 ≤ SNR < -20	11	3				
-20 ≤ SNR < -30	2	2		2	1	
-30 ≤ SNR < -40					2	
SNR ≤ -40					6	
N	3					1
A						
L				2	1	
-	6		1		1	
M	3	1		4	4	15

introduced with Figure 3 and used in Appendix B. The data are summarized in Table 4-IV.*

Table 4-IV illustrates many important features. Perhaps most importantly, of the observations noted by Kugel as undergoing interference, all were predicted to be modally disturbed (flags M or N). The primary objective of coverage studies is to indicate where signals may be used safely. Coverage indications were developed conservatively so as to attempt to assure signal deletion if necessary even at the expense of occasionally deleting signals which were usable. There were, however, a significant number of instances where modal inteference was expected but where Kugel did not note it.

Signals were expected to be unperturbed at better than -20 db signal-to-noise ratio in 100 Hz bandwidth in 45% of the samplings. In these circumstances, tracking was nearly solid. In three percent of the instances tracking was less tha 100%, but even for these exceptions the average tracking was 90%.

---

* As with any summary comparison of multi-facited data, certain procedures and precidences were used. Scientific accuracy demands that the assiduous reader be informed of these.

Usually there was no ambiguity in mapping data from Table 4-II to 4-III, e.g., on flight 7 receiving Norway the entire prediction--observation pair would be attributed to 99% utilization with predicted coverage corresponging to SNR above -20 db but not above -10db. For analysis purposes, a circumstance such as observing Hawaii on Flight 7 was handled by attributing the observation equally to both of the predicted conditions, e.g., a half prediction--observation pair for coverage level 2 and a half for coverage level 3. As can be seen by perusal of the table, the only instance where this approach could cause serious distortion was during flights 21 and 22 when observing Argentina near Melbourne. For these measurements, the aircraft was passing near the antarctic "shadow line" and thus observed coverage would depend in detail on when the aircraft was in one region or another. Because of this inability to properly partition the observation, these two observations were excluded from the comparison table. When flags were encountered, they were used exclusively according to the precidence M, N, L, -. Similarly, observations were credited as being solely modal when identified as modal by Kugel.

This type of performance should certainly be expected. However, it does suggest that there was nothing grossly noisy about the aircraft itself or the particular LTN-211 installation employing the loop antenna. Further, it suggests that the particular parametric model used to estimate field strength produces more or less plausible signal-to-noise ratios when used in conjunction with CCIR noise estimates even with the aforementioned seasonal difference. Considering that atmospheric noise levels may differ significantly from day to day or from hour to hour on any given day, and, further, the aircraft itself may be subjected to triboelectric charging depending on local weather conditions, one should not expect 1:1 correspondence between observed tracking ability and predicted signal-to-noise ration. Actual usage was highly supportive of the theoretical model.

One would also hope that signals in the range from -20 to -30 db could be reliably tracked. The table shows this range to be about the tracking limit with the observed usage ranging from 100% to none. The SNR tracking limit for the particular installation appears nearer -30 db than -20db. Generally, signals which were predicted to be usable were in fact used by the receiver. Unfortunately, some improper signal usage also was noted. That is, some "use" was made of signals which were predicted and observed to be undergoing self-interference.

Whereas comparison of theoretically predicted signal availability and actual signal use was reasonable and meaningful, comparison of predicted accuracy from an optimal receiver using only 10.2 kHz with that from an actual receiver using three of the four Omega frequencies is much less meaningful. Not the least of the various problems is that the true location of the aircraft

at 1800 GMT was not known. The location of the aircraft was known before take-off and after landing. Theoretical predictions indicate abnormally poor fix accuracy (4 mile c.e.p. or more) at 1800 GMT in a generally equatorial belt from Khartoum through Colombo to Singapore but accuracy of 1-2 miles otherwise. For flights airborne at or near 1800 GMT, half of the abnormally poor landing errors were in the equatorial belt. Otherwise, errors on landing were typically slightly over two miles. Typical errors before takeoff were slightly better than one mile. Considering dissimilarities in theretical model and actual implementation and the crudeness of the spot comparison, the agreement is better than might be expected.

5. INDIVIDUAL STATION COVERAGES

INDIVIDUAL STATION COVERAGE ANALYSIS:

As previously noted, potential utility of a signal in a particular area at a particular time depends primarily on the signal structure and secondarily on the prevailing signal-to-noise ratio. The structure can be described in terms of the severity of competing types of self-interference: modal interference, long path interference, or proximity to the transmitter or antipode. Signal self-interference, particularly modal interference, will be addressed first.

SELF-INTERFERENCE

The fundamental design concept of Omega assumes that phase changes regularly with distance from a station. With the aid of predicted propagation corrections (PPCs), this circumstance is well approximated in most locations. Indeed, during daytime illumination conditions, the spherical waveguide between the earth and ionoshpere supports only about one propagation mode and the variation of phase with distance may be extraordinarily regular. At night, particularly near the equator, multiple modes may be supported. In this case the phase will be somewhat advanced or delayed from nominal depending on how the perturbing modes are phased with respect to the nominal dominant mode. Figure 5-1 shows the phase and amplitude perturbations expected from a simple model with one dominant mode and a single perturbing mode. It shows that when the preferred mode dominates by only as little as a few decibels, the resultant phase scatter is only on the order of ten centicycles. Under usual hyperbolic geometry this would correspond to about a one mile error at 10.2 kHz and less at the other frequencies. This is not of particular consequence to a general purpose worldwide navigation system of nominal accuracy such as Omega. Nor would the 14-16 db signal fade typically preclude reception. The problem occurs if the competing signal should become dominant.

The theoretical consequences of a change of modal dominance have been described by Swanson and Dick (1975). Suffice it to note that if different modes are dominant at different times or at different locations, then the

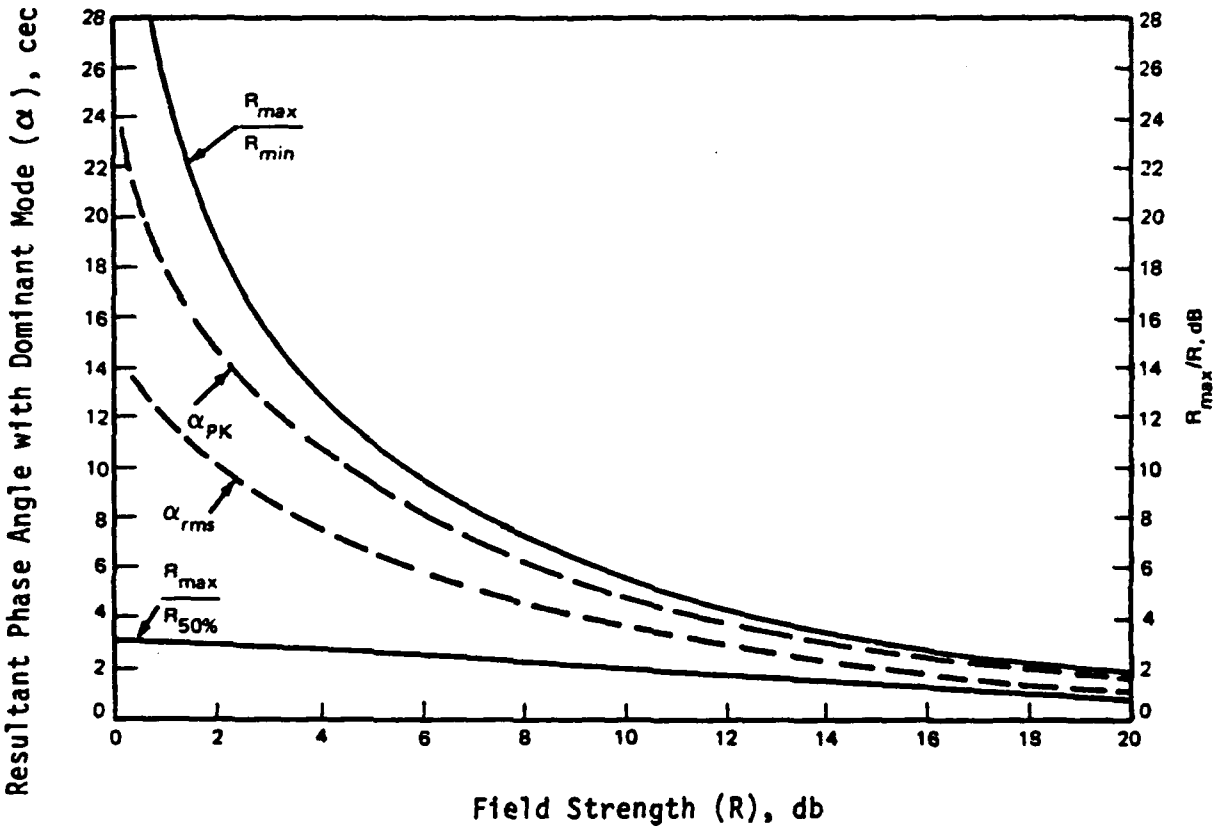

Figure 5-1. Nomograph Showing Phase and Amplitude Spatial Irregularities as Functions of First mode to Second mode amplitude ratios.

competing modes must necessarily be of equal magnitude at some point when transitioning from one region to another. When this occurs, the competing modes could be in phase in which case there would be no perturbation. They could be out of phase, in which case there would be no signal. More likely, the phasor sum will produce some intermediate phase at a significant amplitude. As normal temporal and spatial changes occur, the locus of the phasor sum will vary. Depending on whether this sum circles the origin, and how often, cycle jumps, cycle slips, or normal variation may occur. Navigational errors of a full lane may be introduced. The possibility of inducing blunders into the navigational solution warrants attention to the modal structure from the safety viewpoint as well as the viewpoint of nominal accuracy.

Potentially unpredictable behavior has weighed against the development for phase predictions for other than the usual first mode even in areas where the second mode might prove useful at night. A second disincentive for developing phase predictions for the second mode is that the phase stability is expected to be poorer than that of the first mode. For whatever reason, second mode phase predictions are not available and the first mode must dominate for Omega signals to be used in the usual way.

Another form of signal self-interference is long path interference in which the signal receive over the propagation path going more than half way around the world dominates over that received over the short path. This situation can easily arise at long range because of the non-reciprocity of vlf propagation. Obviously if a long path situation existed and was not recognized, a displacement to the east could be interpreted by an Omega receiver as a displacement to the west. If the direction of arrival is known, some limited research indicates long path signals may be used for navigation (Morris et al., 1982). However, there are some practical predictive problems. First, the predictions for long path are especially uncertain and largely unproven. Whether a signal is received by long path in an area

depends on minor differences in attenuation rates between the long and short paths which, combined, propagate completely around the world. Knowledge of these differences is not yet sufficient to predict long path boundaries with precision. Secondly, the effect on the signal will depend on the velocity and direction of an aircraft as well as the relative field strength of the signals over the long and short paths. In particular, once phase lock is obtained, the Doppler shift may be sufficient to keep a dominating long path signal outside the tracking bandwidth.

Near field limitations for Omega are essentially analagous to regions of skywave-groundwave interference encountered with high frequency signals. The usual waveguide model employed to assess signals at vlf becomes untractable at relatively short distances because of the large number of modes which must be considered. Details of nearfield limitations have been investigated near North Dakota by Kugel (1982; 1983). However, modeling has shown near field limitations to be azimuth and transmitter dependent. Near field limits shown on coverage diagrams are somewhat arbitrary range limits suggesting the range necessary to be free of skywave groundwave interference.

The antipode presents reception limitations somewhat analagous to those in the near field. Signals propagate outward from a transmitter in all directions and eventually will all reach a point on the opposite side of the earth at about the same time. Indeed, the field strength does indeed build up in the vicinity of the antipode. Effectively the antipode can be regarded as virtual signal source. Note that the antipodal limitation stems from a resonance condition from signals propagating in all directions through the spherical wave guide formed between the earth and ionosphere. It is a distinct limitation from long path which is a competition of signals from over two "paths" -- a long and direct path. Since it is very unlikely that one

would be attempting to rely on a signal near the antipode some coverage guidance uses a 2,000 Km radius to cause deselection--a value believed rather generous.

SIGNAL TO NOISE:

Although Section 2 provides full mathematics as to how to optimally process Omega signals in the presence of noise, this report has thus far offered little in editorial discussion of signal-to-noise limitations. This has been for the dual reasons that: 1) noise is not usually a consequential problem and 2) it would take an extremely inept user (or receiver design) to place undue credence on a noisy signal. This is in marked contrast to problems in identifying signal self-interference which has been discussed in detail. Never the less, noise does pose some limitations and these should be noted.

At the outset, a distinction should be drawn between natural noise, local man-made noise, and interference. It is only the natural noise which can be well addressed in terms of system coverage limitations. Man's activities are too varied and too localized to make any specific coverage predictions.

Natural noise at VLF is primarily due to impulsive radiations associated with lightning strikes in thunderstorms. Prediction of noise is based either on a global data base leading to CCIR noise maps or to a model based on radiations from thunderstorm centers. Both have their limitations. Both noise predictions vary seasonally and diurnally. Neither, of course, can predict precisely what will be happening at any given location at any given time. On the other hand, any receiver can easily measure the actual noise being experienced at any given moment. Further, measurement will reflet to some degree whatever additional noise man may be locally generating. Noise

prediction for Omega is of interest more or less exclusively to the system designer or major route planner. An actual navigator can easily measure the noise effecting him at the particular moment he needs to know.

"Clean" Omega installations which are more or less immune to locally generated noise are rare on aircraft but probably relatively common on ships. Acceptable installations are common on all platforms. Reception in aircraft is effected by stray power harmonics carried in currents throughout the skin of the aircraft. It is usual to perform a "skin map" before antenna installation to find a good location. Treboelectric ("precipitation") charging of aircraft is also common. Wicks are usually installed to dissipate this charge. Loop antennas have the reputation of being insensitive to precipitation static.

Apparently, actual receiver performance will depend on the quality of the receiver, care of installation, and actual environmental conditions on an instantaneous basis. Despite the statistical nature of noise prediction and other limitations on prediction of Omega signal-to-noise ratios, it is believed predictions are sufficiently accurate that a user who repeatedly fails to obtain as many usable signals as predicted would be well advised to check out his installation.

EXPERIMENTAL IDENTIFICATION OF SELF-INTERFERENCE

Because of the slow rise time of Omega signals and the fact that they are essentially continuous wave transmissions, the modal components combining to form the resultant signal cannot be directly observed experimentally. Nor, under typical receiving conditions at a stationary receiver, would it be apparent whether a signal was received over the long or short propagtion path. Thus indirect methods and scientific inference must be used in coverage

assessment. It is also a reason coverage assessment is so important; practical receivers are very limited in the means they may employ to detect self-interference.

One of the best methods of assessing signal character is to measure a signal while flying radially toward or away from a station. Although it is the character of the phase behaviour which is of primary interest, it is more convenient to measure amplitude. If only one mode is present, both phase and amplitude will vary regularly. If there are competing modes, neither will vary regularly. Since accurate knowledge of position is needed to interpret phase measurements which vary through a complete cycle each wavelength, amplitude is examined as knowledge of position need be only approximate to support interpretation. As amplitude also varies temporally, one prefers to examine data measured while the entire propagation paths remain dark. Differences may also occur if there are changes of terrain over which the signal propagates. This latter consideration is not usually too consequential unless signals propagate over regions of anomalously high attenuation such as the Greenland or Antarctic ice caps. Apparently terrain effects can be compounded if slant paths to stations are flown rather than true radials. Amplitude variations may also be induced by irregular solar activity. Interpretation of field strength as a function of distance measurements is greatly aided by performing measurements at several frequencies at the same time. Ordinary ionospheric temporal changes tend to effect all frequencies similarly. Likewise, changes in path geometry also tend to effect all frequencies. similarly. However, modal interference will not effect all frequencies similarly at the same place or time. A complication is identification of a region where a single mode may be dominate but not the mode usually prevalent and assumed for Omega. These areas may be inferred since they are contained within other regions where a modal interference boundary has been identified. They may also be inferred if fixed site temporal variations have been recorded. Since the usually assumed dominant mode expected during the day, an irregular temporal variations may indicate a change of modal dominance.

AD-A194 458 INDIAN OCEAN VALIDATION(U) COAST GUARD ALEXANDRIA VA 2/2
OMEGA NAVIGATION SYSTEM CENTER E R SWANSON ET AL.
01 SEP 87 USCG-ONSCEN-02-87

UNCLASSIFIED F/G 17/7 NL

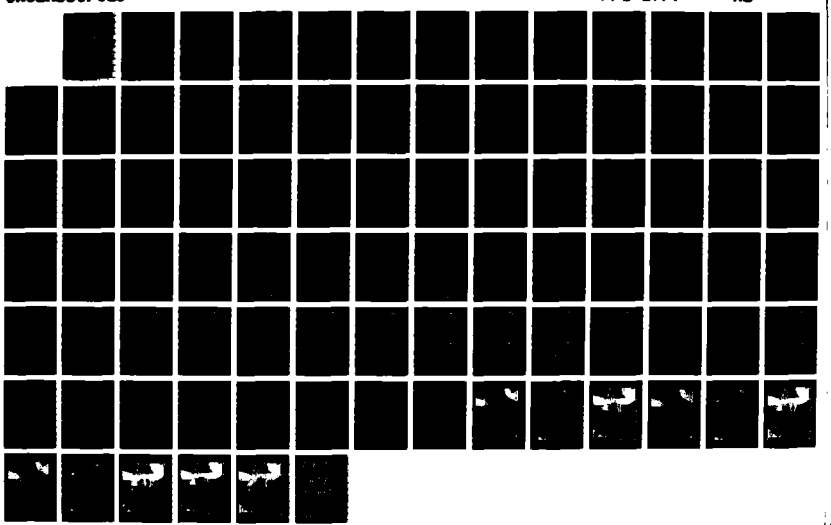

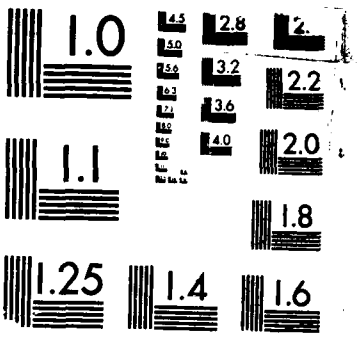

Since the primary method of determining coverage limitations in this validation is the interpretation of recordings of amplitude measure in aircraft flights throughout the region, some discussion of the practical limitations is in order. If strongly received signals are undergoing marked amplitude variation with distance which is not correlated between measurements at various frequencies, it is easy to identify the region as one of modal interference. Smooth variations do not necessarily indicate the signals are appropriate for use in the area. First, there may be a dominant mode but not the usual one. Second, if range variation is limited, it might be that the observations only cover a small sample of constructive interference. If signals are weak, it may be very difficult or impossible to distinguish between modal interference and the normal variations expected when trying to record a weak signal. One advantage of conducting the coverage assessment with attention to theoretical global coverage approaches is that this tends to validate the global coverage assessment methods themselves. Thus, confidence is gained beyond the simple agreement that may occur at a particular location and time. In this the detection of any unambiguous exceptions is particularly important. As Einstein observed, no number of experiments can prove a theory true, but it only takes one to prove it false. In interpreting records, if a weak signal was expected and a noisy track indicative of a weak signal observed, it would be interpreted as compatible with theoretical prediction. If normal propagation conditions were expected to prevail, this compatibility of the records with expectations would not necessarily rule out self-interference; simply indicate that with the quality of the recording nothing incompatible was indicated.

Coverage boundaries shown on overlays are based on a criterion wherein phase variations from nominal due to higher order modes are not more than 20 cecs. Parametric computations use a 1 db margin for the preferred mode. These criterion are essentially equivalent if two modes are competing. In this case, the amplitude fades is shown on Figure 5-1 to be 28 db. While the criterion can be used easily within the mathematical models, it is not reasonable to attempt to apply such a large fade criterion to data available in the present study. As already noted, the measurement method when using the LTN-211 introduces dynamic range limitations. These would generally be

expected to limit the maximum observable fade to less than 28 db. Alternatively, the spectrum analyzer measures coherently so the maximum apparent fade would be the difference between the signal level and noise which, except in the near field, is also expected to be less than 28 db. As a practical matter, fades near but not over 10 db could generally be identified as occurring in a region containing some modal interference but not an areas sufficiently near a boundary to produce larger fades. Fades above 12 db were usually interpreted as indicative of serious modal interference as might occur near a boundary. Fades of 11 or 12 db, or occasionally larger when close to a transmitter, were interpreted with care considering the expected field components. Maximum fades observed were generally less than 20 db.

Perhaps insight into the interpretation of amplitude recordings may be obtained by comparison with a radiologist interpreting x-rays. Both recordings show the cumulative effect of signals (Omega or x-ray) from the effects of various intervening media (portions of the anatomy or geophysical conditions on path). In either case the reader has a fundamental knowledge of what is to be expected under normal and abnormal conditions. The radiologist has knowledge of anatomy and also the pathology of abnormalities--such as whether tumors or aneurysms are likely to have smooth or convoluted edges. The physicist knows the appearance of modal interference especially as compared with variations caused by diurnal or regular spatial changes, solar bursts, or long path interference. Both readers know the limitations of the measurement process. It is also important to note that both readers have access to ancillary information, e.g., medical reports or fixed measurements or predictions.

Before attempting to analyze the amplitude measurements recorded in flight, each flight was annotated to indicate the prevailing illumination conditions on paths from each station. Records were then read in accord with the principles mentioned. Since the records in loose leaf from occupy over 1/3 meter of shelf space, this was a substantial task. Detailed appraisals by station follow.

SUMMARY OF INDIVIDUAL STATION COVERAGES

NORWAY:

No modal or long path coverage limitations are expected throughout the region. Depending on time of day, weak signals were predicted for South Africa, Australia and portions of the south western Pacific near 0500 GMT.

No modal or long path limitations were noted. Weak signals were not encountered in the western Pacific, nor would they have been expected considering the flight schedule. Signal-to-noise ratios near South Africa appeared to be better than the -20 to -30 db expected during the worst times. However, signal-to-noise ratios in southern Australia appeared worse than the -10 to -30 db expected there.

An anomalous field strength variation was noted in the Bay of Bengal. It occurred on both flights 8 and 19 and can be associated with bearing from Norway rather than time of day. The variation is shown in Figure 5-2 as recorded on flight 19. It is imperceptible at 10.2 kHz, noticeable at 11 1/3 kHz and marked at 13.6 kHz. This type of effect has not been observed before. The effect appears to be confined to a small geographic region.

LIBERIA:

With some limitations, Liberia has been expected to provide excellent service throughout the extended Indian Ocean area.

The major limitations in the extended Indian Ocean region and Australia have been expected to be 13.6 kHz modal interference in the Arabian Peninsula and northeast Africa and low signal levels at certain times in Australia.

For the particular flight times, good signals were expected and observed in Australia and up through the Philippines. The flights on which modal interference would be expected in Africa are 10, 11, and 12 flying from Bahrain to Khartoum to Nairobi to La Reunion. These just skirt an

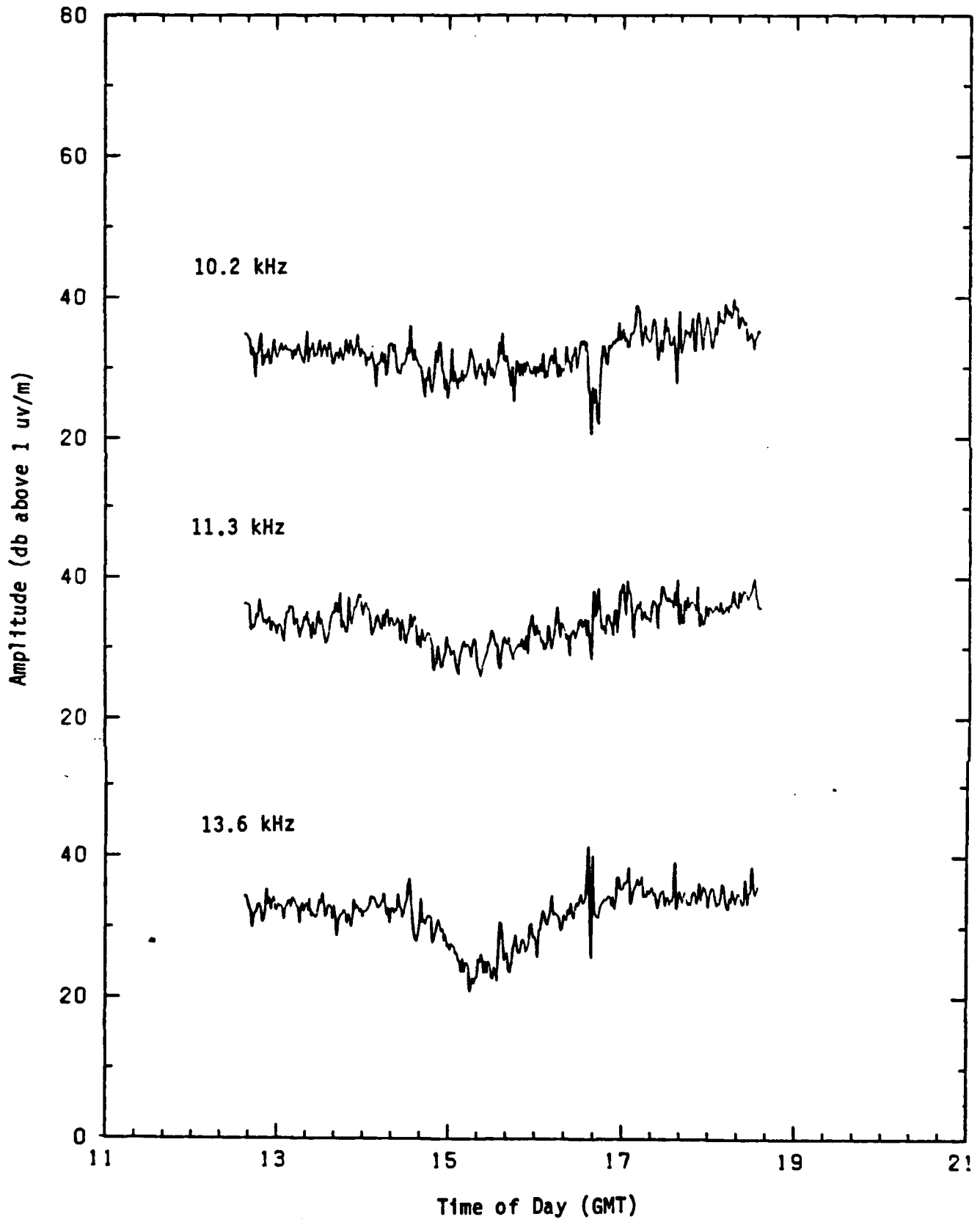

Figure 5-2. Amplitude Variation of Omega Norway in Bay of Bengal

interference region shown on overlays for 10.2 -kHz but not currently modeled parametrically. The data do suggest some competing mode at 10.2 kHz but not sufficient to preclude reliable operation. That is, the expectations were essentially confirmed. One expects 13.6 kHz to have modal interference on the night portions of all of these flights. Of the flights, that from Bahrain to Khartoum shows fades of about 12 db at both 12.0 an 13.6 kHz confirming significant interference in the region. The flight from Khartoum to Nairobi showed little presumably because it was flown largely a constant distance from Liberia. That from Khartoum to Nairobi did not exhibit 13.6 kHz modal interference, although it would be expected to have been observed. However, moderate interference was observed at 12.0 kHz on this flight. It is possible the 13.6 kHz modal boundary extends further east toward La Reunion than presently believed. However, no interference was noted on other flights from La Reunion (excepting possibly flight 14).

One difference: A strong signal was observed in the south Australian area in flight, at Perth and on three ships while a weak one was expected.

HAWAII:

Hawaii was expected to be nearly useless on all the test flights in the Indian Ocean area. An exception might have been flight 10 from Bahrain to Khartoum except that the Hawaii segments were used for injection on this flight so no data were obtained. The limitations were, however, identified differently between the overlays and the parametric model. Overlays identify modal interference over the entire area whereas the parametric model shows 24-hour long path dominance in the Arabian Sea. Additionally, the parametric model shows a very small area of potentially usable weak signal southeast of the Cape of Good Hope.

While it might prove academically interesting to attempt to determine the nature of the limitations in the region, a practical complication is the extremely low signal levels often received by whatever means. Thus, as a practical matter, the signals are not likely to be particularly useful in any case. In a broad sense, the predictions are confirmed.

The data do seem to suggest that there may be a brief period of signal utility near 1800Z on flights 13 and 14 (between South Africa and La Reunion). This would be in accord with the parametric model but not the overlays.

NORTH DAKOTA:

No solid coverage from North Dakota is predicted for Australia, the Indian Ocean or East Africa. Low level signals are expected some of the time throughout East Africa while low level signals may also be occasionally useful in Australia.

As the North Dakota segments were routinely used for injection in Australia and the Indian Ocean, little data were obtained. Other segments were used during portions of flights from the Arabian Peninsula to East Africa. In these cases, reception appeared better than expected being free of interference and at fair signal-to-noise ratio.

LA REUNION:

Coverage predictions show solid coverage over most of the Indian Ocean and Australia. Overlay and parametric predictions both flag a small areas in the La Reunion near field at 10.2 kHz. However, the overlays for 13.6 kHz also show a very marked region of modal interference extending almost to the Philippines. Conversely, the 10.2 kHz parametric coverage shows modal limitations in northwest Africa which are not indicated on the overlays.

One of the most obvious features of the flights was the extensive modal interference on 13.6 kHz northeast of the station. This was observed on all flights where it would be expected. As predicted, the region appears to extend at least to Singapore. Some modal interference is also seen in the Arabian Sea but perhaps not sufficient to cause the region to be flagged by normal coverage considerations. There is also a suggestion that interference toward South Africa, while present, may not be sufficient to warrant flagging the region. Effectively, 13.6 kHz coverage is in accord with predictions.

Coverage at 10.2 kHz is very much more extensive than that at 13.6 kHz. Modal limitations suggested by the parametric model between Khartoum and Nairobi appear to be an artifact of that model and not real, although, of course, it is possible that the second dominance was so complete as to indicate regular variation. The size of the near field limitation about La Reunion is about right but the shape is more realistic on the overlay.

All in all, coverage is much as predicted. This amounts to a considerable triumph for full wave theory, especially in predicting the 13.6 kHz coverage limitation to the northeast.

ARGENTINA:

Argentina is expected to provide solid coverage in the western but not in the eastern Indian Ocean. Additionally, solid coverage in South East Australia and New Zealand is expected. Important additional coverage is expected in the Bay of Bengal although the signal-to-noise ratio may be weak near 1200Z. The limitation is primarily due to Antarctic shadow although 13.6 kHz overlays show modal limitations also within the shadowed region.

Flight data are very much in accord with expectations.

AUSTRALIA:

Coverage diagrams for 10.2 kHz show limitations due to near field in southeastern Australia and limitations due to modal interference or other limitations in the important areas of the Arabian peninsula, Arabian Sea, India, the Bay of Bengal, Indochina, and much of the South China Sea. Coverage throughout most of Australia and the vast majority of the Indian Ocean is expected to be solid. Limitations at 13.6 kHz are expected to be more severe. Use in the Indian Ocean north of the equator is expected to be precluded at night by modal interference while the near field region in southeastern Australia is expected to be more extensive than at 10.2 kHz and preclude operation at night throughout the Tasmanian Sea.

Coverage diagrams for 10.2 kHz show limitations due to near field in southeastern Australia and limitations due to modal interference or other limitations in the important areas of the Arabian peninsula, Arabian Sea, India, the Bay of Bengal, Indochina, and much of the South China Sea. Coverage throughout most of Australia and the vast majority of the Indian Ocean is expected to be solid. Limitations at 13.6 kHz are expected to be more severe. Use in the Indian Ocean north of the equator is expected to be precluded at night by modal interference while the near field region in southeastern Australia is expected to be more extensive than at 10.2 kHz and preclude operation at night throughout the Tasmanian Sea.

Coverage appears to be as expected. Signals on flight 17, Diego Garcia to Bahrain, were weaker than expected. No interference was noted at 13.6 kHz suggesting perhaps the boundary is too conservative (i.e., to far south). However, it might also be that the second mode was completely dominant for the flight. While the data may be suggestive of a 13.6 kHz coverage boundary change, none is yet warranted. Elsewhere over the extended Indian Ocean, predictions appear quite good. Flight 7 from Alice Springs to Singapore is a particularly good example. It shows regular variation at 10.2 and 11 1/3, but a modal complexity at 13.0 and 13.6 kHz about where predicted in Indonesia.

The near field region of Australia is best assessed by analyzing the data in close comparison with the predicted field including the predicted interaction of the various modes. Particularly at 13.6 kHz the predicted limits are established by the first minimum on westerly radials while the second minimum controls on easterly radials. The range at which these minima occur is predicted to be quite constant independent of direction from the station. On the flights in the directions of Darwin, Alice Springs and Perth, the second minimum is noted to occur at a range of 2.2 $\pm$ .1 MM and have a magnitude of 14 $\pm$ 2 db. Quite obviously significant modal interference is occurring. The question, however, is whether or not this second minimum should define a modal boundary. Theory predicts the observed fades and indicates the first mode should exceed the competing mode by several decibels. Thus, the data can be interpreted to confirm the present theoretical boundaries. It would, however, be useful to conduct a ground

based near field survey such as was conducted about North Dakota (Kugel, 1982).Long term monitoring at Alice Springs might also indicate the utility of signals throughout normal temporal variations.

JAPAN:

Theoretical predictions indicate use of Japan should be limited in the Indian Ocean due to modal interference at night. Additionally, use will be restricted in east Africa due to long path or low signal levels. Coverage throughout Australia should be good except possibly in the extreme west. Depending on prediction, indications are that 10.2 kHz but not 13.6 kHz may be usable in the Arabian peninsula, Arabian Sea and the Bay of Bengal.

Because of differences between parametric and overlay coverage and the complexity of coverage contours in the area, many of the flight records of Japan are of abnormal interest.

Unfortunately, some of the records of greatest interest cannot be interpreted unambiguously. Particularly interesting flights include 8, 9, 18, and 19 (to and from Singapore, Columbo, and Bahrain) and flight 20 to Perth.

Flights 9 and 18 flew the same path between Columbo and Bahrain in opposite directions. Measurements at 10.2 kHz do not agree between flights nor do those at 11 1/3 kHz agree either between flights or resemble the equivalent 10.2 kHz measurements. Measurements at 13.6 kHz are noisy but there is a similarity between measurements from the two flights apparently indicating greater amplitude variation than would be expected if a single mode were dominant. Tentatively, one would conclude that 13.6 kHz is undergoing modal interference in the Arabian Sea and that the predictions are correct in this regard. No conclusions are possible for 10.2 kHz.

Flights 8 and 19 were between Singapore and Columbo with flight 8 detouring off the great circle path well into the Bay of Bengal. Both flights show modal interference at all frequencies. While the data cannot differentiate between the 10.2 kHz boundaries indicated by parametric model or overlay, either one appears to be reasonably well located.

Coverage from Japan near Perth at 10.2 kHz is a matter of special interest. Parametric coverage indicates the signal is expected to be perturbed but usable at Perth. However, an extrapolation of the boundary identified in the Western Pacific validation suggests the limit is significantly to the West. Overlay coverage 10.2 kHz suggests the boundary is to the East of Perth while that for 13.6 kHz shows the boundary to the West. Where is the 10.2 kHz boundary? The last leg of the flight into Perth from Singapore was flown on a radial from Japan. No marked modal interference was observed on 10.2 kHz or any other frequency. Nor, indeed, was significant modal interference observed when flying out from Perth toward Melbourne although, in this case, the flight was more or less tangential to the Japan radial and hence one would not necessarily expect to observe an interference pattern. Never the less, lane slips have been long observed at Perth during transitions and often phase variation throughout the night is quite irregular at 10.2 kHz (although not necessarily at other frequencies). How can this be?

Full wave computations at 10.2 kHz show clear first mode dominance by more than 20 db on a southerly (180 degree) radial from Japan at all ranges beyond the near field. However, for a radial South by Southwest, 235 degrees, several modes contribute significantly. Near the equator, three modes are within a spread of only 3 db on this radial. Thus a two mode model is too simplistic for this bearing. Full wave mode sums showing the amplitude expected on various radials from Japan toward Perth were computed for the test plan (figures 5-3 and 5-4). Apparently the interference phenomona is not so much a general feature of radial distance from Japan but lateral displacement transverse to the radial near Perth. This is a most unusual expectation but illustrative of what can happen with more than two modes of significant amplitude. The computations suggest a boundary perhaps 140 miles east of Perth in the vicinity of Perth but at or West of Perth both to the North and South. A complication is that the modal boundary would then curve East to the 192 degree Perth bearing near the equator before shifting again to the West eventually reaching the northern portion of the South China Sea. This is close to the present parametric coverage with the important exception of the area of Perth itself. Present overlay coverage is good if slightly conservative and can be modified to indicate some coverage along the Australian coast near and to the north of North West Cape.

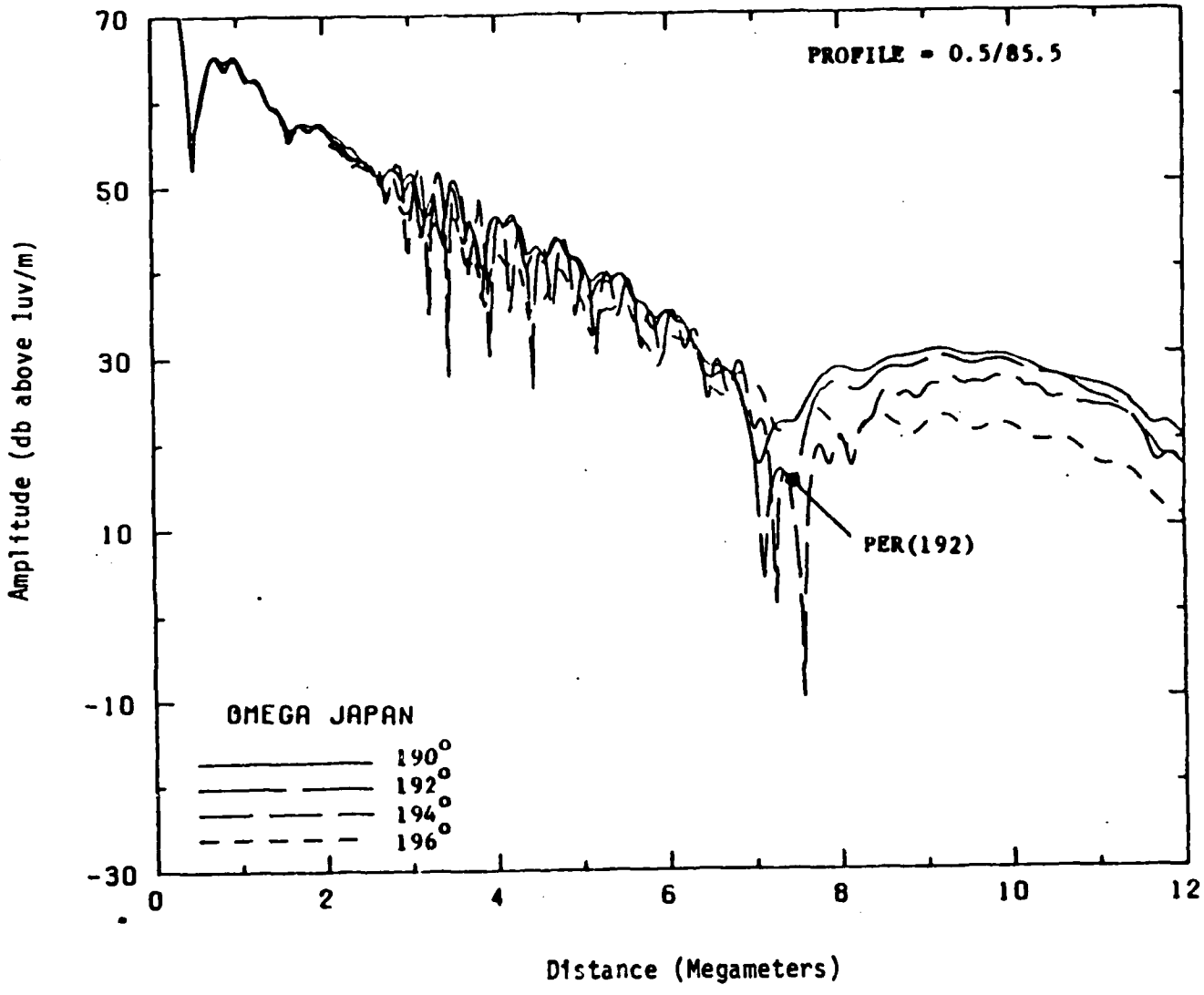

Figure 5-3. Predicted 10.2 kHz Nighttime Signal Level on Various Bearings from Japan toward Perth (PER).

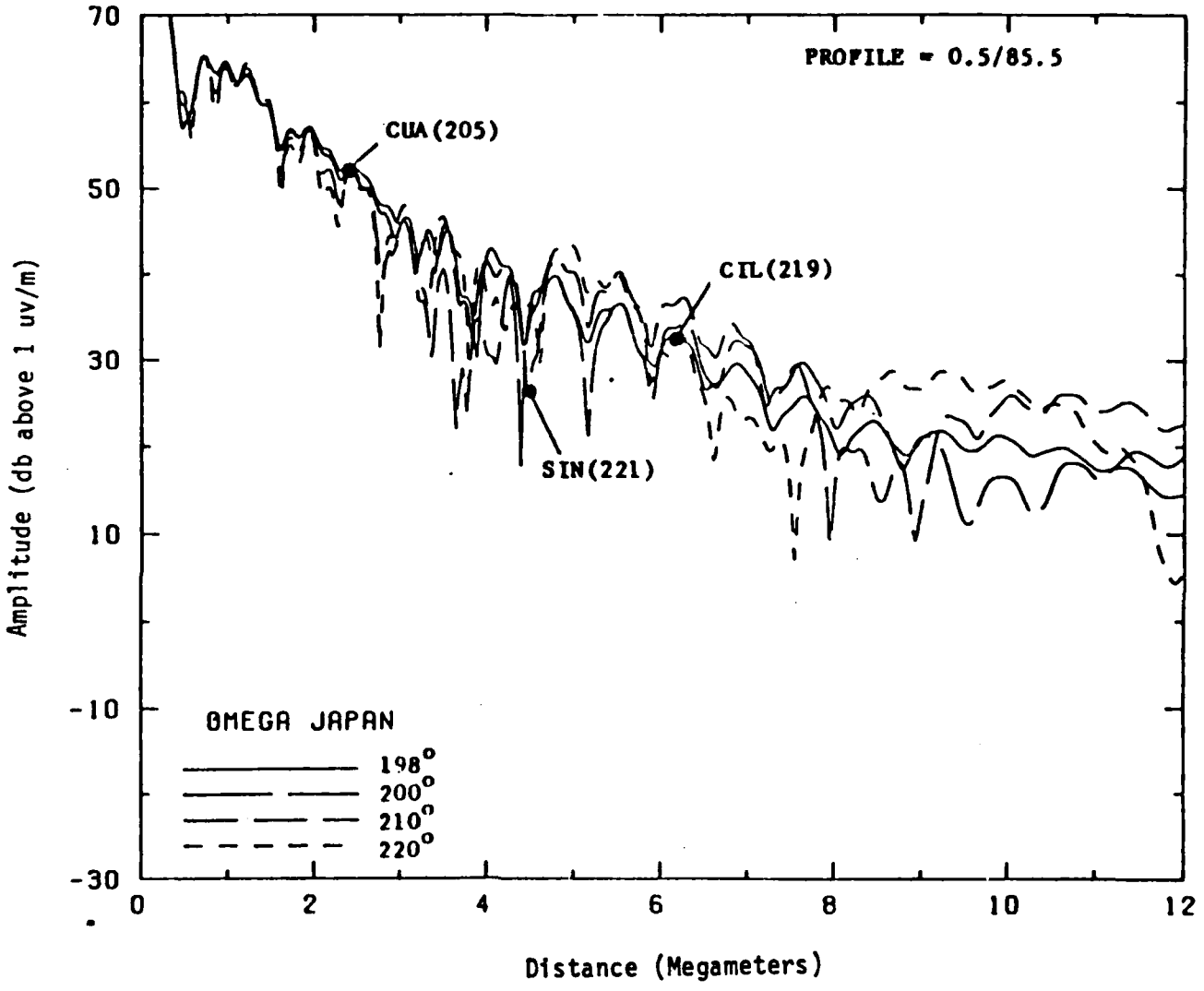

Figure 5-4. Predicted 10.2 kHz Nighttime Signal Level on Various Bearings from Japan toward Cubi Pt., Philippines (CUA); Cocos Is. (CIL) and Singapore (SIN).

The question should be asked as to why the modal limitation at Perth was not observed on a flight program designed to detect it. The answer can be seen in figures 5-5, 5-6 and 5-7 which show phase recordings at Perth over several nights including that of the inward flight on 17 September. Ordinarily the phase is seen to be exceptionally erratic as might be expected if it resulted from the sum of several destructively interfering modes. However, on the 17th itself, the phase variation was normal except for a cycle slip at sunrise. Apparently the ionosphere was just sufficiently abnormal to yield stable results on the one nite. This is a good illustration of the need for long term ground monitoring in critical areas.

Circumstances at Perth, with several modes mutually interfering, also illustrate how occasional local areas may exhibit coverage counter to the usual trend in that 10.2 kHz coverage may be excluded while that at the higher frequencies is not.

The observations and detailed computations warrent a boundary adjustment of the interference region near Perth. The general boundary above and below Perth seems to be much as computed by the parametric model. However, the boundary should be changed to show the interference region extending slightly east of Perth near Perth and toward Southwest Australia, that is, more toward the limit shown on by the coverage overlay.

With the foregoing exception, coverage within the extended Indian Ocean area for Japan was consistent with expectations.

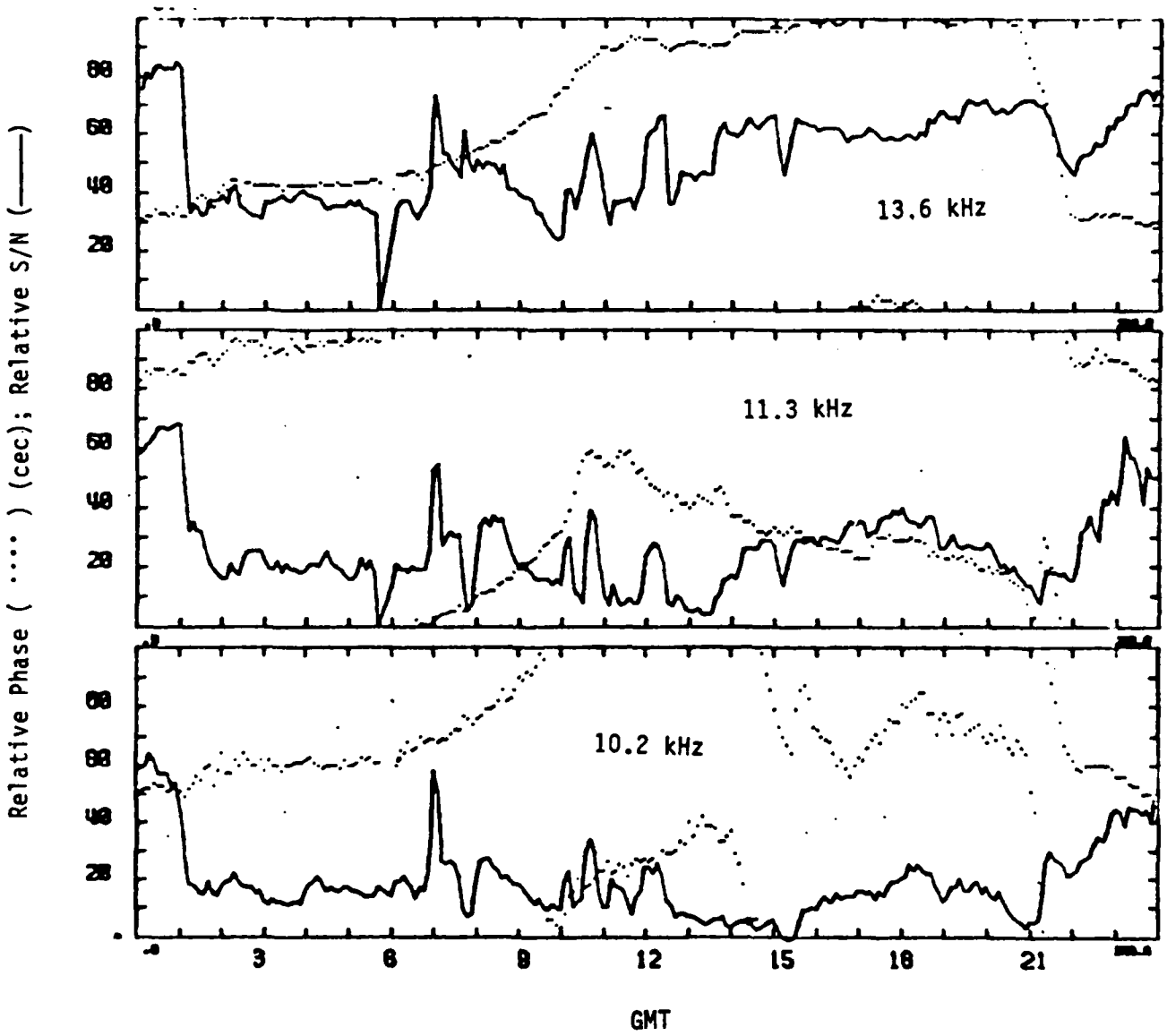

Figure 5-5. Relative Phase and Signal-to-noise Ratio (S/N) of Japan Recieved in Perth, Australia 16 September 1983.

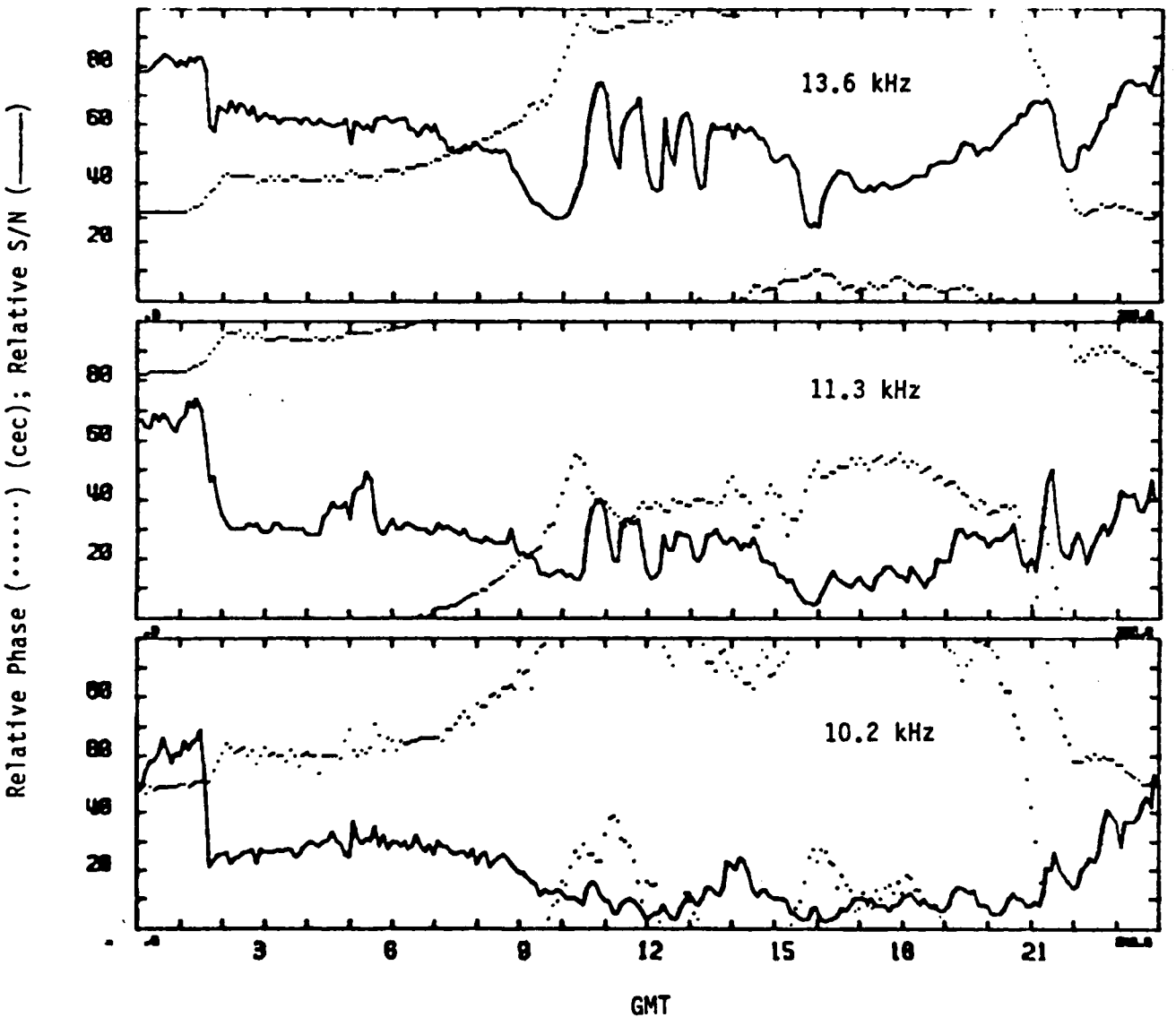

Figure 5-6. Relative Phase and Signal-to-noise Ratio (S/N) of Japan Received in Perth, Australia 17 September 1983.

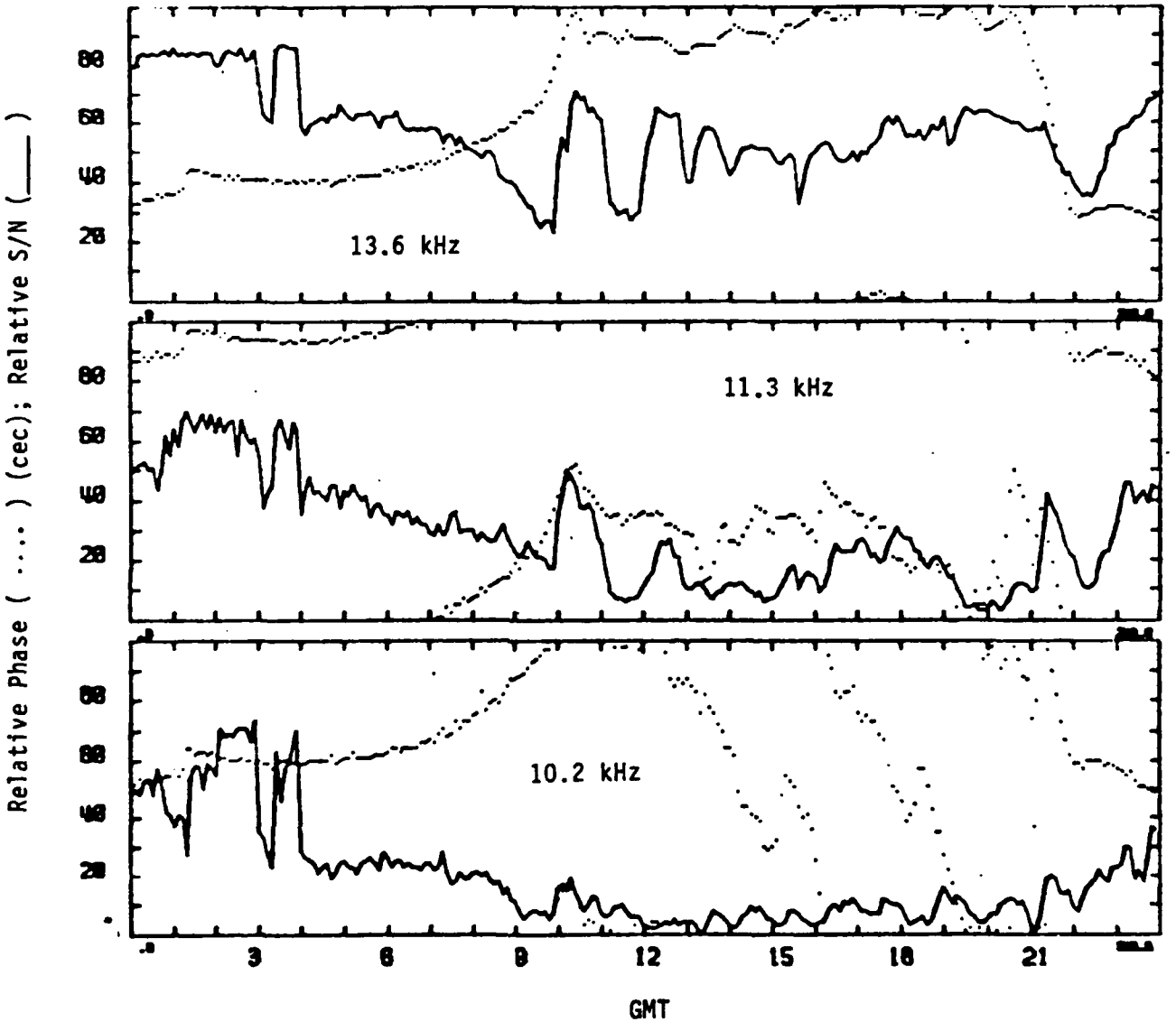

Figure 5-7. Relative Phase and Signal-to-noise Ratio (S/N) of Japan Received in Perth, Australia 18 September 1983.

SHIPBOARD MEASUREMENTS

As previously noted, equipment was installed in three merchantmen operating in the area: MV NEDERBURG, MV SIENA, and MV VISHVA MOHINI. The equipments included both Omega and NAVSAT and automatic recording of both types of information. Because of the arranged conditions and the fact that for tne most part the ship tracks were very straight and predictable, it is believed that a spline smoothing technique applied to the NAVSAT fixes could usually provide an adequate "reference" for Omega from which most significant error could ususally be attributed to Omega.* Thus, the Omega outputs could be processed to provide phase errors on various lines-of-position as compared with predictions. Also recorded was the signal-to-noise ratio deduced from phase variance for each of the Omega signals received.

It should be mentioned that the equipments were operated by the respective crews of the ships as an adjuct to their normal duties. Under these conditions, their efforts can be much appreciated and the good data obtained gratefully analyzed while never the less anticipating some incidental data errors due to the necessity of personnel giving higher priority to navigation of their ships. These circumstances dictate a data processing approach which is defensive of incidental errors in the data. In particular, recognizing regions of modal interference would be difficult. This is not only because of the slow speed of the vessels but also because of the difficulty of distinguishing between unusual events such as a lane slip due to modal interference as compared with one due to incidental equipment malfunction. It is especially difficult to distinguish these after the fact when proper operation can no longer be verified. A conservative data processing approach relying on medians of grouped data sets is appropriate.

Shipboard data augments the other measurements in two important areas:

1. Indicates signal reception aboard operating merchant vessels, and

2. Provides data from the southern portion of the Indian Ocean which was not otherwise well covered (Cf. Figure 5).

---

* results cited herein are based on only those Omega fixes simultaneous with a NAVSAT pass.

Observed signal-to-noise ratios (SNR's) are compared with predictions in Figure 5-8. While the results are less clear cut than it may appear, it will be well to discuss the comparisons first and caveats second. The comparisons are for 10.2 KHz only although SNR's were recorded for 11.33 KHz and 13.6 KHz as well. In general, SNR's at the other frequencies were slightly more favorable than at 10.2 KHz so that directing attention to 10.2 KHz is appropriate. The initially tabulated data included observations taken on various voyages. Analysis was restricted to the voyages indicated in Figure 5 which occured from June to August while measurements on each voyage were grouped with a single median taken to represent conditions on the voyage (analysis was further restricted to voyages with more than one single observation). Comparison predictions were taken from the parametric predictions of Appendix B. In the event coverage was anticipated to be modal, antipodal or the change substantially during a voyage, no comparison was made. Major changes in predictions occured, for example, on measurements of Argentina where a voyage crossed the Antarctic "shadow" line. Approximately 100 comparisons were obtained for observations within two hours of 0600Z and another hundred comparisons for observations within two hours of 1800Z. Comparisons at the two times were orginally plotted separately but found to be remarkably similar. Figure 5-8 contains data for both times. The ordinate and absicissa labels follow the code of Appendix B showing signal-to-noise ratios in db in 100 Hz bandwidth.

Since perfect agreement would have yielded all data confined to squared on a 45-degree diagonal, several features are apparrent. First, only two percent of the time was the observed signal-to-noise ratio worse than prediction. Prediction and observation agreed about half the time (46%). The other half of the time observed SNR's were more favorable than predicted. The discrepancy seems to be about 10 db or perhaps slightly more. If real, this would be welcome new since it indicates substantially better reception than was expected. Several factors need to be mentioned.

Use of parametric results in Appendix B for this comparison was somewhat inappropriate since, strictly, Appendix B applies to the vernal equinox while the ship data were measured in the austral winter. In the austral winter the noise is zero to six db less. This could easily explain some of the

Observed SNR	#	3	2	1	0	Blank
Blank 0			2 4	6 5	12 11	31 31
0 -0's		1	12 2	11 11	5 3	
1 -10's	1 1	4 1	3 3	5 13	1	
2 -20's	2 1	1	1 3	1 1		
3 -30's	4 4		1			
# 40	1 2			Percentage Occurrence Upper entry 0600 GMT Lower entry 1800 GMT		
Grade Range (db)	# 40	3 -30's	2 -20's	1 -10's	0 -0's	Blank 0
	Predicted SNR					

Figure 5-8. Shipboard Signal-to-noise Comparison

difference--but probably not most.

Larger uncertainties may be associated with the calibration of the phase variance measurements within the Magnavox to SNR's. Acalibration curve developed by Magnavox was used. Past work at NOSC has indicated a curve

differing from that of Magnavox by a few db. There may also be differences from one receiver to another and the particular unit used was not specifically calibrated. More inherently, the true SNR can be related to measurement only knowing the noise statistics. While further research might enable one to attribute the apparent results to local variation of noise statistics, the practical result would be as already indicated: better performance than heretofore expected.

Another possibility might be that merchant ships are substantially quieter than the land sites from which the noise base was derived. Again, this conclusion would lead to the same practical result: better performance than heretofore expected.

A safe interpretation of Figure 5-8 is that the merchant vessels experienced a signal environment at least as good as expected. Since the expected environment is more than adequate for practical navigation, there should be no unexpected limitations to maritime applications in the area.

The effect of the antarctic "shadow" line on reception of Argentina was evident in the recorded observations on which Figure 5-8 was based. These were examined to determine if the changes in SNR were occurring in the locations expected or whether, perhaps, some diffraction or other effect were causing marked difference. No differences were discernable.

A region of major disagreement was found in the extended area south of Australia and to the southwest of Australia when receiving Liberia. This was primarily expected to be SNR level "2" (-20 to -30db) while in fact, it was level B (Blank) (>0 db). The disagreement was at least 20 db and was observed on all three ships. Ground based measurements at Perth also show markedly better SNR than predicted for Liberia. Reception of a strong signal from Liberia in this region is especially welcome becasue of the effects of Antarctic absorption on signals from Argentina. Geometrically, Liberia subtends an angle of about 180 degrees with Hawaii in this area--a most welcome circumstance.

Phase measurements comparing lines-of-position (LOP's) with those expected for the postion derived from the NAVSAT observation were also compared on a spot basis. Generally, signal reception was about as expected. Line of position descipancies were on the order of ten centicycles--about as expected.

In general, the shipboard data indicate that stations reception at sea is at least as good as in the air but most probably better. Coverages is clearly adequate in the southern Indian Ocean and, in the case of Liberia, substantially better than expected.

6. SYSTEM COVERAGE AND ERROR CHARACTERIZATION

SYSTEM COVERAGE:

In the previous section, the structural suitability of signals for navigation was assessed together with their adequacy with respect to atmospheric noise sources. This is a necessary but not sufficient part of determining system coverage. Additionally, it is necessary to determine the inaccuracies which may be induced in the phase measurements which will eventually be processed to obtain a fix. In this way the performance of an optimum receiver can be assessed.

The 10.2 kHz parametric model was shown in the previous section to predict modal boundaries reasonably well. By inference, the model can, thus, also predict the statistical effect on accuracy of a multimode signal environment where competing modes may cause errors but not lane slippage. Similarly, one expects the effects of noise to be statistically modeled reasonably well. Other errors include the inherent phase repeatability from day to day due to minor ionospheric differences, σ_r, and the predictive error, σ_p, due to inability to predict the long term average phase properly. The existing error budget has been:

TABLE I

ERROR BUDGET FOR 10.2 kHz PARAMETRIC MODEL

Path Illumination	σ_r	σ_p
Day	3 cec	4 cec
Night	5	4
Transition	4	15

We must now compare this error budget with actual observations in and around the Indian Ocean.

Fixed land based monitoring has long been conducted worldwide including the region. A subset of semi-monthly phase difference measurement blocks from sites in and around the Indian Ocean over a several year period was selected. This very large data base then was processed by the method used in the North Pacific validation. Of particular interest are cumulative

statistics for the median random propagational variation, median "absolute phase error", and median "rms variation about the absolute phase error". Since two propagation paths contribute to a phase difference measurement, the random propagational variation so obtained is equivalent to $\sqrt{2}\,\sigma_r$ while $\sqrt{2}\sigma_p$ is equivalent to the rss combination of the other two terms. Estimates were made for 24-hours, "Day" and "Night". During the "Day", σ_r computes to be 2.6 cec while 4.1 cec is obtained at night or on a 24-hour basis. Obviously, the agreement appears to be excellent. However, there is an important difference. As used within the parametric model, "Day" or "Night" applies as the entire propagational path is illuminated or dark. In combining the Indian Ocean ground based statistics, "Day" was taken to be from 0500 - 0700 GMT while "Night" was 1700 - 1900 GMT. While these periods reasonably represent the region, they do not represent the component propagation paths forming a phase difference. By parametric standards, most of statistical entries in the cumulative tables represent transitional propagation conditions. Thus, the long established error budgets could be slightly conservative. The interpretive distinctions between "Day" and "Night" become much more important in comparing estimates of σ_p as the gross prediction bias during transitions can be expected to override the nominal "Day" and "Night" estimates. Computation yields σ_p = 9.2 cec (Day), 9.6 cec (Night) and 10.7 cec (24-hr). By comparison, a path or collection of paths undergoing transition one third of the time would be expected to yield an rms bias of 9.3 cec while one undergoing transition half the time would yield 11.0 cec. Since the actual illumination mix has not been determined, the agreement can only be called nominal. However, the results are certainly compatible with the assumed budget.*

Day and night predictive biases also may be assessed through perusal of average phase difference errors measured for the semi-monthly data blocks

* Similar estimates were also made for 13.6 kHz, although the utility of these is somewhat moot as the parametric model is not yet extended to this frequency. Estimates of $_p$ averaged 10% higher corresponds to a 17% greater navigational precision because of the shorter wavelength. Estimates of $_r$ were markedly lower ranging from 2.1 to 3.8 cec. These suggest that in multi-frequency fixing, the 13.6 kHz accuracy will dominate.

under the appropriate illumination conditions. This was done manually for the various locations in and around the Indian Ocean to determine: 1) whether the nominal 4 cec error budget for predictive errors was realistic and 2) whether any particular stations/sites, or lines of position exhibited anomalous errors. Predictive biases over single paths appear about 4 cec or slightly less during the day and 4 cec or slightly more at night. No anomalous predictive biases were found.

Another estimate of phase measurement errors can be obtained from actual observations at sea on several merchant ships. These ships were especially instrumented with Magnavox MX 1105 receivers to provide meaningful comparisons of measurements from Omega with those from Navsat. Ordinarily, such comparisons yield only differences which cannot properly be attributed to one system or another. Whereas Navsat provides outstanding accuracy to a docked ship, accuracy degrades at sea. Should high ship dynamics result in large unknown set and drift, Navsat fixes may well be worse than those obtained with Omega. For the installations discussed here, merchantmen were operating on ordinary trade routes with very low dynamics. Further, speed and heading were automatically input to the Navsat equipment while special cubic spline smoothing was employed in making the fix comparisons. Under the arranged conditions, it is believed that usually most of the discrepancy can be attributed to Omega. To avoid complexity introduced by combining various lines of position to obtain a fix, the best comparison for the present purposes will be that of phase difference discrepancies between the various lines of position which can be measured and the Navsat indicated ship position. The median line of position error obtained from the median errors on each of several voyages from each of the several ships was 15.5 cec at 10.2 kHz. This suggests a typical instantaneous measurement error of $15.5\sqrt{2}$ = 11.0 cec over each of the component propagation paths which may by compared with the rss combination of σ_r and σ_p as measured over 24-hours at land sites, viz: $\sqrt{4.1^2 + 10.7^2}$ = 11.5 cec. Apparently, the observed phase discrepancies at 10.2 kHz at sea are in good agreement with those observed on land and, as previously shown, in agreement with the assumed error budget.*

* The median discrepancy at 13.6 kHz was 11% higher indicating 17% higher accuracy capability using 13.6 kHz.

It is not reasonable to attempt a similar comparison of airborne phase measurements. Although a Global Positioning System (GPS) receiver was carried, there were few periods of common operation. Further, asynchronism in the data recording could prove significant at aircraft speeds.

The foregoing and the previous sections indicate that individual station coverages at 10.2 kHz are well represented by the parametric model and further that the assumed error budget is reasonable. Therefore, accuracy forecasts based on the parametric model are credible in the Indian Ocean region. Figures 6, 7, 8 and 9, reproduced from the 1984 Seattle meeting of the International Omega Association, show accuracy expected from an optimal receiver using 10.2 kHz transmissions alone. They may be considered validated for the Indian Ocean. The figures show excellent accuracy at 0000 and 0600 GMT throughout the Indian Ocean while figures for 1200 and 1800 GMT show somewhat poorer accuracy in many areas with markedly worse accuracy at times in a belt from the Arabian Sea through Sri Lanka, the Bay of Bengal, Singapore, the Straits of Malacca, and into the South China Sea. Occurrence of periods of poor accuracy in this belt has long been recognized. It is nearly equitorial and signals propagated at night from the east cannot be used in this region because of modal interference. Those signals which are usable all arrive from the west and, therefore, present poor geometry. It is ironic that the worst accuracy is located on the heaviest trade routes. The areas near Singapore and the Straits of Malacca warrant further study. Currently, use of Japan and Australia is precluded here because of modal interface. However, the boundaries are rather close and a detailed regional study might indicate it safe to use Japan or Australia in this important region. Additional data should be gathered during the forth-coming western Pacific validation.

Accuracy of an optimum multi-frequency Omega receiver is conjectural since the parametric model has not yet been extended beyond 10.2 kHz. Optimal use of 13.6 kHz would not be expected to help much in the belt of poorest accuracy since modal limitations on 13.6 kHz are even more severe than at 10.2 kHz. Certainly, however, the general accuracy would improve. In particular, in the unusual case where noise introduces significant inaccuracy, a four-frequency Omega receiver would have about twice the accuracy of a single frequency receiver.

Perhaps one of the more important results from this validation is the credence added to the parametric model itself. The model has many uses. It can be used as a tool for system analysis. Accuracy can be predicted not only for optimum conditions but for suboptimum conditions as well. An important set of suboptimal conditions is that arising from station outages. Validation of the parametric model also means particular receiver implementations can be emulated. The model may also be used to assess the potential accuracy from possible differential Omega installations. It is also applicable to assessing anticipated performance on proposed routes. Probably the important application will be incorporation of the model in receivers so as to improve accuracy and radically reduce the probability of rare large errors.

A traditional output from area validations has been a composite coverage diagram. Figure 10 shows such a diagram indicating the 10.2 kHz signals which are usable throughout the region. The boundaries primarily reflect nighttime modal limitations, but have been drawn with attention to other limitations as well. The navigator should select lines of position from the signals indicated with attention to geometry and station maintenance schedules. It is advisable to consult other coverage guidance to determine the types of limitations which may be expected at various times. For example, parametric individual station coverages for idealized day and night conditions will show the propagationally limiting conditions. Of the coverages indicated, Norway (A) may be weak at times in the southeast, but is usable if it can be received. Additionally, North Dakota (D) will provide usable, if occasionally weak, signals off South Africa. Also, North Dakota and Hawaii (C) will be occasionally useful in the northeast. Both Australia (G) and Japan (H) cover nearly the entire region during periods when the respective propagation paths are illuminated. "Daytime" long path limitations occur on Australia in the Red Sea and on Japan off East Africa as well as near-field limitations immediately around the stations. Some use of Argentina (F) in southwest Australia may be possible when Antarctica is dark.

The actual performance of widely-sold Omega receivers is of some, if tertiary, interest. The Magnavox MX 1105 receivers used at sea are combined Omega/NAVSAT units. At sea, integrated fixes were obtained. For evaluation,

fixes were by postprocessing phase errors developed in Sec.5. From available lines-of-position, best fixes were selected by comparison with NAVSAT -- an unscientific procedure. Using 10.2 kHz alone, medians were 1.2 n.mi. neaar 0600 GMT, 1.8 n.mi. near 1800 GMT and 1.9 n.mi. over 24-hours.

One of the two airborne Litton LTN-211 receivers was allowed to operate in the usual way using a loop antenna. Unfortunately, the location of the aircraft was rarely known precisely when airborne even though the aircraft was equipped with an Inertial Navigation System (INS) as well as a Global Positioning System (GPS) receiver. The GPS satellite "window" rarely occurred during flights and the receiver failed half way through the validation while the INS proved less accurate than the Omega sets. While detailed airborne accuracy assessment is not supported, gross performance experience can be noted. In nearly two hundred hours of flight time, neither receiver failed. This is consistent with the high mean time between failure (MTBF) expected for a mature commercial avionic product. Occasional in-flight inter-comparisons between the two Omega sets, often using different signals, or between either Omega and the INS suggests that fixes were never in error by much more than the errors on landing. This is particularly noteworthy when it is remembered that the flights were especially selected to investigate areas of modal interference.

When the aircraft was on the ground, it could be confidently located at least to an uncertainty corresponding to the size of the airfield. Table II shows the median accuracy obtained using the LTN-211 with loop antenna using three frequencies on takeoffs and landings. The table has been separated into two columns depending on whether the parametric coverage model for 10.2 kHz alone indicates an accuracy of about one mile or two miles or more for the particular location and time of each takeoff and landing.

TABLE II

LTN-211 MEDIAN ACCURACY

	Expected Accuracy	
	~1 nmi	≳2 nmi
Takeoff	1.1 nmi	0.7 nmi
Landing	2.1	4.9
Median	1.6	2.8

The overall median accuracy from the actual LTN-211 receiver using three frequencies is of the order predicted by the parametric model for an ideal receiver using 10.2 kHz alone. Looking in more detail, important differences are noted. First, the takeoff errors are markedly less than those on landing. This may relate to the recent initialization and the long tracking time constants used by the LTN-211 on the ground. In this case the landing errors would be more valid. Secondly, too many large errors of over four miles were observed on landing. The occasional occurrence of larger errors is a matter of grave concern because of the possible impact on safety. An Omega receiver should be in error by more than four miles only very rarely. Large errors on landing occurred at Alice Springs (4.9 nmi), Nairobi (9.9 nmi), Singapore (5.0 nmi), Sri Lanka (6.4 nmi), Khartoum (7.6 nmi), and Melbourne (6.4 nmi). Of these, only the errors at Singapore and Sri Lanka can be reasonably attributed to the possible effects of poor signal availability and geometry. It is speculated that the other four may have been the result of poor signal utilization within the LTN-211. The only coverage guidance incorporated in the LTN-211s used was that for 10.2 kHz as guidance for 13.6 kHz was published less than two months before the start of the validation. Two of the landing errors, Alice Springs and Melbourne, could have resulted from using inappropriate near-field criteria from Omega Australia at 13.6 kHz compared with that for 10.2 kHz. Comparison of nighttime modal interference differences between 10.2 kHz and 13.6 kHz suggests that it would almost have been surprising if there were not large landing errors at Khartoum and Nairobi. For the flight to Khartoum, major coverage differences between 10.2 kHz and 13.6 kHz were theoretically indicated for stations B, C, E, and H, while for the flight to Nairobi differences occur on B, E, and G. Although coverage differences could have led to improper signal utilization and, hence, large landing errors at several other sites, it is speculated that redundant processing techniques within the LTN-211 prevented large errors elsewhere. All in all, the few large landing errors seem to provide graphic examples of the need for validation and coverage guidance.

Operationally, during flights especially selected to study modal interference, tracking and navigation were continuous throughout the entire region. The error on landing was always less than 10 miles. Use of proper coverage guidance could probably have reduced or eliminated the few larger

errors. Typical accuracy was probably about two miles. Although the LTN-211 software can and is being improved, the actual navigation experienced represents a considerable accomplishment.

CONCLUSIONS

By far the most important result of the validation was the demonstrated correspondence between theory and measurement. Even the modification of the Japanese coverage boundary in west Australia was reflective of clerical limitations in originally drawing the boundary rather than limitations of full-wave propagation theory. Full-wave overlays for both 10.2 and 13.6 kHz were well supported as was the parametric coverage for 10.2 kHz. Coverage studies and the validation process have combined to render the system as an entity much better understood now than it was a few years ago.

Theoretical calculations indicate an accuracy capability of 2 nmi (c.e.p.) or better throughout the region on a 24-hour basis with the unfortunate exception of the trade routes from the Red Sea, around the tip of India, through the Straits of Malacca, and up to the South China Sea. When signal paths from Australia and Japan are both dark, about 1500 GMT, there is a small region directly astride the trade routes where neither Australia nor Japan can be used and the usable stations provide poor geometry. Fix accuracies as poor as about 5 nmi (c.e.p.) may then occur. However, intensive additional study of this small region is warranted. Installation of Differential Omega may be desirable. Uncertainties in the boundary locations are such that either Australia, Japan or both may actually prove usable.

Performance of the LTN-211 flown on the validation flights was noteworthy: both for what it did right and what it did wrong. On the positive side, the set navigated continuously throughout the entire validation effort maintaining a median accuracy of about two miles. Considering the duration of the test, miscellaneous intervening Omega station outages, various weather conditions, and the fact the flights were deliberately planned to investigate problems, this level of system performance and robustness is

exemplary. Comparison with other aids indicated that no truly gross errors ever occurred. However, a few larger (but less than ten mile landing errors did occur. At least some of these apparently resulted from inadequate coverage guidance being incorporated into the LTN-211 at the time of the validation. The exceptions emphasize the need for coverage guidance.

REFERENCES

REFERENCES

Bancroft (1985) Bancroft, S., "An Algebraic Solution of the GPS Equations", IEEE Trans. AES, V AES-21, n. 7 Jan 1985. pp. 56-59.

Campbell et al. (1980) Campbell, L. W., T. M. Servaes and E. R. Grassler, "Omega Validation in the North Atlantic," Proc. of the 5th Annual Meeting of the Int'l Omega Association, 5-7 August 1980, Bergen, Norway, pp 24-1 to 24-23.

DMA (1981) U.S. Defense Mapping Agency Hydrographic/Topographic Center, Omega Coverage Diagrams 10.2 kHz (Prototype), July 1981.

Doubt (1984) Doubt, R. J., "Omega Navigation System Regional Validation Program," NAVIGATION, 31, 3, 155

Gupta (1975) Gupta, R. R., Omega Transmitter Signal Radial Profiles, The Analytic Sciences Corporation Technical Information Memo. 343-27, 24 March 1975.

Gupta and Morris (1983) Gupta, R. R. and P. B. Morris, "Modal Interference Maps," Proc. 8th Annual Meeting of the Int'l Omega Association, 18-22 July 1983, Lisbon, Portugal, (ISSN: 0278-9396), pp 15-1 to 15-8.

Gupta and Morris (1984) Gupta, R. R., and P. B. Morris, "Assessment of Omega 13.6 kHz Signal Modal Interference," Proc. 9th Annual Meeting of the Int'l Omega Association, 6-10 August 1984, Seattle, WA, (ISSN: 0278-9396), pp 16-1 to 16-18.

Gupta, et al. (1980) Gupta, R. R., S. F. Donnely, P. B. Morris and R. L. Vence Jr., "Omega Station 10.2 kHz Signal Coverage Prediction Diagrams," NAVIGATION, 27, 4, pp 142

Gupta et al. (1980) Gupta, R. R., S. F. Donnelly, P. B. Morris, and R. L. Vence, Jr., "Omega System 10.2 kHz Signal Coverage Prediction Diagrams," Proc. of the 5th Annual Meeting of the Int'l Omega Association, Bergen, Norway, 5-7 August 1980, pp 22-1 to 22-36.

Gupta et al. (1983) The Analytical Sciences Corporation Rept. EM-2271, Graphical Display of 13.6 kHz Signal Radial Profiles, by R. R. Gupta, R. L. Geddes and T. M. Watson, Aug 1983. 392pp.

Gupta et al. (1985) Gupta, R. R., P. B. Morris, and R. J. Doubt, "Omega Signal Coverage Prediction Diagrams for 13.6 kHz" Proc. of the 10th Annual Meeting of the Int'l Omega Association, 22-26 July 1985, Brighton, England. (ISSN: 0278-9396) pp. 14-1 to 14-25.

Karkalik (1978) Karkalik, F. G. "Omega Validation Over the Western Pacific Area," NAVIGATION, 25, 4, pp 395

Karkalik et al. (1978) Karkalik, F. G., G. F. Sage and W. R. Vincent, Western Pacific Omega Validation, USCG Rept. ONSOD 01-78. Vols. I and II.

Kugel (1982) Naval Ocean Systems Center Technical Note 1237, Omega Near-Field Modal Interference Model Development, by C.P.Kugel, 22 December 1982.(An informal document intended primarily for use within the Center).

Kugel (1983) Naval Ocean Systems Center Technical Note 1259, Omega Near-Field Modal Interference Model Development: Data Supplement to NOSC TN 1237, by C.P.Kugel, 18 April 1983. (An informal document intended primarily for use within the Center).

Kugel (1984) Kugel, C. P., "Indian Ocean Omega Signal Validation," Proc. 9th Annual Meeting of the Int'l Omega Association, 6-10 August 1984, Seattle, WA, (ISSN: 0278-9396), pp 20-1 to 20-8.

Kugel and Bickel (1983) Kugel, C. P., and J. E. Bickel, Indian Ocean Omega Validation Test Plan, (An informal working paper), Naval Ocean Systems Center, 1 August 1983.

Kugel et al. (1978) Kugel, C. P., J. A. Ferguson, W. R. Bradford, and J. E. Bickel, Airborne and Groundbased Measurements in Support of the Western Pacific Omega Validation, USCG Rept. CG-ONSOD-02-78, 31 March 1978, 154 pp.

Lee (1975a) Lee, H. B., "A Novel Procedure of Assessing the Accuracy of Hyperbolic Multilateration Systems," IEEE TRANS. AES, Vol, AES-11, n.1, January 1975, pp 2-15.

Lee (1975b) Lee, H. B., "Accuracy Limitations of Hyperbolic Multilateration Systems," IEEE Tran. AES, Vol. AES-11, n.1., pp 16-29.

Levine and Woods (1981) Levine, P. H. and R. E. Woods, North Pacific Omega Navigation System Validation, USCG Rept. CG-ONSOD-01-81, 31 December 1981, 372 pp. (ADA 212 105)

Levine and Woods (1981a) Levine, P., and R. Woods, "Omega Validation in the Northern Pacific," Proc. of the 6th Annual Meeting of the Int'l Omega Association, Montreal, Quebec, Canada, 18-20 August 1981, (ISSN: 0278-9396).

Lynn (1983) Lynn, K. J. W., "Transequatorial Omega/VLF Reception in Australia," Proc. 8th Annual Meeting of the Int'l Omega Association, 18-22 July 1983, Lisbon, Portugal, (ISSN: 0278-9396), pp 16-1 to 16-6.

Morfitt et al. (1981). Morfitt, D. G., J. A. Ferguson and F. P. Synder, "Numerical Modeling of the Propagation Medium at ELF/VLF/LF," Medium, Long and Very Long Wave Propagation (At Frequencies Less than 3000 kHz), J. S. Belrose, Ed., AGARD-CP-305. (From the EM Wave Propagation Panel, Brussels, 21-25 September 1981), pp 32-1 to 32-14.

Morris et al. (1982) Morris, P.B., J L.Shuhy, and C.E.Quade, "Long-Path Prediction Errors", Proc. 7th Annual Mtg., Int'l Omega Assoc. 12 14 Oct 1982 Arlington, VA. pp 23-1 to 23-4.

Morris and Swanson (1980). Morris, P. B. and E. R. Swanson, "New Coefficients for the Swanson Propagation Correction Model", Proc. of the 5th Annual Meeting of the Int'l Omega Association, Bergen, Norway, 5-7 August 1980, pp 26-1 to 26-24.

NAVELEX (1981) Naval Electronic Systems Engineering Center, Vallejo, CA document 14203-124804, AN/SRN-12 Omega Receiver Navigators and Operators Information Bulletin5, May 1981.

Pappert et al. (1967). Pappert, R. A., E. E. Gossard, and I. J. Rothmuller, "A Numerical Investigation of Classical Approximations Used in VLF Propagation", Radio Sci., v. 2, pp 387-400, Apr. 1967.

Pierce (1947). Pierce, J. A.., Cruft Laboratory, Harvard University Technical Report 17, RADUX, 11 July 1947. 13 pp.

Pierce et al. (1964). Pierce, J. A. (Chairman), W. Palmer, A. D. Watt, and R. H. Woodward, Omega: A World-wide Navigational System, 1 June 1964. (P&B Pub. No. 886).

Reder (1981). Reder, F., "Omega and VLF Propagation," Proc. of the 6th Annual Meeting of the Int'l Omega Assoc., Montreal, Quebec, Canada, 18-20 August 1981, (ISSN: 0278-9396).

Swanson (1967). Swanson, E. R., "Time Dissemination Effects Caused by Instabilities in the Medium," Phase and Frequency Instabilities in Electromagnetic Wave Propagation, K. Davies, Ed. (Proc. AGARD/EPC Symposium, Ankara, 9-12 October 1967), pp 181-198.

Swanson (1972) "Use of Propagation Corrections for VLF Timing,"Proc. 4th Annual DOD Precise Time Interval (PTTI) Strat. Plan. Meeting. 14-16 November 1972, pp 310-323.

Swanson (1974) Naval Electronics Laboratory Technical Report 1974 Omega Coverage in India: A Case Study, by E. R. Swanson 15 January 1976. AD-A022035

Swanson (1976) Naval Electronics Laboratory Technical Note 3910, Omega Signals Coverage in Australia, by E. R. Swanson, 15 July 1976.

Swanson (1977) Swanson, E. R., "Propagation Effects on Omega," AGARD-CP-209 (Propagation Limitations of Navigation and Positioning Systems), published February 1977, pp 15-1 to 15-21. (French translation is "Effet de la propagation sur "l'Omega," NAVIGATION: Revue Technique de Navigation Maritime Aerienne at Spatiale, 1re parti, v.XXV, n.100, Octobre 1977; 2e parti, v.XXIV, n.101, Janvier 1978, pp 385-407 + 27-51.)

Swanson (1978) Swanson, E. R., "Geometric Dilution of Precision", NAVIGATION, v. 25, n. 4 (Winter 1978-9). pp. 425-429.

Swanson (1983) Swanson, E. R., "A New Approach to Omega Coverage Diagrams," Proc. 8th Annual Meeting of the Int'l Omega Association, 18-22 July 1983, Lisbon, Portugal, (ISSN: 0278-9396), pp 20-1 to 20-24.

Swanson (1983) Swanson, E. R., "Omega", Proc. IEEE, 71, 10 (Oct 83) pp 1140-1155.

Swanson (1984) Swanson, E. R., "Omega Coverage: Accuracy at Specified Times," Proc. 9th Annual Meeting of the Int'l Omega Association, 6-10 August 1984, Seattle, WA, (ISSN: 0278-9396), pp 19-1 to 19.10.

Swanson (1984) Swanson, E. R., "On Omega Signal Availability at 10.2 Khz," Proc. 9th Annual Meeting of the Int'l Omega Association, 6-10 Aug 1984, Seattle, WA, (ISSN: 0278-9396), p 25-1.

Thompson (1977) Thompson, A. D., "Omega System Performance Predictions," NAVIGATION, v. 24, n.4, Winter 1977-78, pp 304-311.

Watt (1983) Watt, T., "Results of the South Atlantic Omega Validation," Proc. 8th Annual Meeting of the Int'l Omega Association, 18-22 July 1983, Lisbon, Portugal, (ISSN: 0278-9396), pp 17-1 to 17-9.

LIST OF SUPPORTING DOCUMENTS

The following documents are supplements containing data on which this report is based. They are quite lenghty containing, literally, thousands of figures.

Indian Ocean Omega Validation Data Supplement: In-Flight Measurements,
ONSCEN Rept. No. CG-ONSCEN-03-87

Indian Ocean Omega Validation Data Supplement: Fixed Site Measurements,
ONSCEN Rept. No. CG-ONSCEN-04-87

Indian Ocean Omega Validation Data Supplement: Miscellaneous Measurements,
ONSCEN Rept. No. CG-ONSCEN-05-87

The In-Flight Measurement supplement contains primarily measurements of amplitude as functions of time during the various flights. Additionally, some flights were processed to show amplitude as a function of distance radially from a station. The Fixed Site Measurement volume contains data from only those sites calibrated for absolute amplitude measurement (Those listed in Table 3-IV). Data from some other fixed sites is included as a part of the local area coverage assessment supported by statistics in the Miscellaneous volume. Shipboard data are also supported by the Miscellaneous measurement volume.

APPENDIX A

AMPLITUDE PREDICTION

FIELD STRENGTH PREDICTION

Since this validation has been conducted within a global perspective, examination of amplitude prediction has not been limited solely to the Indian Ocean area. Indeed, perusal of the literature shows that a considerable amplitude data base is now available. This appendix presents the available 10.2 kHz data base. Comparisons with parametric predictions developed several years ago by Swanson (1983) and used in the parametric coverage are also included.

The usual Omega measurement is that of the difference in phase between signals received from two or more stations. Receivers typically limit signals so amplitude is not measured directly. Only phase or phase variance measurements are made. Indeed, Gupta has attempted to model field strength indirectly through relating phase variance to signal-to-noise ratio and hence phase variance ratios to signal ratios. Occasionally, however, accurate amplitude measurements are made. Over a period of years, these infrequent amplitude measurements now add up to a significant data base.

The Table contains data for both 10.2 and 13.6 kHz but comparisons of observation with prediction only for 10.2 kHz. This is due to the fact that the parametric model has not yet been extended to 13.6 kHz. It should also introduce some caution regarding the 13.6 kHz tabulated values since they have in no way been cross checked. They may very well contain a few errors from clerical or tabulational causes.

Predicted amplitudes are based on coefficients developed by Swanson in 1983. These use the identical modeling forms as have been used for Predicted Propagation Corrections (PPC's) although the particular formulation is not especially well suited to amplitude prediction. Further, the coefficients were developed empirically so as to best yield the observed (or full wave predicted) coverage maps. This approach emphasized the prediction of the relative field strength of competing modes when they were near equality. This is not the same as a prediction scheme based on regression analysis which will weigh all relative levels equally and seek to minimize the total root-mean-square (rms) discrepancy. Especially when considering the second mode, it was not regarded as especially important whether the mode was, say, 20 or 40 db below the first mode when it was in fact well dominated by the first mode.

Rather, attenuation rates were adjusted so as to weight the predictions when he competing modes were nearly equal. The existing data base is now sufficient to support regression analysis. This would surely result in a "better" fit in the sense of a lower rms discrepancy. However, the resulting set of coefficients might well not be as useful for their intended purpose.

Field strength observations and predictions are tabulated in Table Comments indicate instances of second mode dominance, long path dominance, or when either of these field contributions are close to that expected from the first mode. The source documentation for each measurement is listed at the end of the table. The table contains 163 specific daytime measurements of which 12 are presumed to be long path dominant. It also contains 146 nightime observations of which 30 are presumed second mode dominant. Median prediction error for the first mode dominant observations is just over 2 db both during the day and at night with corresponding rms discrepancies between 4 and 5 db. The median prediction error for second mode dominant observations at night is 6 db with the rms discrepancy just below 9 db. In computing these statistics, no allowance was made for the fact that significant signal contributions from more than one propagation mechanism may have been contributing simultaneously to the total field so that the actual observation may have included effects of constructive or destructive interference.

Particularly regarding modal interference at night, it is probably significant that the second mode was presumed to be dominant in 21% of the measurements and sufficient to seriously perturb measurements in many additional first mode dominant observations. Although no claim is made that the selection of measurements to perform was unbiased with respect to modal dominance, neither is there any reason to expect that it was deliberately biased. Thus, the data are suggestive of about a one in five probability of a randomly chosen Omega signal at a random location being mode dominant at night.

The data are probably not a reasonable base for estimating the corresponding probability for long path dominance in the day. Many field strength measurements are made directly by spectrum analyzer. This equipment lacks sensitivity when compared with Omega receivers. Thus, the probable occurrence of dominant long path signals during the day may well exceed the 7% contained in the data.

TYPICAL FIELD STRENGTH RECEIVED AT VARIOUS SITES

LOCATION	DATE	STATION	DAY				NIGHT				COMMENT
			10.2 KHz			13.6 KHz	10.2 KHz			13.6 KHz	LP = Long Path
			Obs.	Pred.	Diff.	Obs.	Obs.	Pred.	Diff.	Obs.	SP = Short Path
Meppen, Germany (55N 5E)	78	A	55	62	7	57	54	60	6	58	
		B	41	41	0	42	43	45	2	46	
		C	≤15*	-18	--	8	7**	--	--	4*	* Noise
											** No night path
		D	17	17	0	14	28	30	2	27	
		E	18	16	-2	28	18	24*	6	19	* Mode 2 (1:2dB lower)
		F	23	24	1	29	34	38	4	40	
		TR	26	--	--	30	34	--	--	32	
		H	17	17	0	23	32	29*	-3	37	* Mode 1 (2:9dB lower)
Scheinfurt, Germany (50N 10E)	78	A	53	59	6	56	56	57	1	52	
		B	42	44	2	43	44	48	4	49	
		C	≤10*	-7	--	14	21**	--	--	20**	* Noise
											** No night path
		D	20	19	-1	22	32	32	0	28	
		E	23	19	-4	31	20	27*	7	26	* Mode 2 (1:2dB lower)
		F	26	22	-4	31	35	38	3	37	
		TR	27	--	--	31	34	--	--	31	
		H	24	19	-5	30	38	30*	-8	39	* Mode 1 (2:9dB lower)
Amberg, Germany (50N 10E)	78	A	52	59	7	52	--			--	
		B	42	44	2	44	--			--	
Aschau/Surendorf, Germany (55N 10E)	78	B	42	41	-1	46	44	45	1	49	
		C	13	12	-1	18	14*	--	--	16*	* No night path
		D	15	17	2	17	26	31	5	25	
		E	23	20	-3	34	26	24*	-2	30	* Mode 1 (2:1dB lower)
		F	28	22	-6	34	39	37	-2	44	
		TR	26	--	--	32	36	--	--	41	
		H	18	19	1	30	30	30	0	36	
Essen (1,2), Germany (50N 5E)	78	A	54	58	4	55	--			--	
		B	43	44	1	44	--			--	

TYPICAL FIELD STRENGTH RECEIVED AT VARIOUS SITES

LOCATION	DATE	STATION	DAY				NIGHT				COMMENT
			10.2 KHz			13.6 KHz	10.2 KHz			13.6 KHz	LP = Long Path
			Obs.	Pred.	Diff.	Obs.	Obs.	Pred.	Diff.	Obs.	SP = Short Path
Pfettrach, Germany (50N 10E)	78	A	52	59	7	53	--			--	
		B	44	44	0	45	--			--	
		E	--			31	--			--	
		TR	--	--	--	29	--	--	--	--	
Ascension Island, Atlantic Ocean (8S 14E)	80	A	26	26	0	30	--			--	
		B	60	54	-6	60	52	55	3	52	
		C	33	11*	--	34	--			--	* LP (1:13dB lower)
		D	33	18	-15	36	43	33	-10	42	
		E	32	39	7	33	43	42*	-1	41	* Mode 1 (2:3dB lower)
		F	47	39	-8	47	50	47	-3	47	
		TR	36	--	--	38	39	--	38	—	
		H	40	27*	--	40	--			--	* LP (1:35dB lower)
Blumenau, Brazil (27S 48W)	80	A	--			17	--			--	
		B	36	36	0	40	28	48*	20	33	* Mode 2 (1:8dB lower)
		C	--			--	--			45	
		D	32	25	-7	33	36	34	-2	38	
		E	--			28	--			37	
		F	56	57	1	55	55	56	1	58	
		TR	30	--	--	33	26	--		33	
Trelew, Argentina (43S 65W)	80	A	--			24	--			--	
		B	32	26	-6	38	33	40*	7	30	* Mode (1:11dB lower)
		C	38	33	-5	40	44	46	2	50	
		D	31	26	-5	34	37	35	-2	36	
		E	--			--	--			26	
		TR	29	--	--	28	19	--	--	35	
Wahiawa, Oahu Island, Hawaii, USA (21.5N 158W)	77	A	22	25	3	25	--			--	
		D	36	38	2	38	41	41*	0	40	* Mode 1 (2:9dB lower)
		E	29	26	-3	32	37	45	8	40	
		H	46	43	-3	50	51	49	-2	53	

TYPICAL FIELD STRENGTH RECEIVED AT VARIOUS SITES

LOCATION	DATE	STATION	DAY				NIGHT				COMMENT
			10.2 KHz			13.6 KHz				13.6 KHz	LP = Long Path
			Obs.	Pred.	Diff.	Obs.	Obs.	Pred.	Diff.	Obs.	SP = Short Path
Orote Point, Guam (13.5N 144.5E)	77	C	32	33	1	40	32	34	2	33	
		E	39	34	-5	40	43	46	3	42	
		H	57	56	-1	58	58	55	-3	60	
Clark Air Base, Philippines (15.2N 120.5E)	77	A	22	22	0	21	31	34	3	28	
		B	27	21	-6	22	37	39	2	34	
		E	42	40	-2	40	43	48	5	40	
		H	53	56	3	56	48	52	4	46	
Darwin, Australia (12.5S 131E)	77	B	29	21	-8	32	40	40	0	40	
		C	22	21	-1	29	25	35*	10	24	* Mode 2 (1:10dB lower)
		E	45	39	-6	44	51	46	-5	45	
		H	44	44	0	46	38	42	4	40	
Port Moresby, Papua, New Guinea (9.3S 147E)	77	B	28	20	-8	27	40	42	2	39	
		C	27	30	3	36	27	40*	13	29	* Mode 2 (1:9dB lower)
		E	39	31	-8	40	48	42	-6	46	
		H	46	46	0	54	42	47	5	49	
Jakarta, Indonesia (6.2S 107E)	77	B	23	24	1	33	41	41	0	43	
		C	28	11*	--	17	23	32**	9	20	* LP (SP:3dB lower) ** Mode 2 (1:16dB lower)
		E	49	46	-3	48	50	50	0	51	
		H	40	42	2	45	34	43*	9	36	* Mode 2 (1:4dB lower)
Atlantic City, New Jersey USA (39N 75W)	78	A	30	26	-4	35	--			--	
		B	32	32	0	40	32	36*	4	33	* Mode 2 (1:2dB lower)
		C	40	35	-5	40	48	43	-5	46	
		D	57	57	0	56	59	57	-2	50	
		E	30	17*	--	33	33	15**	-18	32	* LP (SP:27dB lower) ** Mode 2 (1:8dB lower)
		F	29	22	-7	33	31	28	-3	31	

TYPICAL FIELD STRENGTH RECEIVED AT VARIOUS SITES

LOCATION	DATE	STATION	DAY				NIGHT				COMMENT
			10.2 KHz			13.6 KHz		10.2 KHz		13.6 KHz	LP = Long Path
			Obs.	Pred.	Diff.	Obs.	Obs.	Pred.	Diff.	Obs.	SP = Short Path
Sebana Seca, Puerto Rico (18N 66W)	78	A	31	33	2	40	--			--	
		B	33	34	1	40	32	43*	11	29	* Mode 2 (1:7dB lower)
		E	27	25*	--	32	23	19**	-4	30	* LP (SP:27dB lower)
											** Mode 2 (1:7dB lower)
		F	33	32	-1	36	29	39	10	36	
		H	<23*	0	--	26	--			--	* Noise
Frobisher, NWT, Canada (64N 69W)	78	A	≤12*	20	≥8	5	21	36	15	27	* Noise
		B	29	33	4	33	30	36	6	32	
		D	45	54	9	47	51	55	4	49	
		F	≤12*	7	--	11	15	18	3	15	* Noise
Natal, Brazil (6S 35W)	78	A	25	26	1	33	--			--	
		B	50	50	0	55	34	57*	23	47	* Mode 2 (1:12dB lower)
		C	27	22	-5	28	40	39	-1	42	
		D	--			37	--			45	
		E	23	17*	-6	31	29	30**	1	35	* Mode 1 (LP:4dB lower)
											** Mode 2 (1:5dB lower)
		F	43	43	0	46	49	48	-1	49	
Bermuda (32N 65W)	78	A	39	39	0	--	--	43	--	--	
		B	37	36	-1	--	35	41*	6	--	* Mode 2 (1:4dB lower)
		F	≤32*	28	--	--	33	30	-3	--	* Noise
		H	≤33*	-4	--	--	--			--	* Noise
Gander, New Foundland, Canada (49N 55W)	78	A	45	47	2	--	--			--	
		B	38	37	-1	--	32	38*	6	--	* Mode 1 (2:2dB lower)
		D	45	48	3	--	49	51	2	--	
		F	28	22	-6	--	31	29	-2	--	
Bodo, Norway (67N 14E)	78	E	19	17	-2	--	22	29	7	--	
		F	23	19	-4	--	38	34	-4	--	
		H	20	19	-1	--	33	30*	-3	--	* Mode 1 (2:7dB lower)

TYPICAL FIELD STRENGTH RECEIVED AT VARIOUS SITES

LOCATION	DATE	STATION	DAY				NIGHT				COMMENT
			10.2 KHz			13.6 KHz	10.2 KHz			13.6 KHz	LP = Long Path
			Obs.	Pred.	Diff.	Obs.	Obs.	Pred.	Diff.	Obs.	SP = Short Path
Keflavik, Iceland (64N 23W)	78	A	56	60	4	57	58	58	0	56	
		B	35	38	3	37	40	57*	17	39	* Computational Anomaly
		D	23	24	1	20	--			--	
		E	15	10	-5	21	21	19*	-2	25	* Mode 1 (2:1B lower)
		F	20	20	0	24	33	32	-1	32	
Lajes, Terceira, Azores (39N 27W)	78	A	49	49	0	49	52	50	-2	50	
		B	43	48	5	46	40	45	5	42	
		C	≤21*	8	--	20	--			--	* Noise
		D	35	38	3	36	42	44	2	39	
		E	≤20*	5**	--	22	23	26***	3	23	* Noise ** Mode 1 (LP:3dB lower) *** Mode 2 (1:11dB lower)
		F	32	30	-2	35	39	40	1	40	
Monrovia, Liberia (6N 11W)	78	A	24	32	8	32	24	34*	10	33	* Mode 1 (2:1dB lower)
		D	30	31	1	35	41	40	-1	43	
		E	23	21	-2	37	27	36*	9	36	
		F	39	43	3	43	47	49	7	46	
Singapore (1N 104E)	84	E	51	46	-5	43	--			--	
		H	45	44	-1	50	--			--	
Rota, Spain (37N 6W)	78	A	44	50	6	--	50	50	0	--	
		B	50	50	0	--	50	50	0	--	
		E	--			--	31	31*	0	--	* Mode 2 (1:10dB lower)
		F	33	27	-6	--	40	40	0	--	
Whidbey Island, Washington USA (48N 123W)	79	A	≤18*	-10	--	15	--			--	* Noise
		B	≤21*	14	--	26	24	24**	0	23	* Noise ** Mode 1 (2:8dB lower)
		C	53	49	-4	53	56	51	-5	57	
		D	57	58	1	56	61	56	-5	54	
		F	≤18*	10	--	23	22	25**	3	22	* Noise ** Mode 2 (1:7db lower)
		TR	24	--	--	27	32	--	--	34	
		H	42	35	-7	47	--			--	

TYPICAL FIELD STRENGTH RECEIVED AT VARIOUS SITES

LOCATION	DATE	STATION	DAY				NIGHT				COMMENT
			10.2 KHz			13.6 KHz	10.2 KHz			13.6 KHz	LP = Long Path
			Obs.	Pred.	Diff.	Obs.	Obs.	Pred.	Diff.	Obs.	SH = Short Path
Anchorage, Alaska USA (61N 150W)	79	A	42	41	-1	44	--			--	
		C	48	47	-1	49	--			--	
		D	43	48	5	42	--			--	
		H	48	41	-7	49	--			--	
Wake Island, USA (19N 166E)	79	A	25	23	-2	28	--			--	
		C	44	46	2	--	44	48*	4	32	* Mode 2 (1:3dB lower)
		D	28	26	-2	30	32	33*	1	35	* Mode 1 (2: 8dB lower)
		E	32	30	-2	34	38	45	7	42	
		F	20	18*	--	22	21	24**	3	23	* LP (SP:20dB lower)
											** Mode 2 (1:12dB lower)
		TR	26	--	--	20	28	--	--	21	
		H	52	52	0	--	57	53	-4	--	
Adak, Alaska USA (52N 177W)	79	A	38	36	-2	40	--			--	
		C	48	49	1	51	50	48*	-2	45	* Mode 1 (2:6dB lower)
		D	36	40	4	39	45	44	-1	43	
		E	17	15	-2	21	30	33	3	34	
		F	17	17*	--	23	17	18**	1	24	* LP (SP:18dB lower)
											** Mode 2 (1:6 dB lower)
		TR	11	--	--	14	20	--	--	22	
		H	50	48	-2	54	56	51	-5	49	
Juneau, Alaska USA (58N 135W)	79	A	30	18	-12	--	--			--	
		C	48	47	-1	--	--			--	
		D	50	53	3	--	--			--	
Barking Sands, Kauai, Hawaii USA (22N 160W)	79	A	26	25	-1	28	--			--	
		B	28	17*	--	29	--			--	* LP (SP:17dB lower)
		D	35	37	2	39	41	40*	-1	37	* Mode 1 (2:8dB lower)
		E	26	26	0	31	36	44	8	41	
		F	18	9*	--	15	21	28**	7	20	* LP (SP:4dB lower)
											** Mode 2 (1:12dB lower)
		TR	15	--	--	24	27	--	--	24	
		H	47	43	-4	51	53	49	-4	58	

TYPICAL FIELD STRENGTH RECEIVED AT VARIOUS SITES

LOCATION	DATE	STATION	DAY				NIGHT				COMMENT
			10.2 KHz			13.6 KHz	10.2 KHz			13.6 KHz	LP = Long Path
			Obs.	Pred.	Diff.	Obs.	Obs.	Pred.	Diff.	Obs.	SP = Short Path
San Diego, California USA (33N 117W)	79	A	<19*	-13	--	19	--			--	* Noise
		B	28	14*	14	21	29	27**	-2	26	* Mode 1 (LP:7dB lower) ** Mode 2(1:4 dB lower) Not noise (day)
		C	55	50	-5	53	56	52	-4	59	
		D	55	56	1	55	57	55	-2	52	
		F	26	17	-9	33	30	31*	1	33	* Mode 2 (1:8dB lower) Not noise (day)
		TR	30	--	--	34	41	--	--	39	
		H	40	32	-8	44	51	42	-9	53	
Midway Island USA (28N 177W)	79	A	30	26	-4	--	--			--	
		C	56	57	1	--	53	54*	1	--	* Mode 1 (2:2 dB lower)
		D	36	34	-2	--	40	39	-1	--	
		H	51	48	-3	--	57	51	-6	--	
Perth, Australia (32S 116E)	84	A	15	15	0	22	22	30	8	33	
		B	28	20	-8	34	34	36	2	42	
		C	16	11*	-5	26	14	26**	12	19	* Mode 1 (LP:9 dB lower) ** Mode 2 (1:6dB lower)
		E	48	43	-5	52	46	48	2	48	
		G	50	53	3	54	48	53	5	52	
		H	30	32	2	42	13	32	19	34	
Pretoria (26S 28E)	84	A	25	16	-9	32	27	25	-2	37	
		B	46	44	-2	50	46	48	2	50	
		D	16	11	-5	26	35	30	-5	40	
		E	51	52	1	54	53	52*	-1	56	* Mode 1 (2:9 dB lower)
		F	41	37	-4	44	48	45	-3	47	
		G	31	25	-6	38	41	35	-6	42	

TYPICAL FIELD STRENGTH RECEIVED AT VARIOUS SITES

LOCATION	DATE	STATION	DAY				NIGHT				COMMENT
			10.2 KHz			13.6 KHz				13.6 KHz	LP = Long Path
			Obs.	Pred.	Diff.	Obs.	Obs.	Pred.	Diff.	Obs.	SP = Short Path
Bahrain (26N 51E)	84	A	45	41	-4	47	49	46	-3	52	
		B	43	39	-4	45	46	47	1	48	
		C	30	14*	--	34	33	19**	-14	26	* LP (SP:11 dB lower)
											** Mode 1 (2:3 dB lower)
											Very short night (½ hr)
		E	44	43	-1	51	37	47*	10	44	* Computational Anomaly
		F	30	20	-10	36	43	37	-6	44	
		G	22	12*	--	30	22	22**	0	24	* LP (SP:5 dB lower)
											** Mode 2 (1:3 dB lower)
		H	22	24	2	32	40	33*	-7	43	* Mode 2 (1:1 dB lower)
Diego Garcia (7S 72E)	84	A	38	29	-9	37	44	36	-8	41	
		B	40	33	-7	38	44	44	0	41	
		C	25	24*	--	28	15	27**	12	15	* LP (SP:30 dB lower)
											** Mode 2 (1:22 dB lower)
		E	59	57	-2	55	56	57	1	52	
		F	38	25	-13	36	48	39	-9	44	
		G	34	29	-5	36	47	36*	-11	41	* Mode 1 (2:9 dB lower)
Rome, New York USA (43N 75W)	63	C	34	35	1	--	46	43	-3	--	
Farfah, Canal Zone (9N 80W)	63	C	41	40	-1	--	47			--	
Miami, Florida USA (25N 80W)	63	C	40	38	-2	--	48	46	-2	--	
San Diego, California USA (32N 117W)	63	C	53	50	-3	--	55			--	

TYPICAL FIELD STRENGTH
RECEIVED AT VARIOUS SITES

LOCATION	DATE	STATION	DAY				NIGHT				COMMENT
			10.2 KHz Obs.	10.2 KHz Pred.	Diff.	13.6 KHz Obs.	10.2 KHz Obs.	10.2 KHz Pred.	Diff.	13.6 KHz Obs.	LP = Long Path SP = Short Path
Whidbey Island, Washington USA (98N 123W)	63	C	46	49	3	--	50	51	1	--	
		C	46	49	3	--	50	51	1	--	
Point Barrow, Alaska, USA (71N 157W)	63	C	37	41	4	--	--				
College, Alabama USA (65N 148W)	63	C	45	45	0	--	51	47	-4	--	
Thule, Greenland (77N 69W)	63	C	29	29	0	--	40			--	

APPENDIX A REFERENCES

Reference dates are generally the same as the dates of the data themselves. This, and geography, can be used to key individual table entries in the table to specific sources. Data from 1984 were measured explicitly as a part of the Indian Ocean Validation and are not otherwise referenced.

Naval Ocean Systems Center Preliminary Report, North Pacific OMEGA Validation, by C.P.Kugel, J.A.Ferguson, K.B.Rider, W.A.Pieper, W.R.Bradford, and J.E.Bickel. (Undated--but data are from 1979). [This is an informal document prepared by NOSC for CNSOD rather than the final report North Pacific Omega Navigation System Validation by P.H.Levine and R.E.Woods, Report CG-ONSOD-01-81].

USAF ASD/SD26 Technical Memorandum 79-01, OMEGA/VLF Signal Availibility for Navigation within the European Area, (No author listed but apparently C.P.Kugel, W.R.Bradford, K.B.Rider, J.E.Bickel, and J.A.Ferguson (NOSC)), February 1979.

Naval Ocean Systems Center Data Supplement, North Atlantic OMEGA Validation "Final (Draft)" by C.P.Kugel, J.A.Ferguson, K.B.Rider, W.R.Bradford, and J.E.Bickel, 1 June 1979. [An informal document prepared for ONSOD].

Naval Ocean Systems Center Preliminary Report, South Atlantic OMEGA Validation by C.P.Kugel, J.A.Ferguson, and J.E.Bickel, (Undated but data are from 1980). [An informal document prepared for ONSOD].

Naval Ocean Systems Center Report CG-ONSOD-02-78, Airborne and Groundbased Measurements in Support of the Western Pacific Omega Validation: Data Supplement, by C.P.Kugel, J.A.Ferguson, W.R.Bradford and J.E.Bickel. 31 March 1978. 330pp.

U.S.Naval Electronics Laboratory (now NOSC) Report 1239, Electromagnetic Field Strength Measurements at 10.2 Kilocycles per Second, by E.R.Swanson, 17 September 1964. [AD 450 739]

APPENDIX B

INDIVIDUAL STATION COVERAGES

at 10.2 kHz

AT SPECIFIED TIMES

INDIVIDUAL STATION COVERAGE PREDICTIONS
FOR 10.2 kHz at 0000, 0600, 1200 and 1800 GMT

A method of determining station coverage of individual Omega stations based on a parmetric description of propagation has been described by Swanson (1983, 1984). The first referenced paper described a prediction method for idealized day and night conditions while the second extended the work to provide coverage at particular times of the day. Both works address only 10.2 kHz. Results of both studies have been used in analyzing the Indian Ocean validation. Since the complete set of individual station coverages at particular times has not heretofore been published, they are included herein. Those at 1800 GMT, in particular, have been used in this validation.

Details are provided in the two references while the second paper also includes a few illustrative examples from those presented here. The amplitude parametrization has been briefly described in the previous appendix. Symbols used to indicate coverage limitations on the individual station coverage diagrams are as indicated in Table B-1. Precedence is in the order listed. For example, a "3" means that the signal to noise ratio is in the -30's of db in 100 Hz bandwidth and is not otherwise compromised through significant modal interference, Long Path interference, etc.

TABLE B-1

COVERAGE DISPLAY CODE

Character	Limitation/Meaning	Elaboration
N	Near	Within 1 Mn of station and potentially subject to skywave-groundwave interferences
A	Antipode	Within 2 Mn of antipode and subject to antipodal interference
#	No Signal	SNR worse than -40 dB in 100 Hz bandwidth
M	Modal	Second mode dominates or is within one dB of first mode
L	Long Path	Long path dominant or equal to short
-	Disturbed	Unwanted self interference within 10 dB; either long path or second mode
3	SNR in -30's	$-40 < SNR \leq -30$ dB in 100 Hz bandwidth; usable by well installed good receiver
2	SNR in -20's	$-30 < SNR \leq -20$ dB in 100 Hz bandwidth
1	SNR in -10's	$-20 < SNR \leq -10$ dB in 100 Hz bandwidth
0	SNR in -0's	$-10 < SNR \leq -0$ dB in 100 Hz bandwidth
Blank	Loud and Clear	Signal should be well received by poorly installed mediocre receiver under water

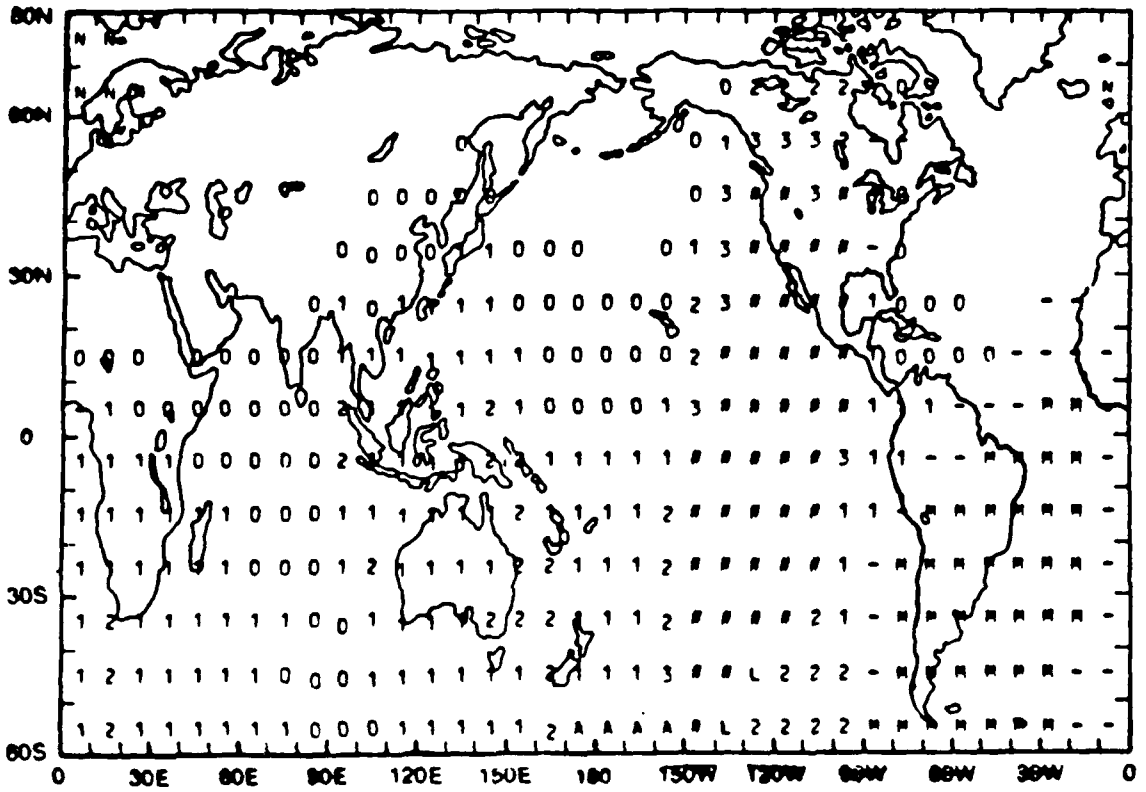

Omega Norway 10.2 KHz
0000 GMT

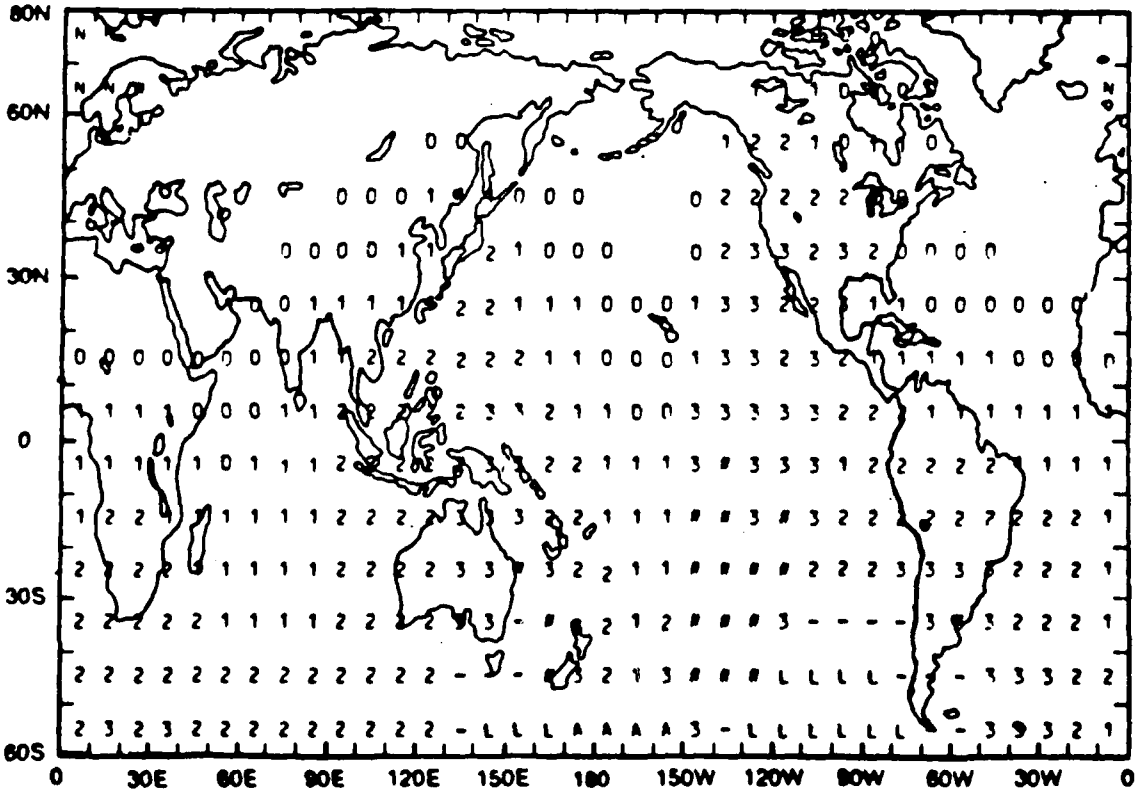

Omega Norway 10.2 KHz
0600 GMT

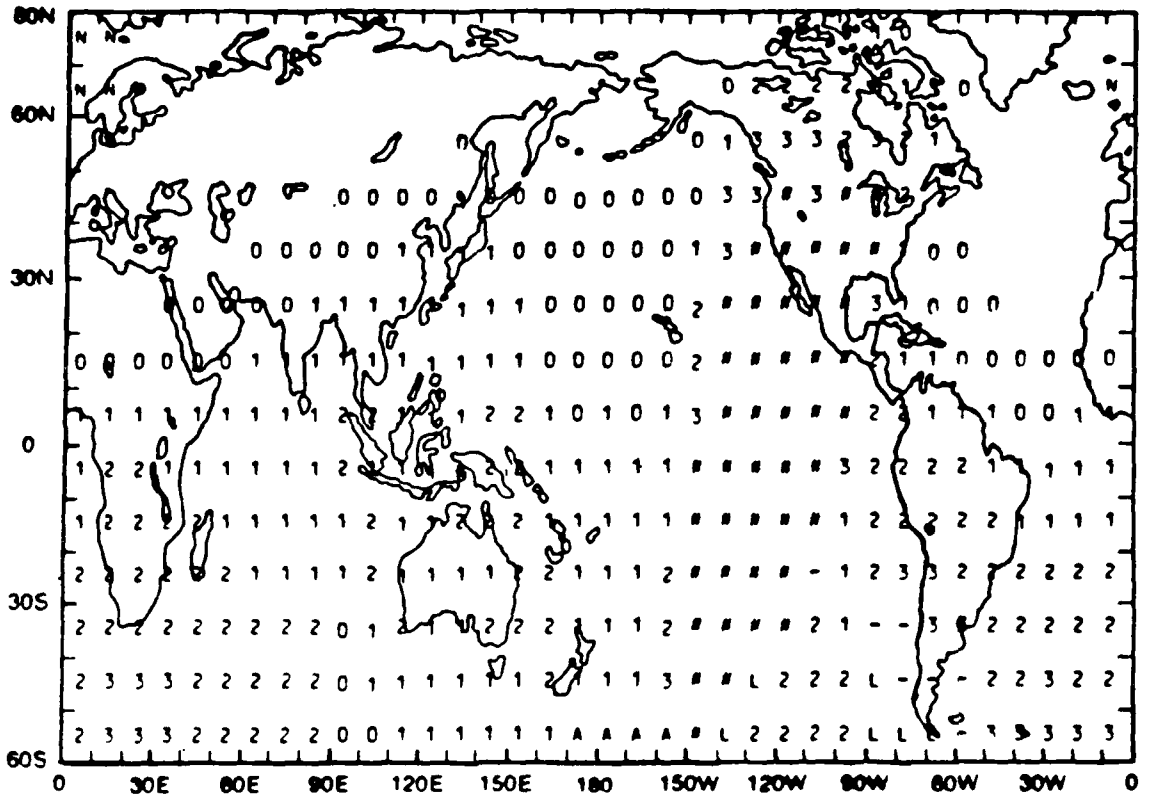

Omega Norway 10.2 KHz
1200 GMT

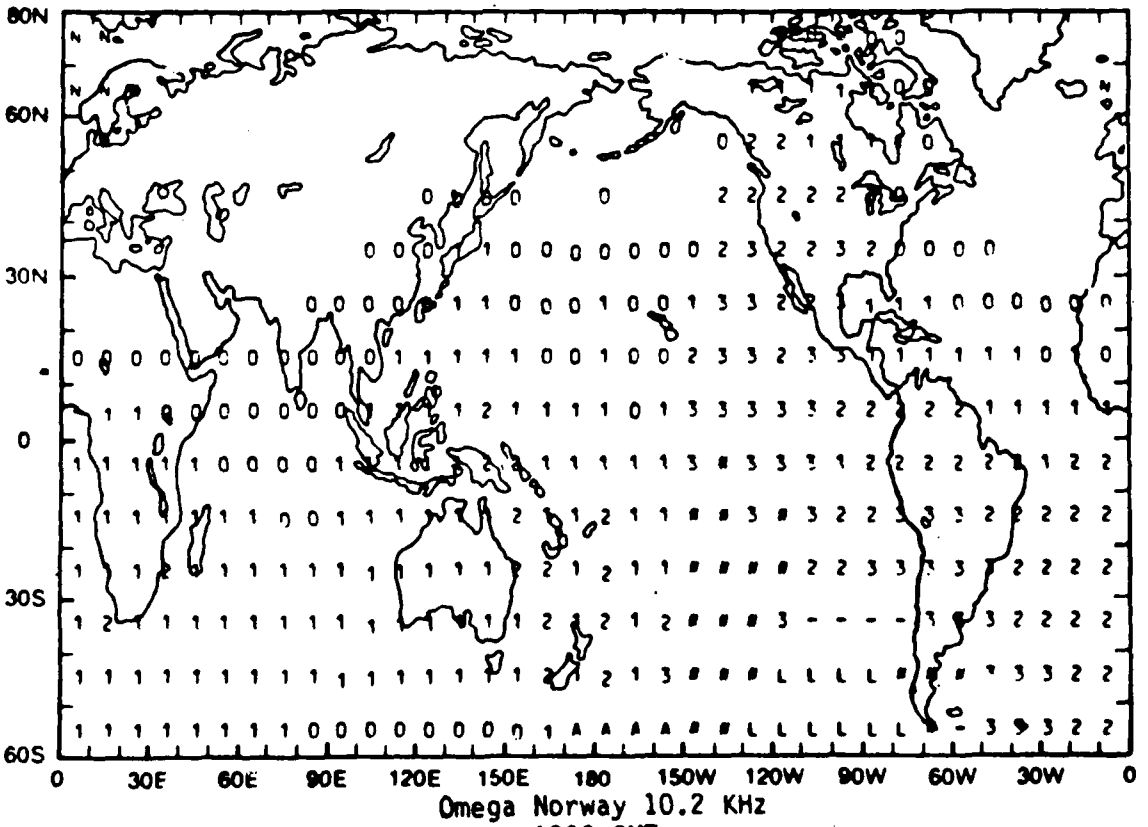

Omega Norway 10.2 KHz
1800 GMT

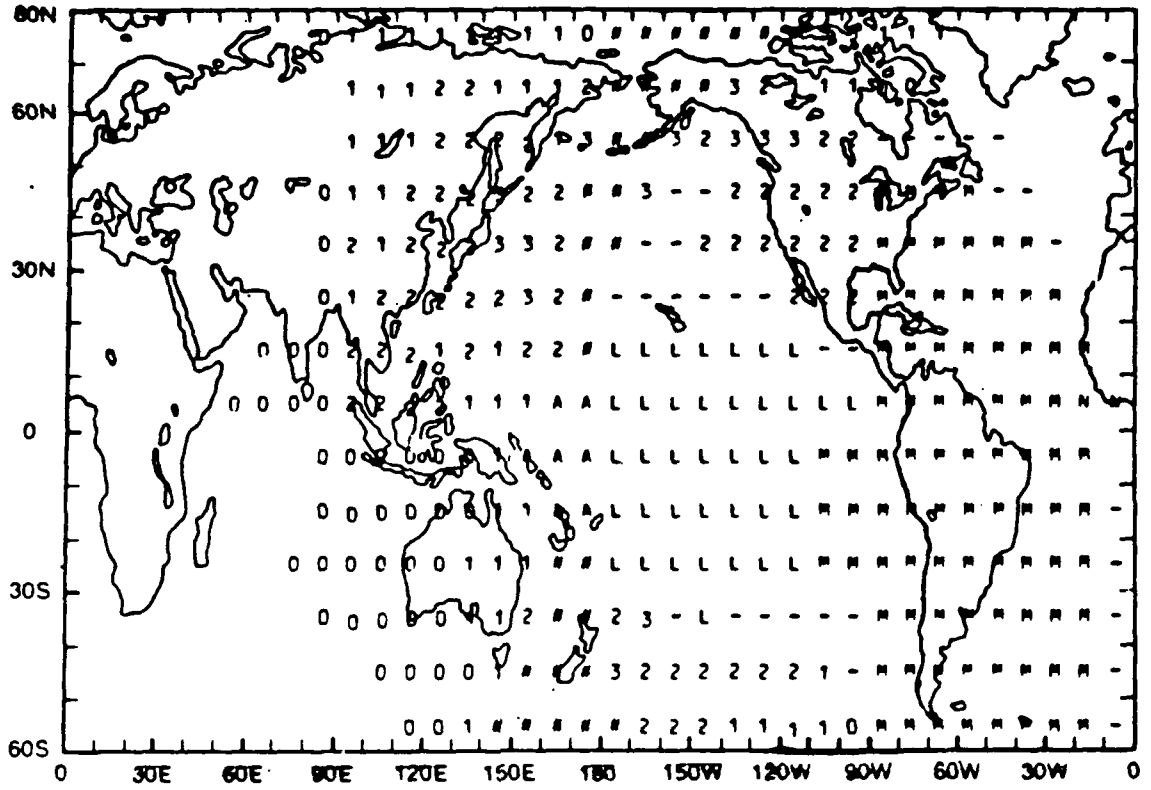

Omega Liberia 10.2 KHz
0000 GMT

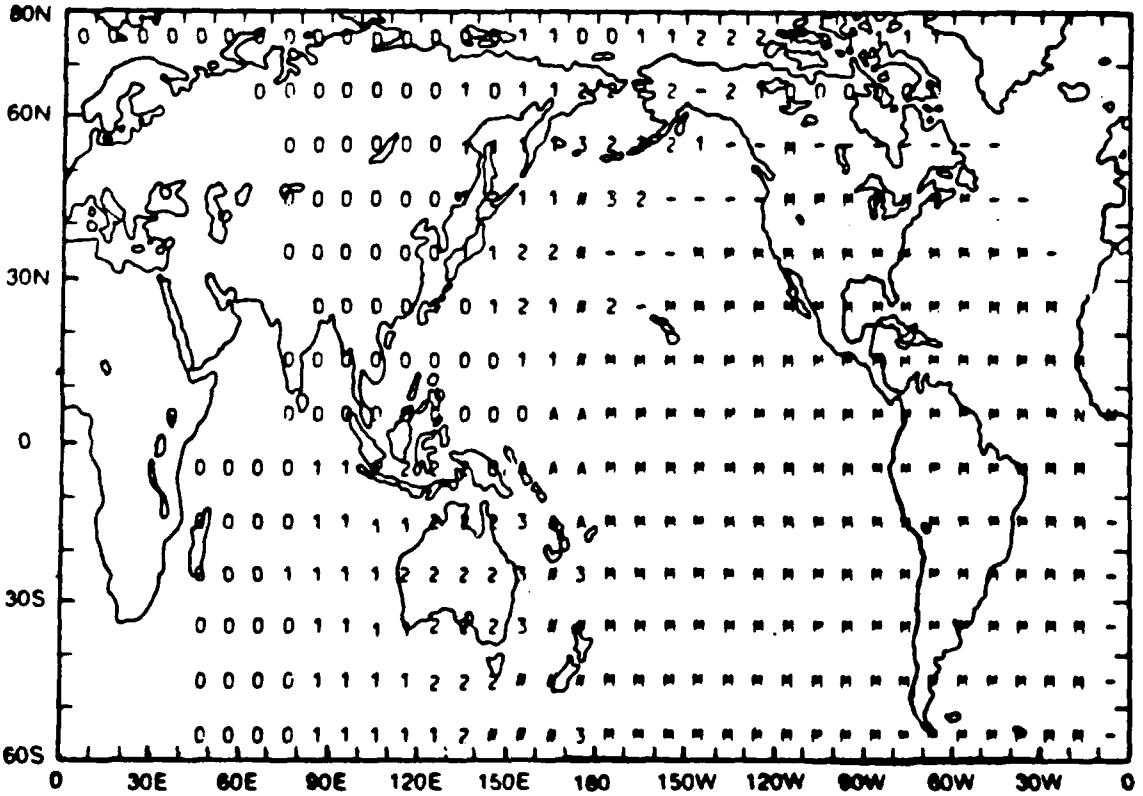

Omega Liberia 10.2 KHz
0600 GMT

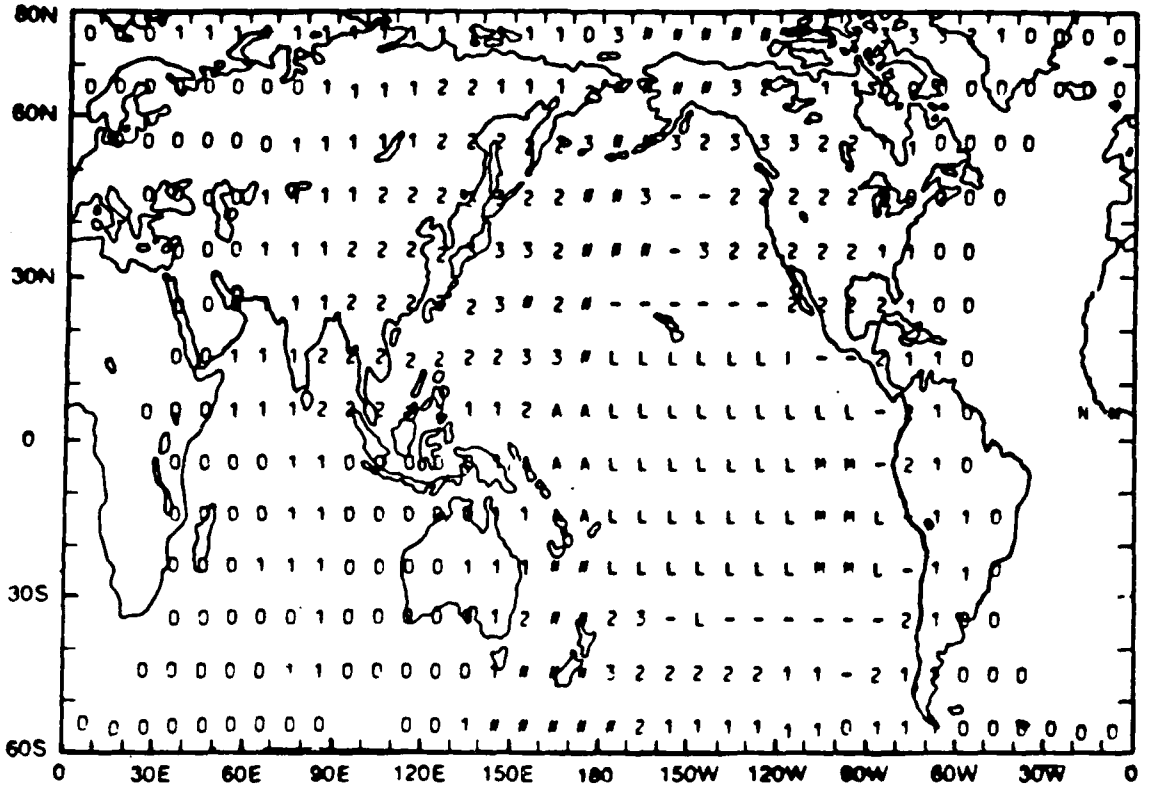

Omega Liberia 10.2 KHz
1200 GMT

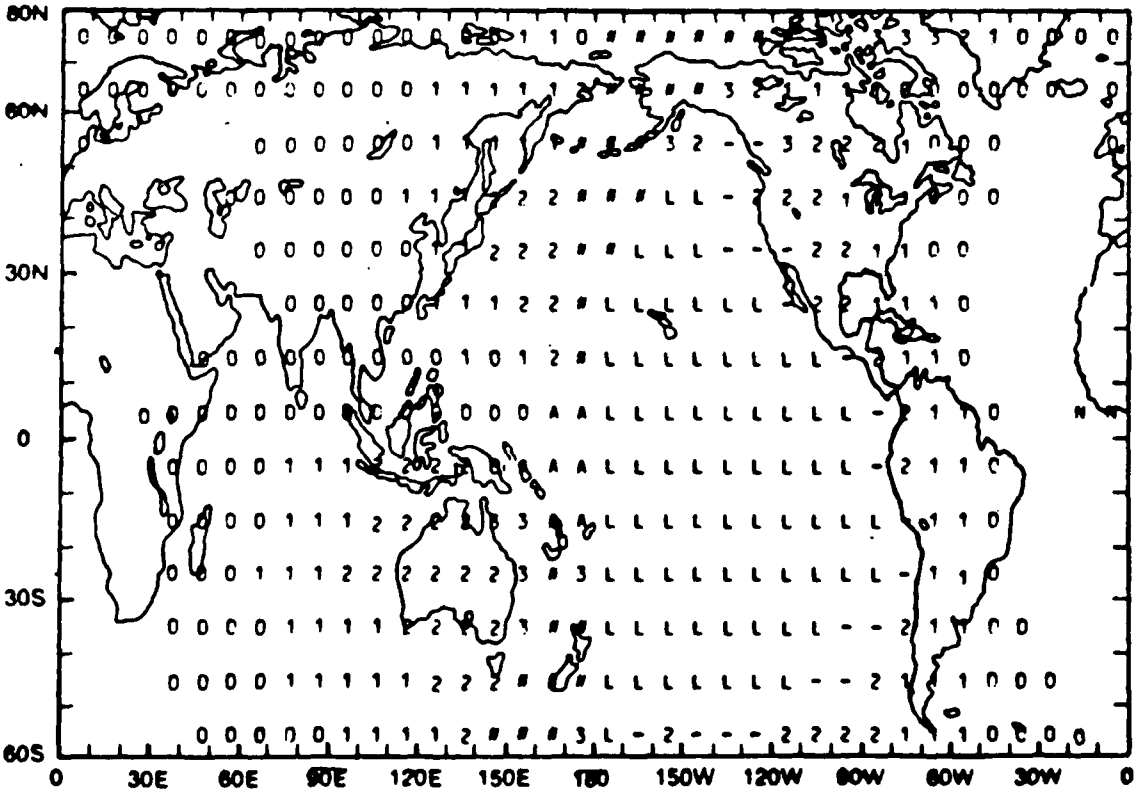

Omega Liberia 10.2 KHz
1800 GMT

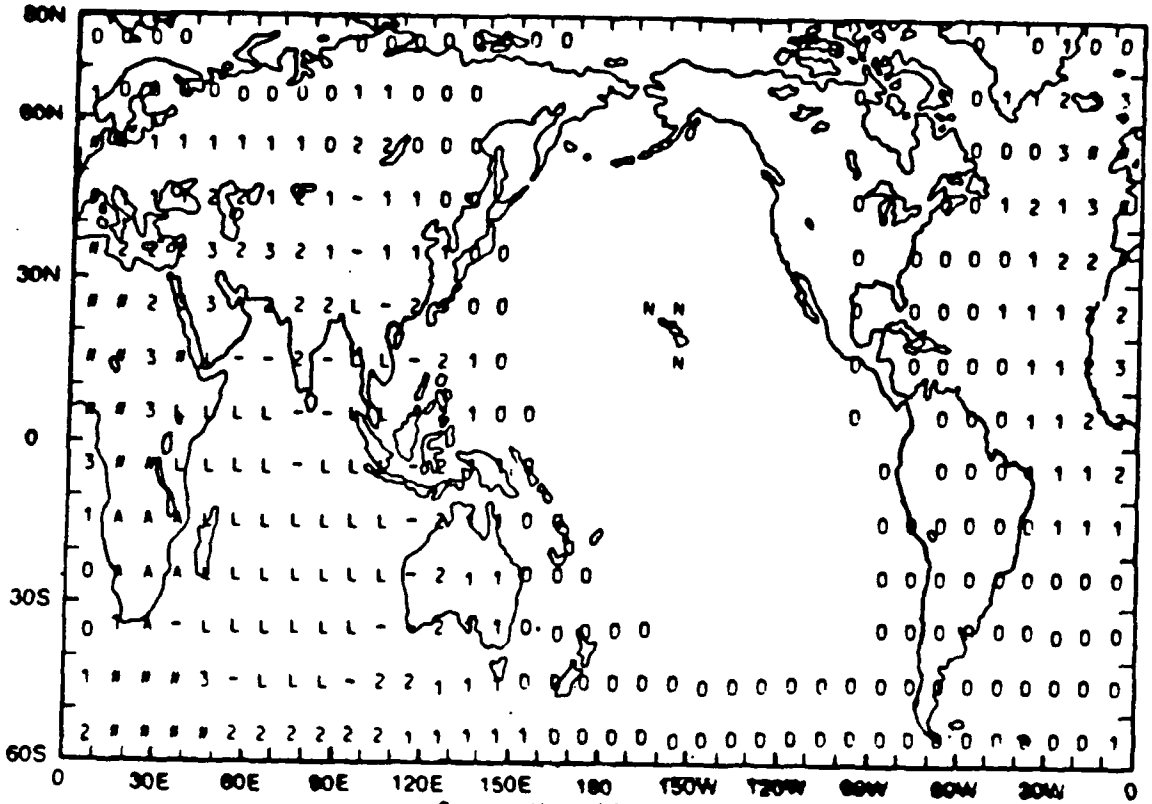

Omega Hawaii 10.2 KHz
0000 GMT

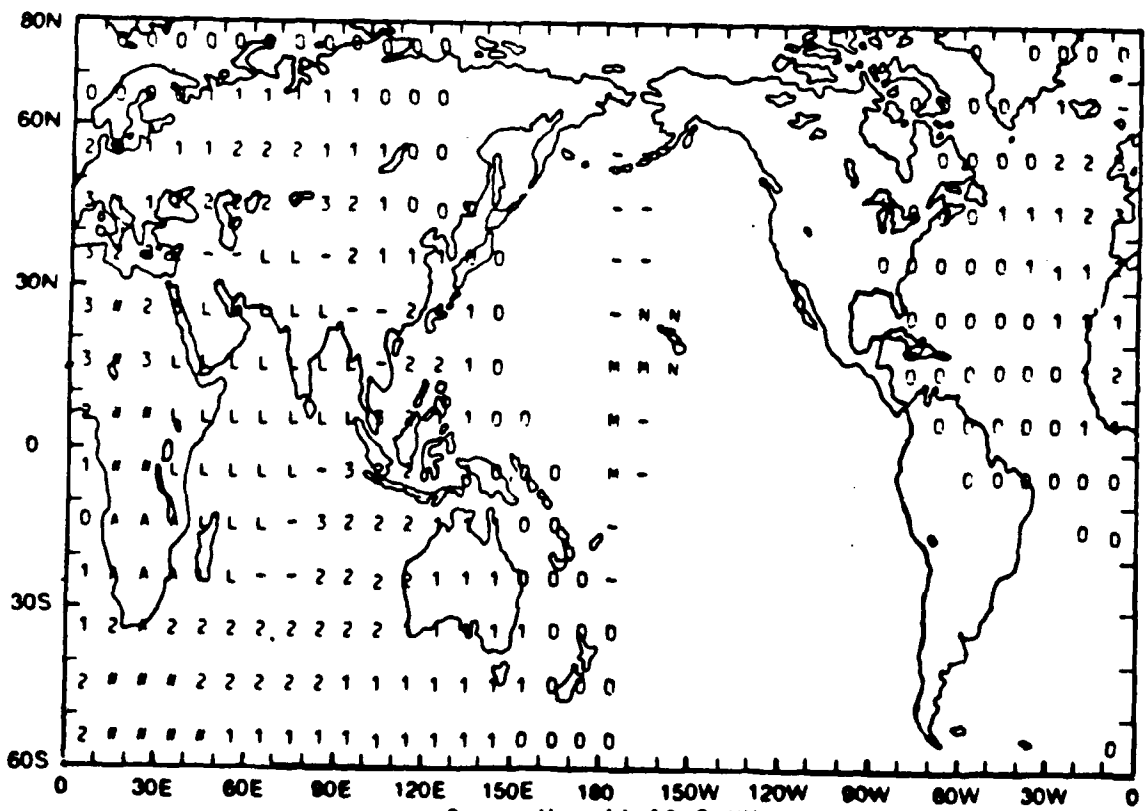

Omega Hawaii 10.2 KHz
0600 GMT

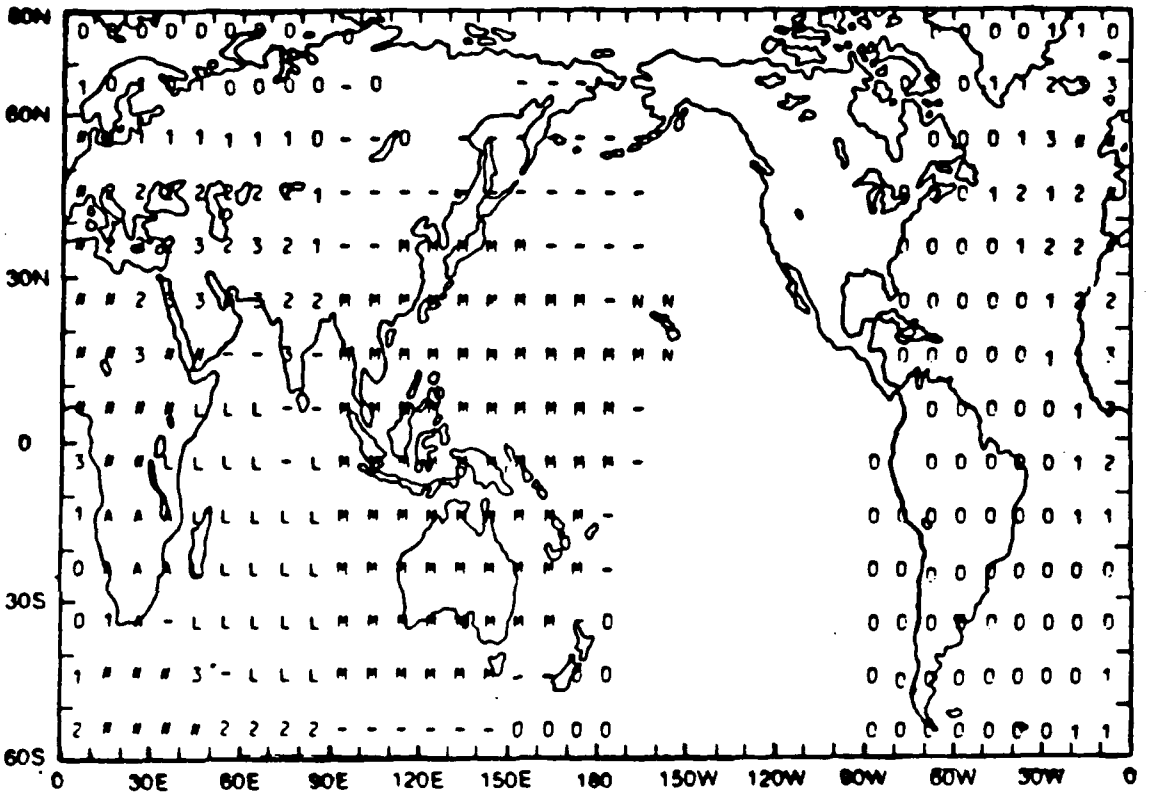

Omega Hawaii 10.2 KHz
1200 GMT

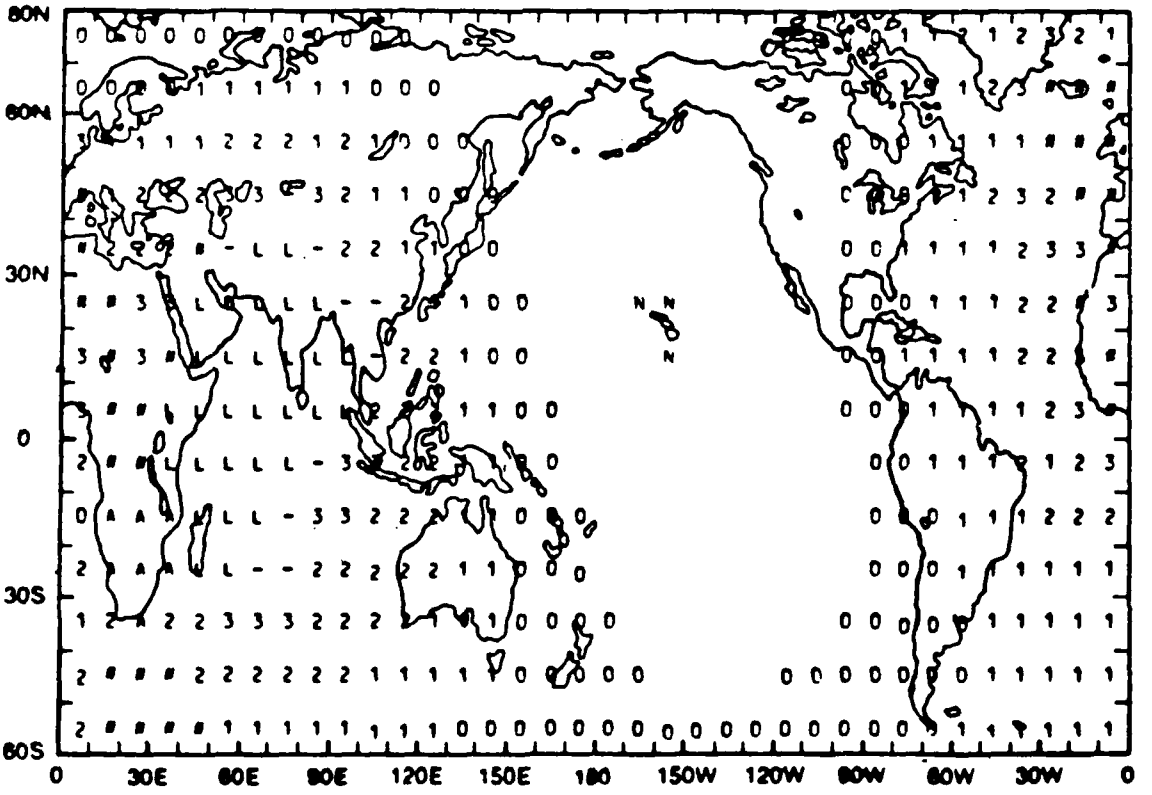

Omega Hawaii 10.2 KHz
1800 GMT

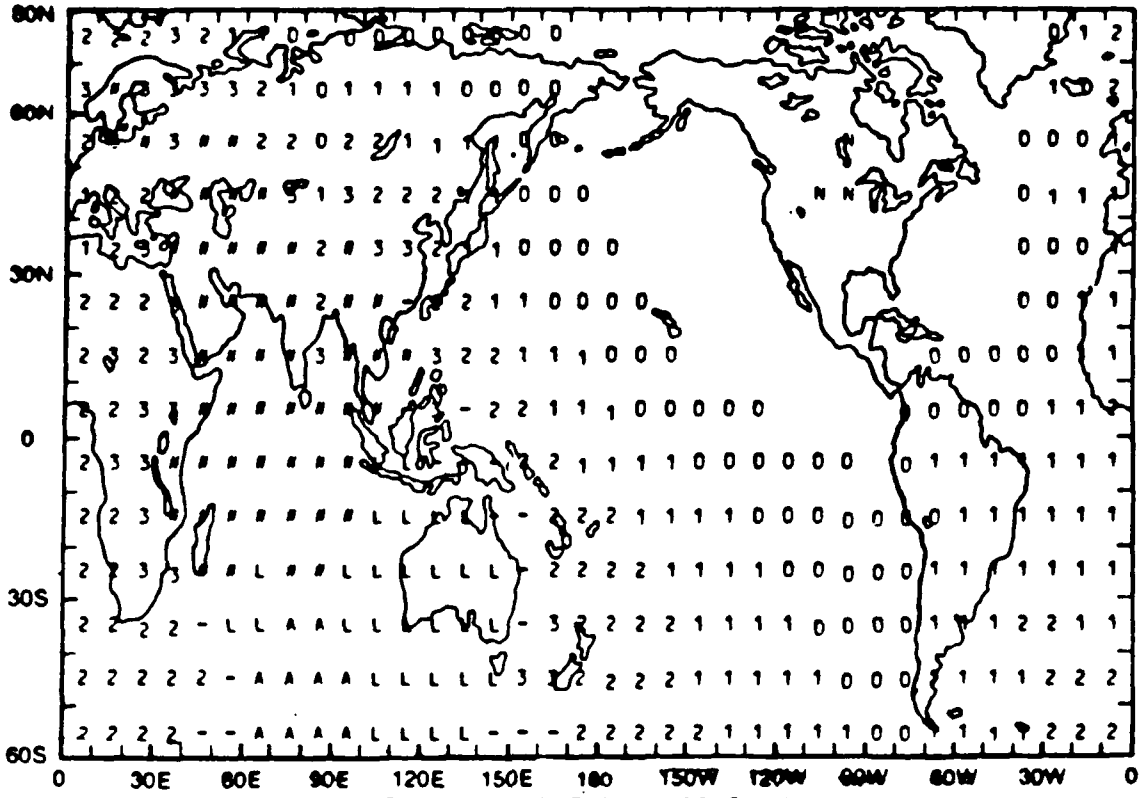

Omega North Dakota 10.2 KHz
0000 GMT

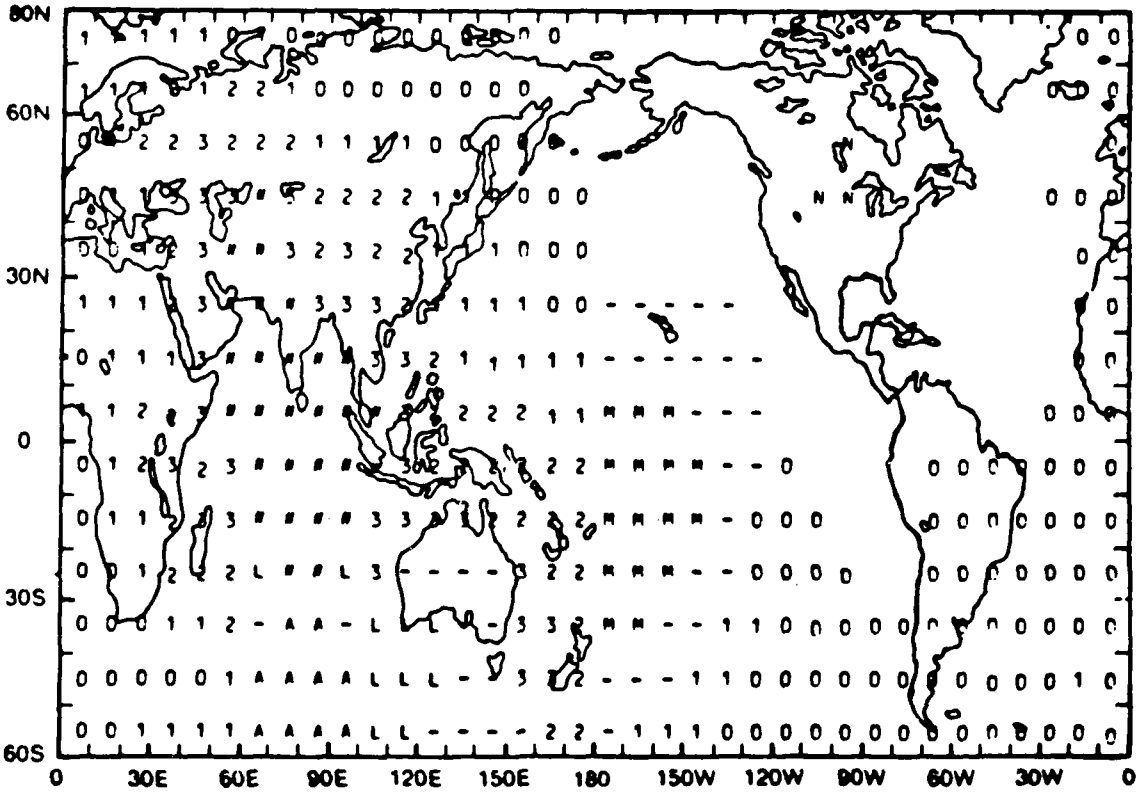

Omega North Dakota 10.2 KHz
0600 GMT

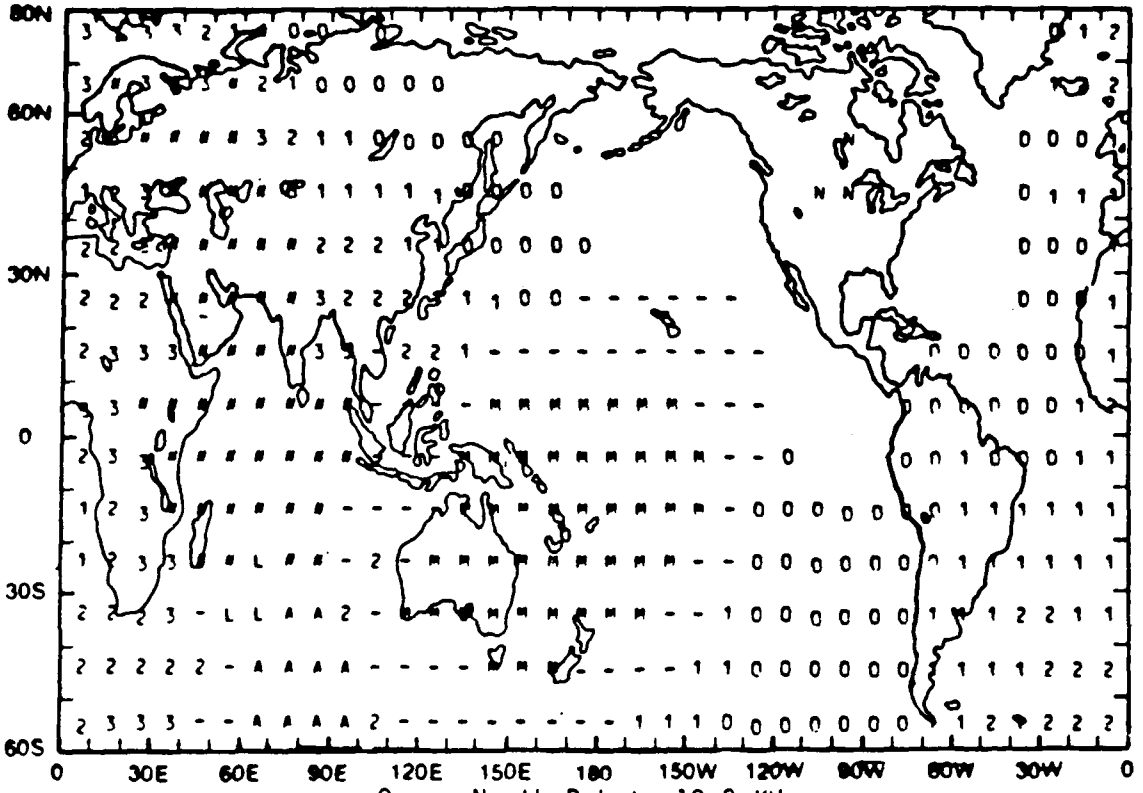

Omega North Dakota 10.2 KHz
1200 GMT

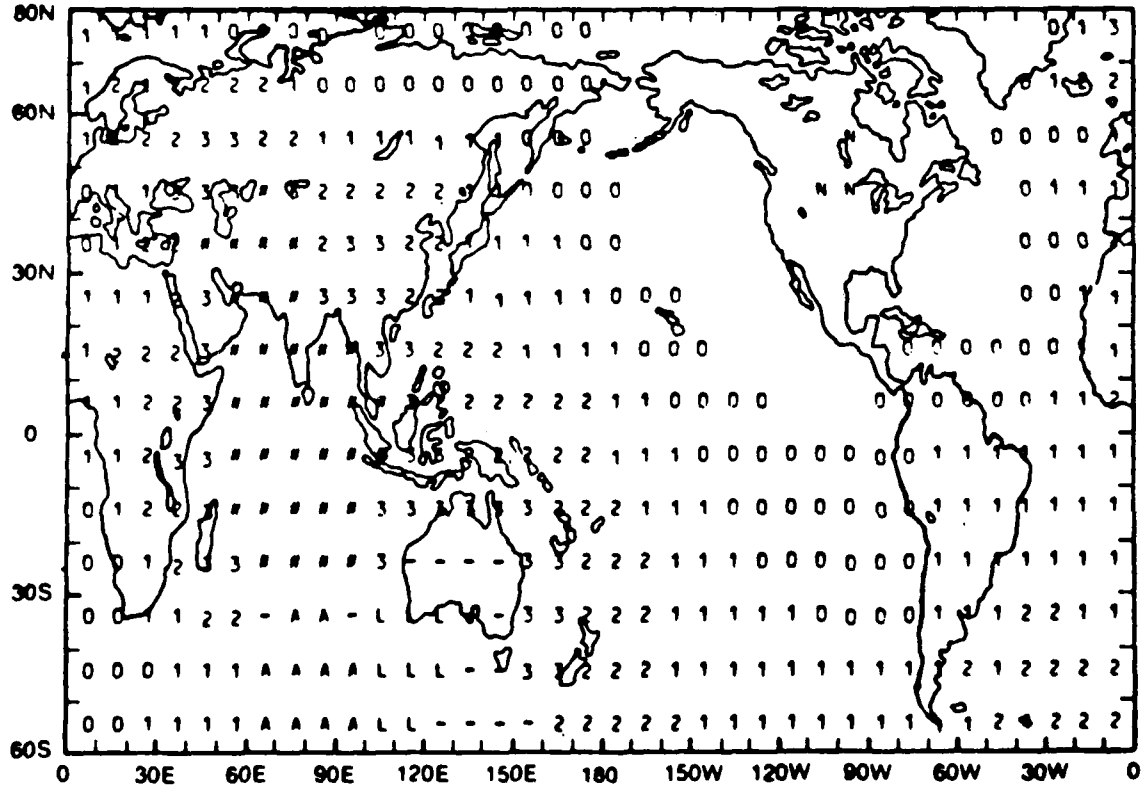

Omega North Dakota 10.2 KHz
1800 GMT

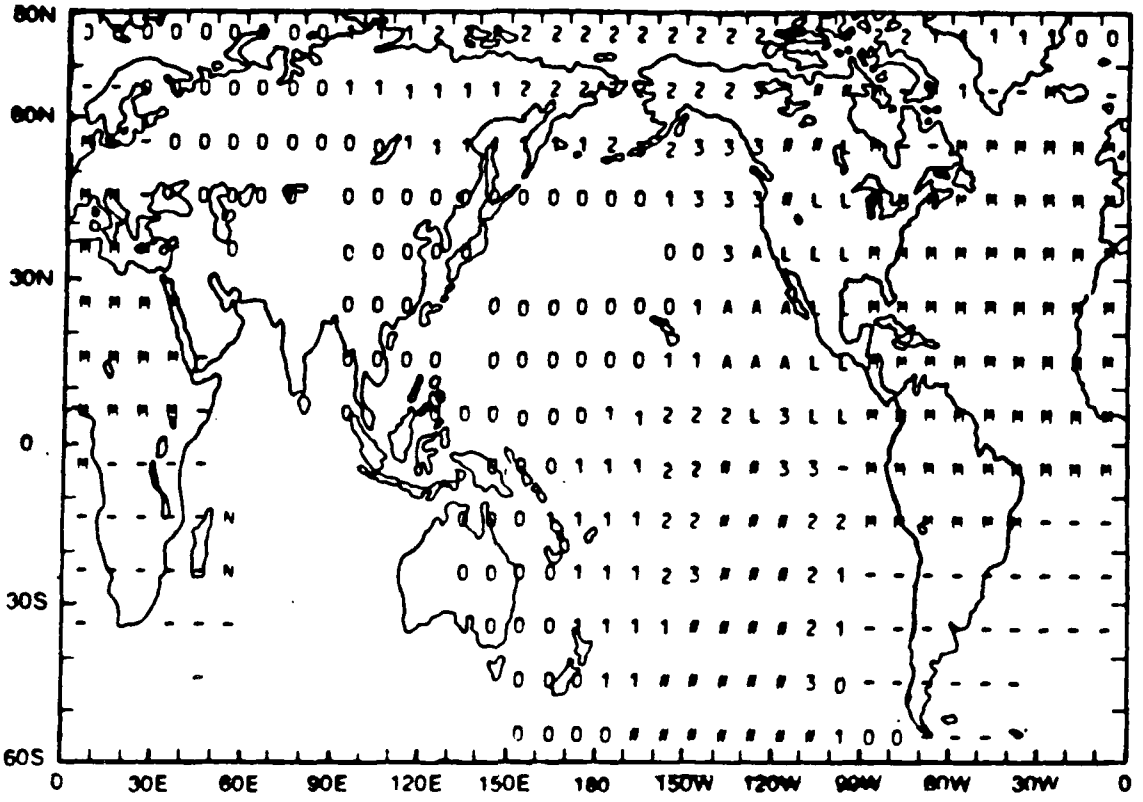

Omega La Reunion 10.2 KHz
0000 GMT

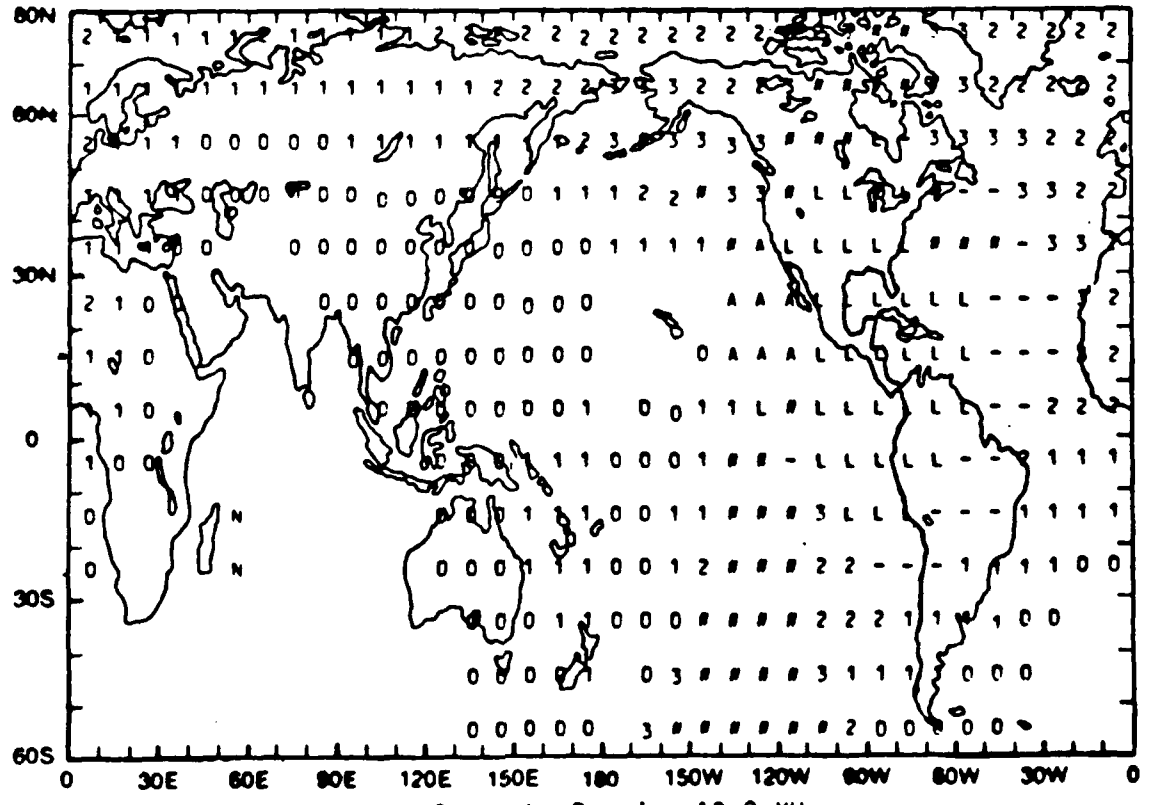

Omega La Reunion 10.2 KHz
0600 GMT

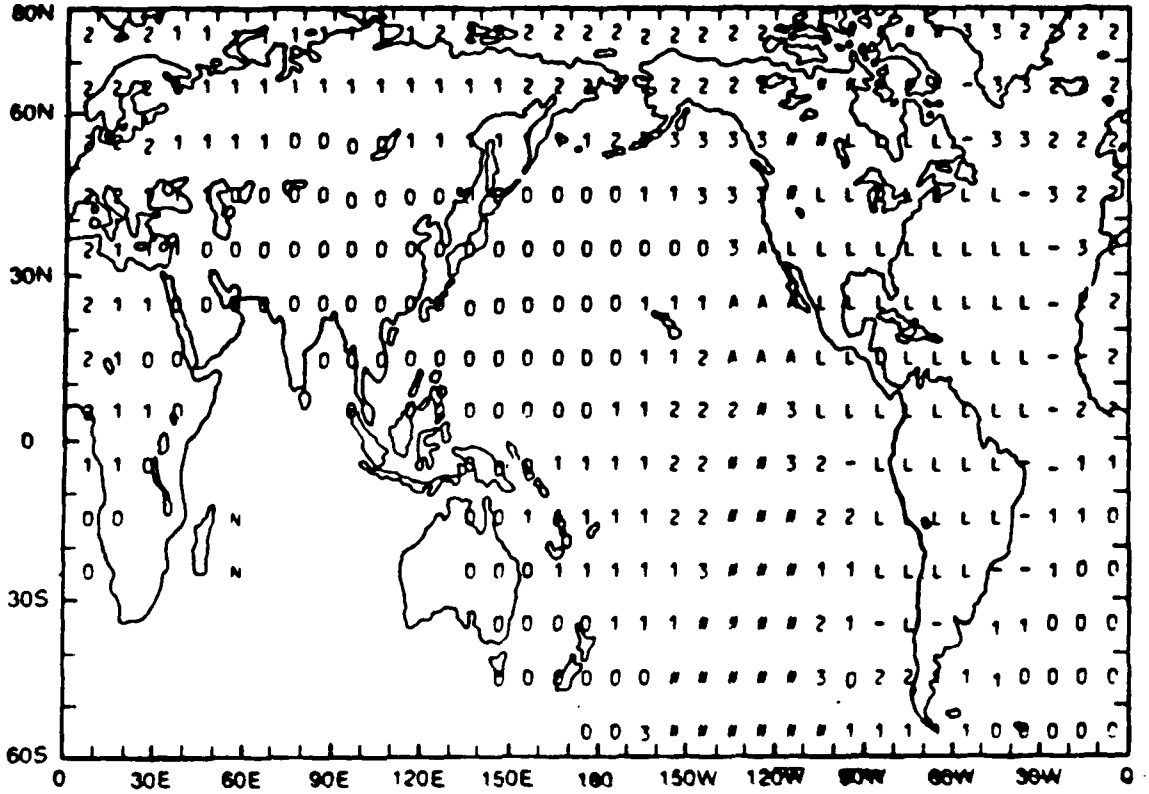

Omega La Reunion 10.2 KHz
1200 GMT

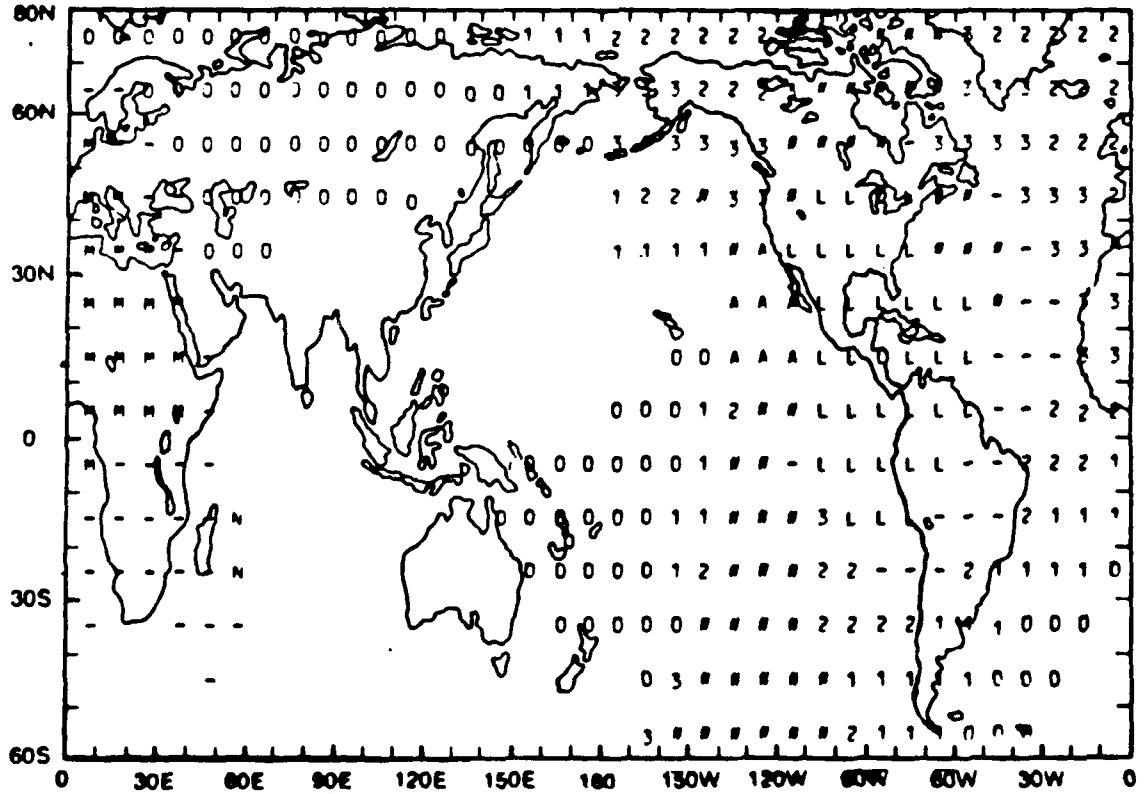

Omega La Reunion 10.2 KHz
1800 GMT

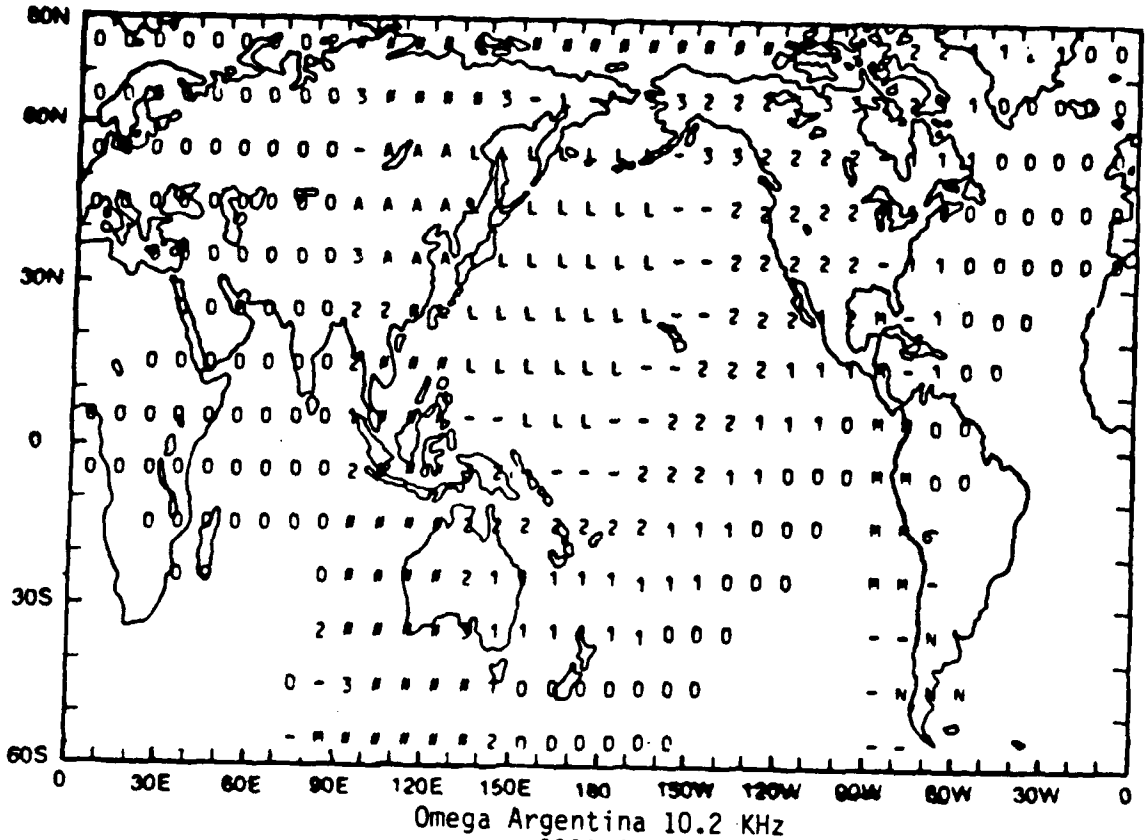

Omega Argentina 10.2 KHz
0000 GMT

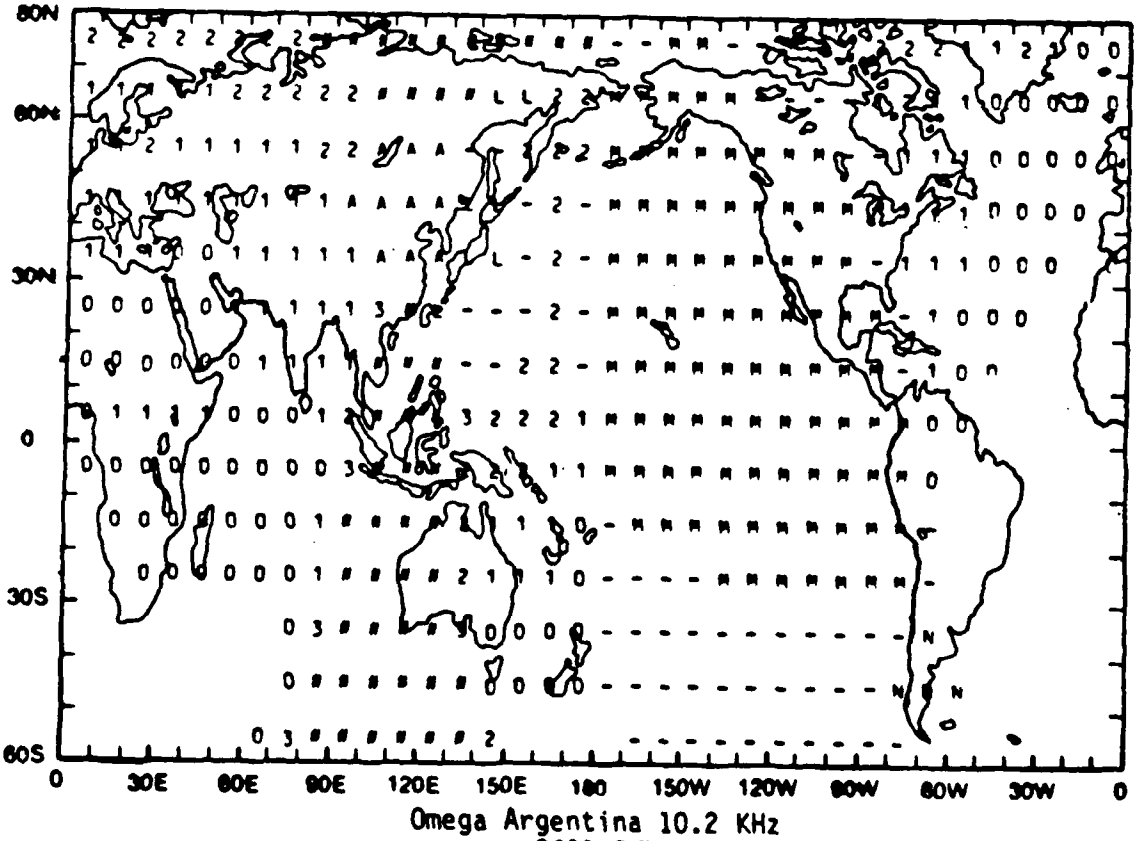

Omega Argentina 10.2 KHz
0600 GMT

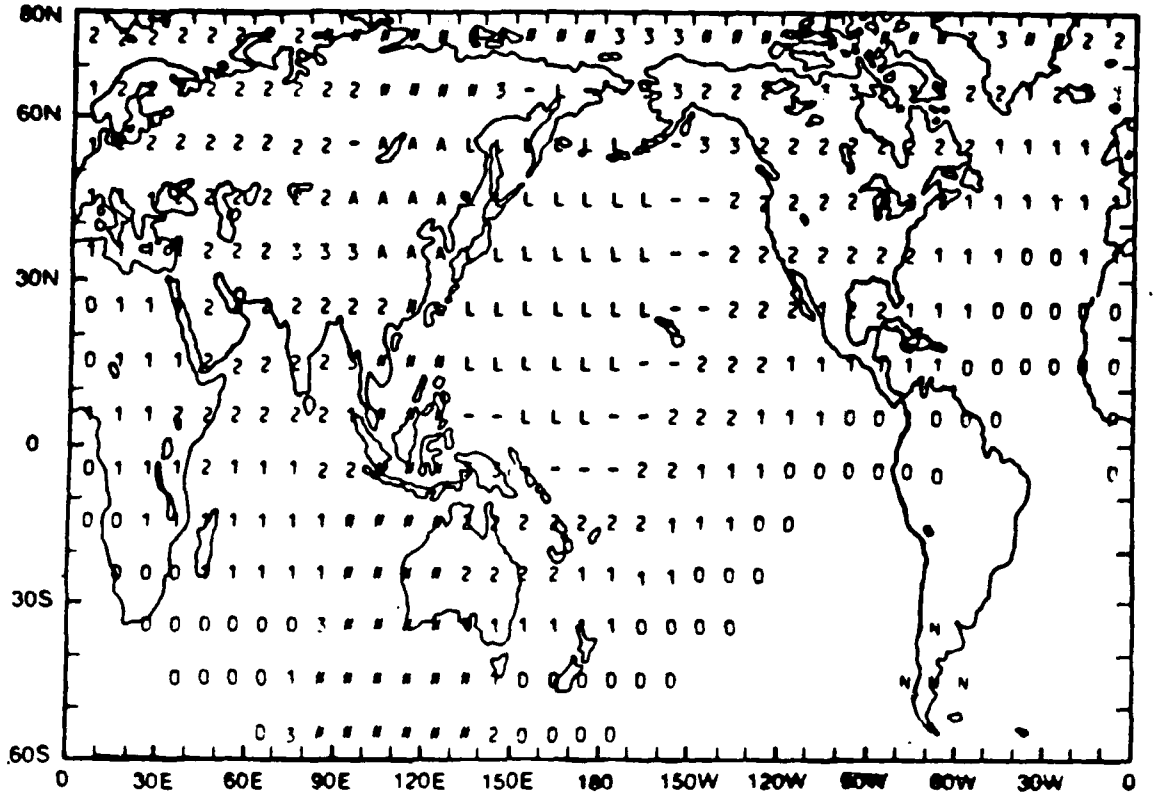

Omega Argentina 10.2 KHz
1200 GMT

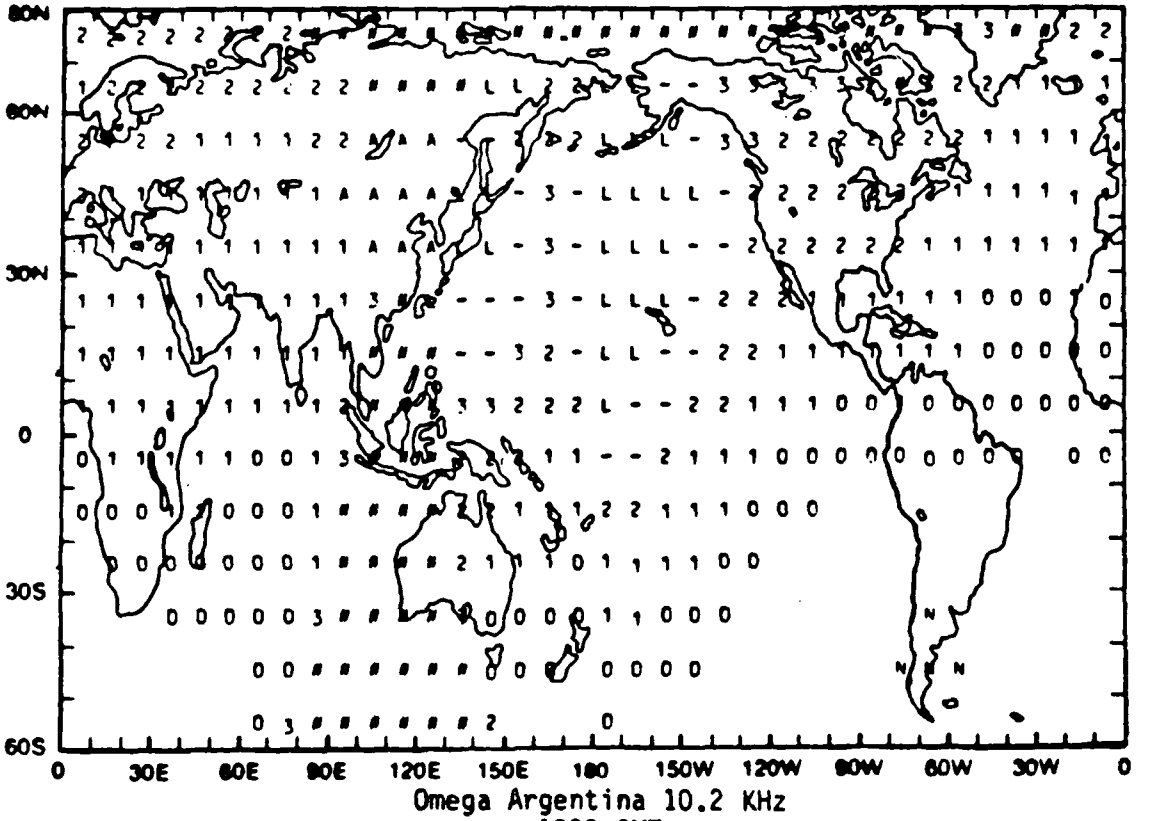

Omega Argentina 10.2 KHz
1800 GMT

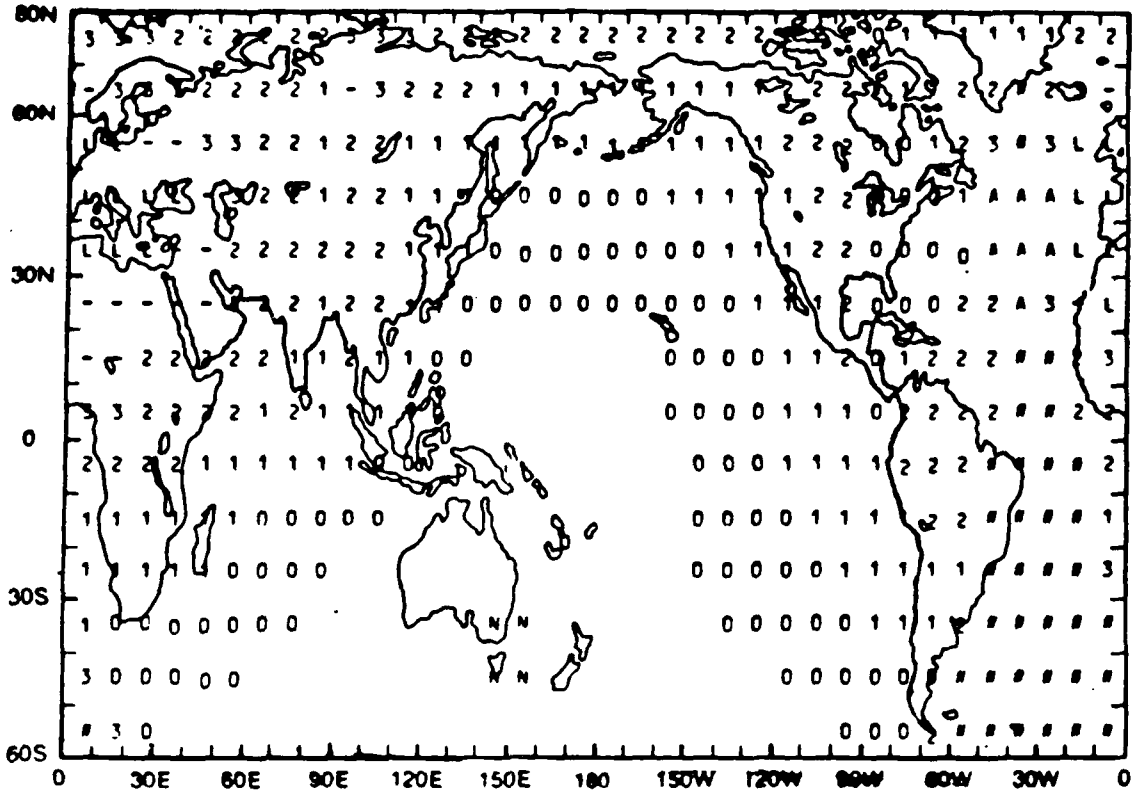

Omega Australia 10.2 KHz
0000 GMT

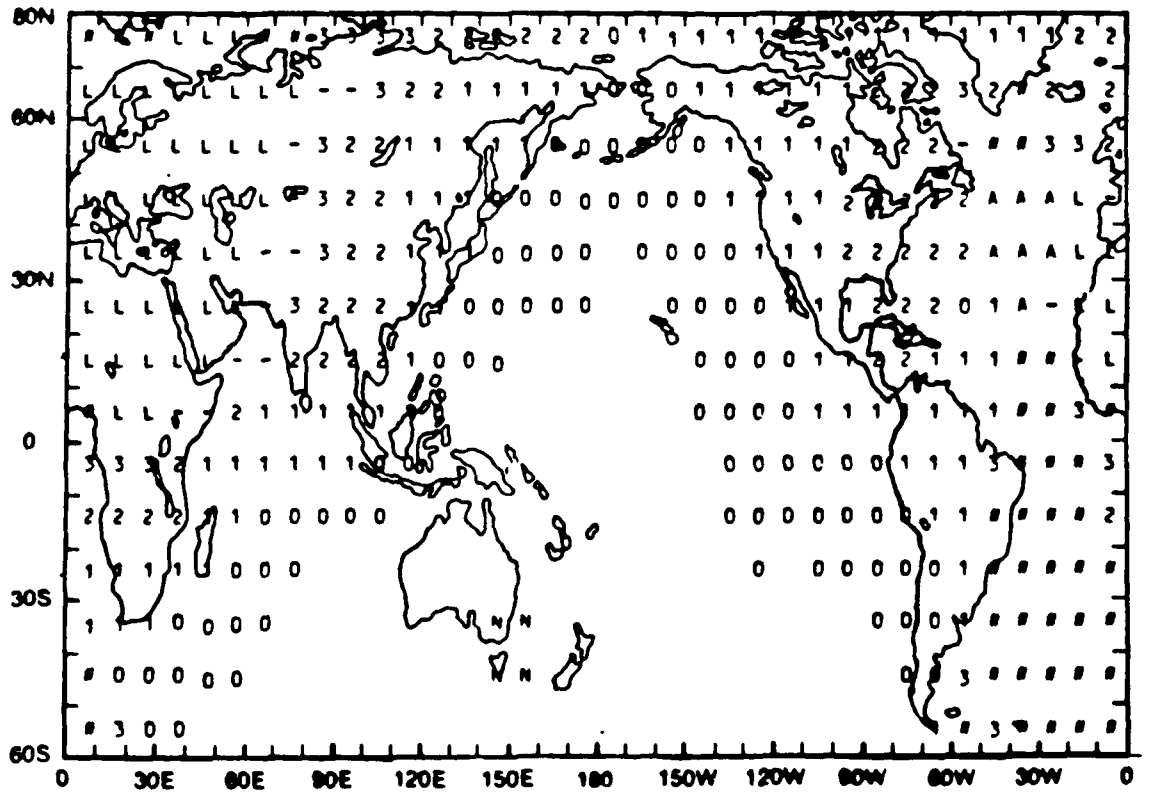

Omega Australia 10.2 KHz
0600 GMT

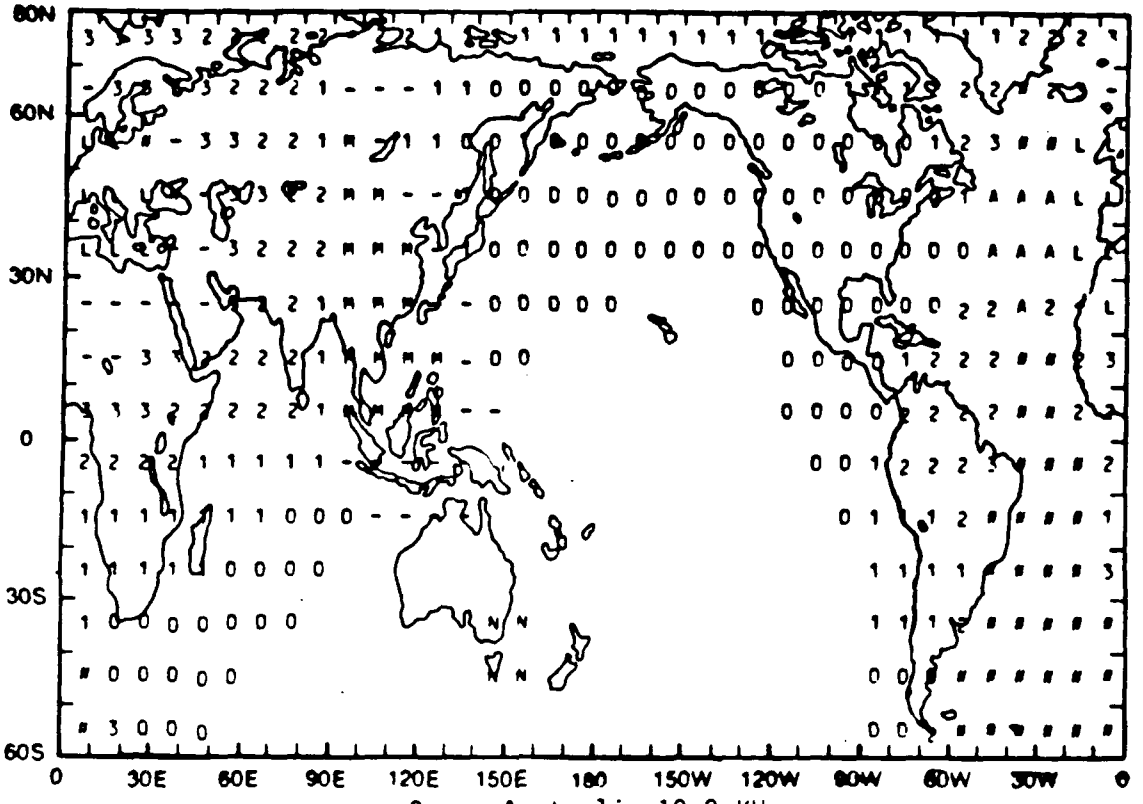

Omega Australia 10.2 KHz
1200 GMT

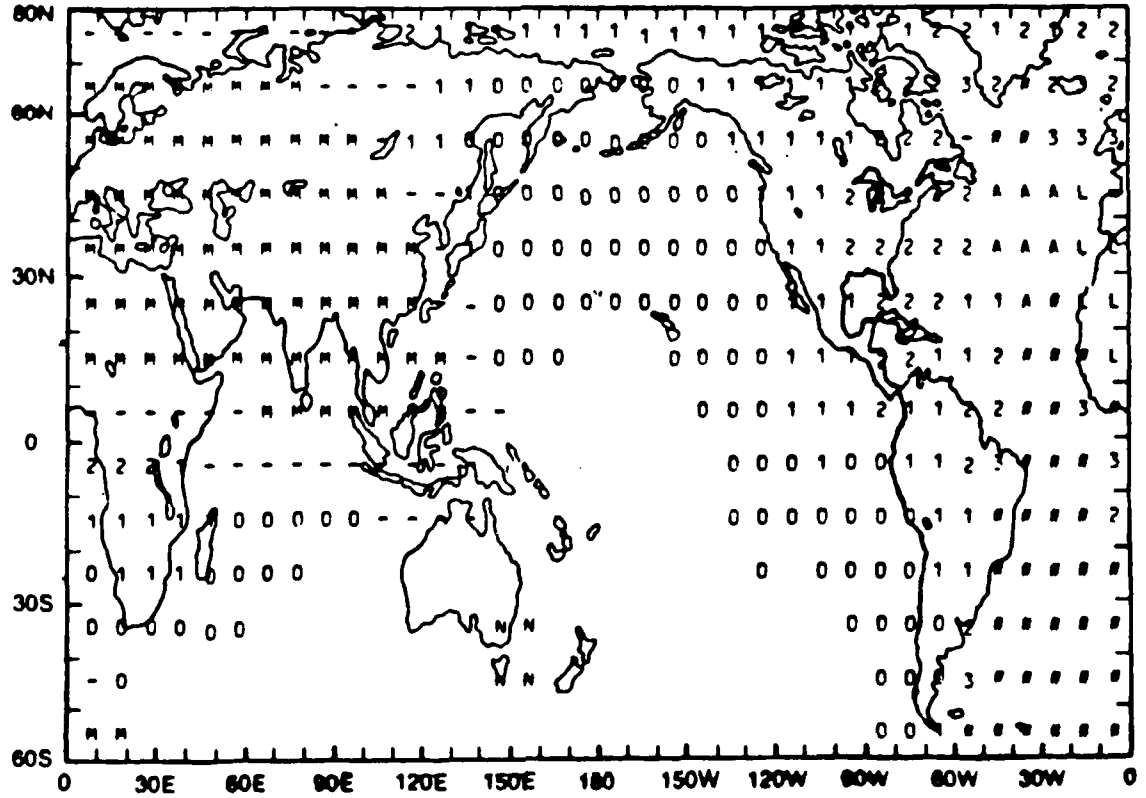

Omega Australia 10.2 KHz
1800 GMT

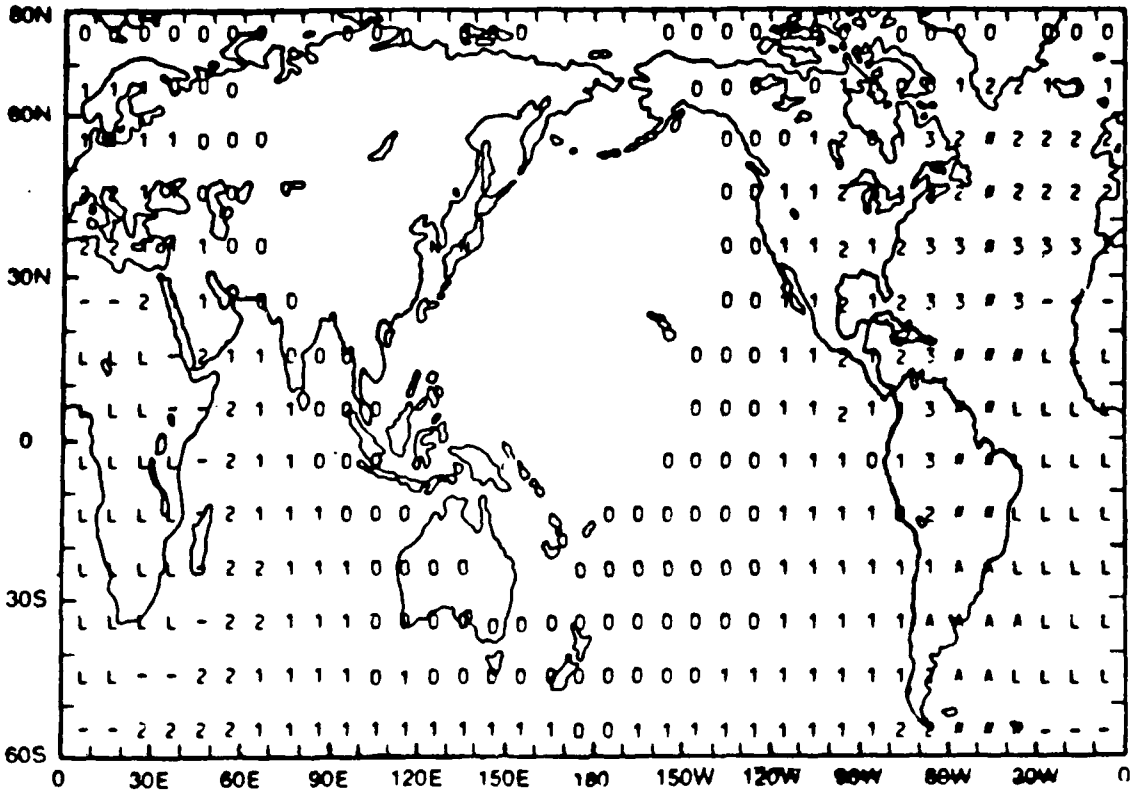

Omega Japan 10.2 KHz
0000 GMT

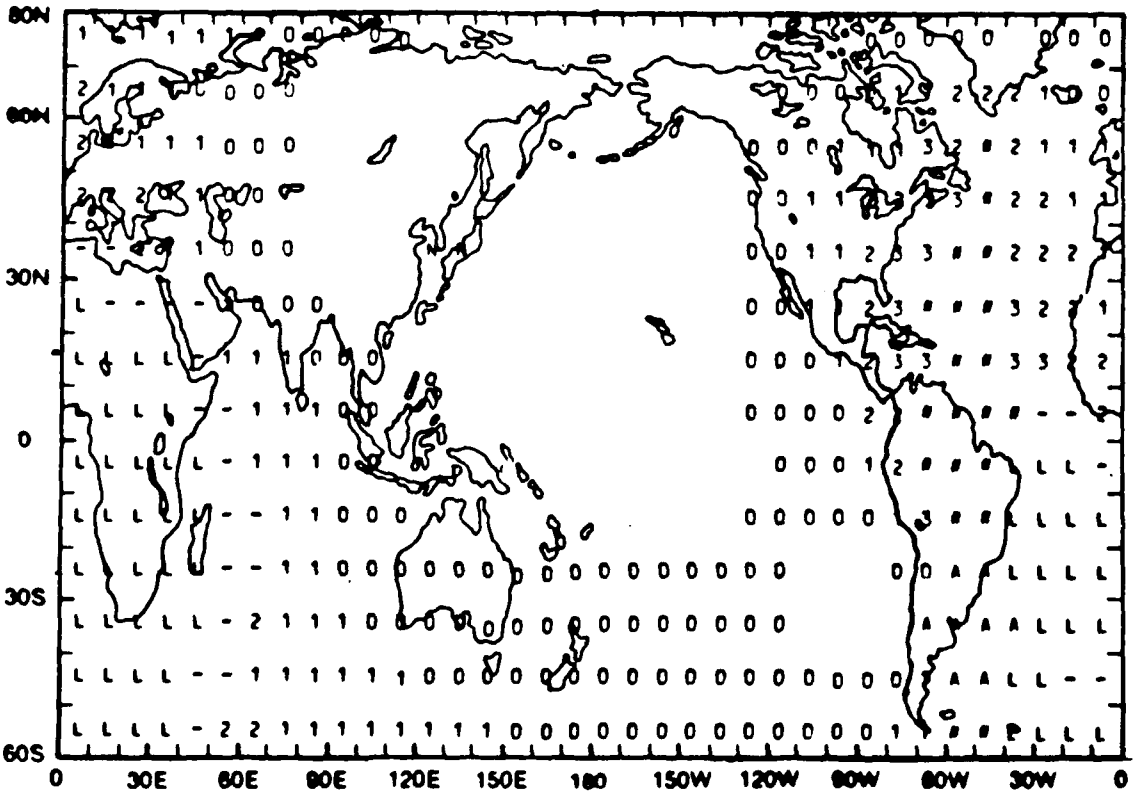

Omega Japan 10.2 KHz
0600 GMT

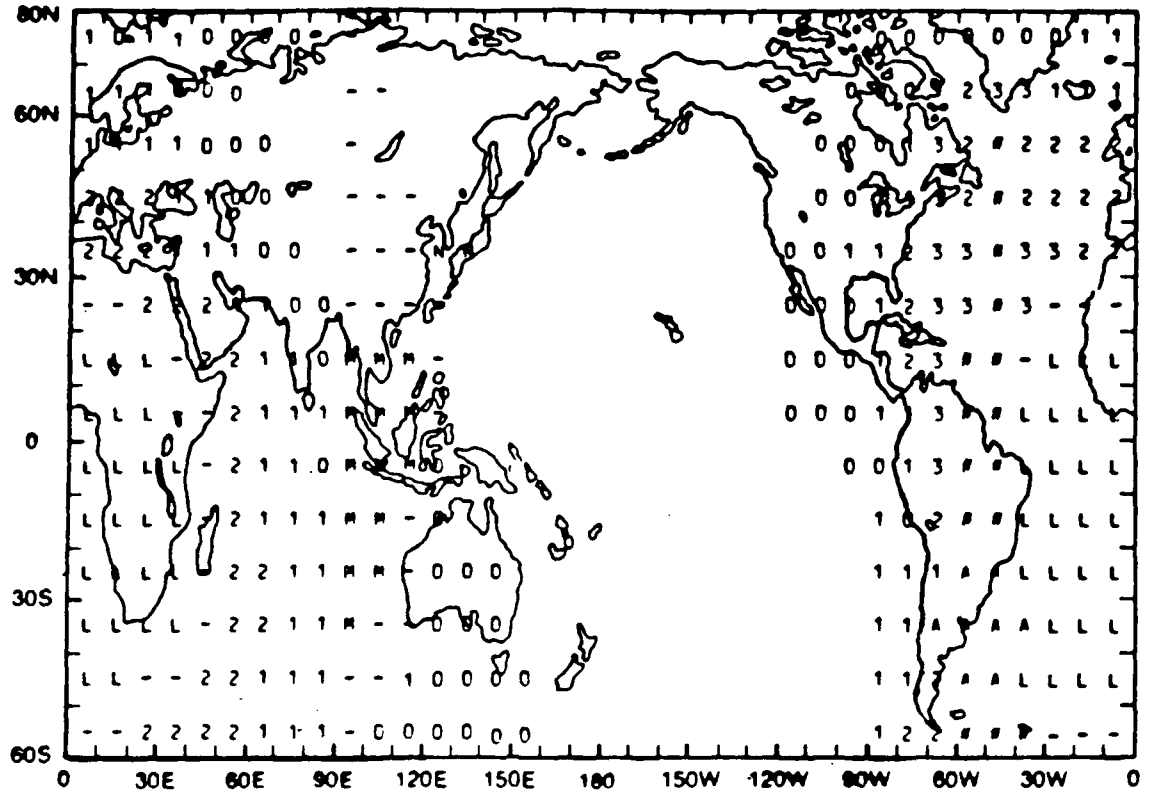

Omega Japan 10.2 KHz
1200 GMT

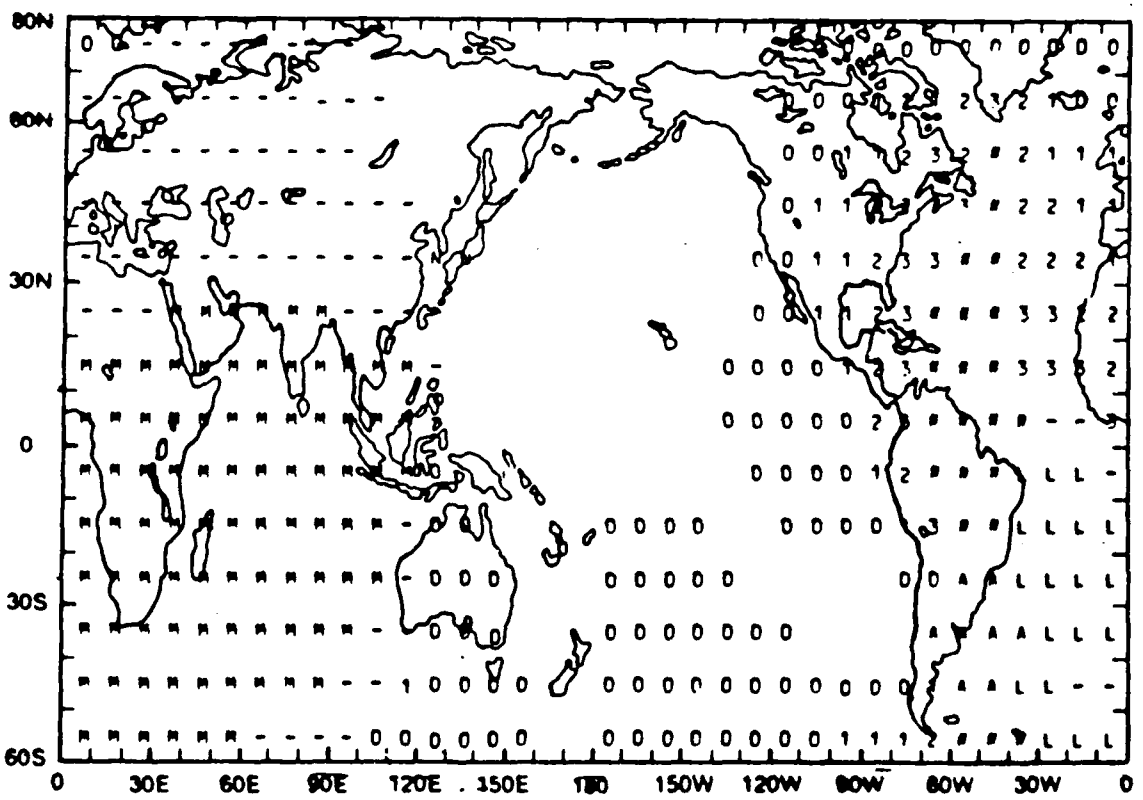

Omega Japan 10.2 KHz
1800 GMT

APPENDIX C

ALTERNATIVE COVERAGE ANALYSIS

LOCAL COVERAGE ANALYSIS

A method of coverage analysis was developed in conjunction with the North Pacific validation and has been documented by Levine and Woods (1981). The approach had considerable success in describing performance in the North Pacific and has also been similarly applied to the Indian Ocean. As previously mentioned, the theoretical approach seems equivalent to that used by Swanson (1983; 1984a) based on earlier work by Thompson (1977) and, especially, Lee (1975a; 1975b). In practice, the Levine-Woods methodology has been applied rather differently than the application by Thompson and Swanson. In the latter approach, the errors are modeled as well as possible physically and then incorporated into the global coverage prediction arithmetic. The Levine-Woods approach treats the error models more statistically on a local basis. While the authors have a distinct preference for the global modeling approach, it is at least prudent to present results from the previously successful analysis when applied to the present coverage region. The numeric results presented herein were computed by Dr. Levine for this validation.

A detailed description of the "Local" Levine-Woods approach is beyond the scope of this document. It is, however, fully described in laudible algebraic detail in the previously mentioned reference (Levine and Woods; 1981) and may be summarized as follows.

Error characterization is a major problem to be addressed in any method of coverage assessment. Levine and Woods do this statistically starting with the Omega Master File data. This data base includes hourly phase difference measurements at many sites over a long period of time. Also incorporated are Predicted Propagation Corrections (PPC's) so that phase errors can be generated. For this analysis, selected local subsets of Master File data were processed separately for 10.2 kHz and 13.6 kHz and, for each frequency, grouped into "Day" (0600 GMT ± 1 hour), "Night" (1800 GMT± 1 hour) and 24-hour. Summary statistics were prepared for each of these periods at the two frequencies. The statistics were then partitioned so as to apportion a portion to each of the two stations composing each station pair (line-of-position) in the Master File. The resultant error statistics were then combined with coverage overlays to determine areas of useful coverage and then the coverage model used to obtain system accuracy for the region.

Histogram summarizing statistics are given in Figures C-1 to C-3. These statistics were used to obtain coverage maps shown in Figures C-4 through C-14 showing coverages for day, night and 24-hours and for various statistical accuracy measures: C.E.P., RMS and 95th percentile. Figures C-4 through C-12 show results of accuracy calculations including allowance for PPC BIAS whereas Figures C-13 and C-14 show 24-hour coverage estimated with the effect of PPC BIAS removed. Coverage Printout symbology includes "#" if less than three stations are available and otherwise shows the integral part of the anticipated accuracy in n. mi. Special symbols include blank used for accuracy better than one n. mi. and ">" for accuracy worse than 10 n. mi. [note that this is not the convention used in Appendix B where the indication is of nominal accuracy, e.g., "1" means accuracy between 0.5 and 1.5 n. mi. instead of 1.0 to < 2.0 n. mi. used here].

A few comments may be in order. First, the Master File now contains a regretable number of errors--perhaps 30% of the data are effected. The size of the Master File precludes proper editing which is well beyond any level of realistic effort as a part of the present project. The use of averages or standard deviations in the analysis is likely to have resulted in significant error. [It could be speculated that the use of medians might have lead to estimates which would be more plausible if still in error.]

Second, the partitioning of statistics from those measured for lines-of-position to the individual station contributions is based on a rather arbitrary procedure assuming equal variance contributions. This is probably not very realistic and could be improved.

Third, in preparing the fix accuracy maps, the frequencies are combined based on zero correlation. Again, this is unrealistic. This introduces roughly a factor of two in the accuracy to be obtained from a four-frequency receiver compared with one operating at either 10.2 kz or 13.6 kHz alone. [It is especially important to remember this fact when comparing results with those in Appendix B which are for 10.2 kHz alone. To a substantial extent this mitagates the overly high error estimates obtained as result of errors in the Master File.]

Fourth, the coverage overlays used were based on a requirement for a 20 db signal-to-noise ratio in a 100 Hz bandwidth. As previously noted, this is much too conservative. It leads to the prediction of large areas within which the system will not function when, in fact, navigation is possible.

All in all, the local coverage predictions tend to reflect a relatively constant error budget with proper accounting for geometric effects but with usage controlled by overly conservative coverage overlays.

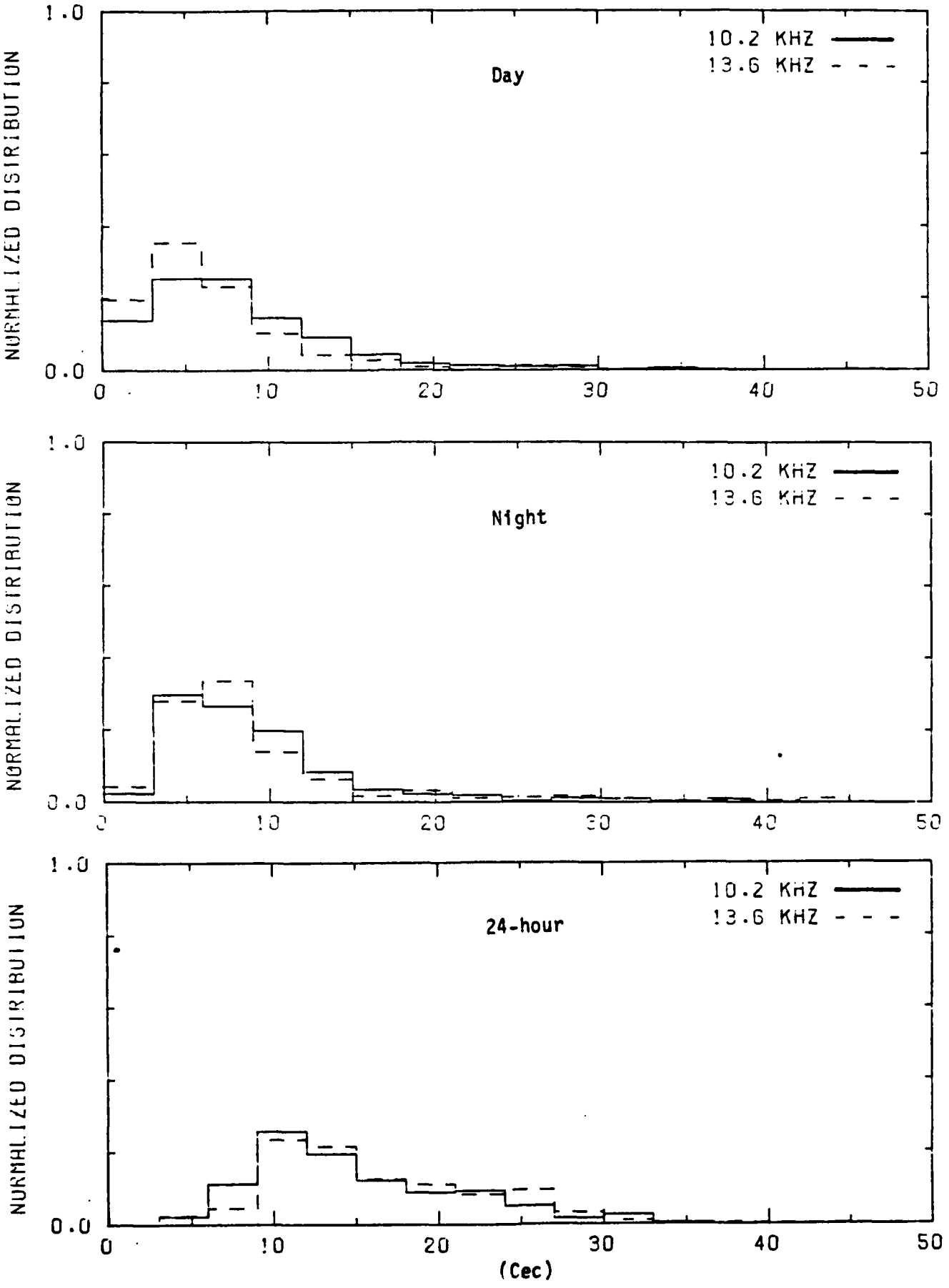

Figure C-1. RMS Phase Error Histograms

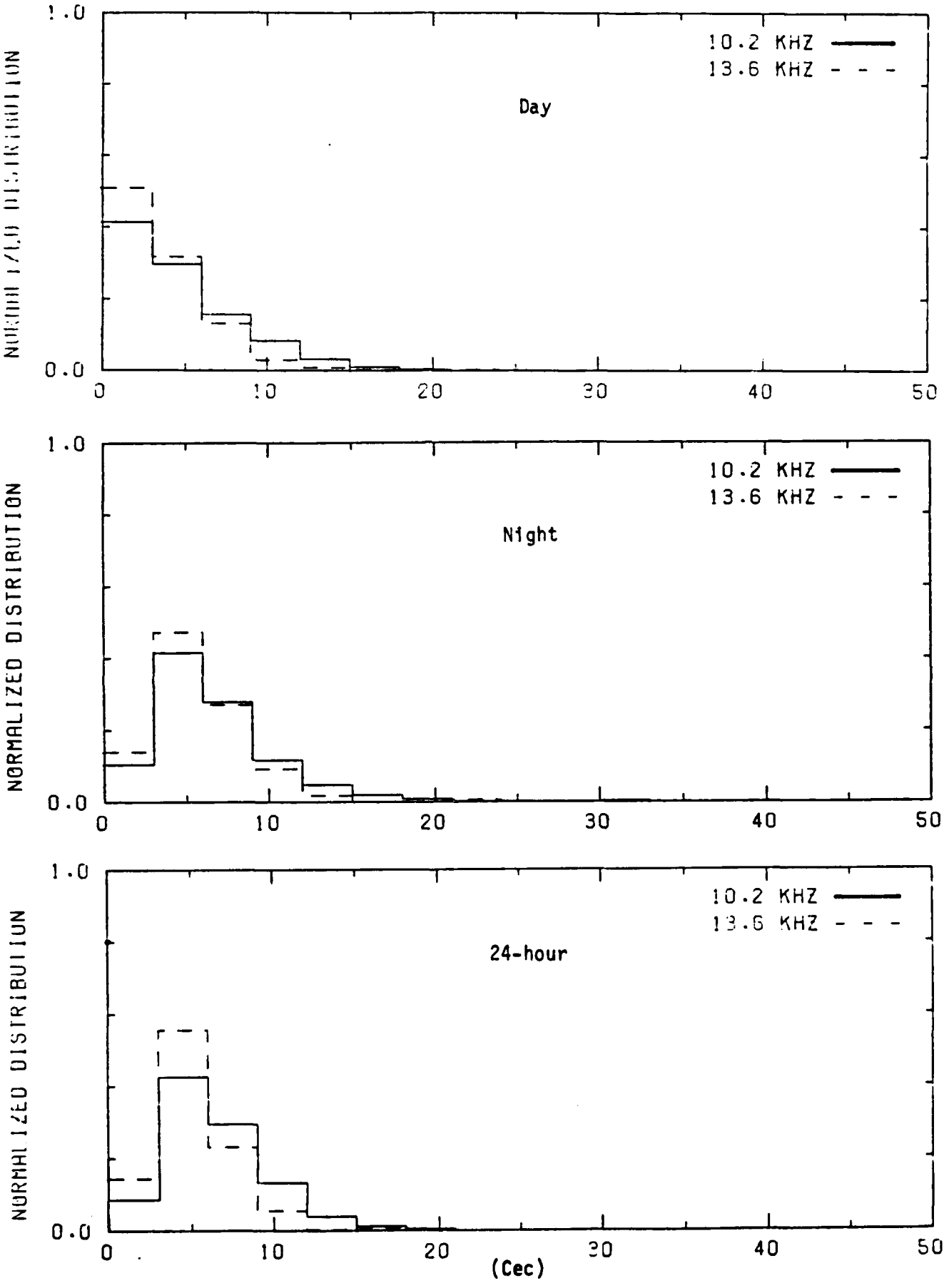

Figure C-2. Random RMS Phase Error Histograms

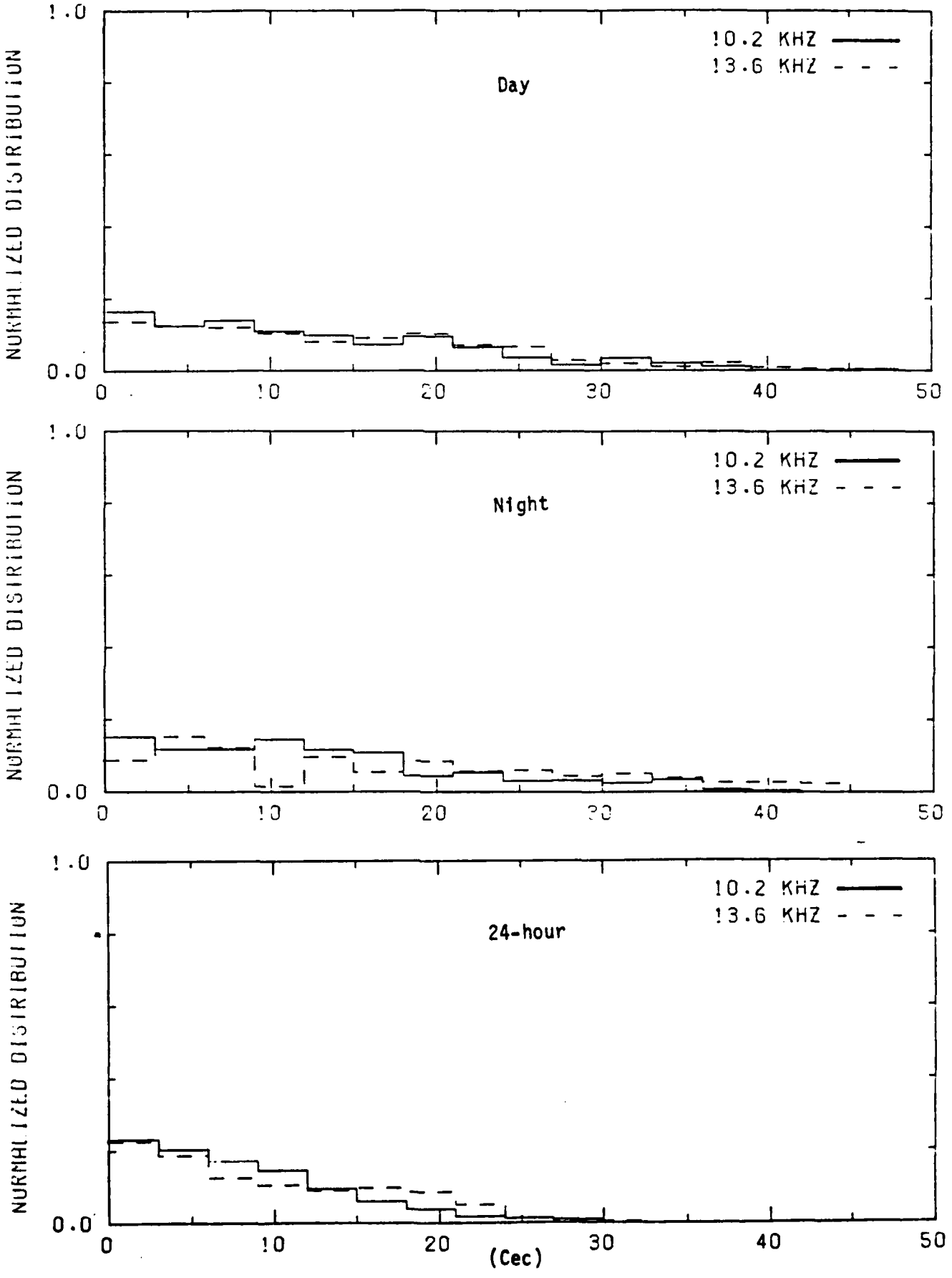

Figure C-3. Absolute Phase Error Histograms

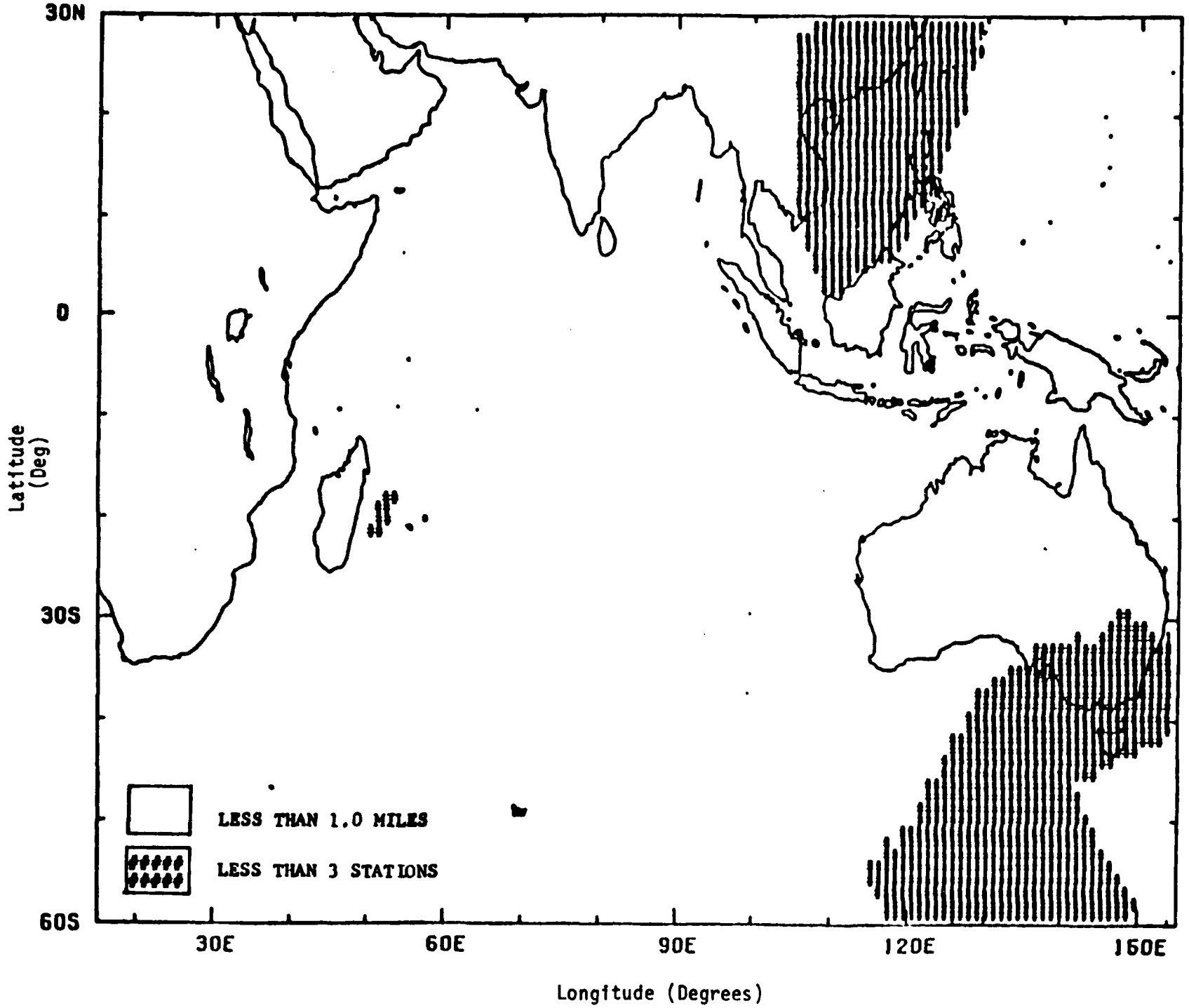

Figure C-4. Daytime Coverage: C.E.P.

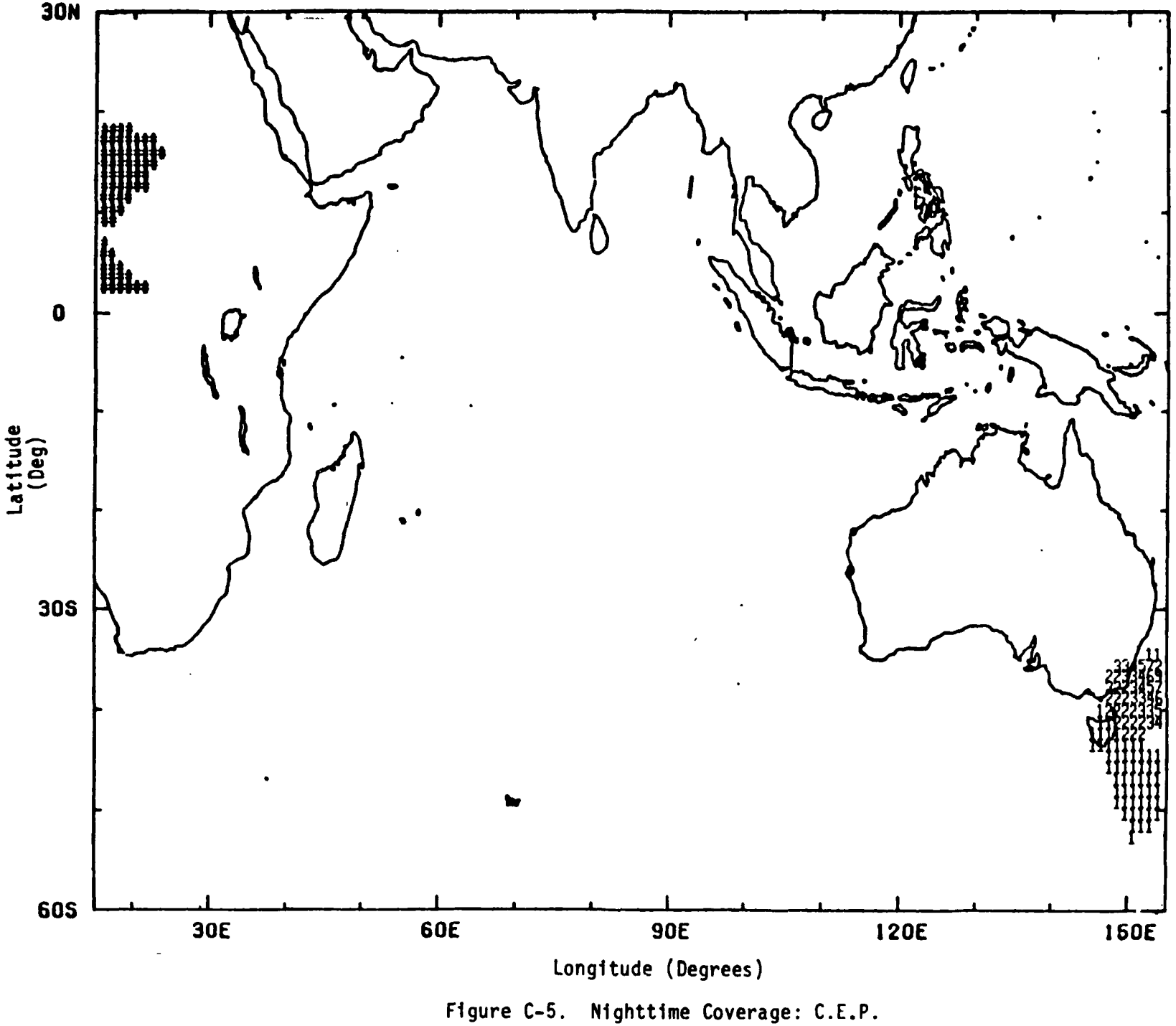

Figure C-5. Nighttime Coverage: C.E.P.

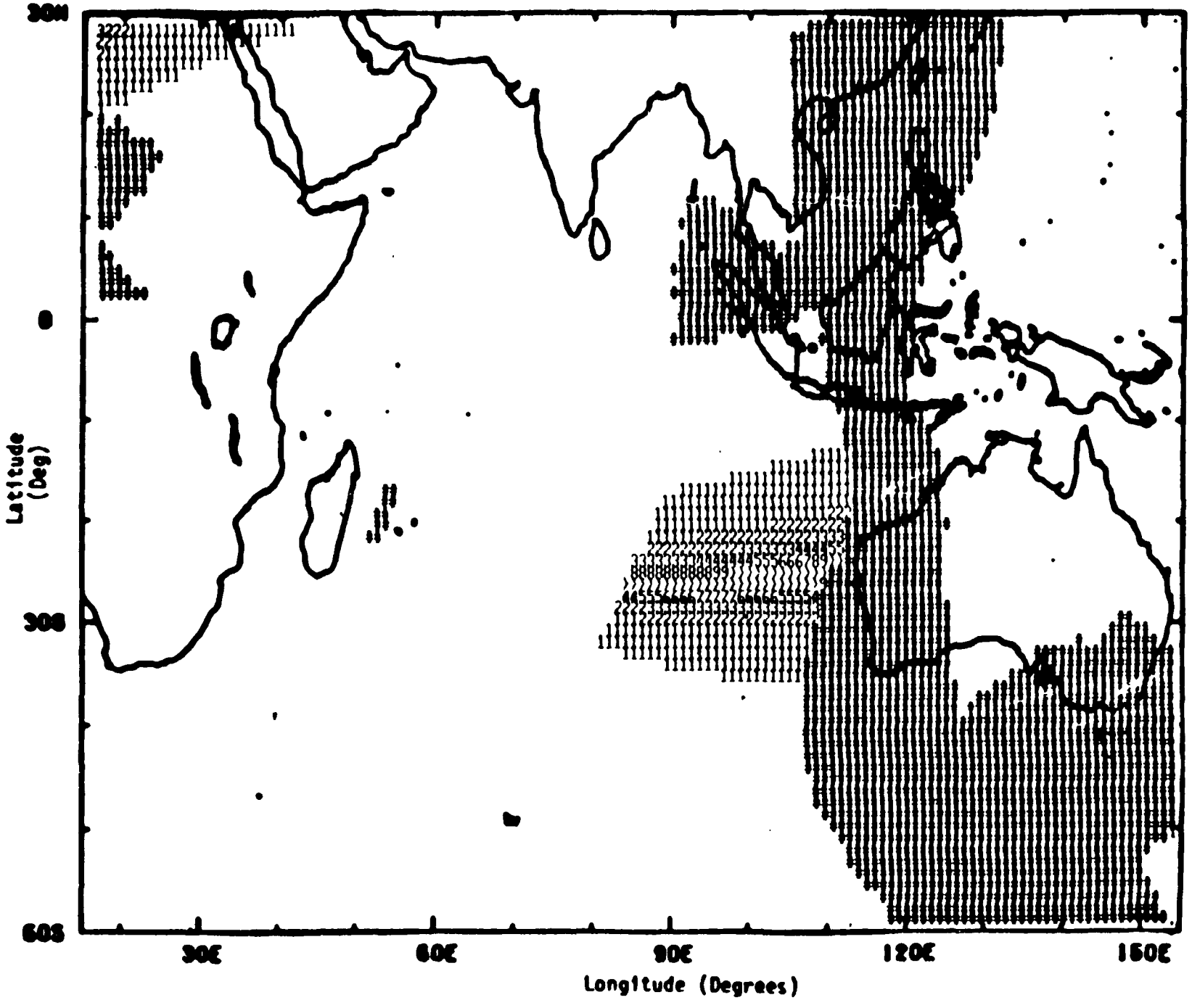

Figure 6. 24-hour Coverage: C.E.P.

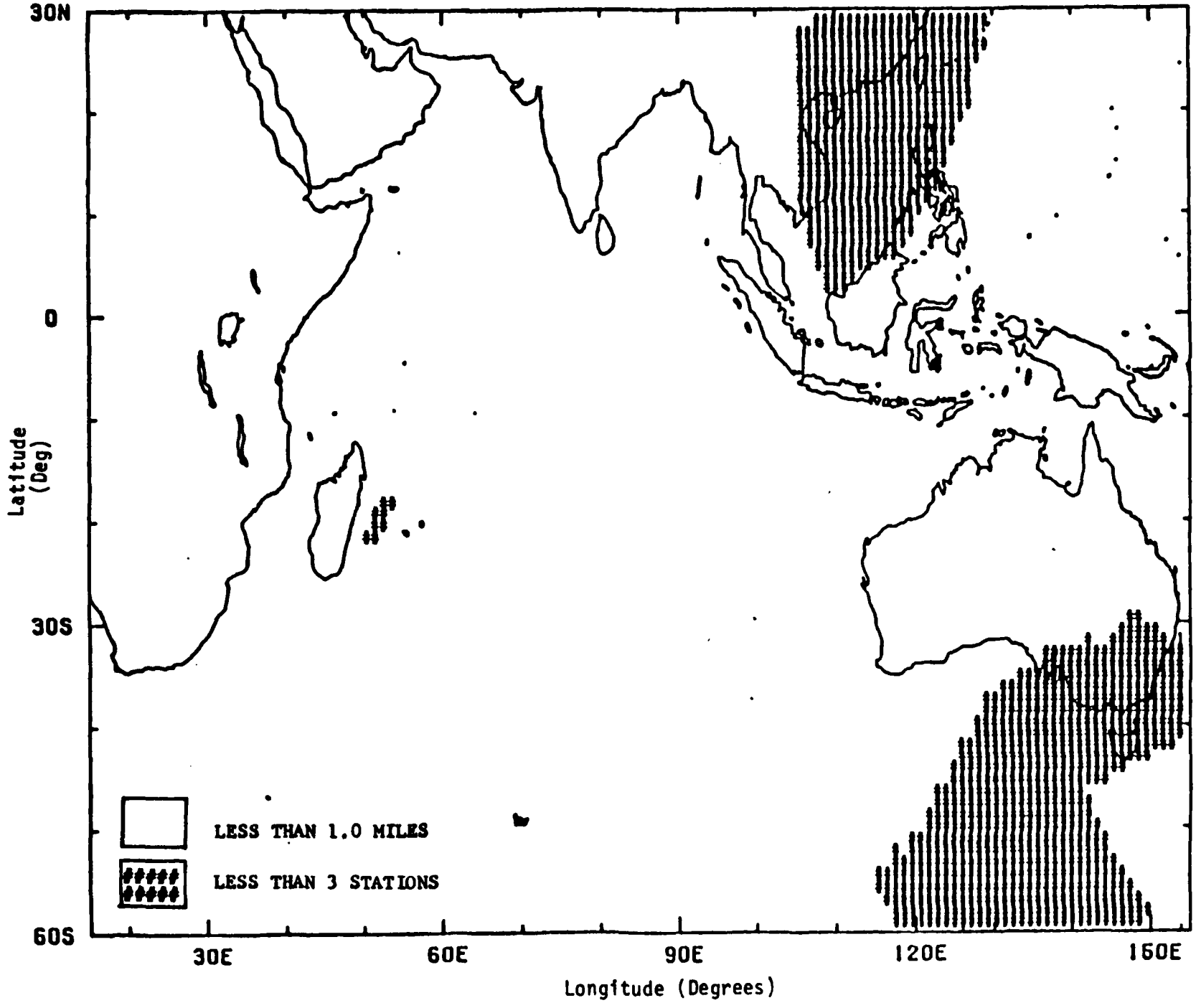

Figure C-7. Daytime Coverage: RMS

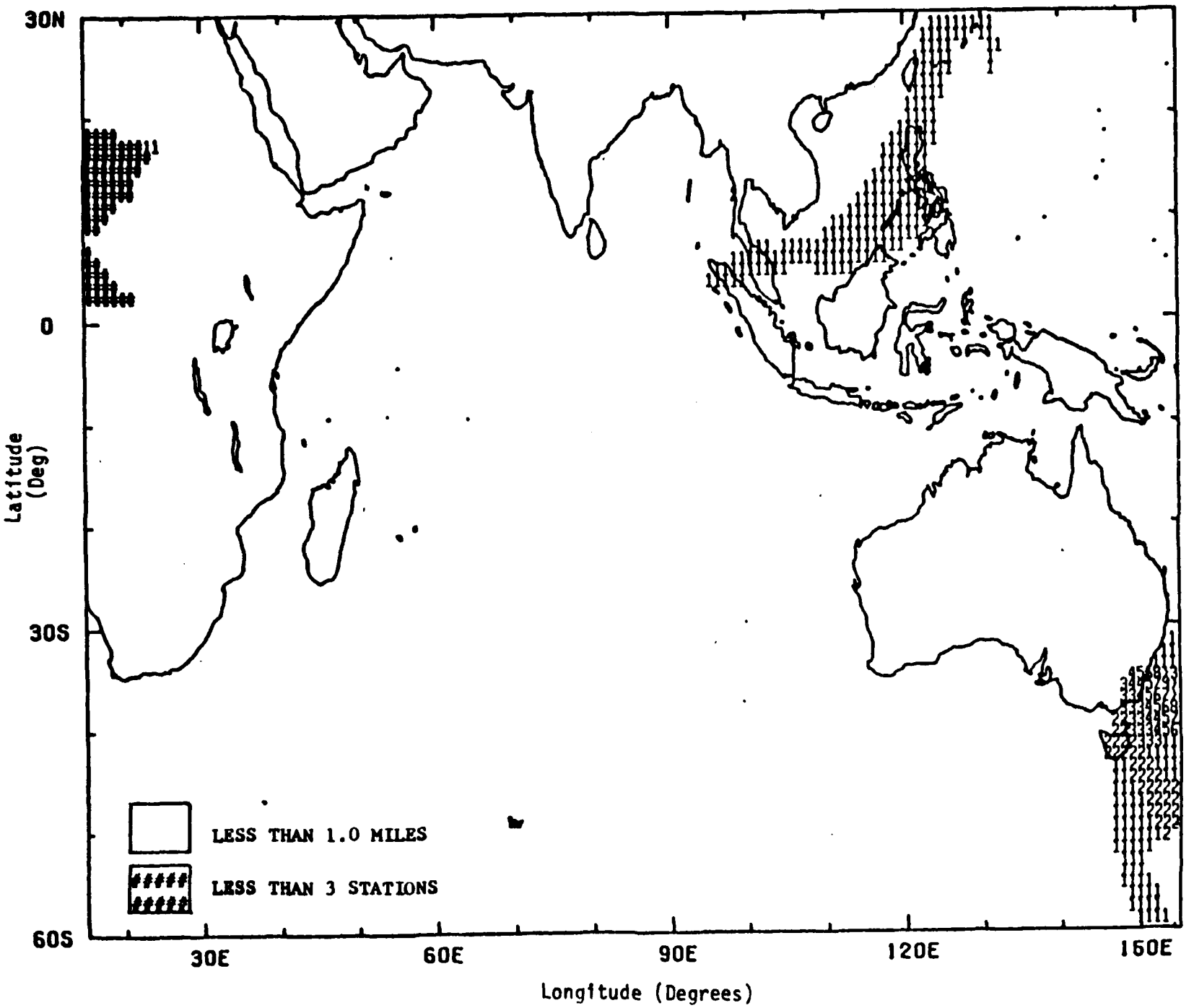

Figure C-8. Nighttime Coverage: RMS

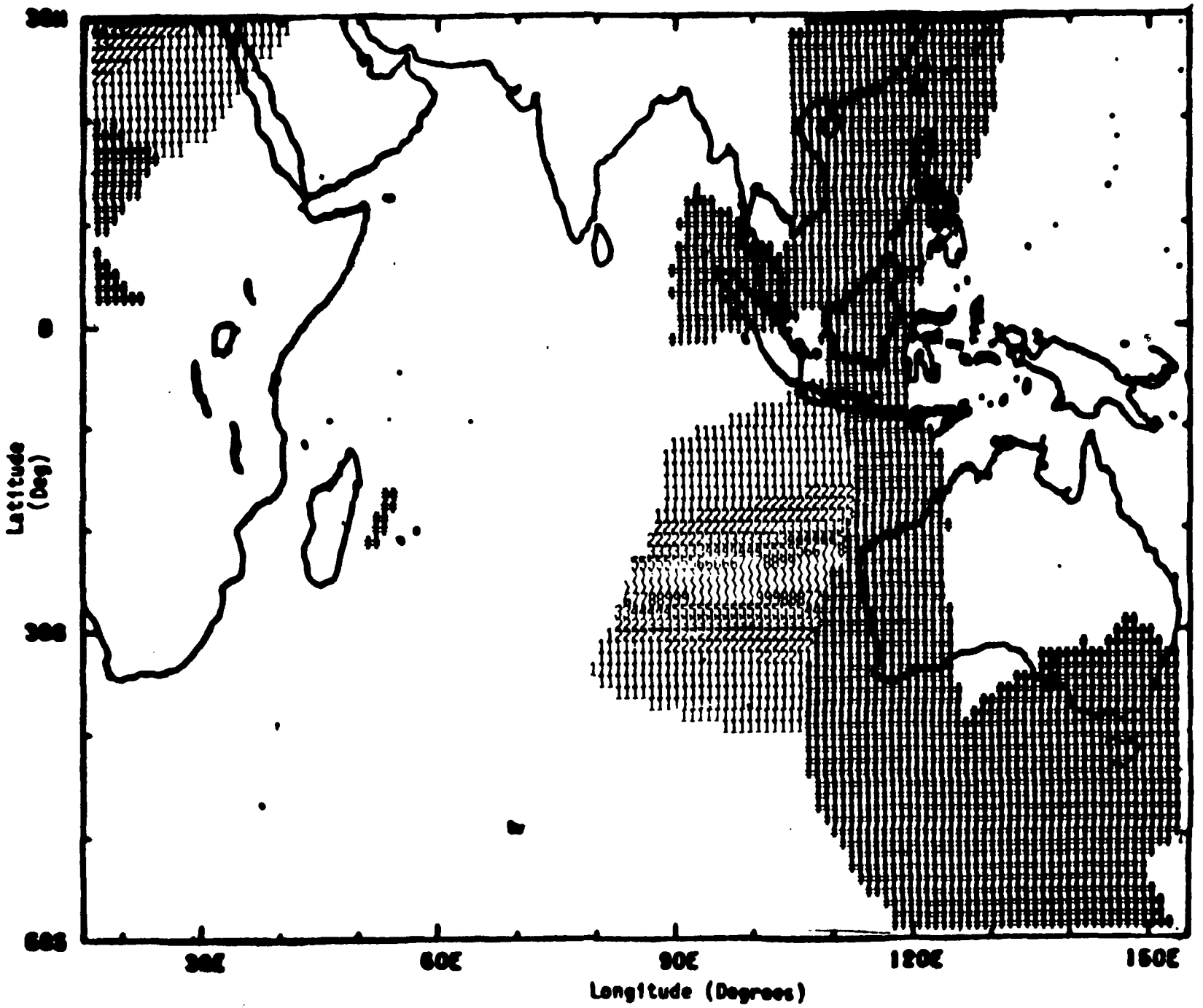

Figure C-9. 24-hour Coverage: RMS

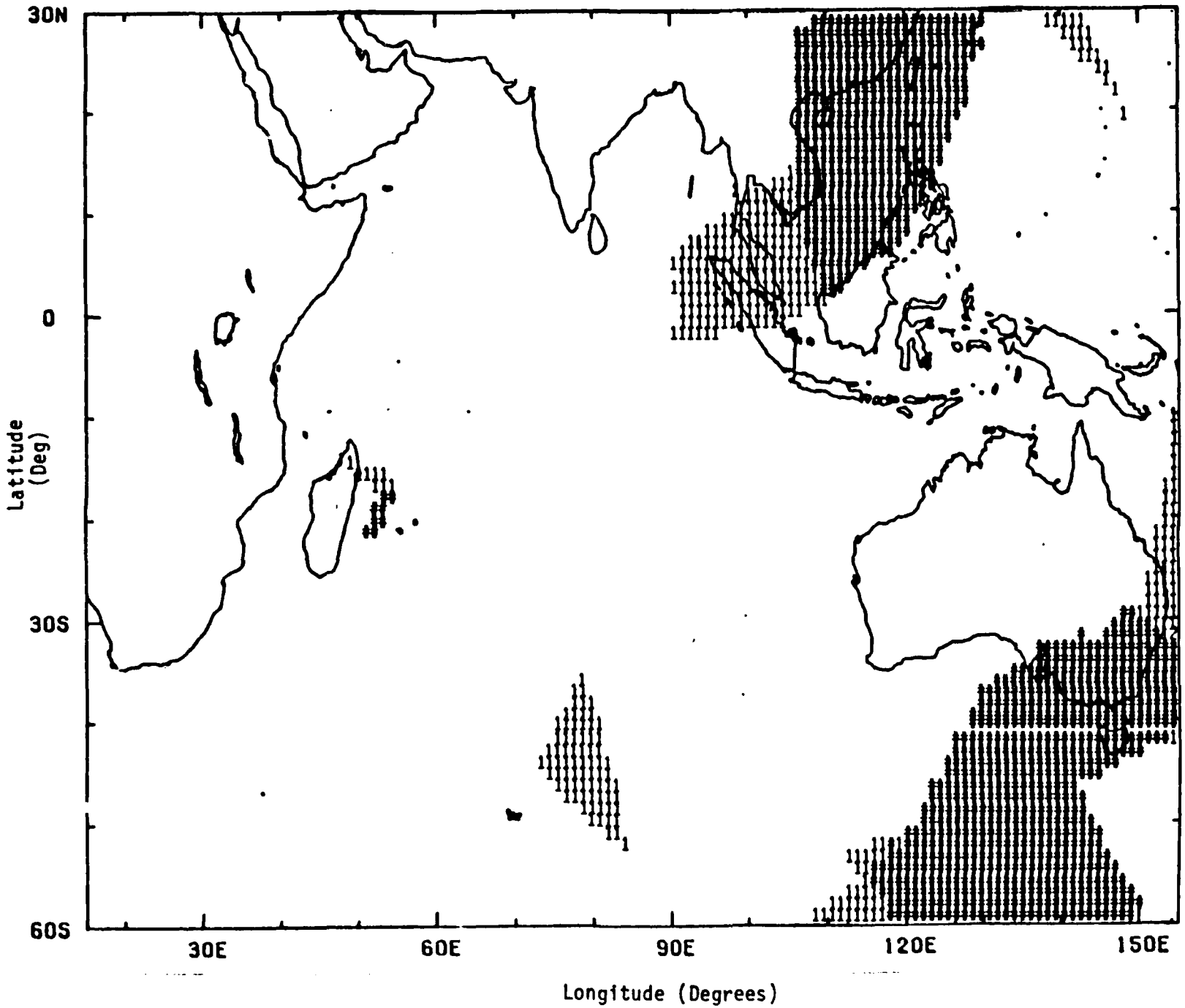

Figure C-10. Daytime Coverage: 95th Percentile

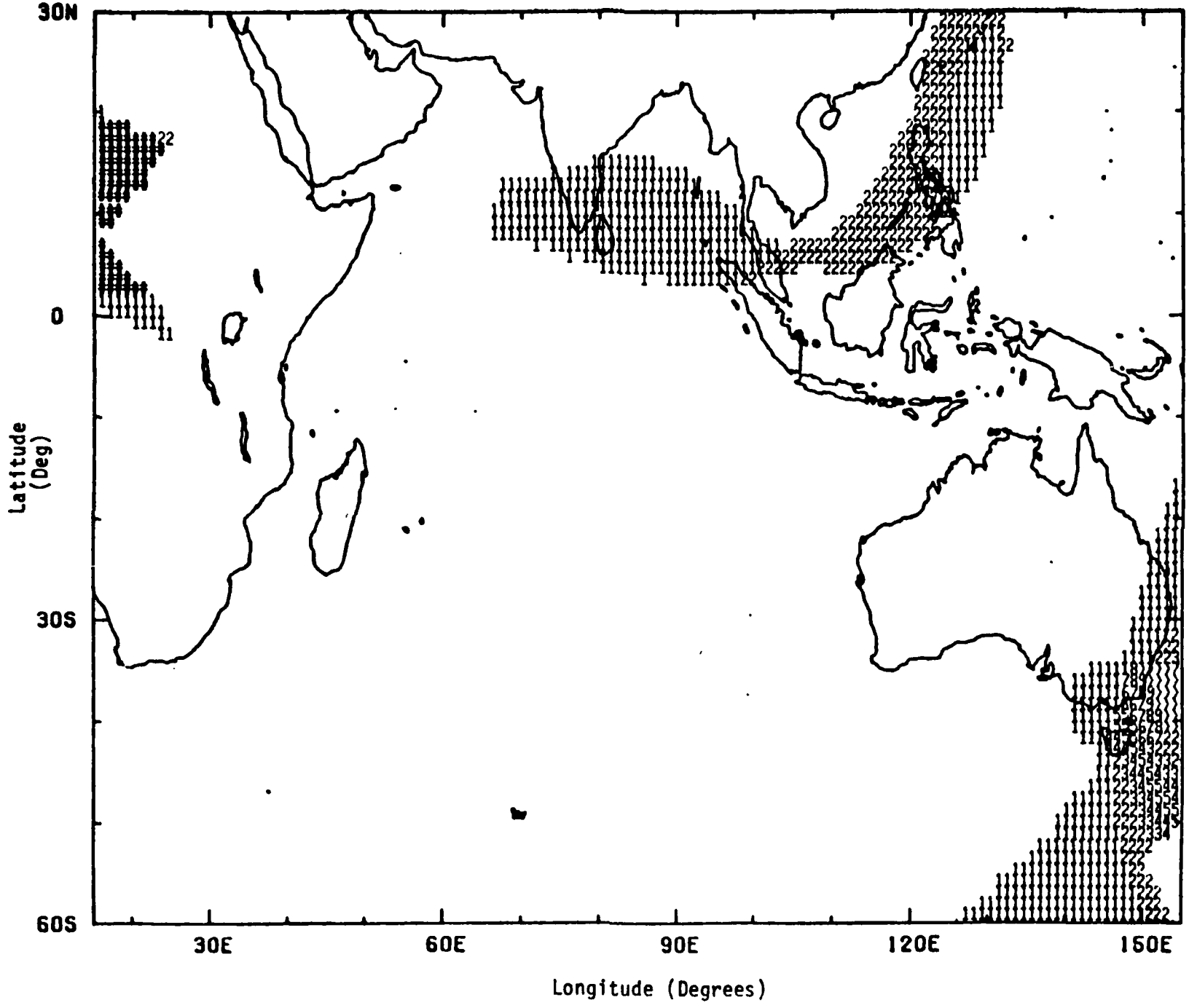

Figure C-11. Nighttime Coverage: 95th Percentile

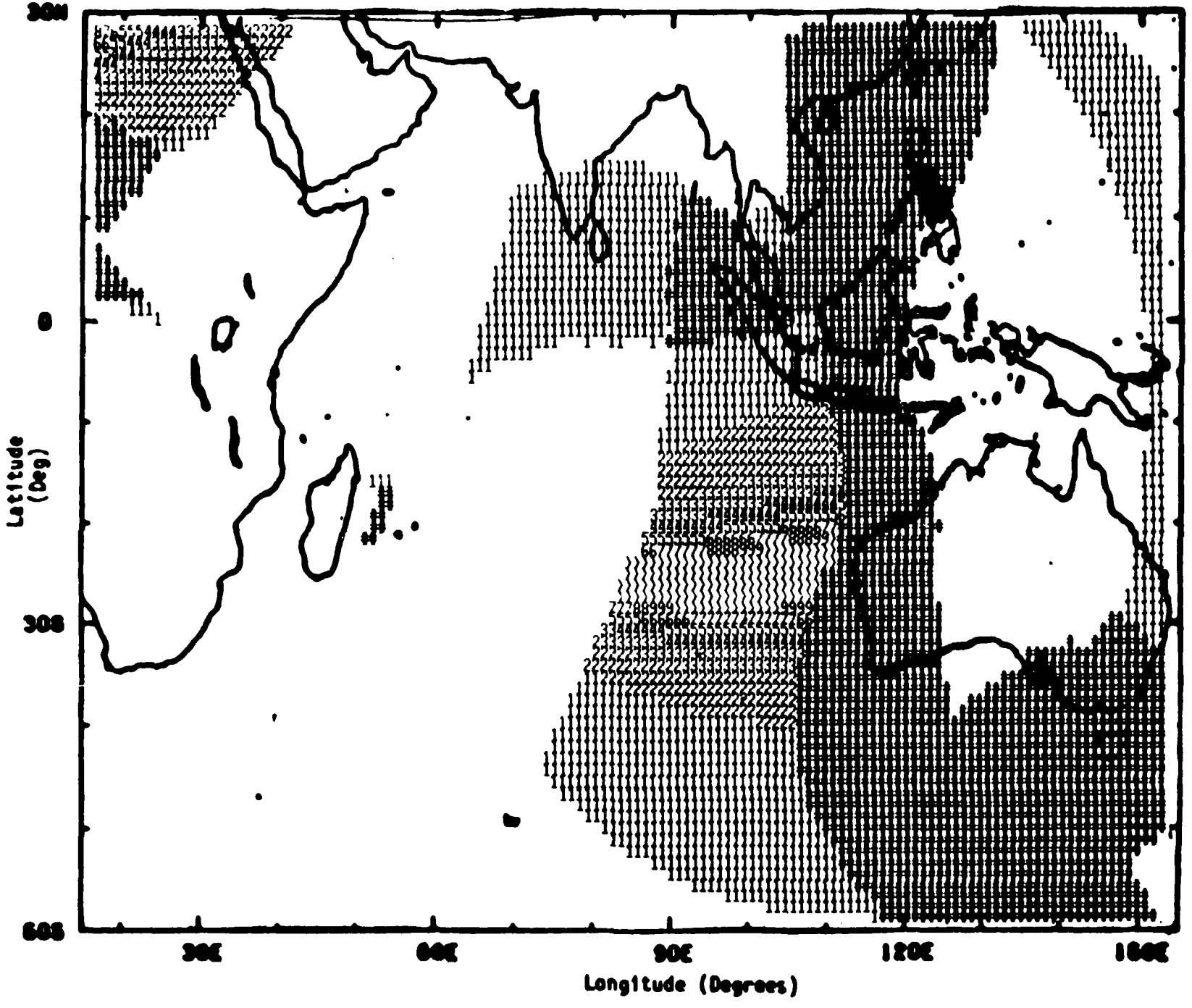

Figure C-12. 24-hour Coverage: 95th Percentile

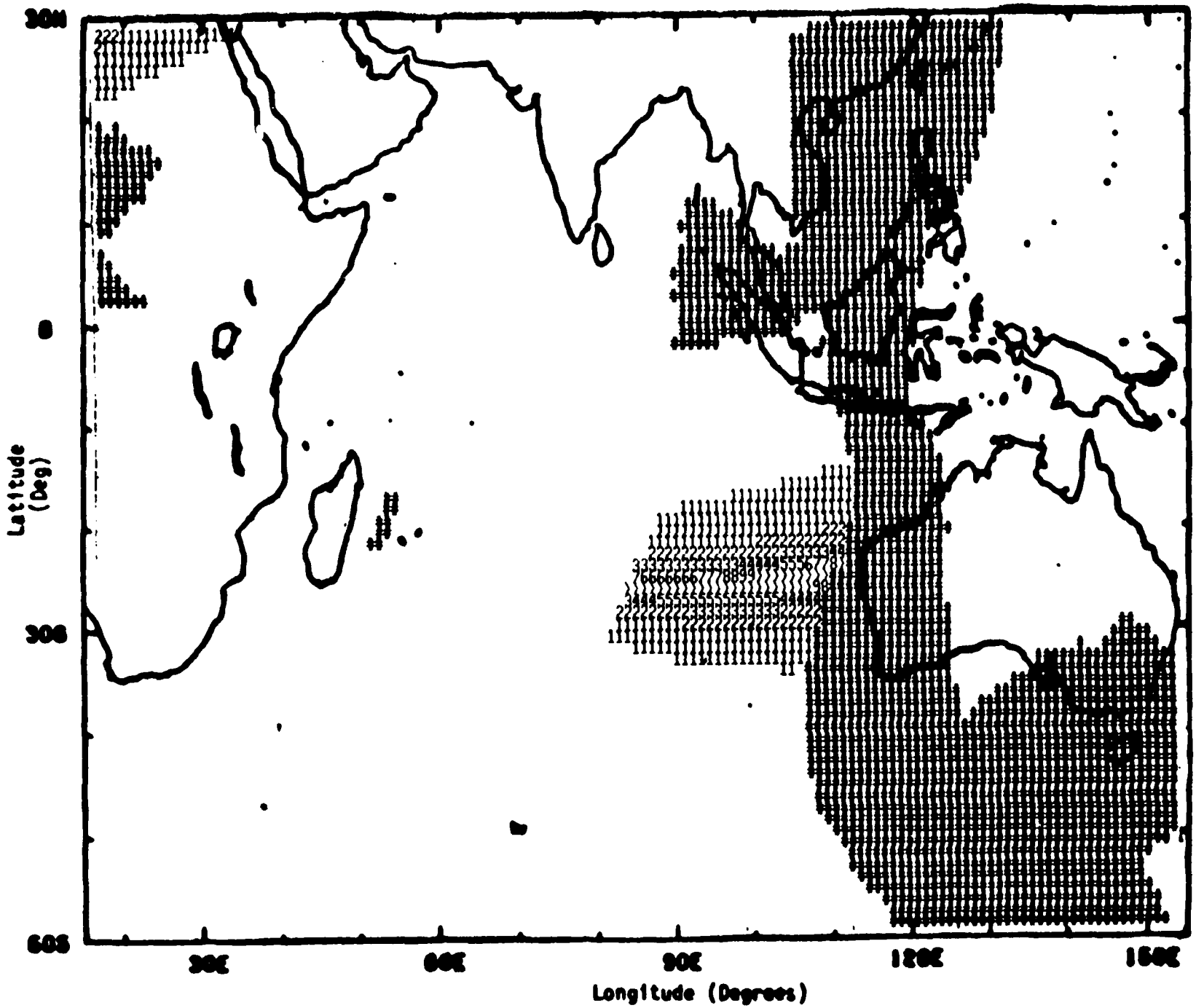

Figure 13. 24-hour Coverage : C.E.P. with PPC Bias Removed

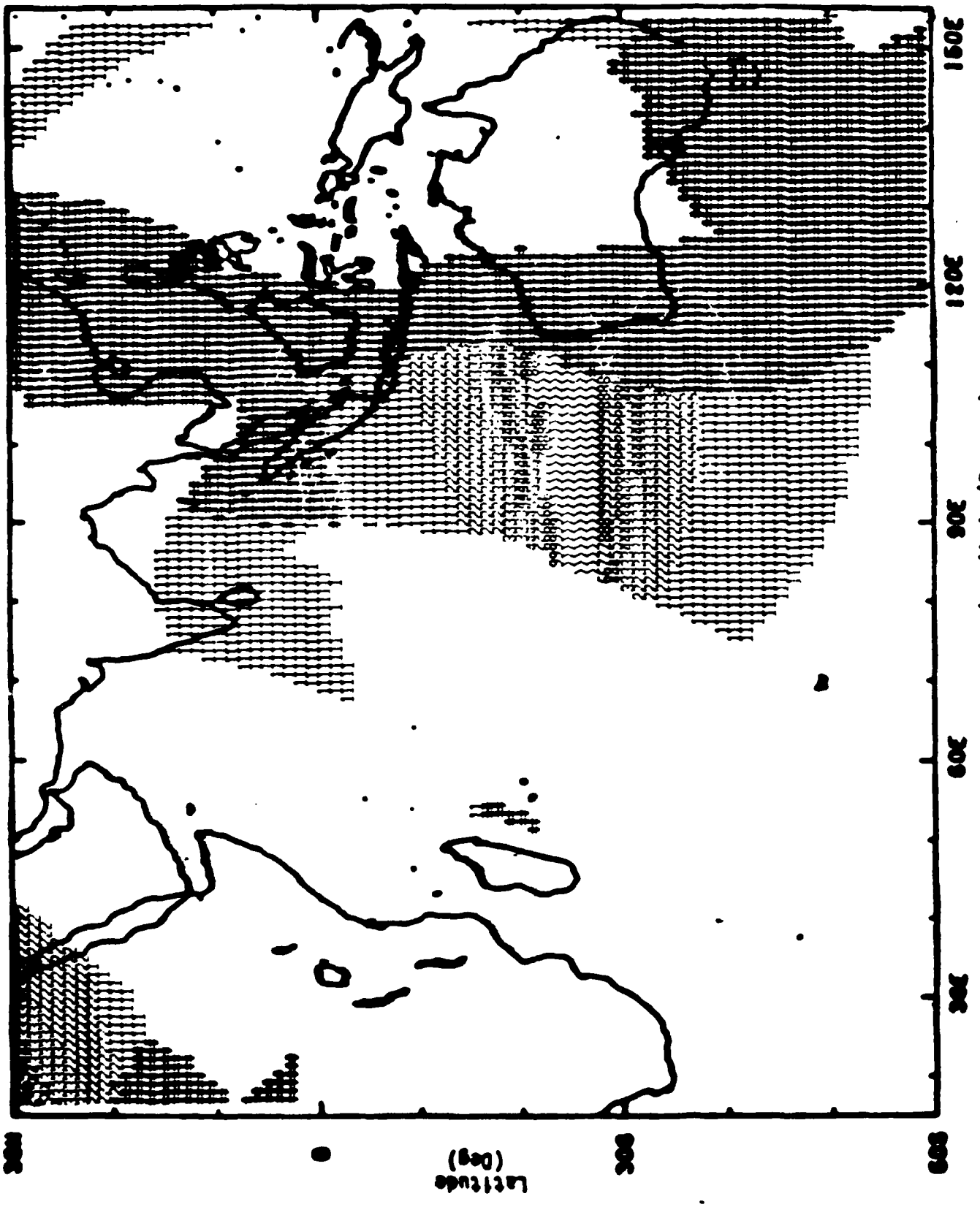

Figure 14. 24-hour Coverage: 95th Percentile with PPC Bias Removed

END

DATE

FILMED

8-88

DTIC